The importance of pollen and local spatial structure in the evolution of reproduction in flowering plants

Stewart-Cox, James

Award date:
2005

Awarding institution:
University of Bath

The Importance of Pollen and Local Spatial Structure in the Evolution of Reproduction in Flowering Plants

---

submitted by

James Stewart-Cox

for the degree of Doctor of Philosophy

of the

University of Bath

Department of Mathematical Sciences

September 2005

ProQuest LLC
789 East Eisenhower Parkway
P.O. Box 1346
Ann Arbor, MI 48106-1346

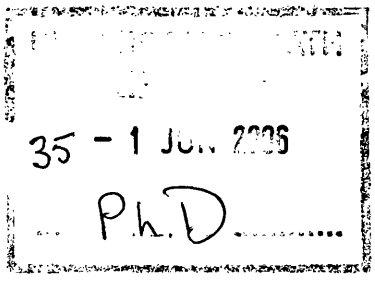
35 - 1 Jun 2006
Ph.D

"He's thrown a kettle over a pub, what have you done"

Gareth Keenan, The Office, Series 1.

Contents

Acknowledgements

I would like to thank the following for their support during the preparation of this report:

- Prof. Nick Britton for his always insightful support and constructive guidance throughout the preparation of this report and its scaffolding of publications, conference presentations, grant proposals and biannual reviews. And for convincing me of the need for sophisticated mathematical approaches in the modelling of flowering plant breeding systems.
- Dr. Mike Mogie for his excellent support and guidance and for his inspirational determination to challenge the limits of current approaches in spatial ecology. And for convincing me of the need for close attention to reproductive biology in the preparation of models of flowering plant breeding systems.
- EPSRC for funding my research.
- Dr. Jane White, Prof. Victor Galaktionov and John Harris for taking time to dispel some, but by no means all, of my mathematical shortcomings.
- Al Kasprzyk for spending an exceptional amount of time coaxing the reluctant computer programmer out of me.
- Peter Hancock, Matthew Dorey, Dr. Guler Ergun and Dr. Hartmut Schwetlick for regularly asking and answering numerous mathematical biology questions.
- Dr. Andrew Ward, Prof. Laurence Hurst, Prof. Rod Scott and Dr. Rinke Vinkenoog for responding patiently and intelligibly to my molecular genetical queries.
- Joanne Allsop and my Family for all the support and input in so many areas of my life over the past three years.

Publications

The work in this report that has been previously published is identified as follows:

- Chapter 2 (pp 31-49) was published in its entirety in an article entitled *Endosperm triploidy has a selective advantage during ongoing parent conflict by genomic imprinting* by J.A. Stewart-Cox, N.F. Britton and M. Mogie in 2004 in the Proceedings of The Royal Society series B, volume 271, number 1549.

- Material in derivations and sexual species models in chapters 5 (pp 144-173) and 6 (pp 193-209) reflects the general framework and example published in an article entitled *Timescale separated Pollination-colonization models* by J.A. Stewart-Cox, N.F. Britton and M. Mogie in 2004 in the proceedings of the 6th international conference on cellular automata for research and industry, ACRI 2004, Lecture Notes in Computer Science, Volume 3305.

- The pair approximation to the sexual species interacting particle system model, and analysis thereof, described in chapter 6 (pp 196-209) was published in an article entitled *Pollen-limitation or mate search need not induce an Allee effect* by J.A. Stewart-Cox, N.F. Britton and M. Mogie in 2005 in the Bulletin of Mathematical Biology, volume 67, issue 5.

- The pair approximation to the gynodioecy interacting particle system model, and analysis thereof, described in chapter 6 (pp 210-225, 243-246) was published in an article entitled *Space mediates coexistence of females and hermaphrodites* by J.A. Stewart-Cox, N.F. Britton and M. Mogie in the Bulletin of Mathematical Biology, Volume 67, issue 6.

Summary

Sexually reproducing flowering plants are in general immobile. They are obliged to produce mobile gametes, which can be dispersed to the reproductive partner. The necessity of producing and dispersing pollen has had an obvious effect on the physical appearance of flowering plants, but it is also of great significance in the evolution of the many differing modes of reproduction found in extant flowering plant species. This significance is not limited to sexual modes of reproduction, since a hermaphrodite asexual may still produce pollen. Moreover there are species in which individuals producing asexual seeds still require pollination.

A further consequence of immobility is that the local abiotic and biotic environment can change very little over the lifespan of a plant. In particular the immediate biotic environment can dictate fitness. The local presence of inter- and intra-specific competitors influences individual survival, the success of vegetative propagation and the likelihood of establishment of locally dispersed offspring. The local presence of conspecifics to donate or receive pollen can strongly influence reproductive success. Understanding the local spatial arrangement of individuals in a population is therefore vital to understanding the viability of that population. Similarly short-scale interactions are of paramount importance in predicting the spread of novel genetic mutations within populations. In particularly, this will be the case if a novel mutation affects reproductive mode, whereby it has the potential to alter the nature of local interaction.

In this report mathematical models that explore the importance of pollen quality and source and the effects of spatial structure within plant populations are systematically developed. These models, derived in generality, will be deployed to investigate several currently unresolved issues in the evolution of flowering plant reproductive diversity. Namely: The mechanisms of coexistence of females and hermaphrodites in gynodioecious populations; The maintenance of pollen production in pseudogamous apomictic species; And the mechanisms underlying geographic parthenogenesis. Modelling techniques are drawn from classical and modern sources for treating population- and individual-scale phenomena.

PART I

Reproductive Physiology

CHAPTER 1

Flowering Plant Reproduction

Flowering plants are the most numerous and diverse of extant plant groups. They first appear in the fossil record 125 million years ago and today more than 250,000 species have been catalogued worldwide (Crane et al. 1995). For such a recent division flowering plants demonstrate a broad range of morphological variety in reproductive physiology and diversity in breeding systems. Flowering plant sexual diversity interested the earliest evolutionary biologists: Darwin devoted volumes to flower polymorphism and self- and cross-fertility. In this chapter the reproductive physiology and breeding systems of flowering plants that underly the mathematical modelling in this report will be concisely surveyed. This will involve discussion of: The typical reproductive anatomy and biology of sexually reproducing flowering plants; Various mechanisms of self-incompatibility and their purpose; Methods of apomictic or asexual seed production; Evolutionary trends and reproductive polymorphisms.

The profusion of life-history details that might conceivably play a role in the ecology of flowering plant populations presents a challenge for mathematical modelling. This report has favoured the approach of examining piece-wise the explanatory power of relatively simple modelling assumptions. Often the details of plant reproduction will be summarized in only a handful of parameters. While this is a theoretical and mathematical necessity it may at times seem an audacious and insipid dismissal of the vast variety of flowering plants. Part of the role of this chapter is to redress this inequity.

1.1 BASIC PHYSIOLOGY

Accounts in this section are sourced from Richards (1986) unless otherwise referenced.

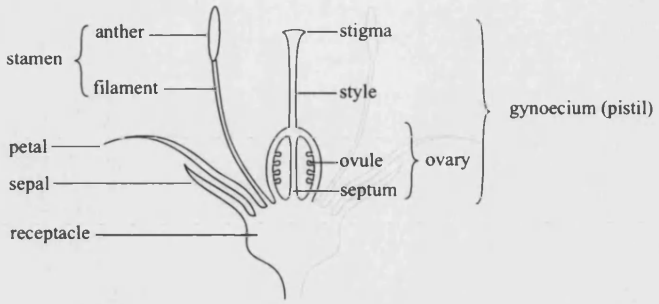

Figure 1-1: Conventionalized diagram of a flower.

Reproductive Anatomy of a Flower

Early flowering plants are likely to have been hermaphrodite, both male and female function are performed by single individuals. Moreover, 95% of extant species include hermaphrodite individuals and of these species 72% produce only flowers containing both functional male and female reproductive structures. The models in this report will usually assume hermaphrodity of some component of the population as a matter of course.

A typical hermaphrodite flower has the form depicted in Figure 1-1. The stem (peduncle) terminates in the receptacle, the base of the flower, from which four concentric whorls of floral parts develop. The outer whorl, the calyx, is comprised of sepals which are leaf-like in form and often photosynthetic. The second whorl, the corolla, is comprised of petals which are leaf-like in shape but generally non-photosynthetic, and subject to huge variability across species in size, colouration and number. The third whorl is comprised of stamens, the lobed anthers of which are microsporangia and give rise to pollen grains. The final whorl consists of one or more gynoecia, at the base of which are ovaries which are megasporangia and give rise to ovules.

Male and Female Gametogenesis

Because of flowering plants' immobility, sexual reproduction relies upon a variety of external mechanisms to enable the meeting of gametes from different individuals. Although sometimes very specialized, biotic mechanisms of insect or animal transfer (entomophily, zoophily) or abiotic mechanisms of wind or water transfer (anemophily,

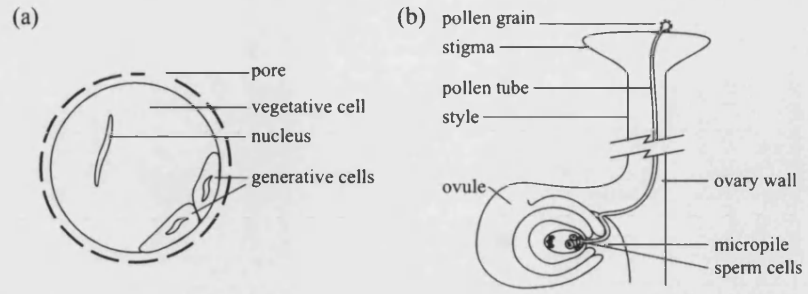

Figure 1-2: (a) Conventionalized diagram of a pollen grain. (b) The development of the male gametophyte (pollen tube) that precedes the union of gametes in double fusion.

hydrophily) are always highly inefficient. Consequently gametes must be numerous and motile to stand a good chance of reaching the gametes of another individual. Gametes must also be well provisioned to ensure that the zygote has sufficient resources to begin embryogenesis. In flowering plants, as in the vast majority of sexual species, these requirements have been accommodated by the evolution of anisogamy: whereby these criteria are allotted to separate genders. In flowering plants the small, abundant and motile gametes of the male function are produced in pollen sacs within the anthers (microsporangia); whilst the large, well provisioned and sessile gametes of the female function are produced in ovules within the ovaries (megasporangia.)

Within a pollen sac a single initial diploid archesporial cell divides mitotically to form many pollen grain mother cells. Mitosis is the cellular process of nuclear division in which a replicate nucleus with a complete complement of chromosomes is produced within a cell. Here mitotic division is used to imply mitosis followed by cytokinesis: the arrangement of cellular matter into two daughter cells each containing one nucleus. Each pollen grain mother cell undergoes meiosis to produce microspores. Meiosis produces haploid cells from diploid cells, and is the basis of all sexual reproduction. In meiotic division chromosomes are initially duplicated and then split into their component chromatids, each complete complement of chromatids is surrounded by a nuclear membrane and partitioned into a separate cell. In many species, including all flowering plants, chromatids, once separated, align and one non-sister pairing (i.e. one chromatid from each chromosome) exchange sections of genetic material. This process of recombination, together with the random segregation of chromatids into nuclei, is a major source of variation in sexual species. A single meiosis yields four non-identical mi-

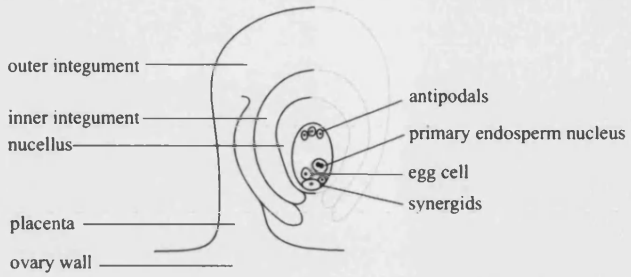

Figure 1-3: Conventionalized diagram of a mature seven-celled embryo-sac.

crospores described as a tetrad, which separate to form pollen grains. Within a pollen grain two mitoses occur with timings that vary widely between species from minutes to months. The first mitosis is asymmetrical resulting in a vegetative cell which dominates the space within the pollen grain and a generative cell. The second mitosis is of the generative nucleus only and yields two genetically and physiologically identical sperm cells. Figure 1-2(a) illustrates a pollen grain in this final three-celled state.

Ovules are attached to the ovary wall by a placenta. Ovules consist of two layers of protective integuments, destined to become the seed coat, surrounding the nucellus. Cells of the nucellus differentiate to become archesporium tissue a single cell of which, the archespore, grows to become an embryo-sac mother cell. The embryo-sac mother cell undergoes meiosis to form a tetrad of megaspores. The tetrad is linear and the last three cells (counting from the end closest to the placenta, the chalazal end) are terminated and disappear. Because the cells of the tetrad are genetically different the selective abortion of three of them is a potential source of kin conflict (Trivers 1974). There is evidence that the mother inserts a rigid substance, callose, between the cells to prevent spiteful, preemptive poisoning, by the other cells of the tetrad, of the cell chosen to survive (Haig 1986). The surviving megaspore undergoes three mitoses resulting in eight unwalled cells. These cells have roles of varying importance to successful fertilization and viable seed production. They comprise: Two synergids, one of which is much larger than the other and dominates the end of the embryo-sac furthest from the placenta (the micropile); The egg cell adjacent to the large synergid; Two polar nuclei, located more centrally which fuse to form the primary endosperm nucleus; and three antipodal cells at the chalazal end of the embryo-sac. Figure 1-3 illustrates the mature seven-celled embryo-sac.

Both male and female gametogenesis result in a haploid self-sustaining tissue known as a gametophyte. The male gametophyte is the pollen tube which grows from the pollen grain when it alights upon a stigma and the female gametophyte is the embryo-sac. The gametophyte is a phase in the *alternation of generations* common to all plants, in which diploid tissue, the sporophyte, gives rise to haploid tissue, the gametophyte, and fusion between certain cells of male and female gametophytes produces a diploid zygote which will develop into a sporophyte. The gametophyte phase in flowering plants is much reduced and consists of only a handful of mitoses. Nevertheless the haploidy of the reduced gametophyte phase serves to unmask recessive mutations, since a gametophyte with compromised function will fail to mature. Thus heterozygous genetic load in plants is reduced in comparison with animals.

Double Fusion and Seed Development

Once a pollen grain alights on a stigma it is hydrated and germinates. Usually a single pollen tube grows from a pore of the pollen grain, penetrates the stigma and grows down the inside of the style. Any of these steps can be interrupted by the female function, on detection of incompatibility. Such physiological incompatibility mechanisms will be discussed further in section 1.2. The generative cells of the pollen grain migrate along the pollen tube, remaining close to the growing tip. Meanwhile the vegetative cell degenerates. Pollen tube growth is controlled by a poorly understood but highly effective mechanism. Travelling down the ovary wall, the tube turns sharply into the placenta of an unfertilized ovule, bypassing fertilized ovules or even being redirected in the event that the target ovule becomes fertilized before the pollen tube arrives. The tube exits the placenta at the base of the ovule and reenters at the micropile, adjacent to the embryo-sac. Figure 1-2(b) illustrates the path of the pollen tube from the stigma to the micropile of an ovule.

The larger synergid has begun to degenerate during the progress of the pollen tube, while at the same-time developing outgrowths which assist the pollen tube in penetrating the embryo-sac. Inside the remains of the synergid, the sperm cells diverge and align, one with the egg cell and the other with the primary endosperm nucleus. Double fusion then occurs: One sperm cell and the egg cell fuse to form a diploid zygote and the other sperm cell and the primary endosperm nucleus fuse to form a triploid endosperm. The first mitoses of embryogenesis are delayed in the zygote, whilst the endosperm divides rapidly, through a free-nuclear stage with later cellularization,

engulfing the embryo and forming nutrient links to maternal tissue. The endosperm will constitute the bulk of matter in the mature seed. It is a largely uniform food store, that will resource the initial growth of the embryo once the seed germinates. The $2:1$ ratio of maternal to paternal contribution to the endosperm genome (denoted 2m:1p) is important for correct endosperm development. Alternative ratios, achieved by crosses between plants with different ploidy levels, usually result in over- or under-proliferation of the endosperm and seed abortion (Adams et al. 2000).

The tissues of the putative seed thus have three distinct genetic constitutions: the maternal sporophyte; the diploid embryo; and the triploid endosperm. There is potential, therefore, for conflict over how much maternal resource should be set aside for the embryo within the seed. The fact that there are three participants in this conflict, and the endosperm's unusual triploid genome, suggest an intriguing evolutionary history. Current opinion concerning this history will be covered in section 1.4 and chapter 1 will explore this history in even greater detail, providing models for crucial incidents.

The process of double fusion was once considered unique to flowering plants but is now known to occur very rarely in some closely related plant groups (Friedman & Floyd 2001).

1.2 SELF-INCOMPATIBILITY

It is often suggested that the need to avoid inbreeding has contributed greatly to the evolution of the myriad morphological and physiological adaptations of flowering plants. In hermaphrodite species inbreeding, resulting from the transfer of pollen to stigmas within the same flower (autogamy) or a different flower of genetically the same individual (geitonogamy), is an immediate problem. The offspring of such crosses are often low in vigour and fertility. This effect, termed *inbreeding depression*, was studied extensively by Darwin and is supported by a wealth of empirical evidence (Mayo 1987). Inbreeding decreases heterozygosity by 25% per generation giving a high likelihood that deleterious recessive alleles, not expressed in the parental phenotype, will be expressed in that of the offspring. Inbreeding also decreases variability in offspring, this can have negative consequences which will be discussed further, with reference to apomixis, in section 1.3. If ovules are self-fertilized both pollen and ovule are removed from the pool of gametes available for outcrossing (pollen and seed discounting.)

A wide range of inbreeding prevention mechanisms have arisen in flowering plants.

These may be physiological: at any stage following arrival at a stigma, the pollen grain or pollen tube may be recognized by the female sporophyte and further development arrested. Other mechanisms involve preventing pollen from coming into contact with stigmas from the same plant. This may involve controlling the timing of when male and female function are active (dichogamy), or the placement of anthers and stigmas within a flower (herkogamy.)

Although many species go to great lengths to avoid inbreeding, or selfing, some species actively promote it. Such species employ no incompatibility mechanism and may, for example, deliberately prevent flowers from opening until most seed has been self-fertilized (cleistogamy.) In obligate selfing species, fruit and seed set is high, and inbreeding depression is scarcely a problem because in general a seed's parent was itself self-fertilized and successfully survived to reproductive maturity. Heterozygosity and genetic variation in such species is low, so although such species arise frequently, their potential to adapt may be compromised and they may persist for a comparatively short periods. Obligate outcrossing and obligate selfing are subject to positive feedback: Outcrossing increases heterozygosity and thus allows for a greater genetic load, so that inbreeding results in poor viability; Selfing decreases heterozygosity, reducing genetic load in surviving offspring and so minimizing inbreeding depression. Despite the antithesis of the breeding systems, many species find something to be gained by employing a mixture of strategies. For outcrossers autogamy and geitonogamy provide reproductive assurance, suitable mates may not always be available, and producing inbred seed is better than producing no seed at all. For selfers occasional outcrossing introduces variability and provides lineages with access to novel genetic material.

Physiological Mechanisms

Gametophytic Self-Incompatibility

In gametophytic self-incompatibility (GSI) the haploid genotype of the pollen grain determines the compatibility phenotype. Alleles from the same loci in the male gametophyte genome and the female sporophyte genome are expressed at some point between pollen arrival and fertilization. The interaction of expression products either prevents or permits continued pollen tube growth. Usually only a single compatibility locus is involved whose alleles are conventionally denoted S_i. So, for example in diploids, a pollen grain bearing an S_i allele will succeed in fertilizing only S_jS_k females

where $i \neq j, k$. Thus pollen from the same plant is always detected and fertilization is prevented. If individuals are parent and offspring or full siblings, they will typically share one compatibility allele, in this case half of all crosses will be compatible and half incompatible. This effect amongst closely related individuals is described as semi-compatibility. In a GSI breeding system all offspring will necessarily be heterozygous and so a minimum of three alleles are required for the species to persist. In natural populations it is common to find many more than three alleles, polymorphism is maintained by frequency-dependent selection favouring rare alleles. The presence of GSI strongly correlates with a range of phenotypic characteristics: Long-lived pollen is typically transferred in binucleate form and adheres to a sticky exudation of the stigma, which hydrates the pollen grain and promotes initial pollen tube growth. The stigma surface is discontinuous allowing the pollen tube direct entry to the style where it grows through cells. When pollen is incompatible, pollen tube growth is arrested in the style.

In some cases two or more loci may be involved in a GSI breeding system. In a multi-locus system all alleles present in the male gametophyte must match alleles in the female sporophyte in order for pollen to be rejected. This improves specificity: selfed pollen is always rejected, but in a two-locus system typically only 25% of crosses between close relatives, who are themselves the product of outcrossing, will be rejected. Multi-locus GSI systems are a more efficient way of preventing selfing without prohibiting reproduction with a large contingent of the population. Most grasses (Poaceae) have a two-locus incompatibility system. Interestingly, however, they bear none of the phenotypic hallmarks of the system, bearing instead the hallmarks of sporophytic incompatibility (see below) It is likely that the incompatibility system in grasses is secondary, having re-evolved from self-compatible ancestors.

Gametophytic self-incompatibility is widespread and probably present in more than 50% of extant species across a broad range of orders including primitive dicotyledons and monocotyledons (Richards 1986, p 207). The mechanism's ubiquity coupled with the presence of similar mechanisms in gymnosperm and pteridophyte groups give credence to the long standing belief that it is primitive to flowering plants (Whitehouse, 1950 and Bateman, 1952 cited in Richards (1986, p207).)

Sporophytic Self-Incompatibility

In multi-allelic sporophytic self-incompatibility (SSI) the genotype of the male sporophyte that produced the pollen grain determines the compatibility phenotype. Semi-

compatibility cannot occur, and all crosses between two individuals will either all succeed or all fail. Dominance and codominance relationships are commonly reported between compatibility alleles. So, if S_1 dominates S_2 the compatibility phenotype of S_1S_2 will be S_1. This is intriguing, because the compatibility phenotype may not match the allele carried in the pollen grain and homozygotes can result. Dominance and codominance relationships between alleles may differ between male and female sporophyte. It is not however likely that reciprocal dominance relationship will arise (S_i dominates S_j in pollen, but S_j dominates S_i in stigma) because S_iS_j individuals would be fully self-compatible. It is typically the case that dominance hierarchies govern pollen compatibility phenotype, but alleles are expressed independently on stigmas. The presence of multi-allelic SSI also strongly correlates with a range of phenotypic characteristics: Short-lived pollen is typically transferred in trinucleate form and adheres by virtue of it own sticky surface to a dry stigma Incompatible pollen is rejected at the stigma and often fails to hydrate or germinate.

Sporophytic self-incompatibility is sometimes diallelic with only two alleles: the dominant S and the recessive s. When present S dominates the compatibility phenotype on both pollen and stigma. A population thus contains heterozygotes Ss and homozygotes ss which are cross-compatible, but self-incompatible. Such systems are usually found in heteromorphic populations featuring reciprocal herkogamy (see below)

Pseudocompatibility and Breakdown

Under circumstances of poor or unreliable outcrossed pollen supply self-incompatibility may be disadvantageous. Such circumstances may be temporary, for example at the very beginning or end of a season, or persistent, a result of biotic or abiotic environmental change.

Richards (1986, p 222-224) reviews experiments which have demonstrated that gametophytic incompatibility does not operate on immature or over mature stigmas or in late opening flowers in certain species. These effects may well be adaptive. If immature stigmas or late flowers accept selfed pollen this may provide a baseline of reproductive success, albeit inbred, regardless of what the season might bring. This carries the risk that if outcrossed pollen proves to be abundant some ovules will be fertilized with selfed pollen and fitness may be sub-optimal. If over-mature stigmas accept selfed pollen, the same risk is not incurred since, if outcrossed pollen has been abundant, few if any ovules will remain to be fertilized. Very little selfed pollen may be accepted by such

pseudocompatibility mechanisms. However, a small amount of self-compatibility can prove to have highly significant consequences for a hermaphrodite species' chance of establishment and also it's vulnerability to invasion by male sterility genes (Chapters 3 and 4.)

If circumstances of poor pollen supply persist a selective pressure for bypassing or dismantling self-incompatibility will arise. The reproductive assurance that self-compatibility provides is clear empirically: Fruit set in self-compatible hermaphrodite species averages 72.5% compared with only 22.1% in self-incompatible species (Sutherland and Delph, 1984 cited in Richards (1986, p41).)

The operation of physiological compatibility systems have been discussed here for diploids. Many species of flowering plant have more than two complete sets of chromosomes, they are described as polyploid. Polyploidy arises in numerous ways in natural populations and duplicate chromosome sets may be derived from the same species (autopolyploidy) or through hybridization, usually between closely related species (allopolyploidy.) In self-incompatible diploid species autopolyploidization, which is rare in nature but can be induced experimentally, tends to disrupt the incompatibility mechanism on the male side. Selfed crosses succeed as do back crosses in which the diploid parent is female (Richards 1986, p 220). It is presumed that that multiplicity of functional compatibility loci in autopolyploids is somehow responsible for the breakdown in compatibility. When allopolyploids are formed by hybridization, self-incompatibility may or may not break down. It is likely to be broken down only if both parent species are self-incompatible with compatibility controlled by the same (i.e. homologous) loci (Richards 1986, p 220).

Temporal and Morphological Mechanisms

Dichogamy

Dichogamy refers to the the temporal separation of male and female activity within hermaphrodites flowers. Typically the active gender of the flower changes once during its life span. Pollen may be released in advance of stigma maturity (protandry) or subsequent to stigma senescence (protogyny). Dichogamy is very common, it is estimated that 74.6% of species have some within flower dichogamy and 97.0% have between flower dichogamy (Bertin 1993). Moreover, dichogamy is found more or less equally frequently in self-compatible and self-incompatible species (Bertin 1993) suggesting that its pur-

pose is not solely to prevent inbreeding. Barrett (2002*b*) notes that whilst physiological incompatibility mechanisms increase female fitness by reducing the number of inbred seeds produced, they do not improve male fitness since they do nothing to promote pollen export. Irrespective of the presence of a physiological incompatibility mechanism, it is therefore worthwhile for a species to employ temporal and morphological mechanisms to reduce the amount of pollen lost to autogamy and geitonogamy. Insect pollinated flowering plants must balance inflorescence size to maximize pollinator visits but minimize unwanted geitonogamous pollen transfer (Klinkhamer & de Jong 1993). Dichogamy can permit increased inflorescence size by exploiting pollinator behaviour. For example on the spiked inflorescence of the fox glove (*Digitalis purpurea*) the lower flowers will be older than those above. If pollinators typically forage from lower to higher flowers protandry will improve fitness, because the lower flowers in female phase will receive mainly imported outcrossed pollen, and geitonogamy will be minimized for the higher flowers in male phase (Bertin & Newman 1993).

Herkogamy

Herkogamy refers to the spatial separation of stamens and gynoecia within hermaphrodite flowers. Naturally all species practise herkogamy to some extent by virtue of producing male and female gametes in different structures. The greater the separation between anther and stigma the lower the chance of self-pollination. Too great a separation, however, would prevent pollinator visits from serving the dual purposes of importing and exporting pollen. Heteromorphy is an ingenious solution to this problem that has evolved numerous times. Within a population two or more distinct morphological forms occur both with significant herkogamic separation of anthers and stigmas. Morphs are complementary for anther and style position so that pollinators transfer pollen most effectively between the different morphs. Heteromorphy occurs in 25 families of flowering plants across 18 orders (Richards 1986, p244). The most common form is distyly in which two reciprocal morphs have long styles and short anthers (pin) or short styles and long anthers (thrum). In this way within flower sexual interference is minimized and pollen is transferred precisely (Barrett 2002*a*) from pin anthers to thrum stigmas and vice versa on different parts of the pollinators body. Figure 1-4(a) illustrates distyly. Distyly is controlled by a single locus diallelic mechanism, in general heterozygotes Ss are thrum and homozygotes ss are pin. Since morphs are maintained at $1:1$ by frequency dependent selection only 25% of alleles are the dominant S allele. It is usual to

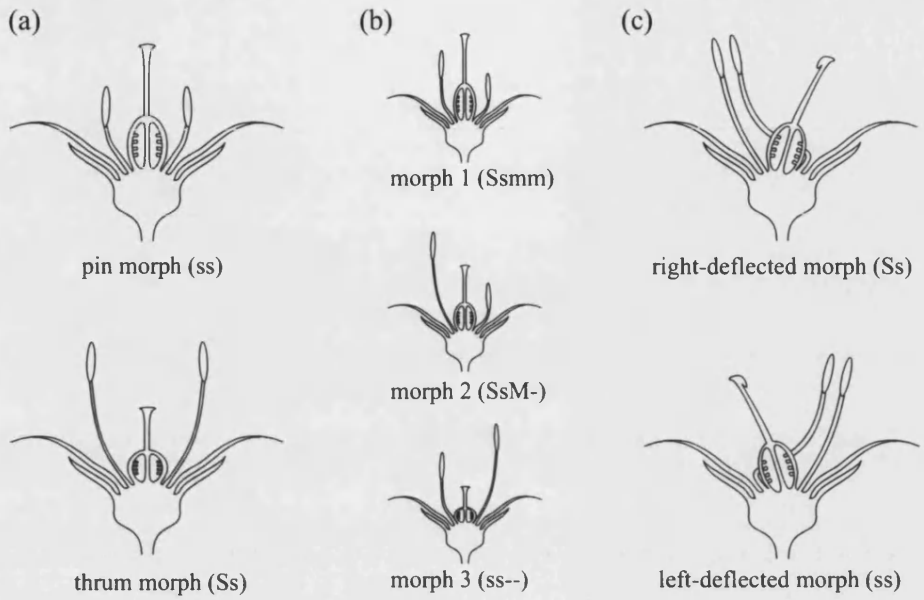

Figure 1-4: Examples of reciprocal heteromorphy. (a) The common form of distyly seen for example in *Primula* species. (b) The tristyly polymorphism seen in *Lythrum Salicaria* (c) Dimorphic enantiostyly seen in *Wachendorphia paniculata.*

find SSI controlled by the same alleles, supporting distyly and policing legitimate pollen transfer (i.e. between reciprocal morphs.) As with dichogamy Barrett (2002*a*) explains that this is not a redundancy of inbreeding prevention mechanisms. SSI promotes female fitness by limiting inbreeding and heterostyly promotes male fitness by improving outcrossed pollen transfer. Occasionally three style morphs can coexist within a population. This mechanism, tristyly, has been reported in just three unrelated families (Richards 1986, p247) and is always under two-locus control. As with two-locus GSI, specificity is improved and a greater proportion of pairs selected randomly from the population are potential mates. Figure 1-4(b) illustrates tristyly. The rarity of tristyly and the absence of more elaborate stylar polymorphisms is almost certainly caused by the difficulty of depositing pollen at multiply segregated sites on pollinators' bodies (Barrett 2002*a*). In fact, the vagaries of pollen transfer mean that even distylous mechanisms rarely achieve anything like exclusive intermorph pollination (Richards 1986, pp 249-250).

A less studied heteromorphy involves mirror-image flower morphs in which styles

and stamens bend in opposite directions. Enantiostyly is most commonly observed with both flower morphs occurring on the same plant (monomorphic enantiostyly), in which case there is no prevention of geitonogamous pollen transfer. By contrast, in the more rarely seen dimorphic enantiostyly, reciprocal mirror-image morphs occur on different plants. In this case control of the polymorphism is by a single diallelic locus, and ratio of morphs is 1:1, precisely as observed with distyly. Interestingly in the dimorphic enantiostylous *Wachendorphia paniculata* no SSI system accompanies the heteromorphism suggesting the mechanism is highly successful at promoting intermorph mating (Barrett 2002*a*). Figure 1-4(c) illustrates enantiostyly.

In several species of tropical ginger (*Alpina*) a mechanism called flexistyly has been reported that combines dichogamy and herkogamy (Li et al. 2001). Populations are dimorphic and flowers last a single day: Cataflexystyled flowers open with a single unreceptive stigma held above the dehiscent anthers; Hyperflexystyled flowers open with a receptive stigma curved downward below the indehiscent anthers. During the course of the day, the stigmas of both morphs move in strict synchronization across the population: The stigma of a cataflexystyled flower moves down below the anthers which cease dehiscing; The stigma of a hyperflexystyled flower elongates and straightens until it is held above the anthers which then begin dehiscing. Thus pollination of hyperflexystyled flowers with pollen from cataflexystyled flowers occurs early in the day and the reverse occurs later in the day. Assuming that pollen is short-lived the timing and strict synchronization should ensure exclusively intermorph pollen transfer. The genetics underlying flexistyly are not currently understood, but like dimorphic enantiostyly the mechanism seems to be exclusively responsible for preventing self-pollination since no physiological incompatibility system is present (Li et al. 2001). Flexistyly is an example of heterodichogamy in which protandrous and protogynous morphs coexist (Barrett 2002*a*).

1.3 APOMIXIS

The reproductive processes mentioned so far in this chapter have all concerned the fusion of gametes. The fusion of haploid nuclei to form a zygote is generally considered the defining feature of sexual reproduction. Thus although autogamy and geitonogamy involve only one individual they are regarded as sexual in the same respect as outcrossing (xenogamy.) Richards (1986) states that apomixis includes both vegetative propagation and the production of fertile seeds in the absence of sexual reproduction (although

this is by no means the only or even the accepted usage of apomixis.) Vegetative propagation includes, for example, the production of bulbs or modified horizontal stems the lie above or below ground (stolons, rhizomes.) It is becoming increasingly conventional to classify vegetative propagation as growth, and exclude it from discussions of reproduction, primarily because most flowering plant species engage in some form of vegetative propagation irrespective of their mode of seed production (Mogie 1992). Vegetative propagation will not play a role in any of the example models considered in this report, although points at which it can be incorporated will be highlighted in model derivations in chapter 3 and chapter 5. This section will discuss non-vegetative apomixis and throughout this report 'apomict' will refer to an individual producing fertile seeds non-sexually.

The evolution and maintenance of sexual reproduction has received enormous attention from evolutionary biologists from the early part of the twentieth century onward (Fisher 1930, Müller 1932, Williams 1975, Maynard-Smith 1978, Stearns 1987, Michod & Levin 1988, Hamilton et al. 1990, Hurst & Peck 1996, Kondrashov & Kondrashov 2001). Any discussion of the relative merits of sexual and asexual reproduction faces two main novelties in flowering plants. The first is the immediacy of the problem. Apomixis is seen is roughly 15% of flowering plant families and is especially common in the Compositae, Gramineae and Rosaceae (Richards 1986, p426). There are many mechanisms for producing apomictic seed which are likely to have arisen independently several times over. Moreover, apomixis may be facultative and numerous species produce both sexual and apomictic seed. So whereas in most higher animal species asexual reproduction was abandoned in the distant evolutionary past, in flowering plants sexual and apomictic reproduction are repeatedly interacting. Secondly flowering plants are generally hermaphrodite. So crucially every individual in a population produces eggs and there is no two-fold cost of sex (Maynard-Smith 1978, pp 1-10) arising from the need for sexuals to produce non-egg-producing males. A further consequence of hermaphroditism is that apomictic seed production need not entirely disable male-function. Apomicts may produce viable pollen and may therefore be able to sire apomictic offspring on sexual relatives (Mogie 1992, pp 117-137). By contrast in asexual animal species it is rare for retained male function to have any capacity for spreading asexuality (Lynch 1984). Charlesworth (1980) points out that the ability of apomicts to sire offspring on sexuals partially reinstates the cost of sex. Depending on the genetic control of apomixis and on apomictic pollen quality the cost of sex is up to 1.5-fold. As a result of the first novelty contemporaneous sexual and apomictic

conspecifics are found in natural populations, for example the dandelion species *Taraxacum officinale*; as a result of the second novelty the interaction between reproductive modes is significantly more complex than straight-forward competition for resources.

Mechanisms of Apomixis

Apomictic seed production is invariably comprised of elements of sexual seed production together with some legerdemain to avoid male gamete input into the embryo. Methods of apomixis can be grouped in many mechanistic ways, for example according to whether the embryo develops from an egg cell or otherwise. However, probably the most significant practical dichotomy is whether or not the seed produced is necessarily genetically identical to the maternal sporophyte producing it.

Clonal methods, in which the seed is genetically identical to the maternal sporophyte, generally avoid meiosis altogether. The embryo in the seed develops either from the archesporium or from other cells of the nucellus. In the former case, mitotic diplospory, an unreduced embryo-sac is produced through mitoses, as seen in the daisy *Antennaria alpina.* In the latter somatic cells of the nucellus may divide mitotically to produce an unreduced embryo-sac, this is apospory and is seen in the grasses *Poa pratensis* and *Poa alpina* (Richards 1986, p405). Alternatively somatic cells may mitotically differentiate an embryo directly, this is adventitious embryony and is seen in species of the *Citrus* family (Richards 1986, p402).

In non-clonal methods of apomixis, in which the seed produced need not be genetically identical to the maternal sporophyte, some form of meiosis of the embryo-sac mother cell is initiated but does not always succeed. In meiotic diplospory, as seen in the dandelion *Taraxacum officinale*, an unreduced embryo-sac is produced through non-disjunctional meiosis; that is the meiosis fails. In *Allium*-type parthenogenesis, seen for example in *Allium nutans*(Mogie 1992, p23), an endomitotic doubling of chromosomes precedes meiosis so that the embryo-sac developing from a member of the meiotic tetrad contains an egg cell with the sporophyte chromosome number. In Replicative haploid parthenogenesis, meiosis proceeds as normal and a haploid embryo-sac is produced. The egg cell of the embryo-sac divides spontaneously but the nuclei of the first division then fuse to produce a diploid cell which develops into the embryo. Replicative haploid parthenogenesis is seen in some species of the *Brassica* family (Eenink, 1974, cited in Mogie (1992, p23).) Note that in non-clonal types of apomixis material from

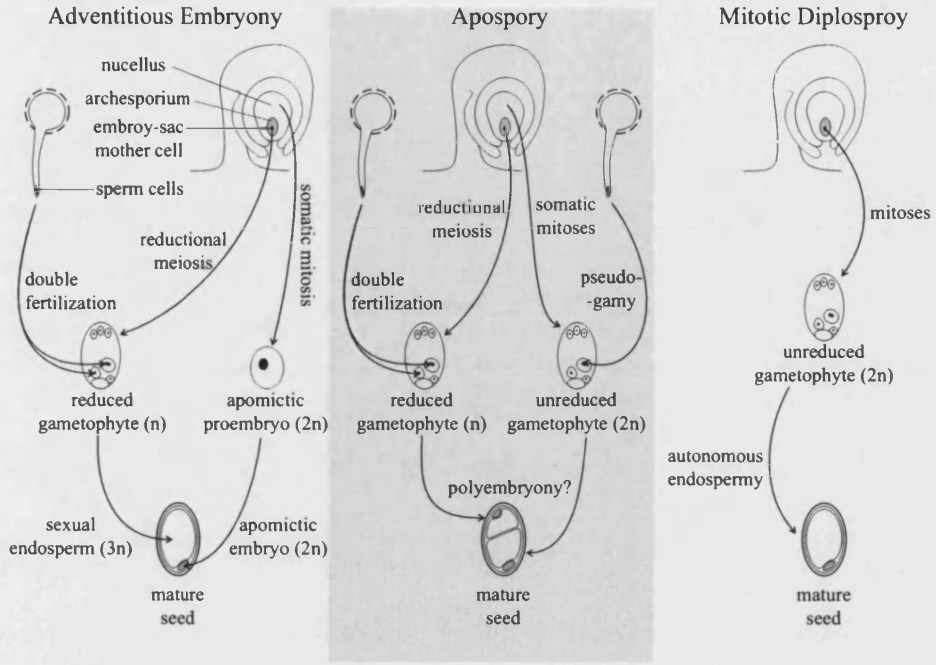

Figure 1-5: Methods of clonal apomictic seed production in flowering plants. Genotype of maternal sporophyte and apomictic offspring identical.

the maternal genome may be discarded. This is always the case in Replicative haploid parthenogenesis. It may be the case in *Allium*-type parthenogenesis if non-sister chromosomes pair during meiosis (Mogie 1992, p27). It may be the case in meiotic diplospory depending on how far meiosis proceeds and whether recombination occurs (Richards 1986, p405). In diploids, replicative haploid parthenogenesis produces offspring homozygous at every locus. So for obligate replicative haploid parthenogens reproduction is effectively clonal since all descendants will bear the same homozygous genome.

An autonomously developing embryo cannot form a viable mature seed without an endosperm. All the above mentioned methods of apomixis, excepting adventitious embryony, are parthenogenetic, that is they involve the female gametophyte as an intermediate stage (also known as gametophytic apomixis.) In this case a primary endosperm nucleus is available alongside the embryo in the embryo-sac. The primary endosperm nucleus may develop autonomously or may require fertilization by sperm cells from pollen.

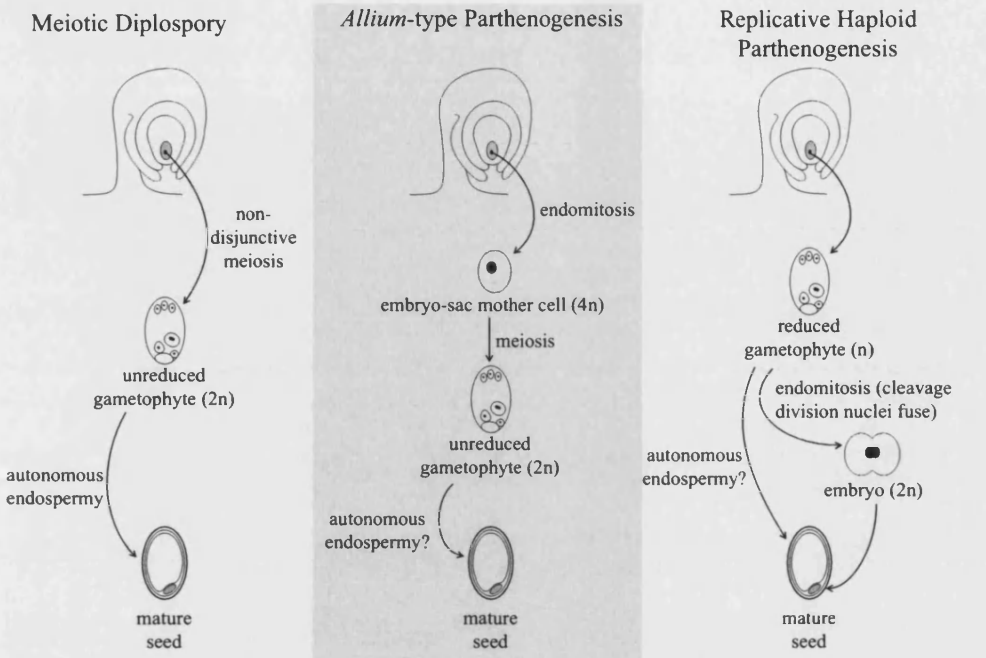

Figure 1-6: Methods of non-clonal apomictic seed production in flowering plants. Genotype of maternal sporophyte and apomictic offspring may differ.

Diplospory is generally associated with autonomous endospermy, so that mature seeds are produced entirely in the absence of male gametes. The endosperm usually has twice the ploidy level of the embryo, but clearly the 2m:1p ratio crucial for normal endosperm in sexual seeds is not met. Although *Allium*-type parthenogenesis proceeds somewhat similarly to diplospory, it is not clear whether endosperm always develop autonomously. Kim et al. (1999) found autonomous endospermy to be present in some apomictic *Allium* species and absent in others.

Apospory is strongly associated with non-autonomous endosperm development requiring fertilization. This requirement of male input in a non-procreative role is termed pseudogamy. The genetic composition of the endosperm will depend on the ploidy of the pollen received. In a diploid species with normal male meiosis, pollen will be reduced so the endosperm will be 4m:1p. However, in apomictic species, male-meiosis is rarely completely normal (Nogler 1984) and non-reduced pollen may arise yielding a 4m:2p endosperm with the optimal 2:1 balance. Endosperm may also achieve optimal balance when pollinated by reduced pollen if both of the sperm-cells fuse with

the primary endosperm nucleus. Such double fertilization occurs in 69% of self-crosses in the tetraploid buttercup *Ranunculus auricomus* (Rutishauser (1954) cited in Nogler (1984)). Richards (1986) observes that because an aposporously developed embryo-sac does not displace the archesporium, a normal haploid embryo-sac is often also present in the ovule. This may also be fertilized leading in some cases to polyembryony, multiple embryos both sexual and apomictic within a seed. Aposporous apomixis is usually therefore found to be facultative, except in circumstances when normal meiosis is disrupted by odd ploidy or otherwise.

Adventitious embryony also does not affect the archesporium and for this reason also tends to occur alongside normal sexual reproduction. Because of the absence of the gametophyte stage, however, the so-called, apomictic proembryo has no adjacent primary endosperm nucleus. It is therefore compelled to invade the embryo-sac, following successful fertilization, and commandeer the endosperm of the sexual embryo (Richards 1986, p406). Therefore, like apospory, Adventitious embryony is also pseudogamous. Unlike apospory, however, adventitious embryony cannot proceed without sexual reproduction and so must be facultative. Polyembryony is rare, because of the presence of a single endosperm in the ovule, but occasionally sexual and apomictic embryos share the endosperm.

The clonal methods of apomictic seed production outlined above are illustrated in Figure 1-5, and the non-clonal methods are illustrated in Figure1-6.

Advantages and Disadvantages of Apomixis

With a maximum 1.5-fold disadvantage of sex (Charlesworth 1980), sexual and apomictic modes of reproduction are theoretically more evenly matched for fitness. Many factors contribute to the success of one or the other, but most proposed advantages carry caveats and some have not been empirically substantiated. The sophisticated multidimensional character of the choice to produce sexual or apomictic seed is presumably the reason that apomictic lineages have established successfully in some flowering plant families and are not found in others. It is also the reason why numerous species prefer to maintain facultative apomixis. For these species it would seem that the variable selective pressures of their evolutionary history have not been able to distinguish a clear-cut winner. There follows a, by no means exhaustive, review of some of the principle factors contributing to the advantage of sexual or apomictic seed production.

Variation

Sexual fusion of gametes introduces a huge amount of variation into sexually produced offspring, which is multiplied by the meiotic processes of segregation and recombination. The *Tangled Bank* hypothesis (Bell 1982) suggests that in a spatially and temporally heterogenous environment this variation maximizes the fitness and abundance of DNA by permitting it to fill as many niches as possible (Dawkins 1976). From the perspective of a female, producing variable offspring can increase fitness by reducing inter-sibling competition. This effect is, however, dependent on the level of environmental heterogeneity, mutation rates and fecundity being sufficiently high (Felsenstein 1988). Richards (1986, p18) observes that if all possible niches are already filled by differently adapted asexually reproducing individuals, competing sexuals will fare no better. So that temporal variation and the regular creation and destruction of niches is crucial to a persistent advantage for sexuals.

The postulate of very rapid temporal variation in the biotic environment characterizes the application of the *Red Queen* hypothesis (van Valen 1973) to the advantage of sex. The Red Queen hypothesis suggests that continual cycling and recycling of phenotypic variation may be necessary to maintain constant fitness. Hamilton et al. (1990) demonstrated that variation in intrinsic immunities to different parasites among offspring can provide an advantage in evading infections prevalent in the previous generation. The typically rapid evolution of parasites compared with their hosts means that there is no single optimum genotype, instead fitness is maximized by the continual intermixing of an array of good resistance genes. Hamilton et al. (1990) point out that this advantage to sex remains in circumstances of low fecundity and mutation rates which can stymie the Tangled Bank advantage.

When biotic and abiotic environmental heterogeneity is low, apomixis may be favoured for it's ability to directly replicate an existing successful genotype. In these circumstance apomixis will avoid the *cost of meiosis* (Williams 1975, p8-9), the obligatory production of offspring with lower-than-maternal fitness. This cost is, however, most acute when fecundity is low, which is rarely true of flowering plants. A corollary to this point is that apomixis avoids the segregational load inherent in the maintenance of heterozygosity in a sexual population. Heterozygosity can become fixed in an asexual population.

Offspring variation is not exclusive to sexual reproduction. The non-clonal methods of apomictic seed production described above can all produce offspring that differ from

the maternal genotype and each other. This may reduce sibling competition marginally, although variation is limited to recombinations of the maternal genotype, so is scarcely likely to meet the requirements of the Red Queen hypothesis. Moreover, non-clonal methods of apomixis tend to reduce heterozygosity over time (Bell 1982, Mogie 1992), limiting the amount of variation available through recombination and segregation.

Some of the methods of apomixis outlined above are compatible with a mixed strategy of sexual and asexual seed production. Occasional sexual reproduction avails a facultative apomictic population of some variation and the opportunity to combine advantageous genes. Mixed strategies in flowering plants, such as those commonly observed in aposporous *Poa*, *Potentilla* and *Ranunculus* species, are particularly intriguing in the light of theoretical results which suggest that only a few offspring need be produced sexually in order to reap most of the benefits (Green & Noakes 1995, Hurst & Peck 1996). This is contentious, however, and it is also possible that the rare sexually produced offspring of facultative asexuals may be poorly adapted when compared with their apomictically produced siblings (Peck & Waxman 2000).

A mixed strategy can also be ascribed to obligate apomicts that retain male-function and coexist with sexual conspecifics, since they have the opportunity sire variable sexual offspring (Mogie 1992, pp 117-137).

Beneficial and Deleterious Mutations

In an obligate clonally apomictic lineage the entire genome can be considered as a single linkage group. This has consequences for both beneficial and deleterious mutations. Beneficial mutations may become 'stranded' on an otherwise low fitness genome and consequently be doomed to extinction as more rounded genomes become fixed (Fisher 1930). Which is to say that beneficial mutations cannot be recombined and evolution is slowed and the lineage is ill-equipped to deal with environmental change. Meanwhile deleterious, but non-lethal, mutations that arise in similar lineages accrue, since they cannot be eliminated from offspring. The aggregation of deleterious mutations and consequent deterioration of asexual lineages is known as *Müller's Ratchet* (Müller 1932, Müller 1964).

Kondrashov (1988) has suggested that if fitness has a particular functional response to the accumulation of weakly deleterious mutations, specifically a decreasing and accelerating response (synergistic epistasis), then sexual reproduction is more efficient at removing these mutations from the gene pool. The *deterministic mutation hypothesis*

argues that recombination frequently brings these mutations into the same genome, where their combined effect may be lethal. By contrast in an asexual population the slower accumulation of these mutations in all lineages will depress total population fitness. In addition to the specified functional form Kondrashov's (1988) theory requires an extremely high mutation rate to give sexual reproduction a significant advantage.

The retention of male-function in apomicts provides an escape route for 'stranded' beneficial mutations. Where apomicts coexist with sexuals, the ability of the sexual population to rapidly combine beneficial mutations can be exploited by apomicts who sire apomictic offspring on the fittest sexuals. Mogie (1992, p119) observes that when apomixis arises in a sexual population it need not be confined to the first genome it arises in, but can move from genome to genome. Moreover, if apomixis gradually replaces sexual reproduction, the last surviving sexuals would tend to be the fittest. This all but ensures that, when apomixis fixes, the best genes available from the sexual gene pool are retained.

The non-clonal methods of apomixis provide an escape from Müller's Ratchet. If a novel deleterious mutation arises in an individual, some of that individual's offspring will avoid that mutation. This is most clear for replicative haploid parthenogenesis, where only 50% of offspring will contain the chromosome on which the mutation arose.

Reproductive Assurance and Colonization

Apomixis can convey reproductive assurance, a single individual can reproduce via seed production in the absence of pollination. The fate of such apomicts would not be linked to that of pollinator species. Also single individuals would be able to found or perpetuate populations, suggesting that apomicts may be better colonizers than sexual relatives (Stebbins 1950). Note that there are several reasons why retention of seed production may be preferable to vegetative propagation. Through seed production a 'clean egg' is obtained, which, by virtue of having developed from a single cell, may have a reduced viral load. The dispersal range of seeds is often further than that of vegetative propagation, and distance is covered in a more energetically efficient way since it does not require connected tissue growth between parent and offspring.

However, as discussed above, apospory and adventitious embryony are typically pseudogamous and do require pollination to produce seeds. Thus reproductive assurance and superior colonizing ability may not be available to these apomicts. Or, as in the case of some pseudogamous blackberry species (*Rubus*), self-fertilization may have

evolved to conserve pollen and avoid the need for insect visits (Nybom 1985). Noirot et al. (1997) suggest that pseudogamous species may adopt an evolutionarily stable strategy of conserving a large proportion of pollen, since in exclusively pseudogamous populations exporting pollen does not increase fitness.

The advantages of reproductive assurance and superior colonization ability are also available to sexuals who are self-compatible. Stebbins (1950) observes that few if any apomictic species appear to have evolved from self-compatible cosexual ancestors. This suggests that self-compatibility and apomixis may provide different solutions to the problem of poor pollen availability. If this is the case then self-compatibility in extant pseudogams may have resulted from selective pressures that became active when apomixis arose, or may be a consequence of polyploidy (as discussed in section 1.2) that is also strongly implicated in the emergence of apomixis.

Polyploidy and Hybridization

Polyploidy is strongly associated with gametophytic apomixis (Asker & Jerling 1992, pp 109-120). This relationship has long been conjectured to be causative: Hybridization of distinct species can produce a polyploid genome which is sexually sterile because meiosis is disrupted, such a species could only persist if capable of apomixis (Darlington 1958, pp 157-168). But polyploidy is widespread in flowering plants species where apomixis is absent. Moreover, sexual hybrids and polyploids have been generated experimentally in species of *Taraxacum* where naturally occurring polyploids are apomictic (Stebbins 1950, pp 380-417).

Richards (1986, pp 396-450) points out that being hybrid and polyploidy should make apomicts highly heterozygous and very vigourous. When polyploid apomicts dominate sexual relatives it is therefore challenging to disentangle the advantages resulting from apomixis per se, from those resulting from polyploidy (Bierzychudek 1987, Mogie et al. submitted). Despite their vigour, hybrids will most likely not be adapted to a very specific niche (Richards 1986, pp 396-450). This may be disadvantageous confining apomicts to transitory or unstable habitats, or newly opened up territory from which they are soon displaced. It may prove advantageous, however, if apomicts undergo selection to acquire *general-purpose genotypes* (Lynch 1984) in which case they may be able to endure a wider range or environmental conditions. When sexuals and apomicts are contemporaneous, it is often seen that apomicts occupy a wider range encompassing habitats of poorer quality (Bierzychudek 1987).

Apomixis and Polymorphism

Pseudogamous Gynodioecy

Natural populations of pseudogamous apomicts tend to retain male function. But male function does not add directly to reproductive success, since no male genetic material finds its way into the embryo. A pseudogamous population in which pollen is abundant might, therefore, be vulnerable to invasion from male-sterile mutants which avoid the cost of producing male gametes and reinvest this saving in enhancing the number or viability of their seeds.

The fate of such a male-sterility mutation might well depend upon whether or not the pseudogamous population was capable of self-fertilization. In self-compatible pseudogamous apomicts male function does contribute indirectly to fitness by supplying pollen to fertilize endosperm. It is not know in general how widespread self-compatibility is amongst pseudogamous species, there is a dearth of field data. However, two conjectures may be drawn from the known interactions of the traits of apomixis, polyploidy and self-incompatibility. Apospory is a pseudogamous form of gametophytic apomixis and consequently shows a strong association with polyploidy. Polyploidy can disrupt self-incompatibility mechanisms and so aposporous pseudogams are likely to be self-compatible. This is certainly the case for aposporous species within the *Rubus* genus (Nybom 1985). By contrast adventitious embryony is an example of sporophytic apomixis with which polyploidy is much less often associated. Consequently a self-incompatible species in which adventitious embryony arises is likely to retain the incompatibility mechanism at least initially. The author is not aware of any direct evidence of this this, however, self-incompatibility is common in *Citrus* species, a genera in which apomixis usually arises by adventitious embryony.

Self-compatible species which derive some fitness from a retained male-function might be expected to be less vulnerable to the invasion of male sterility mutations. This is, however, confounded by the only well known example of male-sterility in pseudogamous apomicts, found in aposporous *Potentilla tabernaemontani* (Smith 1963).

Maynard-Smith (1978) offers two explanations for the retention of pollen production in self-incompatible pseudogamous apomicts. The first is that pollen production is still valuable if apomixis is facultative and occasional sexuals are produced. The second is that, if dispersal is local, pseudogams will be growing near to relatives who are clonally

identical and pollen production is therefore meritorious since it increases the fitness of neighbouring clones. But this argument is sensitive to the self-incompatibility mechanism in operation: Physiological mechanisms of incompatibility would still prohibit this sort of kin fertilization; Herkogamy might be overcome, but this is not so in the case of reciprocal heteromorphy because clones will be the same morph; Dichogamy would permit between clone pollination, so long as the timing within season of anther and pistil dehiscence is not strictly genetically controlled.

The ecological consequences of the interaction of male-sterility and self-incompatibility with pseudogamy will be examined in models in chapters 3 to 6.

Geographic Parthenogenesis

Often apomictic species and the sexual species that probably gave rise to them occupy overlapping habitats (they are sympatric.) It is often observed that when this is the case, the sexual species is confined to a territory in the centre of the apomictic range. This is described as *geographic parthenogenesis* and genera for which the trend is well-documented include the American herbs and shrubs *Parthenium* and *Townsendia* (Bierzychudek 1987) and European herbs *Taraxacum* and *Hiercium* (Stebbins 1950). The reverse relationship is not unknown, however: sexual species of *Antennaria* are widespread in Europe, while related apomictic species are confined to the mountain ranges of Scandinavia (Asker & Jerling 1992, pp 221-239).

As was noted above the coexistence of sexual and apomictic conspecifics may be complicated by the ability of apomicts that retain a male function to sire progeny on sexuals. The ecological consequences of this complication will be modelled in chapters 3 to 6. Explanations of geographic parthenogenesis usually revolve around the assumption that apomicts are differentially adapted to more extreme environments. But Mogie & Ford (1988) point out that this is often insufficient to explain observed patterns and that in particular sexual species of *Taraxacum* appear 'trapped' in southern locations in Europe by apomictic species which dominate more northern regions. It is not the case that the sexual species cannot tolerate low temperatures, since many of them survive at high altitudes. Accordingly the models in this report will assume a homogenous environment and no specific competitive advantage of either reproductive mode. However, having been sexually produced will be assumed to convey some intrinsic level of enhanced viability to seeds. The advantage being drawn from some combination of those outlined above. Initial modelling will be non-spatial (chapter

3), but subsequent spatial models (chapters 4, 5 and 6) will focus particularly on the interaction between sexuals and apomicts at the boundaries of regions dominated by one or other reproductive mode.

1.4 EVOLUTIONARY HISTORY

The rapid and prolific evolution of flowering plants makes their evolutionary history deeply intricate and complex. This section serves to highlight some of the trends and innovations that are of particular current theoretical interest.

Female Gametophyte

Current botanical opinion holds that the earliest angiosperms had four rather than eight nucleate embryo sacs, the result of one fewer developmental mitoses (Friedman & Williams 2004). The ancestral four nucleate embryo sac comprised: an embryo, one polar nuclei, two synergids and no antipodal cells. Double fertilization, which is believed to predate the angiosperm division, would thus result in a diploid endosperm with equal male and female contributions (Williams & Friedman 2002). When double fertilization is reported outside the angiosperms, in gnetales and conifers for example, two viable embryos are formed (Friedman & Floyd 2001). The implication is that in early angiosperms the second embryo surrendered its opportunity to develop into a reproductive individual and instead became a nutritive support tissue for the embryo. Kin selection theory (Hamilton 1964) deems this adaptive if endosperm support more than doubles the survival chances of the embryo, since embryo and diploid endosperm have relatedness 1. Chapter 2 will discuss how the triploid endosperm may have evolved as a strategic female adaptation in the parental conflict over seed provisioning. A selective pressure to increase the female contribution to the endosperm may have motivated an additional mitosis in the early angiosperm gametophyte giving rise to the modern eight nucleate embryo sac.

Evolutionary Pathways to Dioecy

The vast majority (72%) of flowering plants bear hermaphrodite flowers and there is strong evidence that this is the primitive state (Richards 1986, pp 297-356). The remaining species have breeding systems in which one or all of the flowers on individual

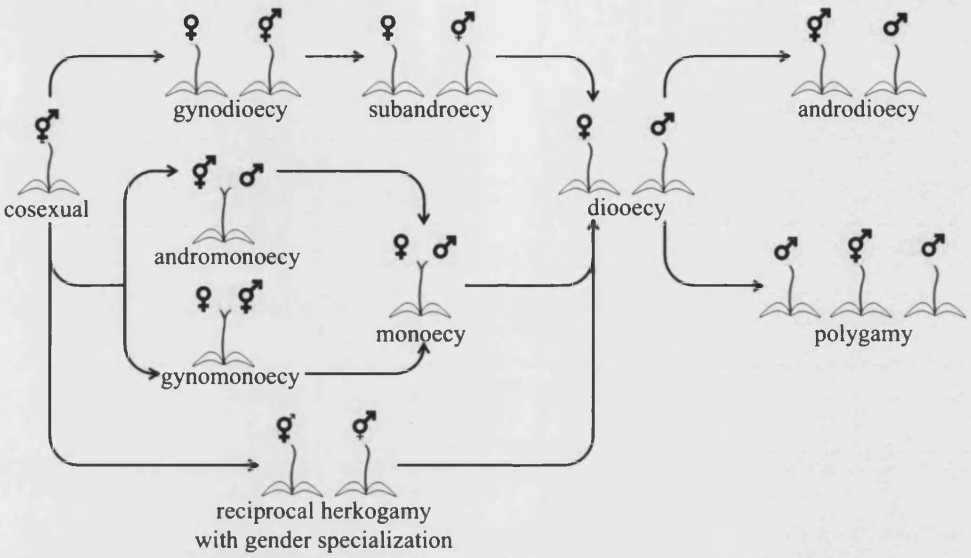

Figure 1-7: Evolutionary pathways to dioecy and beyond. Symbols indicate functional gender of flowers, reduced appurtenances on symbols indicate reduced allocation to one or other gender. Adapted and extended from Barrett (2002, Box 1)

plants do not bear flowers with both functional stamens and gynoecia (dicliny). Dioecy in which some individuals bear female flowers and others bear male flowers account for only about 4% of flowering plant species. The remaining diclinous species employ breeding systems with multifarious combinations of hermaphrodite, female and male flowers on the same or distinct individuals.

There are two widely accepted evolutionary pathways to dioecy that incorporate most diclinous breeding systems and a third for which there is some recent evidence (Barrett 2002*a*). In the first pathway male-sterile mutants invade cosexual populations resulting a mixed population of hermaphrodites and females (gynodioecy). If hermaphrodites in a gynodioecious population are less fit than females, they may be selected to decrease female function resulting in subandroecy where most hermaphrodite investment is in male function. If female function in hermaphrodites is lost altogether then dioecy results. In the second pathway cosexual species evolve to express only a single gender in each flower (monoecy). A monoecious species is still hermaphrodite but, perhaps to limit self-pollination, has isolated reproductive organs in separate flowers. This process may pass through stages in which hermaphrodite and male flowers (andromonoecy) or hermaphrodite and female flowers (gynomonoecy) are both present.

If an even balance of investment into male and female flowers is suboptimum, disruptive selection may drive the evolution of separate genders resulting in dioecy. A possible third route to dioecy is suggested by the morphology of *Chassalia corallioides*, it is distylous but short stamens and short styles are inactive so it is functionally dioecious (Pailler et al. 1998). This suggests that distyly in cosexuals may evolve directly into dioecy through enhanced investment in male or female function in reciprocal morphs. The two main diclinous breeding systems not accommodated in these pathways are both rare: Androdioecy, in which hermaphrodites and males coexist; Polygamy in which males, females and hermaphrodites coexist. These conditions have been assumed to derive from dioecy (Barrett 2002*a*).

Gynodioecy

The first step of the gynodioecy pathway to dioecy has received considerable theoretical attention for two reasons. The first is the apparent ubiquity of simple male-sterility causing mutations in important crop species. Mutations may arise in chromosomal DNA causing so-called nuclear male-sterility or in non-chromosomal DNA borne in the cytoplasm causing so-called cytoplasmic male-sterility. Cytoplasmic male-sterility (CMS) alone has been reported in over 140 species of flowering plant (Laser & Lersten 1972) and is exploited in many commercial crops such as maize, rice, rye, sunflower and wheat to avoid the need for hand-emasculation in creating hybrid cultivars (Schnable & Wise 1998). The second reason is the problem of understanding why male-sterility mutations establish in the first place. Charnov (1982, pp 10-12) observes that a novel female mutant arising in a hermaphrodite population would require a two-fold competitive advantage in order to compensate for the loss of offspring through pollen. That is unless the mutation is cytoplasmic, in which case only a small advantage to female function is required to initiate a successful invasion. This is because cytoplasmic DNA is not inherited through male function and hence has nothing to lose if pollen production is stopped. In most cases the advantage to female function will be less than two-fold, and the fitness of cytoplasmically sterilized individuals will therefore be lower than that of hermaphrodites. More so because male-male competition will be decreased as females spread.

As with pseudogamy the spread and ultimate fate of male-sterility mutations is likely to be significantly affected by self-incompatibility. Unlike pseudogamy, however, self-incompatibility of one type or another is likely to be the rule in the sexual her-

maphrodite populations in which male-sterility mutations arise. The mixed strategies discussed in section 1.2 are significant in this regard, particularly if females come to dominate the population and pollen becomes scarce. Hermaphrodites capable of some self-fertilization will experience the pollen shortage less acutely.

1.5 CONCLUDING REMARKS

It was the aim of this chapter to present some of the physiological innovation and diversity of breeding systems that are found in flowering plants. It is evident that the ecological meaning and evolutionary origin of some of these innovations and breeding systems is incompletely understood. In flowering plants, producing and distributing small motile gametes is a fundamental necessity of sexual reproduction. The consequences of this necessity reverberates through the phylogenetic tree of flowering plants. Most sexual species try to avoid transferring pollen to their own female sexual organs whilst maximizing the pollen export to and import from other individuals. It is of great significance that asexual species inherit pollen production from their sexual ancestors. Through their male-function asexuals can interact with sexuals, promoting the spread of asexuality and alleviating many of the classical costs of asexual reproduction.

Chapter 2 of this report will contribute to the effort to understand an elementary and near universal property of pollen physiology: The presence of two sperm cells in a pollen grain. This discussion will touch upon why double fertilization exists at all and will go further to examine adaptive explanations for the triploid constitution of the endosperm.

It is clear that the understanding of flowering plant breeding systems could benefit from a general modelling framework for examining the ecology of populations in which several reproductive modes occur. It is crucial that pollination often takes place between individuals with different reproductive modes. Inter-mode pollination may be essential for survival, as in is the case with reciprocal heteromorphy and for females in gynodioecious populations; alternatively it may be a complexity in the interaction between independently viable populations, as is the case for contemporaneous sexual and apomictic conspecifics. In chapters 3 and 5 generalized modelling frameworks will be developed for treating the ecology of species in which there is polymorphism for reproductive mode and inter-pollination between morphs. The approach of chapter 3 will be population-based and emerges as an extension of existing competition models. Chapter 4 extend the models of chapter 3 to consider spatially distributed populations.

In chapter 5 a second modelling framework will be developed focussing on the interactions between discrete individuals. Chapter 6 will examine a technique for extracting the significant behaviour of the complicated models the that framework of chapter 5 calls for. In each chapter the modelling technique being presented will be applied to specific examples of reproductive polymorphisms in which the mechanism promoting coexistence is currently incompletely understood. The first of these examples will concern gynodioecy in both sexual and asexual populations. The second example will be the coexistence of closely related sexual and apomictic conspecifics.

CHAPTER 2

Endosperm Evolution

The flowering plant endosperm mediates the supply of maternal resources for embryogenesis. An endosperm formed in sexual reproduction between diploid parents is typically triploid with a 2:1 ratio of maternal to paternal genetic material. Variation from this ratio affects endosperm size, indicating parent of origin specific expression of genes involved in endosperm growth and development. The presence of paternally or maternally imprinted genes can be explained by parental conflict over the transfer of nutrients from maternal to offspring tissue. Genomic imprinting can, for example, provide the male parent of an embryo in a mixed-paternity seed pod with an opportunity for expressing its preference for a disproportionate allocation of resources to its embryo. It has been argued that a diploid 1m:1p endosperm was ancestral and the 2m:1p endosperm evolved following parental conflict, to improve maternal control over seed provisioning. In this chapter a population genetic model is presented which instead places the origin of triploidy early in the parental conflict over resource allocation. It is found that there is an advantage to having a triploid endosperm as the parental conflict continues. This advantage can help to explain why the 2m:1p endosperm prevails among flowering plants. This material was first published in Stewart-Cox et al. (2004*a*).

2.1 INTRODUCTION

The triple fusion which results in the 2m:1p primary endosperm nucleus was first reported in 1898 and was subsequently found in a large proportion of flowering plants (Vijayaraghavan & Prabhakar 1984). Because the 2m:1p endosperm is widespread and disturbance of the genetic ratio upsets development, it has long been believed that an adaptive explanation should be sought for its unusual genetic constitution. Stebbins (1976) argued that all innovations that distinguish the reproductive process in flowering plants from other seed plants are associated with shortening of the time

taken to mature seeds. In this context triploidy is seen as an adaptation to encourage the rapid growth of the endosperm via heterozygote and polyploid vigour and the presence of a greater number of templates for protein synthesis. However there is no reason why the 2m:1p ratio should be crucial to accruing these advantages (Westoby & Rice 1982, Queller 1983, Haig & Westoby 1989).

What was missing from increased vigour explanations, was the careful consideration of inclusive fitness which reveals the distinct and sometimes antagonistic interests of each genetically distinct tissue involved in seed provisioning (Charnov 1979, Queller 1983). Whenever the amount of parental investment in offspring is variable we should expect conflict between all genetically distinct tissues capable of influencing the level of investment. This expectation is an extension of parent-offspring conflict ideas (Trivers 1974). In general (Queller 1989) disproportionate provisioning of the embryo inside a developing seed should be favoured by the associated female gametophyte, the endosperm, and the embryo itself. If there is at least some chance of mixed paternity amongst seeds raised by the maternal plant, the male sporophyte should be added to this list. If reallocation of resources is inefficient, or the fitness of a seed depends non-linearly on its provisioning, the female parent will favour uniform provisioning of all its offspring.

In the ancestors of flowering plants the female gametophyte acted as the nurse tissue for the embryo. Explanations of endosperm evolution must address why the endosperm arose and displaced the gametophyte as nurse tissue and why the triploid 2m:1p genetic configuration was favoured. Williams & Friedman (2002) have shown that diploid endosperm are common among early flowering plant lineages. Queller (1989) produced an inclusive fitness argument for how such a diploid endosperm may have succeeded the gametophyte. Suppose initially both tissues shared the nursing role. Being genetically identical to the embryo the new diploid nurse tissue would be selected to increase acquisition of resources. The gametophyte's best interests would then be served by reducing its acquisitiveness. Eventually the diploid endosperm would replace the gametophyte as the primary acquisitive tissue for the embryo. The subsequent doubling of the maternal contribution to the endosperm can be seen as a maternal adaptation to lower the acquisitiveness of the endosperm (Queller 1984). However it is not clear why the triploid endosperm persists until lower acquisitiveness can be selected (Queller 1989). Two mechanisms have been proposed to explain the doubling of the maternal contribution, one driven by parent-offspring conflict, the other by parental conflict.

Härdling (2001) present a parent-offspring conflict argument. They suppose that endosperm amount (level of resource acquisition) is determined by a single allele, heterozygotes for this allele are assumed fittest so an intermediately provisioned seed is most viable. They suppose there is no dosage effect on doubling the maternal contribution to the endosperm. The allele for endosperm triploidy therefore has no effect on the fitness of seeds, but it is assumed to have an effect on the number of seeds set. Triploidy increases the number of low-provisioned homozygous seeds, but lowers the number of high-provisioned homozygous seeds. They argue that the former increases maternal fitness by more than the latter decreases it and hence triploidy is selectively advantageous. This argument has somewhat awkward assumptions. Optimum viability for intermediately provisioned seeds implies an unusual relationship between provisioning and fitness. The usual relationship is monotonic increasing with diminishing returns (Smith & Fretwell 1974, Parker & Macnair 1978). Härdling's (2001) assumptions are incompatible with Queller's (1989) argument for the diploid endosperm displacing the gametophyte, since increased aggression in the endosperm would not improve fitness.

Haig & Westoby (1989) present a parental conflict argument that makes use of parent-of-origin specific gene expression. If parents can modify the expression of genes responsible for endosperm acquisitiveness, then paternally derived genes would be selected for increased expression. This is particularly true if paternity on the maternal plant is very mixed. In any case, all seeds with increased acquisitiveness fathered by the same individual would have more competitive endosperm. The costs would fall on embryos fathered by other individuals. Antagonistically maternally derived genes for resource acquisition will be selected for decreased expression. The expectation over time then, is that paternally derived genes will have high expression and maternally derived genes will be silenced. The advantage of triploidy consists in the presence of a second set of maternal genes reducing transcription resource availability for paternal genes. This would lower the acquisitiveness of the endosperm. The Haig & Westoby (1989) argument can account for the presence of imprinted genes in the endosperm genome, and can also make successful predictions about the outcomes of some inter-ploidy crosses (Haig & Westoby 1991, Vinkenoog et al. 2002). The assumption about restricted transcription resources is as yet untested but can be circumvented by instead considering parental conflict enacted through the imprinting or silencing of acquisition-promoting or acquisition-inhibiting genes active in the endosperm. Wilkins & Haig (2001) found that a model of this sort would predict that acquisition-promoting genes would be silent when maternally derived, and acquisition-inhibiting genes would

be silent when paternally derived. Although their model was presented in the context of a pair of imprinted genes in mammals, similar results should hold for imprinting in the endosperm.

In this chapter a model is presented which considers the fate of a gene causing endosperm triploidy arising during ongoing parental conflict via imprinting of endosperm resource acquisition genes. The purpose of this modelling is to demonstrate that triploidy has a two-fold advantage. Firstly it is an alternative maternal response to additional paternal imprinting of acquisition inhibiting genes. Secondly once present in a population where triploidy is selectively neutral, the additional active maternal copies of acquisition-inhibiting genes prove an advantage during future invasions of paternally imprinted genes.

2.2 MODELLING

A population genetic model will be constructed which enables consideration of the fate of paternally or maternally imprinted endosperm genes and genes causing endosperm triploidy. This model requires assumptions about imprinting, population dynamics, competition for resources and the effects of polyploidy. These assumptions are discussed in detail here.

Characterization of Imprinting

Genomic imprinting is a mechanism that causes gene expression to vary according to its parental origin. Typically an imprinted gene will be silent when inherited from one parent, but this is not always the case. We do not assume that imprinting can only have a down-regulatory effect on expression. A maternally (paternally) imprinted gene is a gene which when derived from the female (male) parent carries an imprint or expression modifier. The precise mechanism for setting imprints in flowering plants is not known, although certain elements of the mechanism have been established (Adams et al. 2000, Vinkenoog et al. 2002). Barlow (1993) records a simple model for how parent-specific expression can be achieved. According to this model imprints are set during gametogenesis when short sequences in the promoter region of a gene, imprinting boxes, attract an imprinting factor which modifies the gene and alters expression. The modification persists in somatic cells but is erased in early germ cells and reset according to the gender of the new individual. Imprinting boxes and factors must be different for

maternally and paternally imprinted genes.

Our models will assume that new imprinted genes can arise when a gene acquires, through mutation, an imprinting box that attracts extant imprinting factors. A heterozygote for such a mutation will set the imprint in only those gametes that carry the mutation. An alternative hypothesis is that new imprints arise when mutant imprinting factors recognise new sections of promoter sequences. This can lead to a different pattern of inheritance, with all offspring of a heterozygote carrying imprints. This distinction is the same as that recognized by Spencer & Williams (1997) in their modifier locus models of genomic imprinting. This hypothesis was also explored by the authors with similar results to those presented here.

Life History Functions and Basic Model

The models will concern a perennial hermaphrodite sexual ancestor species with no imprinting. Assume random mixis of gametes produces a fixed number of seeds per individual per reproductive season. The provisioning s of these seeds is normalized to 1. Introduce a function $f(s)$ that specifies the viability of a seed provisioned s. This function is usually assumed monotonic increasing and convex in the region of $s = 1$, that is increased provisioning has diminishing returns (Smith & Fretwell 1974, Parker & Macnair 1978). Convexity ensures that maternal fitness is optimized by uniform resource allocation. Suppose $f(0) = 0$ and for convenience that f is differentiable, so f is sigmoidal on $[0, 1]$. The form of f is shown in Figure 2-1. The species is iteroparous so maternal fitness depends on a combination of present offspring viability and the likelihood of survival until future seasons. For this reason conditions must be placed on the relationship of f and parental mortality.

Parental mortality will play a more prominent role here than is usual in population genetic models, because it will be assumed that over-provisioned seeds may have access to maternal reserves not intended for reproduction this season. Since this reserve deficit affects all future offspring equally it is equivalent to increased current mortality in the mother. A function $m(\bar{s})$ is required that specifies the mortality rate per reproductive season of a plant producing seeds with average level of provisioning $\bar{s}$. Suppose m is monotonic increasing, conditions must be imposed on m so that $\bar{s} = 1$ gives an evolutionarily stable balance of offspring viability to parent mortality. To obtain these conditions a model is introduced for a diallelic locus affecting seed provisioning with one

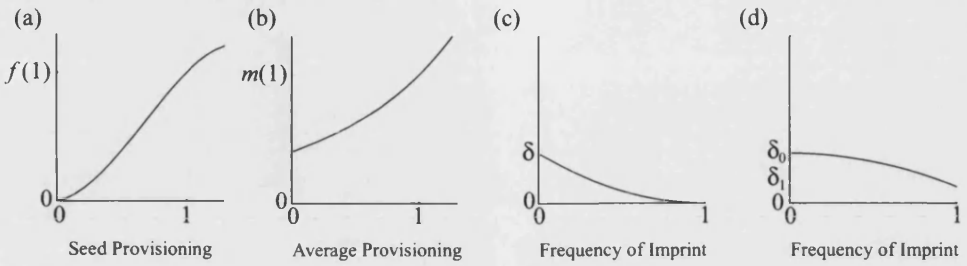

Figure 2-1: Illustrative functions. (a) Seed viability. (b) Parental mortality. (c) Modification to provisioning in this case an increase ($d_s \geq 0$) funded by contemporary siblings. (d) Modification to provisioning funded by maternal reserves. For paternal imprinting d_s and d_m vary with frequency of the imprint in the population. For maternal imprinting d_s and d_m vary with the frequency of the imprint in the maternal genome.

allele dominant over the other. Suppose carriers of the dominant allele produce seeds provisioned s_1 and other individuals produce seeds provisioned s_0. Let u, v and w be the frequency of homozygotes for the dominant allele, heterozygotes and homozygotes for the recessive allele respectively. Assume weak selection for a continuous time model with rates of change for each type are given as follows

$$\begin{aligned}
\frac{du}{dt} &= \frac{M(u,v,w)f(s_1)(u^2+uv+v^2/4)}{F(u,v,w)} - m(s_1)u, \\
\frac{dv}{dt} &= \frac{M(u,v,w)f(s_1)(uv+2uw+v^2/2+vw)}{F(u,v,w)} - m(s_1)v, \\
\frac{dw}{dt} &= \frac{M(u,v,w)f(s_0)(v^2/4+vw+w^2)}{F(u,v,w)} - m(s_0)w,
\end{aligned} \tag{2.2.1}$$

where

$$\begin{aligned}
F(u,v,w) &= f(s_1)(1-(1-u-v/2)^2) + f(s_0)(1-u-v/2)^2, \\
M(u,v,w) &= m(s_1)(u+v) + m(s_0)w.
\end{aligned}$$

Implicit in the formulation of this model is the assumption that any change in mortality of individuals is not substantial enough to destabilize the population. This is consistent with individuals producing a large quantity of offspring only a few of whom will reach maturity. The change in mortality simply accelerates or decelerates

the turnover of individuals. This is why the average mortality M modifies the rate of growth for each type. Since mortality is usually assumed constant and unitary in population genetic models this term rarely appears.

The variables u, v and w are not linearly independent and the model can be written in terms of variables $p = u + v/2$, the frequency of the dominant allele, and v. Hence

$$\begin{aligned} \frac{dp}{dt} &= p\left(\frac{M(p,v)f(s_1)}{F(p)} - m(s_1)\right), \\ \frac{dv}{dt} &= \frac{M(p,v)f(s_1)2p(1-p)}{F(p)} - m(s_1)v, \end{aligned} \tag{2.2.2}$$

where

$$\begin{aligned} F(p) &= f(s_1)(p^2 + 2p(1-p)) + f(s_0)(1-p)^2, \\ M(p,v) &= m(s_1)(p + v/2) + m(s_0)(1 - p - v/2). \end{aligned}$$

Now p and v are independent and the region of interest $\triangle$ in (p, v)-space is the triangle with vertices at $(0,0)$, $(1/2,1)$ and $(1,0)$. The region $\triangle$ is invariant under the flow given above. Clearly $(0,0)$ and $(1,0)$ are equilibria. By linearizing about $(0,0)$ the eigenvalues $-m(s_1)$ and $m(s_0)f(s_1)/f(s_0) - m(s_1)$ are obtained. The former indicates that the v-axis is always a stable manifold, so stability of $(0,0)$ is determined by the sign of the latter eigenvalue. If $s_0 = 1$ the dominant allele cannot invade if $m(s_1)f(1) > m(1)f(s_1)$. The same condition is obtained if instead it is insisted that recessive mutants cannot invade. So for $\bar{s} = 1$ to be evolutionarily stable

$$m'(1) = \frac{f'(1)m(1)}{f(1)} \quad \text{and} \quad m''(1) > \frac{f''(1)m(1)}{f(1)}.$$

It is reasonable to adjust the time scale in the model so that $m(1) = 1$. An appropriate m is shown in figure 2-1.

At this point we have developed a basic model that can describe the population genetics of non-imprinted genes which modify seed provisioning. To incorporate imprinted genes we must consider how imprinting can alter the balance of maternal provisioning of seeds on the mother plant.

Provisioning Functions

Endosperm can exercise a degree of control over their acquisitiveness by deploying haustoria, an invasive absorbing tissue, which tunnel into maternal tissue to obtain nutrients (Johri & Ambegaokar 1984, pp 23-28). Imprinting endosperm resource-acquisition genes will increase or decrease acquisitiveness in the carrier; this will either consume or free up additional resources. In the case of increased acquisition, consuming additional resources must either deprive contemporary siblings or the mother. The first case has been modelled by Law & Cannings (1984) and the second by Queller (1984). For a general model both these components will be incorporated into endosperm over-consumption.

Consider first the modified provisioning of seed with a paternally imprinted endosperm acquisitiveness gene (henceforth paternally imprinted seed) when over-consuming seeds deprive only contemporary siblings of resources. Such a seed is formed from pollen carrying an imprinted endosperm acquisitiveness gene (henceforth imprinted pollen). Assume that prior to the imprint arising all seeds in the pod are provisioned s_0. Let $s_0 + d_s(x)$ be the provisioning of a paternally imprinted seed, where d_s is small and dependent on the proportion of pollen that is imprinted x. The bearers of the imprint will be over-consumers if $d_s(x) > 0$, under-consumers if $d_s(x) < 0$. Fix $d_s(0) = \delta$ and $d_s(1) = 0$, because when $x = 1$ all seeds compete equally for a fixed amount of resources. Suppose d_s is monotonic. If no resources are lost by reallocation then the average provisioning of seeds is expected to remain constant for $x \in [0, 1]$. The provisioning of a seed that is not paternally imprinted is therefore $s_0 - xd_s(x)/(1-x)$. d_s is likely to have $(1-x)$ as a factor, for example, a simple linear model gives $d_s(x) = \delta(1-x)$. If resources are assumed to be acquired by the endosperm at a constant rate over a period of time a concave d_s is obtained, an example for $d_s \geq 0$ is illustrated in figure 2-1. The flexibility of this model can be improved by adding a parameter e describing the efficiency with which resources are reallocated to or away from paternally imprinted seeds. The provisioning of a seed without the paternal imprint is then

$$s_0 - \frac{xd_s(x)}{(1-x)e}.$$

Suppose that reallocation can only incur losses and not gains for total seed provisioning. Thus if $d_s > 0$ then $e \leq 1$ but if $d_s < 0$ then $e \geq 1$. Law & Cannings (1984) choose to have completely independent fitness functions for over-consuming and under-consuming

seeds. This level of flexibility can be obtained in this model by allowing e to vary with x, although our conditions on e constitute a restriction that Law & Cannings (1984) did not impose.

A component is now added that derives from additional maternal resources. Define $d_m(x)$ which describes the modification of the provisioning of a paternally imprinted seed when the proportion of imprinted pollen is x. Fix $d_m(0) = \delta_0$ and $d_m(1) = \delta_1$, and assume d_m is monotone. In the case of over-consumption ($d_m > 0$) assume also that

$$d'_m(x) > \frac{-d_m(x)}{x} \quad \text{for all } x \in [0,1].$$

This ensures that average seed provisioning increases with x. For under-consumption this inequality must be reversed, so that average seed provisioning decreases with x. An appropriate over-consumption function is illustrated in figure 2-1. Combining the two components gives the provisioning of a paternally imprinted seed

$$s_0 + d_s(x) + d_m(x).$$

The modified provisioning of seed with a maternally imprinted endosperm acquisitiveness gene (henceforth maternally imprinted seed) can be split in exactly the same way. From the assumptions a newly arising maternal imprint should be passed on to half of the offspring in the seed pod. So a heterozygote for the mutation causing the imprint will provision maternally imprinted seeds $s_0 + d_s(1/2) + d_m(1/2)$ and other seeds $s_0 - \frac{d_s(1/2)}{e}$. Homozygotes for the mutation will pass it to all offspring; their provisioning will be $s_0 + d_m(1)$.

At this point the preparation that enables modelling of the fate of newly arising paternally or maternally imprinted endosperm acquisitiveness genes is complete. These models are provided in Appendix A. The models produce results that corroborate those of Wilkins & Haig (2001), that paternal imprints will only be selected if they increase endosperm acquisitiveness and maternal imprints selected only if they bring provisioning closer to the maternal optimum. If imprinting is equated with silencing, genes that are paternally imprinted must be genes whose activity inhibits endosperm acquisitiveness. Similarly genes that are maternally imprinted must be genes whose activity promotes endosperm acquisitiveness. Henceforth imprints that would not be selected are not under consideration.

Triploidy and Dosage

The basic model (2.2.2) is sufficient to demonstrate that the addition of a second haploid maternal genetic complement to the endosperm would be selected for if it could bring average seed provisioning closer to the maternal optimum. In the early stages of parental conflict via imprinting, the haploid genomes of embryo sac nuclei should feature a small number of maternally imprinted genes that promote endosperm acquisitiveness, and the full complement of active genes that inhibit endosperm acquisitiveness. If some or all of these inhibition genes have a cumulative effect with increased dosage, then an additional nucleus would be expected to engender a surfeit of gene products that inhibit endosperm acquisitiveness. It is not unreasonable to suppose the imprinted genes in the endosperm have cumulative effects with dosage, since if they did not the 2m:1p ratio would not be so critical. If average seed provisioning is initially above the maternal optimum, additional nuclei could prove advantageous by helping to reduce provisioning. In most species of flowering plants today the addition or loss of an entire haploid genetic complement is disastrous for endosperm development (Scott et al. 1998). For this reason triploidy must arise at an early stage in parental conflict.

Suppose triploid endosperm individuals from a population where $\bar{s} \geq 1$ arrive in a population where a diploid endosperm prevails and similarly $\bar{s} \geq 1$. In this case there will be no immediate selective advantage to triploidy. If a novel paternal imprint arises triploid endosperm carriers of the new imprint have two active maternal copies of the imprinted acquisition inhibiting gene. Seeds with diploid endosperm carry only one. So long as these genes have a cumulative effect with dosage the acquisitiveness of the triploid endosperm will be less enhanced than that of the diploid endosperm. The following model considers carriers of a novel paternal imprint with diploid endosperm to be provisioned $s_0 + d_{2,s}(x) + d_{2,m}(x)$ and carriers with triploid endosperm to be provisioned $s_0 + d_{3,s}(x) + d_{3,m}(x)$. Since the triploid endosperm is expected to be less acquisitive, assume

$$d_{2,s} \geq d_{3,s} \geq 0 \quad \text{and} \quad d_{2,m} \geq d_{3,m} \geq 0.$$

Endosperm Triploidy Model

The effect that the arrival of a novel paternal imprint on the frequency y of a dominant allele for endosperm triploidy in a population mixed for endosperm ploidy is modelled in this section. The frequency of the mutation that causes the novel paternal imprint

PI-seed provisioning	-	$s_0 + d_{i,s}(x) + d_{i,m}(x)$
NPI-seed provisioning	-	$s_0 - xd_{i,s}(x)/(1-x)e$
Viability of PI-seed	$f_i^+(x)$	$f(s_0 + d_{i,s}(x) + d_{i,m}(x))$
Viability of NPI-seed	$f_i^-(x)$	$f(s_0 - xd_{i,s}(x)/(1-x)e)$
Parental Mortality	$m_i(x)$	$m(s_0 + d_{i,m}(x)x)$

Table 2.1: Life history parameters and abbreviations for individuals with diploid (i=2) and triploid (i=3) endosperm. (PI-seeds carry the novel paternal imprint, NPI-seeds do not.)

to be set is given by x. The life history parameters of the model are specified in Table 2.1.

To describe the population dynamics of the dominant allele for endosperm triploidy we reprise the basic model (2.2.2). As with the basic model the variable v is required to describe heterozygote frequency for the triploidy allele. The only difference from the basic model is that average mortality M, average viability F and the viabilities of offspring of carriers of the triploidy allele must now depend on the frequency of the paternal imprint. In place of the offspring viability ($f(s_1)$ in the basic model) the average offspring viability F_3 of triploidy carriers with and without the paternal imprint is required. Similarly F_2 is defined as the average offspring viability of individuals not carrying the triploidy allele.

$$\begin{aligned} F_3(x) &= f_3^+(x)x + f_3^-(x)(1-x), \\ F_2(x) &= f_2^+(x)x + f_2^-(x)(1-x), \\ F(x,y) &= F_3(x)y(2-y) + F_2(x)(1-y)^2, \\ M(x,y,v) &= m_3(x)(y+v/2) + m_2(x)(1-y-v/2). \end{aligned} \tag{2.2.3}$$

The population dynamics for the paternal imprint can now be constructed. Consider the diploid and triploid populations separately. Seeds homozygous for the mutation must have a paternal imprint and so have viability $f^+(x)$, these seeds occur with frequency x^2. Seeds heterozygous for the mutation have a 50% chance of carrying the paternal imprint and so viability is on average $(f^+(x) + f^-(x))/2$. Heterozygotes occur with frequency $2x(1-x)$. Consequently the average viability experienced by the

mutation is

$$f^+(x)x^2 + \left(\frac{f^+(x)+f^-(x)}{2}\right)x(1-x) = \frac{x}{2}(f^+(x) + f^+(x)x + f^-(x)(1-x)).$$

Now combining both diploid and triploid populations the average mutant viability is

$$\frac{x}{2}(y(2-y)f_3^+(x) + f_2^+(x)(1-y)^2 + F(x,y)).$$

Now for notational efficiency define

$$F^+(x,y) = f_3^+(x)y(2-y) + f_2^+(x)(1-y)^2.$$

The same frequency of paternal imprints is found in all individuals in the population and so the mutation experiences the average mortality M. These considerations permit the introduction of paternal imprinting into the basic model as follows

$$\begin{aligned}
\frac{dx}{dt} &= \frac{M(x,y,v)x}{2}\left(\frac{F^+(x,y)}{F(x,y)} - 1\right), \\
\frac{dy}{dt} &= y\left(\frac{M(x,y,v)F_3(x)}{F(x,y)} - m_3(x)\right), \\
\frac{dv}{dt} &= \frac{2M(x,y,v)F_3(x)y(1-y)}{F(x,y)} - m_3(x)v.
\end{aligned} \tag{2.2.4}$$

This model has equilibria $E_0 = \{(0, y, 2y(1-y))|y \in [0,1]\}$, which is consistent with triploidy having no advantage prior to the paternal imprint arising. The following inequality can be demonstrated

$$\frac{f_2^+(x)}{F_2(x)} \geq \frac{F^+(x,y)}{F(x,y)} \geq \frac{f_3^+(x)}{F_3(x)} \geq 1 \quad \text{for all } y \in [0,1].$$

This indicates that the imprinting mutation would be selected more strongly in a diploid population than a triploid population, and for a mixed population the strength of selection will be intermediate. Thus $\dot{x} > 0$ on $[0,1]$, so the paternal imprint must fix.

If $s_0 \geq 1$ the dynamics of the triploidy allele are straight forward, because the relationship of m and f requires

$$M(x,y,v)F_3(x) \geq m_3(x)F(x,y),$$

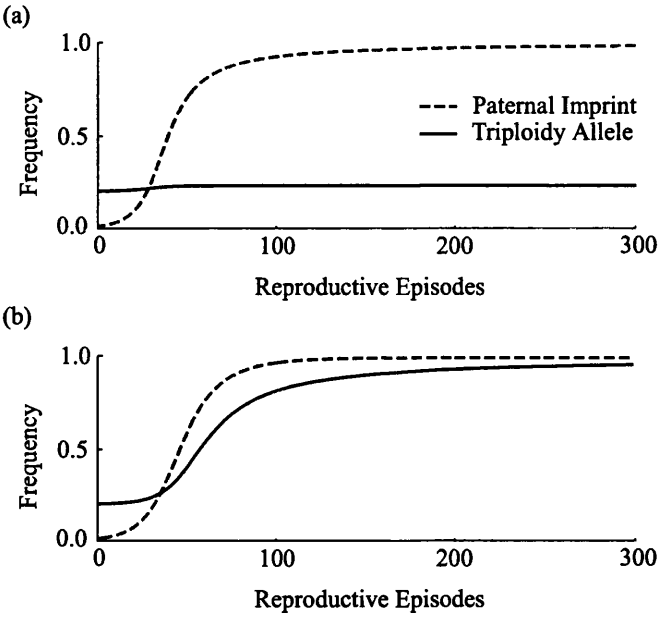

Figure 2-2: The selective advantage of endosperm triploidy during the fixing of a paternal imprint. Individuals carrying the paternal imprint may derive additional resources from contemporary siblings or from maternal reserves. (a) The short lived advantage of triploidy when all additional resources are obtained from siblings. (b) Triploidy fixes when some additional resources are obtained from maternal reserves.

thus y is monotonically increasing on any trajectory from $x = 0$ to $x = 1$. The triploidy allele will fix only if $d_{3,m} > 0$, otherwise

$$M(1, y, v) = m_3(1) = m(s_0) \quad \text{and} \quad F(1, y) = F_3(1) = f(s_0) \quad \text{for all } y, v \in [0, 1].$$

In which case $E_1 = \{(1, y, 2y(1-y)) | y \in [0, 1]\}$ are equilibria. If $s_0 < 1$ the triploidy allele may be selected against for some or all of a trajectory from $x = 0$ to $x = 1$.

2.3 DISCUSSION

It has been shown that an episode of paternal imprinting of endosperm acquisitiveness genes will favour an allele causing endosperm triploidy, so long as seed provisioning is initially at or above the maternal optimum. A selective advantage is available regardless of whether resources for overgrowth come predominantly from contemporary siblings or

from maternal reserves. The triploidy allele will only fix, however, if some overgrowth depends on maternal reserves; this distinction is illustrated in the plots in figure 2-2. Haig & Westoby (1989) developed the original argument that genomic imprinting in the endosperm is the result of parental conflict and that the second female contribution constitutes an escalation of this conflict. This theory allows endosperm triploidy a selective advantage as a mechanism of retaliation against paternal imprinting. The argument here demonstrates that even if endosperm triploidy is initially selectively neutral it will attract an advantage during the fixing of future paternal imprints. This latent advantage can contribute to explaining why endosperm triploidy became widespread when it arose and why it has rarely been displaced by alternative endosperm types. The argument depends explicitly on paternal and maternal imprints affecting antagonistic endosperm development genes and so is not derivable from a model which considers either acquisitiveness-promoting or acquisitiveness-inhibiting genes alone. The advantage to the mother of producing 2m:1p endosperm over 1m:1p endosperm is readily predicted by inclusive fitness theory (Queller 1989, Haig 1997). The additional maternal genetic material increases the endosperm's relatedness to siblings and so brings its interests into closer alignment with maternal interests. Effectively this improves maternal control over endosperm acquisitiveness and in the model above this proves advantageous when paternal imprints arise. Improved maternal control over seed provisioning is also responsible for the selective advantage to endosperm triploidy that Härdling (2001) found. The model here, however, is more general because it does not depend on the optimum endosperm acquisitiveness being maintained by heterozygote advantage.

The story of endosperm evolution is not complete and may yet require components that parental conflict arguments cannot provide. In particular parental conflict is unlikely to be able to explain why additional paternal nuclei have not been introduced to the endosperm. This question cannot be resolved within the scope of the models presented here. Experimental 2x x 4x crosses yield a 2m:2p endosperm whose seed is inviable seed in most species (Vinkenoog et al. 2002) suggesting that presently it is too late for a male-nucleus to be added. In the end it may be that physiological constraints prevented a tetraploid endosperm arising before imprinting strength rose above a prohibitive threshold.

2.A PATERNAL AND MATERNAL IMPRINTING MODELS

This Appendix contains models whose results are not novel, but whose considerations and construction inform the model presented in this chapter.

Paternal Imprinting

For the purpose of this model a paternal imprint is a genomic modification applied during the production of pollen that modifies the acquisitiveness of any endosperm that carry it. Let $s_0 + d_s(x) + d_m(x)$ be the level of provisioning attained by an endosperm bearing the paternal imprint, where s_0 is the initial level of provisioning in the absence of the imprint; x is the proportion of pollen that carries the imprint; and d_s and d_m are functions modelling the modification that carrying the imprint makes on provisioning. The level of provisioning in individuals without the paternal imprint developing in seed pods alongside imprinted individuals is $s_0 - xd_s(x)/(1-x)e$ where e gives the level of efficiency with which resources of under-consumers are converted to those of over-consumers. The viability of a seed provisioned s is given by $f(s)$. The mortality of an individual producing seeds with average provisioning $\bar{s}$ is given by $m(\bar{s})$. Assume random mixis, so every individual's seed set will contain the same proportion of paternally imprinted seeds. Thus every individual suffers the same mortality, the average mortality $M(x)$, which depends on the prevalence of imprinted pollen.

The setting of the paternal imprint is caused by a mutation, consider the rates of change of homozygotes for the mutation, heterozygotes and wild-types without the mutation, labelled u, v and w respectively. Assume weak selection so a satisfactory model for a perennial species is

$$\begin{aligned}
\frac{du}{dt} &= \frac{M(x)f(s_0 + d_s(x) + d_m(x))(u^2 + uv + \frac{v^2}{4})}{F(x)} - M(x)u, \\
\frac{dv}{dt} &= \frac{M(x)(f(s_0 + d_s(x) + d_m(x)) + f(s_0 - \frac{xd_s(x)}{(1-x)e}))(uv + 2uw + \frac{v^2}{2} + vw)}{2F(x)} - M(x)v, \\
\frac{dw}{dt} &= \frac{M(x)f(s_0 - \frac{xd_s(x)}{(1-x)e})(\frac{v^2}{4} + vw + w^2)}{F(x)} - M(x)w,
\end{aligned} \tag{2.A.1}$$

where

$$\begin{aligned}
F(x) &= f(s_0 + d_s(x) + d_m(x))x + f(s_0 - \frac{xd_s(x)}{(1-x)e})(1-x), \\
M(x) &= m(s_0 + d_m(x)x).
\end{aligned}$$

This model reduces by simple algebra to a one dimensional model, describing the rate of change of $x = u + v/2$.

$$\frac{dx}{dt} = \frac{M(x)x}{2}\left(\frac{f(s_0 + d_s(x) + d_m(x))}{F(x)} - 1\right). \tag{2.A.2}$$

This model is straightforward to analyse. Equilibria occur when $x = 0$ or when

$$f(s_0 + d_s(x) + d_m(x)) = F(x).$$

This is satisfied when $x = 1$ or if

$$f(s_0 + d_s(x) + d_m(x)) = f(s_0 - \frac{xd_s(x)}{(1-x)e}).$$

The later is never possible for $x \in [0,1]$ since d_s and d_m have the same sign, $-xd_s(x)/(1-x)e$ necessarily has the opposite sign, and f is monotonic. The stability of the equilibria depend on whether the paternal imprint causes increased or decreased endosperm acquisitiveness. Increased acquisitiveness implies $d_s, d_m > 0$ and consequently $f(s_0 + d_s(x) + d_m(x)) \geq F(x)$, for all $x \in [0,1]$, thus $\dot{x} > 0$ and $x = 0$ is unstable $x = 1$ is stable. Precisely the reverse is true for decreased acquisitiveness, in which case $x = 0$ is stable and $x = 1$ is unstable. The model therefore predicts that regardless of the initial level of seed provisioning, paternal imprints that increase provisioning can always in-

vade, those that decrease provisioning always disappear. If a paternal imprint increases seed provisioning it does not matter whether the resources for over-consumption are derived from siblings or from maternal reserves or a combination, the imprint will always succeed. Seed provisioning after the mutation causing the imprint has fixed will be $s_0 + d_m(1)$, that is it will depend only on the final ($x = 1$) level of over-provisioning derived from additional maternal reserves.

Maternal Imprinting

To model maternal imprinting exactly the same functions as above can be used, but the levels of over and under-provisioning now depend on the maternal genotype. Again the setting of the maternal imprint is caused by a mutation. Homozygotes for this mutation will provision all their seeds $s_0 + d_s(1) + d_m(1)$, that is $s_0 + \delta_1$. Heterozygotes will provision half of their seeds, those carrying the mutation $s_0 + d_s(\frac{1}{2}) + d_m(\frac{1}{2})$, and the other half $s_0 - d_s(\frac{1}{2})/e$. Wild-type individuals without the mutation will continue to provision all their seeds s_0. Since fitness and mortality values are now constant and independent of imprinting frequency we will use the abbreviations in table 2.2.

f_0	$f(s_0)$
$f^+_{1/2}$	$f(s_0 + d_s(1/2) + d_m(1/2))$
$f^-_{1/2}$	$f(s_0 - d_s(1/2)/e)$
f_1	$f(s_0 + d_m(1))$
m_0	$m(s_0)$
$m_{1/2}$	$m(s_0 + \frac{d_s(1/2)(1-1/e)+d_m(1/2)}{2})$
m_1	$m(s_0 + d_m(1))$

Table 2.2: Abbreviations for constants in maternal imprinting models

We first form the model in terms of homozygotes u, heterozygotes v and wild type w.

$$\begin{aligned}
\frac{du}{dt} &= \frac{M(u,v,w)(u+v/2)(f_1u+f^+_{1/2}v/2)}{F(u,v,w)} - m_1u,\\
\frac{dv}{dt} &= \frac{M(u,v,w)((u+v/2)(f_0w+f^-_{1/2}v/2)+(w+v/2)(f_1u+f^+_{1/2}v/2))}{F(u,v,w)} - m_{1/2}v,\\
\frac{dw}{dt} &= \frac{M(u,v,w)(w+v/2)(f_0w+f^-_{1/2}v/2)}{F(u,v,w)} - m_0w,
\end{aligned} \tag{2.A.3}$$

where

$$\begin{aligned}
F(u,v,w) &= f_1u+(f^+_{1/2}+f^-_{1/2})v/2+f_0w,\\
M(u,v,w) &= m_1u+m_{1/2}v+m_0w.
\end{aligned}$$

As in the basic model u, v and w are not linearly independent and the model can be reduced by one equation. There is no great advantage to substitution of variables in this case, so the above model is analysed with the final equation removed and instances of w replaced by $1-u-v$. The region of interest is the triangle with vertices $(0,0)$, $(0,1)$ and $(1,0)$. It is straight forward to verify that this region is invariant. On inspection $(0,0)$ and $(1,0)$ are equilibria. The stability of these equilibria determines whether the maternal imprint can invade and whether it can fix. By linearization $(0,0)$ is unstable if

$$\frac{f^+_{1/2}}{f_0}+1>\frac{2m_{1/2}}{m_0}. \tag{2.A.4}$$

This is the condition for invasion. It can be satisfied only if $s_0<0$ and $d_s(1/2)\geq 0, d_m(1/2)>0$ or if $s_0>0$ and $d_s(1/2)\leq 0, d_m(1/2)<0$. That is a maternal imprint can only invade if it increases provisioning when seeds are under-provisioned, or decreases provisioning when seeds are over-provisioned. By linearization $(1,0)$ is stable and locally attracting if

$$\frac{2m_{1/2}}{m_1}>1+\frac{f^-_{1/2}}{f_1}. \tag{2.A.5}$$

This is the condition for fixation. Equilibria internal to the region of interest are possible but the form of the nullclines of 2.A.3 makes it unlikely that more than one can exist. However, at least one internal equilibrium must exist if condition (2.A.4)

holds and condition (2.A.5) fails. This equilibrium implies that a heterozygote for the imprinting mutation has the fittest balance of mortality and offspring viability.

Whether conditions (2.A.4) and (2.A.5) are satisfied depends upon the particular choice of our functions f, m, d_s, d_m and e, but this does not preclude a general summary of the behaviour of maternal imprinting model (2.A.3). If provisioning is initially low ($s_0 < 1$) maternal imprints that increase provisioning can invade and fix so long as the increase is not too large. Similarly if provisioning is initially high ($s_0 > 1$) maternal imprints that decrease provisioning can invade and fix so long as the decrease is not too large. Imprints with larger effects may invade but not fix, resulting in polymorphism for the mutation causing the imprint. Imprints with particularly large effects (e.g. $d_s(1/2) + d_m(1/2) \gg 2|1 - s_0|$) are incapable of invading, and simply disappear. Maternal imprints that lower provisioning when it is initially low or raise it when it is initially high cannot succeed.

Discussion

The models in this appendix indicate the possible roles that paternal and maternal imprinting of endosperm acquisitiveness genes could have played in the evolutionary history of the endosperm. Paternal imprinting will be selected only if it raises seed provisioning. This increase may occur only prior to fixation or may endure afterwards depending on how over-consumption is resourced. Maternal imprinting is a more subtle tool capable of correcting maternally non-optimal seed provisioning, whether that requires raising or lowering endosperm acquisitiveness. The success or failure of genomic imprints should be viewed in the wider context of all mutations that can affect endosperm acquisitiveness. Maternal imprinting is not only a response to paternal imprinting of endosperm acquisition genes but to any mutation which dislodges seed provisioning from the maternal optimum. In a similar vein maternal imprinting is not the only response to paternal imprinting, since gene silencing that is not parent-of-origin specific could be an alternative, although maternal imprinting of a gene has significant advantages over outright silencing, since there will be no segregational load. For example, heterozygotes for a mutation causing silencing of a gene that increases endosperm acquisition would enjoy a similar fitness to individuals who have a maternal imprint on the same gene. However should the silencing mutation spread, homozygotes will eventually arise who may have significantly lower fitness because they have no active copies of the gene.

PART II

Population-Based Approaches

INTRODUCTION

Population-based, or state variable, approaches have been employed by ecologists for over two centuries. The mathematical formalization of these approaches (Verhulst 1838, Lotka 1956, Volterra 1931, Fisher 1930, Skellam 1951, Wright 1968) marked the inception of the discipline of mathematical biology. The principle of population-based modelling is to lift, from the mechanics of individual demography or from life history data, population-scale rules that determine how population size and structure will develop.

The models in chapter 3 of this report will be derived in the first instance from the pioneering ecological models of Verhulst (1838), Lotka (1956) and Volterra (1931). A scheme of inheritance that reflects a plausible genetic scenario will be imposed in each example model, without recourse to an explicit population genetical approach. This approach endeavours to compromise between biological realism and theoretical flexibility. In common with early ecological models the models in this report will not incorporate size structure, phenotypic variability or spatial heterogeneity of resources. However, the general frameworks developed in chapters 3 and 5 lend themselves to extensions in these directions.

The models in part II incorporate the primary distinguishing feature of population-based models: Population size is modelled as a continuum. This facilitates assembly and analysis of models and in particular has promoted an enduring migration of techniques from the physical sciences. Ignoring the discreteness of individuals is contentious, never more so than when population size is small, and a revision of this assumption will be proposed in part III. The consequences of respecting discreteness will be reviewed at that stage.

All the models in this report will operate in continuous time. This permits a wide range of well understood mathematical analyses. Continuous time implies at least that species' generations overlap, which is true of perennial plant species. An ideal subject species would be involved throughout maturity in all demographic processes: principally pollen and seed production and death. This is true of some tropical plant species, for which the constancy of the climate suppresses annual cycles. It should be noted that by no means all of the species and phenomena discussed in chapter 1 are found in tropical climes. It would be possible to introduce the seasonality experienced by sub-tropical species into the models in this part by using time dependent reproductive

parameters. Arguably the main effect of such a modification would be to slow down population growth and decay because of the shortened periods of reproductive activity. In any case the absence of time dependence in the parameters provides a necessary bench-mark for exploring model behaviour.

CHAPTER 3

Non-spatial Models

In this chapter classical non-spatial population dynamical models with be extended to explicitly incorporate pollination. The extension process is intended to be general and will provide a framework for considering populations of inter-pollinating conspecifics which have been sorted into one or more classes. Conspecific classes may, for example, distinguish between individuals with or without a specific gene. In the examples presented later on in the chapter they will be used to group together individuals with a common reproductive mode.

3.1 DERIVATION

Logistic Model

The treatment begins with the familiar logistic model for a self limiting population attributable to Verhulst (1838)

$$\frac{dN}{dt} = r\left(1 - \frac{N}{K}\right)N. \tag{3.1.1}$$

The logistic model is intended to describe a population of size $N(t)$ whose growth is limited by intra-specific competition. The population is assumed to grow at a rate r in the absence of competition. The growth rate of the population is assumed to decrease linearly with population size. The model is sufficiently general that intra-specific competition can be interpreted either as limiting a mature individual's access to the resources which make reproduction possible, or as inhibiting the establishment of offspring. The population growth rate is zero at a threshold population size $K > 0$, this is described as the carrying capacity of the population and is a stable attracting equilibrium of the dynamical system over $[0, \infty)$.

It will be convenient in what follows to separate the birth and death components

of the growth parameter r. Taking b as birth rate and d as death rate and setting $r = b - d$

$$\frac{dN}{dt} = b\left(1 - \frac{rN}{bK}\right)N - dN.$$

To non-dimensionalize this model a new timescale is chosen with units $t' = dt$, and the dimensionless parameter $b' = b/d$ is introduced

$$\frac{dN}{dt'} = b'\left(1 - \frac{(b'+1)N}{b'K}\right)N - N.$$

The model is tidied up with the introduction of a rescaled population size u where

$$u = \frac{(b'+1)N}{b'K}.$$

Finally the primes on t and b are dropped for simplicity to obtain

$$\frac{du}{dt} = b(1-u)u - u. \tag{3.1.2}$$

The model is now dependent on a single parameter b, and the stable attracting equilibrium now occurs at $u = (b-1)/b$.

The logistic model presented here is a continuous time model suitable for perennial species of plant. It is most ideally suited to the population dynamics of non-seasonal species in which reproductive activity is not synchronized between individuals and occurs with uniform probability throughout the year. These caveats of applicability are, of course, inherited by any models derived from the logistic model.

Lotka-Volterra Competition Model

The Lotka-Volterra inter-specific competition model is an extension of the logistic model to two or more distinct populations that share resources. Here, however, it is intra-specific competition between physiologically very similar individuals that is of interest; as such resource requirements will overlap considerably. This is a special case within the framework of the Lotka-Volterra model and can be recovered by judicious selection of parameters. The model for n competing species

$$\frac{dN_i}{dt} = r_i\left(1 - \frac{N_i + \sum_{j\neq i} a_{ij}N_j}{K_i}\right)N_i, \text{ for } i \in \{1,2,\ldots,n\}. \tag{3.1.3}$$

The population of each species is assumed to grow at the rate r_i in the absence of intra- and inter-specific competition. The growth rate of of each population is assumed to decrease linearly with population size as with the logistic model. In addition the growth rate decreases linearly with the population size of each competing population. The a_{ij}'s parameterize the impact of the j-th population on the i-th population. So that a small value of a_{ij} indicates a weak competitive impact; a large value indicates a strong competitive impact; and $a_{ij} = 1$ indicates that for species i intra-specific competition and inter-specific competition with species j are equivalent.

The competition model is neatly non-dimensionalizable along similar lines to the logistic model if it is assumed that all species have the same death rate. This is not true in general, but is not unreasonable under the circumstances, since all conspecifics belong to the same species. Let $r_i = b_i - d$ as above, rescale time by $t' = dt$ and introduce $b_i' = b_i/d$.

$$\frac{dN_i}{dt'} = b'_i \left(1 - \frac{(b_i'+1)\left(N_i + \sum_{j\neq i} a_{ij}N_j\right)}{b_i'K_i} \right) N_i - N_i. \tag{3.1.4}$$

The model is tidied up with the introduction of rescaled population sizes u_i and competition parameters α_{ij} given by

$$u_i = \frac{(b_i'+1)N_i}{b_i'K_i} \text{ and } \alpha_{ij} = \frac{(b_i'+1)b_j'K_j}{(b_j'+1)b_i'K_i}a_{ij} \text{ for all } i,j \in \{1,2,\ldots,n\}.$$

The matrix $A = (\alpha_{ij})$ is termed the competition matrix. Applying these definitions to (3.1.4) and dropping the apostrophes on the t and b_i parameters, results in

$$\frac{du_i}{dt} = b_i\Big(1 - u_i - \sum_{j\neq i}\alpha_{ij}u_j\Big)u_i - u_i, \text{ for } i \in \{1,2,\ldots,n\}. \tag{3.1.5}$$

This is a model for n competing species. However conspecifics classes are not distinct species and are likely to occupy very similar ecological niches and be highly competitive with each other. With respect to the parameters of (3.1.5) this implies

$$b_i \approx b_j \text{ and } \alpha_{ij} \approx 1 \approx \alpha_{ji} \text{ for all } i,j \in \{1,2,\ldots,n\}. \tag{3.1.6}$$

Conspecifics with different reproductive modes may well be capable of inter-breeding, and viable inter-conspecific crosses may result in offspring with the same reproductive

mode as one or other parent, or may be classed as belonging to a different conspecific group. The Lotka-Volterra model describes distinct species for whom inter-breeding in not possible. In treating classes of conspecifics with this model the possibility of viable crosses between classes is excluded, the model must be developed further to accommodate inter-breeding. Before this can be done a notion of pollination must be introduced to establish the rates of inter-breeding between conspecific classes.

Introducing a Pollination Process

All or some of the conspecific classes produce pollen. These classes may contain hermaphrodite or exclusively male individuals. Similarly all or some of the conspecific classes require pollination in order to set seed. These classes may contain hermaphrodite or exclusively female individuals. Pollen may be involved in sexual reproduction or only required for endosperm fertilization. Self-pollination may occur amongst self-compatible conspecifics.

Considering a single class of sexually reproducing hermaphrodite conspecifics, pollination is assumed to affect the growth rate of the population and is determined by the density of the population. A function $f(u)$ is required which describes the effect of population size u on the proportion of the population successfully pollinated and therefore capable of reproduction. Such a function can be incorporated into the competition model (3.1.5), which for a single class of conspecific resolves to the logistic model (3.1.2).

$$\frac{du}{dt} = bf(u)(1-u)u - u. \tag{3.1.7}$$

Several functional responses could be appropriate here. Pollen availability is a limiting factor in reproduction only in some species and often only when pollen is very rare. (See Willson & Burley (1983, pp 28-31) for a compilation of studies.) So the functional response should increase with pollen availability, particularly when pollen is rare. Conversely when pollen is abundant, artificially raising pollination in many cases has little effect on seed set. So the functional response should be saturating. It would be reasonable to take f linear on $u \in [0, \epsilon)$ and unitary for $u > \epsilon$, this is a Holling type I functional response. However, it is convenient for f to be differentiable as with the Holling type II functional response. Since pollen is a crucial reproductive resource there is no reason to expect threshold effects in the response when pollen is scarce, so the Holling type III response is unsuitable. Various increasing saturating functional

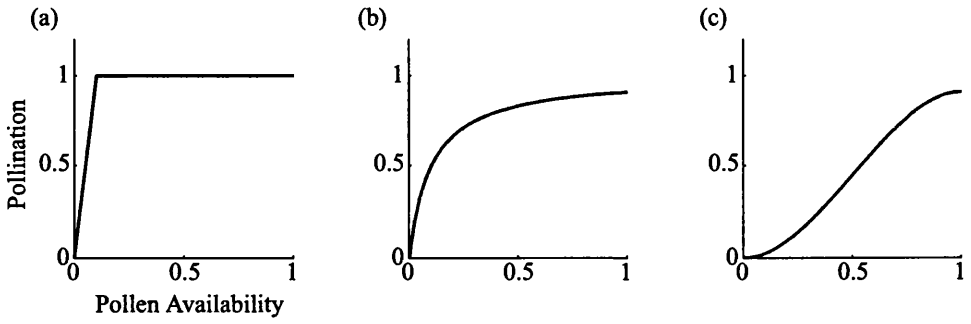

Figure 3-1: Possible increasing saturating pollination responses to pollen availability (a) Holling type I. (b) Holling type II. (c) Holling type III.

responses discussed are illustrated in Figure 3-1.

A Holling type II functional response to the availability of a resource x is given by

$$h(x) = \frac{x}{1+x}$$

The resource here is pollen, and pollen availability is assumed a linear function of population size $pu + s$, where $p \geq 0$ parameterizes the effort put into pollen production and dispersal away from the parent plant by each individual in the population and $s \geq 0$ parameterizes the effort put into self-pollination. A self-compatible hermaphrodite species would have a strictly positive value for both p and s. The proportion of the population successfully pollinated is taken as

$$f(u) = h(pu + s) = \frac{s + pu}{1 + s + pu} \tag{3.1.8}$$

Adjusting p increases or decreases how rapidly the function saturates with population size. When male reproductive effort is isolated and incorporated in a pollination function like this, it is intuitive to consider b as describing female reproductive effort. Since the species is hermaphrodite male and female reproductive effort are limited by the same pool of resources. In this report, however, no trade-off between male and female reproductive effort will be assumed and they will be left as free parameters. The model resulting from substituting (3.1.8) into (3.1.7) is analysed in section 3.2.

The parameter p is specific to the conspecific class. For a general model define p_{ij}, the pollen production and dispersal effort of class j experienced by conspecifics of class

i. The matrix $P = (p_{ij})$ is termed the inter-pollination matrix. Also take s_i to be the self-pollination effort of class i. The functional response of conspecific class i to the pollination effort of class j is given by the multi-species generalization of the Holling type II response

$$f_{ij}(\mathbf{u}) = \frac{s_i\delta_{ij} + p_{ij}u_j}{1 + s_i\delta_{ij} + \sum_{k=1}^{n} p_{ik}u_k}, \tag{3.1.9}$$

where δ_{ij} is the Kronecker delta. For sexual conspecifics: $f_{ij}(\mathbf{u})$ specifies the proportion of ovules produced by conspecifics of class i and fertilized by conspecifics of class j. In the example models treated here it will prove satisfactory to assume $p_{ik} = p_{jk}$, which assumes that differences in how class i and class j respond to pollen from class k are negligible. In reality, however, the assumption is often false: Pollen tubes may exhibit different rates of growth, which may be affected by the other pollen present on the stigma, and may be enhanced or retarded by the intervention of the recipient plant (Richards 1986).

General Inter-pollinating Conspecifics Model

The rate of establishment for a seedling whose maternal parent comes from class i and whose paternal parent comes from class j is given by

$$b_i f_{ij}(\mathbf{u})\Big(1 - u_i - \sum_{j\neq i} \alpha_{ij}u_j\Big)u_i,$$

since f_{ij} specifies the proportion of class i offspring fathered by class j individuals. Such seedlings are described as (i,j)-seedlings. But notice that $p_{ij} = p_{ik} \Rightarrow f_{ij}(\mathbf{u}) = f_{ik}(\mathbf{u})$, so that the establishment rates of (i,j)-seedlings and (i,k)-seedlings are the same. Thus in the above expression the establishment rate does not reflect the specific genetic constitution of (i,j)-seedlings. This can be rectified by introducing both-parent specific reproductive rates b_{ij}, where the first subscript indicates the conspecific class of the maternal parent and the second indicates that of the paternal parent. So the establishment rate of (i,j)-seedlings is instead given by

$$b_{ij} f_{ij}(\mathbf{u})\Big(1 - u_i - \sum_{j\neq i} \alpha_{ij}u_j\Big)u_i.$$

If $b_{ij} > b_{ik}$ this should be interpreted to mean that the sum fitness of (i,j)-seedlings will be greater that the sum fitness of (i,k)-seedlings derived from the same maternal

plant, if that plant was equally pollinated by pollen from class j and pollen from class k. It does not directly imply that (i,j)-seeds are fitter than (i,k)-seeds, or that they are more numerous.

The conspecific class that (i,j)-seedlings belong to must be determined by the classes of their parents. However, not all (i,j)-seedlings need belong to the same class. Consider, for instance, a population of conspecifics sorted into classes differing only in the alleles born at one locus. If class i are heterozygous and class j are homozygous for a given allele, then (i,j)-seedlings may belong to either class i or class j. Clearly the seedlings that establish from either class need to be distinguished. This can be achieved by splitting the reproductive rate b_{ij} into two components, one for each class the offspring could belong to. In general b_{ij} may need to be split over all n classes, so the component reproductive rates b_{ijk} are introduced with

$$\sum_{k=1}^{n} b_{ijk} = b_{ij}.$$

Note that not only the relative proportions of (i,j)-seeds belonging to different classes, but also any differential establishment likelihood can be incorporated into the values $b_{ij1},\ldots,b_{ijn}$. So it need not be the case with the example of heterozygotes and homozygotes that $b_{iji} = b_{ijj} = b_{ij}/2$ if, for example, heterozygotes are fitter than homozygotes. The array $B = (b_{ijk})$ is termed the reproduction array.

The establishment rate of (i,j)-seedlings belonging to conspecific class k is

$$b_{ijk} f_{ij}(\mathbf{u})\Big(1 - u_i - \sum_{j\neq i} \alpha_{ij} u_j\Big) u_i.$$

The recruitment of sexually produced offspring to class k is therefore

$$\sum_{i=1}^{n}\sum_{j=1}^{n} b_{ijk} f_{ij}(\mathbf{u})\Big(1 - u_i - \sum_{j\neq i} \alpha_{ij} u_j\Big) u_i.$$

In addition conspecifics in class k may be capable of autonomous asexual reproduction or vegetative propagation, which will not be pollen limited but will be subject to the same competition as sexual offspring. Additional clonal and asexual reproduction is parameterized by c_i for class i. The general inter-pollinating conspecifics model for n

conspecific classes is

$$\frac{du_k}{dt} = \sum_{i=1}^{n}\sum_{j=1}^{n}(b_{ijk}f_{ij}(\mathbf{u}) + c_i\delta_{ik})\Big(1 - u_i - \sum_{j\neq i}\alpha_{ij}u_j\Big)u_i - u_k, \quad \text{for } k \in \{1,\ldots,n\}. \tag{3.1.10}$$

The following sections of this chapter examine $n = 1$ and $n = 2$ examples of this general model which apply to specific biological phenomena.

3.2 SEXUAL SPECIES

The simplest representative of the class of models developed above which retains the pollination structure describes a sexually reproducing self-incompatible hermaphrodite species. Taking $n = 1$, $c_1 = 0$ and $s_1 = 0$ in (3.1.10) and dropping all unnecessary subscripts

$$\frac{du}{dt} = F(u) = \frac{bpu^2(1-u)}{1+pu} - u. \tag{3.2.1}$$

Biologically reasonable solutions ($u \in \mathbb{R}^+$) of (3.2.1) exist for reasonable initial population size ($u_0 \in \mathbb{R}^+$) for all $t \in [0,\infty)$ by Picard's theorem coupled with the invariance of (3.2.1) on compact sets $K = [0,k]$ for any $k > \hat{u}^+$ given below. The model has three equilibria one trivial and two non-trivial given by

$$\hat{u}^{\pm} = \frac{b-1}{2b} \pm \sqrt{\left(\frac{b-1}{2b}\right)^2 - \frac{1}{bp}} \tag{3.2.2}$$

The non-trivial equilibria exist when $p \geq p_{crit}$ where

$$p_{\text{crit}} = \begin{cases} \dfrac{4b}{(b-1)^2} & \text{for } b > 1 \\ \infty & \text{for } b \leq 1 \end{cases} \tag{3.2.3}$$

For $p \geq p_{crit}$, $\hat{u}^{\pm} \in [0,1]$ with limiting behaviour

$$\hat{u}^- \to 0^+ \text{ and } \hat{u}^+ \to \left(\frac{b-1}{b}\right)^- \text{ as } p \to \infty$$

and

$$\hat{u}^- \to 0^+ \text{ and } \hat{u}^+ \to 1^- \text{ as } b \to \infty.$$

The greater equilibrium $\hat{u}^+$ should be interpreted as the population carrying capacity, it is the largest stable population size. $\hat{u}^+$ is stable and attracting on $(\hat{u}^-, \infty)$. The trivial equilibrium is also stable and attracting on $(-\infty, \hat{u}^-) \supset [0, \hat{u}^-)$. So that populations that fall beneath the threshold size $u = \hat{u}^-$ face extinction.

For $b \geq 1$ and $p < p_{crit}$ and for $b \leq 1$ (3.2.1) has a single equilibrium at zero, which is stable and attracting over $\mathbb{R}$. In this case population persistence is impossible. The region of population viability in (b,p)-space is depicted in Figure 3-2(b). The conclusion of this model must be that population survival is critically dependent on the production of sufficient pollen and seed; this is especially true of small populations.

The bistable population dynamics exhibited by (3.2.1) are characteristic of a critical depensation effect, also termed an Allee effect after W.C. Allee who collected evidence that small populations often perform sub-optimally (Allee et al. 1949, pp. 393-419). Critical depensation requires that small populations experience a negative growth rate. It is clear then that the functional response to pollen availability that was chosen penalizes small populations, for which the level of cross-pollination is so low they cannot persist. When only a few new individuals become established in virgin territory, their reproductive capacity is greatly limited by insufficiency of pollen donors. The model derived here differs slightly in form from the classical model with depensation used to treat populations with Allee effects but also arising in the study of excitable media, and nerve potentials

$$\frac{dv}{dt} = bv(\hat{v} - v)(v - a),$$

where $\hat{v} > 0$ specifies the stable carrying capacity and $a \in \mathbb{R}$ parameterizes depensation. When $a \in (0, \hat{v})$ the model treats critical depensation, and a specifies the threshold viable population size. The classical model can be parameterized so that its equilibria match those of (3.2.1)

$$\frac{dv}{dt} = G(v) = bv(\hat{u}^+ - v)(v - \hat{u}^-). \tag{3.2.4}$$

Notice that

$$F(x) = \frac{px}{1+px}\left(-bx^2 + (b-1)x - 1/p\right),$$
$$G(x) = x\left(-bx^2 + (b-1)x - 1/p\right),$$

so that $px^2 - (p-1)x > 0 \Leftrightarrow |F(x)| > |G(x)|$. For a population of size $x \in [0, (p-1)/p)$

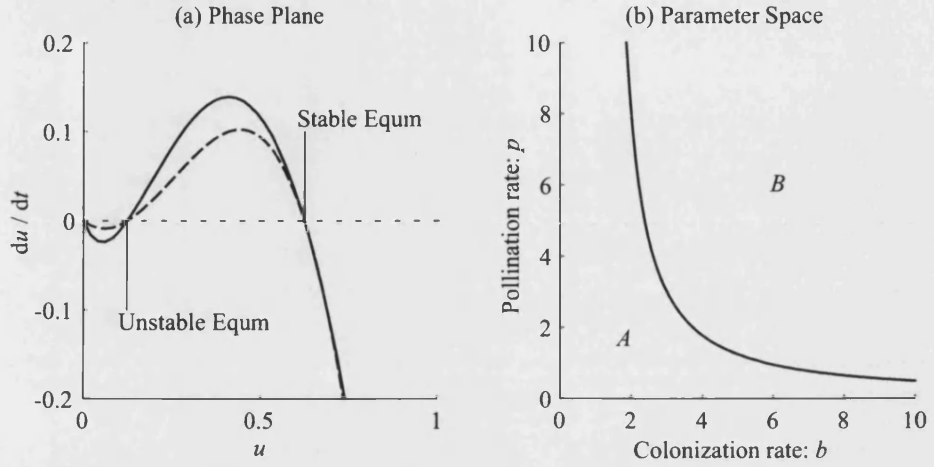

Figure 3-2: (a) Phase diagram for sexual species model (solid line) with classical Allee effect model for comparison (dashed line). (b) (b,p)-Parameter space for the sexual species model is divided into two regions: A - Region of population extinction for all initial population sizes, B - Region of population survival conditional on initial population size exceeding a threshold.

if the population is growing it will grow more quickly, and if it is decaying it will decay more rapidly, under (3.2.1) than under (3.2.4). Outside the region $[0, (p-1)/p)$ the reverse it true. This is illustrated in Figure 3-2(a).

Self-Compatible Sexual Species

Sexual flowering plants are generally outcrossers and some species go to great lengths to prevent self-fertilization. In many cases self-fertilization is not possible due to chemical or physiological incompatibility, but incompatibility may not be complete and occasionally selfed offspring may be produced (see section 1.2). In other species outcrossing is facultative, it is the preferred reproductive strategy but selfed seed may still be set. In particular selfing may be deliberately encouraged if outcrossed pollen availability is low. For species that can tolerate inbreeding, self-fertilization provides reproductive assurance, a greater than zero baseline of reproduction that can be sustained in isolation. Here the sexual species model is amended to incorporate a level of self-pollination. The level of self-pollination effort is given by s and the overall functional response to available pollen is given in (3.1.8). The self-compatible sexual species model is given

by

$$\frac{du}{dt} = \frac{b(s+pu)u(1-u)}{1+s+pu} - u. \tag{3.2.5}$$

Biologically reasonable solutions must exist as with (3.2.1) and the model has three equilibria: zero and $\hat{u}^{\pm}$ given by

$$\hat{u}^{\pm} = \frac{b-1}{2b} - \frac{s}{2p} \pm \sqrt{\left(\frac{b-1}{2b} - \frac{s}{2p}\right)^2 + \frac{(b-1)s-1}{bp}}. \tag{3.2.6}$$

The non-trivial equilibria exist when $p \geq p_{\text{crit}}$ where

$$p_{\text{crit}} = \begin{cases} 0 & \text{for } s > \frac{1}{b-1} > 0 \\ \frac{b}{(b-1)^2}\left(2 - s(b-1) + 2\sqrt{1-s(b-1)}\right) & \text{for } 0 \leq s \leq \frac{1}{b-1} \\ \infty & \text{for } b \leq 1 \end{cases} \tag{3.2.7}$$

Notice however that $\hat{u}^- > 0$ if and only if $s < 1/(b-1)$, so that for large enough levels of self-pollination the model no longer exhibits critical depensation. Non-critical depensation is still exhibited by the model while

$$s < \frac{\sqrt{4p+1}-1}{2}.$$

In this case populations smaller than

$$\frac{\sqrt{p+s+1}-s-1}{p},$$

experience an accelerating growth rate. Note that $\sqrt{4p+1}-1 \leq 2/(b-1) \Rightarrow p \leq p_{\text{crit}}$ so that depensation can only be lost if $s \geq 1/(b-1)$ and cross pollination is sufficiently weak. Figure 3-3 illustrates regions of different model behaviour.

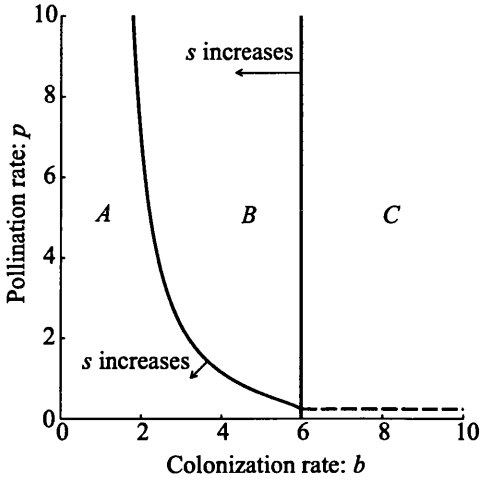

Figure 3-3: (b, p)-parameter space for the self-compatible sexual species model (3.2.5) is divided into three regions of distinct model behaviour: A - Region of population extinction for all initial population sizes, B - Region of population survival conditional on initial population size exceeding a threshold, C - Region of unconditional population survival. For very small cross-pollination rates in region C all depensation is lost (below dashed line), this is because the level of pollination is nearly independent of population size. Parameters $s = 0.2$.

3.3 GYNODIOECY

The case of gynodioecy discussed in chapter 1 section 1.4 can be treated with the general model restricted to two conspecific classes one of females and one of hermaphrodites. A gynodioecious population features sexually reproducing hermaphrodite and female individuals. Female individuals are assumed to bear a non-nuclear male-sterility allele, which has disabled male function. As a result of reallocation of reproductive resources female function in female individuals is assumed to be slightly enhanced. Since the male-sterility allele is non-nuclear individuals inherit their maternal parent's reproductive mode. Hermaphrodite individuals may or may not be capable of selfing, it is assumed that selfed offspring are as fit as outcrossed offspring.

In fact the model derived here will be general enough to treat pseudogamous apomixis (see chapter 1 section 1.3), in which parthenogenetic reproduction requires fertilization of the endosperm. In the pseudogamy case the male-sterility allele of the females need not be assumed cytoplasmic since all embryos are genetically identical to

their maternal parents.

The population size of hermaphrodites is denoted u_1 and that of females u_2. It is assumed that females and hermaphrodites compete for existence within the same niche and are identically competitive so that

$$A = \begin{pmatrix} 1 & 1 \\ 1 & 1 \end{pmatrix}.$$

Since all individuals rely upon hermaphrodites for pollination the inter-pollination matrix for the system is

$$P = \begin{pmatrix} p & 0 \\ p & 0 \end{pmatrix},$$

where it has been assumed that females and hermaphrodites respond to pollen in the same way (i.e. $p_{11} = p_{21} = p$.) Hermaphrodites are capable of self-fertilization at a level s. Females have an enhanced female function and so set more seed with the pollen that they receive. The reproductive matrix for offspring recruited to the hermaphrodite class is

$$B_1 = (b_{ij1}) = \begin{pmatrix} b & 0 \\ 0 & 0 \end{pmatrix},$$

and for the female class

$$B_2 = (b_{ij2}) = \begin{pmatrix} 0 & 0 \\ \mu b & 0 \end{pmatrix},$$

where μ has been introduced to parameterize the ratio of female to hermaphrodite seed production. The resulting model is

$$\begin{aligned} \frac{du_1}{dt} &= \frac{bu_1(s+pu_1)}{1+s+pu_1}(1-u_1-u_2) - u_1, \\ \frac{du_2}{dt} &= \frac{\mu bpu_1u_2}{1+pu_1}(1-u_1-u_2) - u_2. \end{aligned} \tag{3.3.1}$$

Biologically reasonable solutions of (3.3.1) exist for all $t \in [0, \infty)$, since the system is readily demonstrated invariant on any compact set $\triangle_k = \{(x_1, x_2) | \ 0 \leq x_1 \leq k - x_2, \ 0 \leq x_2 \leq k - x_1\}$ with $k > 1$.

Behaviour of Nullclines

$\dot{u}_1 = 0$ is satisfied by $u_1 = 0$ and

$$u_2 = f_1(u_1) = -u_1 + \frac{b-1}{b} - \frac{1}{b(s+pu_1)}.$$

f_1 has an asymptote at $-s/p$ and takes positive values in the first quadrant for $u_1 \in (\hat{u}^-, \hat{u}^+)$ when $s \geq 1$, $b > 1$ and $p > p_{\text{crit}}$, where $\hat{u}^-$ and $\hat{u}^+$ are defined in (3.2.6) and p_{crit} is defined in (3.2.7). f_1 attains a maximum in the first quadrant at

$$\left(\frac{\sqrt{bp} - bs}{bp}, \frac{sb - 2\sqrt{bp} + p(b-1)}{bp}\right).$$

$\dot{u}_2 = 0$ is satisfied by $u_2 = 0$ and when

$$u_2 = f_2(u_1) = -u_1 + \frac{\mu b - 1}{\mu b} - \frac{1}{\mu b p u_1}.$$

f_2 has an asymptote at $u_1 = 0$ and takes positive values in the first quadrant for $u_1 \in (\check{u}_1^-, \check{u}_1^+)$ where

$$\check{u}^{\pm} = \frac{\mu b - 1}{2\mu b} \pm \sqrt{\left(\frac{\mu b - 1}{2\mu b}\right)^2 - \frac{1}{\mu b p}}. \tag{3.3.2}$$

f_2 attains a maximum in the first quadrant at

$$\left(\frac{1}{\sqrt{\mu bp}}, \frac{(\mu b - 1)p - 2\sqrt{\mu bp}}{\mu bp}\right).$$

The equilibria of (3.3.1) occur at intersections of nullclines. The system has a maximum of four biologically relevant equilibria. The system inherits three equilibria from (3.2.5) which describes the behaviour of a hermaphrodite population in the absence of females. In addition there may be one intersection of f_1 and f_2 in the interior of the first quadrant. By considering the behaviour of the nullclines as b, p, μ or s get very large, it can be shown that, where they lie in the first quadrant, the nullclines are always

inside the region $\triangle_1$. Begin by noting that for $u_1 \in (0,1]$

$$\begin{aligned}
b_1 > b_2 \geq 1,\ p \geq p_{\text{crit}},\ s \geq 0 &\iff f_1(u_1;b_1) > f_1(u_1;b_2),\\
b \geq 1,\ p_1 > p_2 \geq p_{\text{crit}},\ s \geq 0 &\iff f_1(u_1;p_1) > f_1(u_1;p_2),\\
b \geq 1,\ p \geq p_{\text{crit}},\ s_1 > s_2 \geq 0 &\iff f_1(u_1;s_1) > f_1(u_1;s_2),\\
b_1 > b_2 \geq 1,\ p \geq p_{\text{crit}},\ \mu \geq 1 &\iff f_2(u_1;b_1) > f_2(u_1;b_2),\\
b \geq 1,\ p_1 > p_2 \geq p_{\text{crit}},\ \mu \geq 1 &\iff f_2(u_1;p_1) > f_2(u_1;p_2),\\
b \geq 1,\ p \geq p_{\text{crit}},\ \mu_1 > \mu_2 \geq 1 &\iff f_2(u_1;\mu_1) > f_2(u_1;\mu_2).
\end{aligned}$$

So that f_1 and f_2 are monotonically increasing with respect to each of their parameters. Now if $u_1 \in (0,1]$ then

$$\begin{aligned}
f_1(u_1) &\to 1-u_1 && \text{as } b \to \infty,\\
f_1(u_1) &\to \tfrac{b-1}{b} - u_1 && \text{as } p \to \infty,\\
f_1(u_1) &\to \tfrac{b-1}{b} - u_1 && \text{as } s \to \infty,\\
f_2(u_1) &\to 1-u_1 && \text{as } b \to \infty,\\
f_2(u_1) &\to \tfrac{\mu b-1}{\mu b} - u_1 && \text{as } p \to \infty,\\
f_2(u_1) &\to 1-u_1 && \text{as } \mu \to \infty.
\end{aligned}$$

It follows that if f_1 and f_2 intersect in the interior of the first quadrant the resulting equilibria must be in $\triangle_1^\circ$ the interior of $\triangle_1$.

Self-Incompatibility

By restricting (3.3.1) to $s = 0$ the fate of females with an enhanced female function in a population of self-incompatible hermaphrodite conspecifics can be examined. Under the self-incompatibility assumption

$$(f_2 - f_1)(u_1) = (\mu - 1)\left(\frac{1+pu_1}{\mu b p u_1}\right),$$

so that $\mu \geq 1 \Rightarrow f_2(u_1) \geq f_1(u_1)$ for all $u_1 \in (0,\infty)$, with equality if and only if $\mu = 1$.

In the case of no female reproductive advantage ($\mu = 1$) there is a curve of equilibria. Solutions follow linear rays through the origin, since hermaphrodites and females have

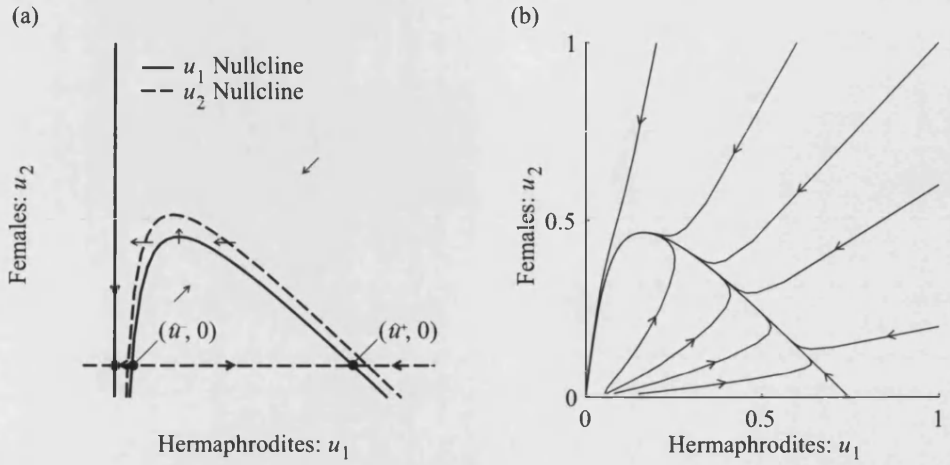

Figure 3-4: A self-incompatible species of sexually reproducing hermaphrodites is vulnerable to non-nuclear male-sterility mutations. If females who bear the mutation have an appreciably enhanced female function ($\mu > 1$) the mutation will spread. The non-spatial gynodioecy model presented here predicts that as the mutation spreads pollen becomes scarce and the population is driven into decline. (a) Nullclines of the gynodioecy model: Arrows indicate the direction of flow; Filled circles highlight equilibria. Under self-incompatibility assumptions ($s = 0$) the non-axial nullclines cannot intersect. (b) Sample solutions with parameters $b = 5$, $p = 5$, $\mu = 1.1$.

the same the per capita growth rate given by

$$\frac{bpu_1(1 - u_1 - u_2)}{1 + pu_1} - 1.$$

Solutions move toward the origin when above the curve of equilibria and away when below. The basin of attraction in the first quadrant for the curve of equilibria is

$$\Big\{(x, y)|\ y \le f_1(x)\Big\} \cup \Big\{(x, y)|x \ge \sqrt{1/2bp},\ y \le f_1\Big(\sqrt{1/2bp}\Big)x\Big\},$$

which is empty if $f_1(x) < 0$. The remainder of the first quadrant is attracted to the origin.

For $\mu > 1$ the model has a maximum of three equilibria: the origin and $(\hat{u}^{\pm}, 0)$ where $\hat{u}^{\pm}$ are equilibria of the hermaphrodite only system given in (3.2.2). The origin is a stable node and for $p < p_{\text{crit}}$ (p_{crit} defined in (3.2.3)) it is the only equilibrium in the first quadrant. The model undergoes a saddle-node bifurcation at $p = p_{\text{crit}}$,

the saddle-node equilibrium $(\hat{u}^+, 0) = (\hat{u}^-, 0)$ present at this point has stable manifold $W_s(\hat{u}^+, 0) = \{(x, 0) | \ x \geq \hat{u}^+\}$. For $p > p_{\text{crit}}$ both non-trivial equilibria exist and are distinct: $(\hat{u}^-, 0)$ is an unstable node and $(\hat{u}^+, 0)$ is a saddle point whose stable manifold lies on the hermaphrodite axis (as is demostrated by the stability of $\hat{u}^+$ under (3.2.1).)

Claim 1. *For $s = 0$ and $\mu > 1$ the origin attracts all orbits in the first quadrant except, when $p > p_{\text{crit}}$, those lying on $\{(x, 0) | \ x \geq \hat{u}^-\}$.*

Proof. $\triangle_k$ is a forward invariant compact set for all $k \geq 1$, with equilibria occurring only on the boundary. By the Poincaré-Bendixson theorem the ω-limit set of each point in $\triangle_k$ must contain one of these equilibria. When they exist and are distinct the stability of the non-trivial equilibria indicates that $(\hat{u}^-, 0)$ attracts no orbits except itself, and $(\hat{u}^+, 0)$ attracts, besides itself, precisely two orbits $W_s^-(\hat{u}^+, 0) = \{(x, 0) | \ \hat{u}^+ > x > \hat{u}^-\}$ and $W_s^+(\hat{u}^+, 0) = \{(x, 0) | \ x > \hat{u}^+\}$. So that all points in $\triangle_k \backslash \{(x, 0) | \ x \geq \hat{u}^-\}$ have only the origin in their ω-limit sets. □

It is instructive to consider the proportion of hermaphrodites in the population

$$q = \frac{u_1}{u_1 + u_2}.$$

On $\triangle_1^\circ$ this value strictly decreases over time since

$$\frac{dq}{dt} = \frac{(1 - \mu) b p u_1}{1 + p u_1} q(1 - q)(1 - u_1 - u_2).$$

So it is clear that hermaphrodites will be driven from the population, with the logical consequence that females cannot persist in their absence. Although it is positive definite and strictly decreasing on $\triangle_1^\circ$, q is not a satisfactory Lyapunov function because it is not defined on an open set of the origin at which it is, in any event, singular.

Behaviour of Boundary Equilibria

For the full gynodioecy model the possible equilibria on the boundary of the first quadrant are the origin and $(\hat{u}^\pm, 0)$ where $\hat{u}^\pm$ are equilibria of the hermaphrodite only system with self-compatibility given in (3.2.6). Clearly for $s = 0$ these equilibria match the self-incompatible case discussed above, so here the discussion concerns the case $s > 0$. The stability of these equilibria and local behaviour of solutions near

these equilibria are obtained by considering the eigenvalues of the Jacobian of (3.3.1) evaluated at the origin. Bifurcation phenomena occur at these boundary equilibria at the critical pollination level $p = p_{\text{crit}}$ (p_{crit} is given in (3.2.7).)

The origin has Jacobian

$$J(0,0) = \begin{pmatrix} \dfrac{bs}{1+s} - 1 & 0 \\ 0 & -1 \end{pmatrix}.$$

Both eigenvalues of the origin are negative if $s < 1/(b-1)$ and the origin is stable and locally attracting. For $s > 1/(b-1)$ the origin is an unstable saddle point, attracting only orbits on the female axis. Similarly if $s = 1/(b-1)$ the origin is unstable and from the first quadrant attracts only orbits on the female axis. In summary

$$(0,0)\begin{cases} \text{is stable and attracting} & \text{if } s < 1/(b-1). \\ \text{is unstable (attracts } u_2\text{−axis)} & \text{if } s \geq 1/(b-1). \end{cases}$$

The non-trivial boundary equilibria exist when $p \geq p_{\text{crit}}$. The Jacobians for the nontrivial equilibria are

$$J(\hat{u}^{\pm}, 0) = \begin{pmatrix} \left(\dfrac{(b-1)p - bs - 2bp\hat{u}^{\pm}}{1+s+p\hat{u}^{\pm}}\right)\hat{u}^{\pm} & \dfrac{\hat{u}^{\pm}}{1-\hat{u}^{\pm}} \\ 0 & \dfrac{\mu bp\hat{u}^{\pm}(1-\hat{u}^{\pm})}{1+p\hat{u}^{\pm}} - 1 \end{pmatrix}.$$

The eigenvalues of $(\hat{u}^{\pm}, 0)$ are thus

$$\begin{aligned} \lambda_1^{\pm} &= \frac{\hat{u}^{\pm}((b-1)p - bs - 2bp\hat{u}^{\pm})}{1+s+p\hat{u}^{\pm}}, \\ \lambda_2^{\pm} &= \frac{\mu bp\hat{u}^{\pm}(1-\hat{u}^{\pm})}{1+p\hat{u}^{\pm}} - 1. \end{aligned} \tag{3.3.3}$$

$\lambda_1^{\pm}$ have associated eigenvectors along the hermaphrodite axis. $\lambda_1^{\pm}$ is negative for

$$\hat{u}^{\pm} > \frac{b-1}{2b} - \frac{s}{2p},$$

as might be expected this always holds for $\hat{u}^+$ and always fails for $\hat{u}^-$ (see (3.2.6)). So that $(\hat{u}^+,0)$ always has one negative eigenvalue and $(\hat{u}^-,0)$ always has a positive one. For $p = p_{\text{crit}}$, $(\hat{u}^-,0) = (\hat{u}^+,0)$ and this equilibrium, which has a zero eigenvalue, is always unstable since $\omega^+(u_1,0) = \{0\}$ for $u_1 < \hat{u}^-$.

λ_2^+ is negative when $f_2(x) = 0$ has no solutions or has solutions the largest of which $\check{u}^+$ is less than $\hat{u}^+$. When $\check{u}^+ = \hat{u}^+$ $(\hat{u}^+,0)$ has a zero eigenvalue. $\lambda_2^+ > 0$ when $\check{u}^+ > \hat{u}^+$. The value of μ for which $\check{u}^+ = \hat{u}^+$ is denoted μ_0 and is given by

$$\mu_0 = \begin{cases} -\frac{\gamma_1}{2} - \sqrt{\left(\frac{\gamma_1}{2}\right)^2 - \gamma_0} & \text{for } 0 < s < \frac{1}{b-1} \\ \frac{(b-1)((2b-1)(b-1)p - b)}{(b^2-(b-1)^2p)((b-1)^p - b)} & \text{for } s = \frac{1}{b-1} \\ -\frac{\gamma_1}{2} + \sqrt{\left(\frac{\gamma_1}{2}\right)^2 - \gamma_0} & \text{for } s > \frac{1}{b-1} > 0 \end{cases} \tag{3.3.4}$$

where

$$\begin{aligned} \gamma_1 &= \frac{p^2 s + bp(2p+2+s(s+1)) - b^2 s(p^2 + p(1+s) + s)}{bp(p+s+1)(bs-s-1)}, \\ \gamma_0 &== \frac{(b-1)ps + b(s-1-p)}{b(p+s+1)(bs-s-1)}. \end{aligned} \tag{3.3.5}$$

For $\mu < \mu_0$ the hermaphrodite-only carrying capacity equilibrium $(\hat{u}^+,0)$ is a stable node, for $\mu > \mu_0$ it is an unstable saddle point. When $\mu = \mu_0$ a transcritical bifurcation occurs, $(\hat{u}^+,0)$ is still locally attracting in the first quadrant, however. In summary

$$(\hat{u}^+,0) \begin{cases} \text{is unstable} & \text{if } p = p_{\text{crit}}. \\ \text{is stable and attracting} & \text{if } p > p_{\text{crit}} \text{ and } \mu \le \mu_0. \\ \text{is unstable (attracts locally on } u_1\text{−axis)} & \text{if } p > p_{\text{crit}} \text{ and } \mu > \mu_0. \end{cases}$$

The eigenvalue λ_2^- is negative when $f_2(x) = 0$ has no solutions or has solutions the smallest of which $\check{u}^-$ is greater than $\hat{u}^-$. This is always true when $\hat{u}^- \le 0$, that is for $s \ge 1/(b-1)$. For $s < 1/(b-1)$ if $\check{u}^- = \hat{u}^-$ then $\lambda_2^- = 0$, and if $\check{u}^- < \hat{u}^-$ then $\lambda_2^- > 0$.

The value of μ for which $\check{u}^- = \hat{u}^-$ is denoted $\mu_{\max}$ and is given by

$$\mu_{\max} = \begin{cases} -\frac{\gamma_1}{2} + \sqrt{\left(\frac{\gamma_1}{2}\right)^2 - \gamma_0} & \text{for } 0 < s < \frac{1}{b-1} \\ \infty & \text{for } s \geq \frac{1}{b-1} \end{cases} \tag{3.3.6}$$

It is practical to define $\mu_{\max} = \infty$ for $s \geq \frac{1}{b-1}$ since in the following section it will be shown that in general the system has an internal equilibrium while $\mu \in (\mu_0, \mu_{\max})$. For $\mu < \mu_{\max}$ the hermaphrodite-only threshold equilibrium $(\hat{u}^-, 0)$ is an unstable saddle point, for $\mu > \mu_{\max}$ it is an unstable node. When $\mu = \mu_{\max}$ a transcritical bifurcation occurs, at this point $(\hat{u}^-, 0)$ attracts no orbits from the first quadrant. In summary

$$(\hat{u}^-, 0) \begin{cases} \text{is unstable} & \text{if } p = p_{\text{crit}}. \\ \text{is unstable} & \text{if } p > p_{\text{crit}} \text{ and } s = \dfrac{1}{b-1}. \\ \text{is unstable (saddle)} & \text{if } p > p_{\text{crit}},\ 0 < s < \dfrac{1}{b-1} \text{ and } \mu < \mu_{\max}. \\ \text{is unstable} & \text{if } p > p_{\text{crit}},\ 0 < s < \dfrac{1}{b-1} \text{ and } \mu \geq \mu_{\max}. \end{cases}$$

Behaviour of Internal Equilibrium

For $\mu > 1$, f_1 and f_2 intersect only once for $u_1 \geq 0$, the resulting equilibrium is labelled $(\hat{u}_1, \hat{u}_2)$ and is given by

$$\begin{aligned} \hat{u}_1 &= \frac{-(s+1)}{2p} + \sqrt{\left(\frac{s+1}{2p}\right)^2 + \frac{s}{p^2(\mu-1)}}, \\ \hat{u}_2 &= f_1(\hat{u}_1) = f_2(\hat{u}_1). \end{aligned} \tag{3.3.7}$$

It was shown above that no intersections occur for $\mu = 1$. For $\mu > 1$, when $f_1(\hat{u}_1) > 0$ and $f_2(\hat{u}_1) > 0$ an internal equilibrium occurs in the first quadrant. Algebraically this is entirely equivalent to requiring that $\hat{u}^{\pm}$, $\check{u}^{\pm}$ exist and $\hat{u}^+ < \check{u}^+$, $\hat{u}^- < \check{u}^-$ for a given μ. In the previous section it was demonstrated that these conditions are satisfied if $p > p_{\text{crit}}$ and $\mu > \mu_0$ or if $s < 1/(b-1)$ and $\mu < \mu_{\max}$. For $s \geq 1/(b-1)$, it is clear

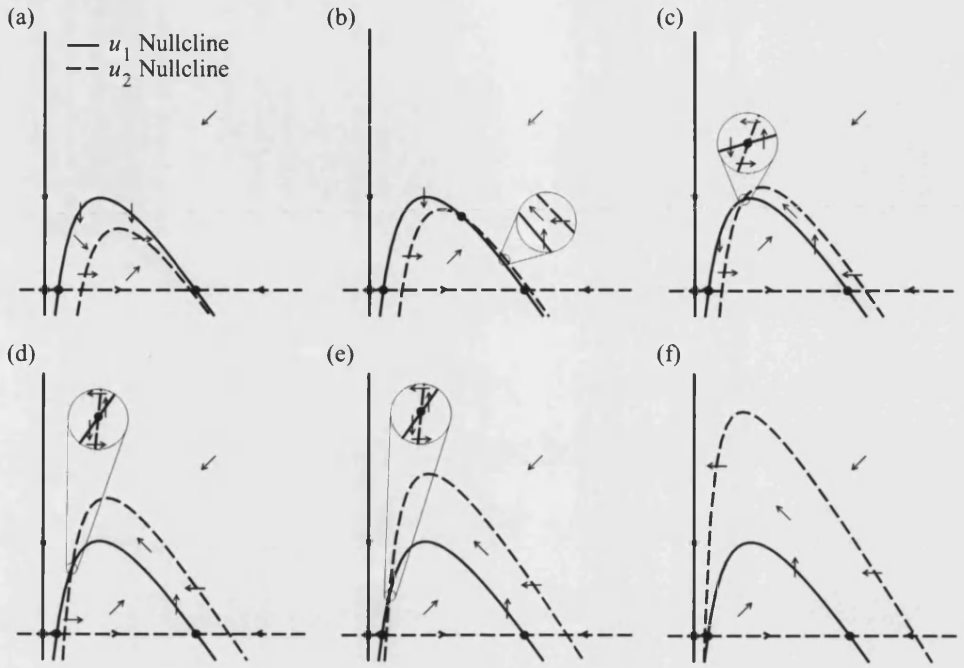

Figure 3-5: Nullclines for the gynodioecy model with selfing ($s > 0$) as the female advantage parameter μ increases, under the assumption that a hermaphrodite only population is viable ($p > p_{\text{crit}}$) but exhibits critical depensation ($s < 1/(b-1)$). Illustration uses specific parameters $b = 3.5$, $p = 3.5$, $s = 0.25$ (a) $\mu = 1$. (b) $\mu = 1.08$. (c) $\mu = 1.2$. (d) $\mu = 1.4$. (e) $\mu = 1.6$. (f) $\mu = 2.4$.

that $\hat{u}^- \leq 0$ and $\check{u}^- > 0$ so that $\hat{u}^- < \check{u}^-$ is satisfied for all μ. For $p > p_{\text{crit}}$ and $s > 0$ the equilibrium $(\hat{u}_1, \hat{u}_2)$ is in $\triangle_1^\circ$ when $\mu \in (\mu_0, \mu_{\max})$. The stability of the internal equilibrium is determined by the determinant and trace of the Jacobian evaluated at $(\hat{u}_1, \hat{u}_2)$. The determinant can be expressed in the following form

$$\det \hat{J} = \frac{p(1-\mu)^2}{\mu s} \sqrt{(s+1)^2 - \frac{4s}{1-\mu}} \left(\frac{\hat{u}_1 \hat{u}_2}{1 - \hat{u}_1 - \hat{u}_2} \right),$$

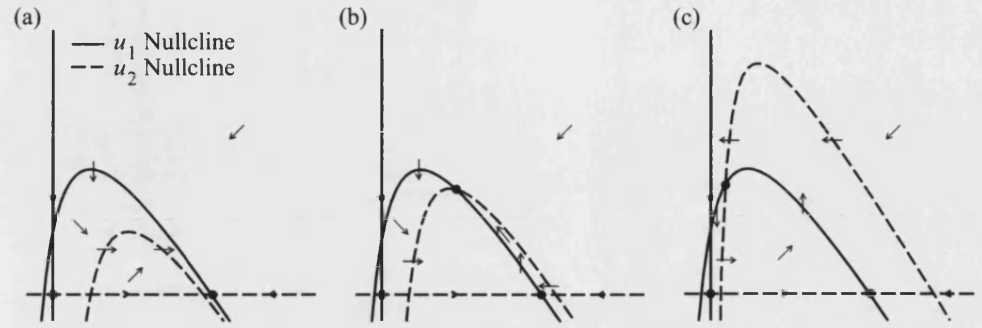

Figure 3-6: Nullclines for the gynodioecy model with selfing ($s > 0$) as the female advantage parameter μ increases, under the assumption that a hermaphrodite only population is viable ($b > 1$) and does not exhibit critical depensation ($s \geq 1/(b-1)$). Illustration uses specific parameters $b = 3.5$, $p = 3.5$, $s = 0.5$ (a) $\mu = 1$. (b) $\mu = 1.2$. (c) $\mu = 2.4$.

so it is readily seen that

$$\det \hat{J} \begin{cases} > 0 & \text{if } \mu \in (\mu_0, \mu_{\max}). \\ = 0 & \text{if } \mu \in \{\mu_0, \mu_{\max}\}. \\ < 0 & \text{if } \mu \in (1, \infty) \backslash [\mu_0, \mu_{\max}]. \end{cases}$$

In the limit of large μ

$$\begin{aligned} \lim_{\mu\to\infty} \det \hat{J} &= \lim_{\mu\to\infty} \frac{\mu-1}{\mu} \left(2 - \frac{(s+1)(\mu-1)p\hat{u}_1}{s}\right) \lim_{\mu\to\infty} \frac{\hat{u}_2}{1-\hat{u}_1-\hat{u}_2} \\ &= \frac{(b-1)s-1}{s+1}, \end{aligned}$$

since

$$\begin{aligned} \lim_{\mu\to\infty} (\mu-1)p\hat{u}_1 &= \lim_{\mu\to\infty} \frac{-(s+1)(\mu-1)}{2} + \sqrt{\left(\frac{(s+1)(\mu-1)}{2}\right)^2 + s(\mu-1)} \\ &= \lim_{\mu\to\infty} \frac{-(s+1)(\mu-1)}{2} + \frac{(s+1)(\mu-1)}{2}\left(1 + \frac{2s}{(s+1)^2(\mu-1)} + O\left(\frac{1}{\mu^2}\right)\right) \\ &= \frac{s}{s+1}. \end{aligned}$$

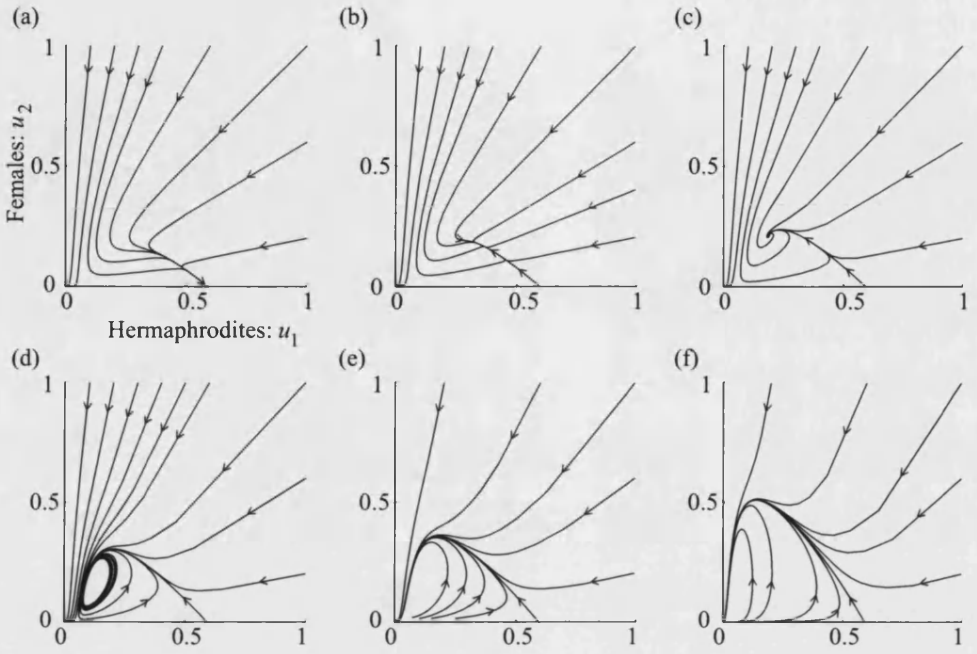

Figure 3-7: Sample solutions for the gynodioecy model with selfing ($s > 0$) as the female advantage parameter μ increases, under the assumption that a hermaphrodite only population is viable ($p > p_{\text{crit}}$) but exhibits critical depensation ($s < 1/(b-1)$). Illustration uses specific parameters $b = 3.5$, $p = 3.5$, $s = 0.25$ (a) $\mu = 1$. (b) $\mu = 1.08$. (c) $\mu = 1.2$. (d) $\mu = 1.4$. (e) $\mu = 1.6$. (f) $\mu = 2.4$.

Since $\det \hat{J} > 0$ when $\mu \in (\mu_0, \mu_{\max})$ the stability of $(\hat{u}_1, \hat{u}_2)$ depends on solely on the trace, which is given by

$$\text{tr}\hat{J} = 1 - b + \frac{b+1}{w} - \frac{s}{w(w-1)},$$

where $w = 1 + s + p\hat{u}_1$. Observe that

$$\mu \to 1^+ \Rightarrow w \to \infty \Rightarrow \text{tr}\hat{J} \to 1 - b,$$

so that for μ near 1 the trace is strictly negative if $b > 1$. The trace is increasing only when $w > w^+$ where

$$w^+ = \frac{b + s + 1 + \sqrt{s(b+s+1)}}{b+1},$$

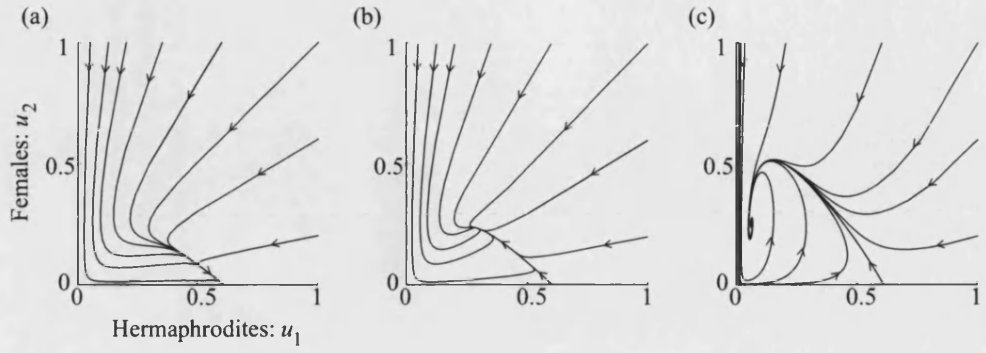

Figure 3-8: Sample solutions for the gynodioecy model with selfing ($s > 0$) as the female advantage parameter μ increases, under the assumption that a hermaphrodite only population is viable ($b > 1$) and does not exhibit critical depensation ($s \geq 1/(b-1)$). Illustration uses specific parameters $b = 3.5$, $p = 3.5$, $s = 0.5$ (a) $\mu = 1$. (b) $\mu = 1.2$. (c) $\mu = 2.4$.

that is to say for $\mu \in (1, \mu^+)$ with

$$\mu^+ = \begin{cases} 1 + \dfrac{1}{w^+(w^+ - s - 1)} & \text{for } s < \frac{1}{b-1}. \\ \\ \infty & \text{for } s \geq \frac{1}{b-1}. \end{cases}$$

Now observe that

$$\mu \to \infty \Rightarrow w \to s + 1 \Rightarrow \mathrm{tr}\hat{J} \to \frac{1 - s(b-1)}{s+1}.$$

This limiting value is strictly positive if $s < 1/(b-1)$ and non-positive otherwise. For $s \geq 1/(b-1)$ as μ increases the trace is always strictly negative. For $s < 1/(b-1)$ as μ increases the trace is initially strictly negative, passes through zero and is thereafter strictly positive. In this case $\mathrm{tr}\hat{J} = 0$ for $\mu = \mu_2$ where

$$\mu_2 = \frac{(b+1) - s(b-1)}{(b+s+1)\sqrt{1 - s(b-1)}} + \frac{s}{b+s+1}.$$

When $\mu = \mu_0$ the equilibria $(\hat{u}_1, \hat{u}_2)$ and $(\hat{u}^+, 0)$ coincide In the above section it was demonstrated that the Jacobian at this point has one negative and one zero eigenvalue and so has a strictly negative trace, therefore $\mu_0 < \mu_2$. It remains to elucidate the local

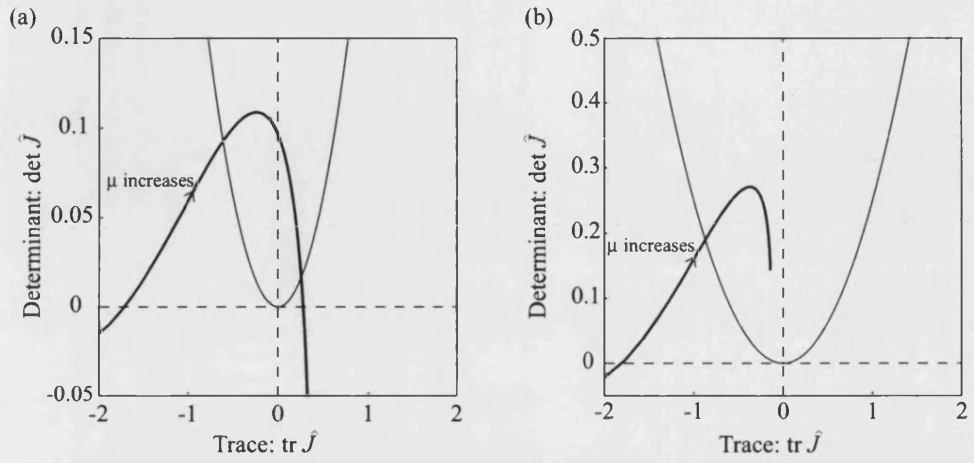

Figure 3-9: The stability of the internal equilibrium and behaviour of local solutions is prescribed by the determinant and trace of the Jacobian evaluated at the equilibrium. The figures show sample trajectories in $(\mathrm{tr}\hat{J}, \det \hat{J})$-space as the female reproductive advantage parameter μ increases on $[1, \infty)$. Note that while $\det \hat{J} < 0$ there is no internal equilibrium in $\triangle_k$. (a) Sample trajectory for low self-pollination ($0 < s < 1/(b-1)$), parameters: $b = 4$, $p = 4$, $s = 0.2$. (b) Sample trajectory for high self pollination ($s \geq 1/(b-1)$), parameters: $b = 4$, $p = 4$, $s = 0.4$.

behaviour of solutions when the internal equilibrium is stable and when it is unstable. In fact the internal equilibrium is sometimes a node and sometimes a focus but there are not elegant expressions for the value of μ at which this transition occurs. The path traced through $(\mathrm{tr}\hat{J}, \det \hat{J})$-space as μ increases is illustrated in Figure 3-9(a) for an example with $s < 1/(b-1)$ and in (b) with $s \geq 1/(b-1)$. The intersections of the curve with $\det \hat{J} = (\mathrm{tr}\hat{J}/2)^2$ indicate when the equilibrium switches between a node and a focus. For $s < 1/(b-1)$ intersections occur once when $\mathrm{tr}\hat{J} < 0$ and once when $\mathrm{tr}\hat{J} > 0$. The value of μ at the former is denoted μ_1 and at the latter μ_3. If $s \geq 1/(b-1)$ then $\mathrm{tr}\hat{J} < 0$ for all values of μ, an intersection is assured, since

$$\lim_{\mu \to \infty} \mathrm{tr}\hat{J} = - \lim_{\mu \to \infty} \det \hat{J}.$$

The value of μ at this point is also labelled μ_1. A summary of the transitions in stability and local behaviour for the internal equilibrium is provided in Figures 3-10 and 3-11.

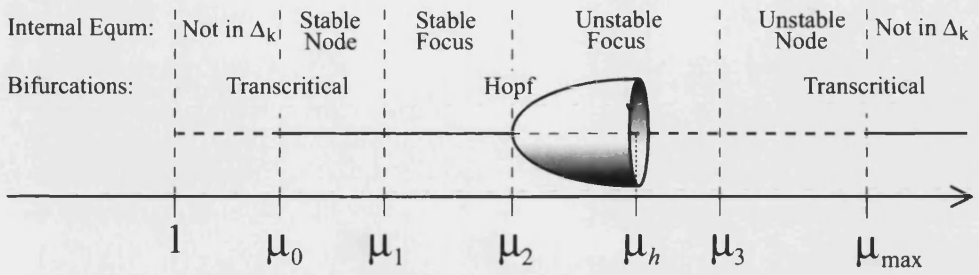

Figure 3-10: Summary of the behaviour of the internal equilibrium for the gynodioecy model with low selfing as μ increases, under the assumption that a hermaphrodite only population is viable ($p > p_{\text{crit}}$) but exhibits critical depensation ($s < 1/(b-1)$).

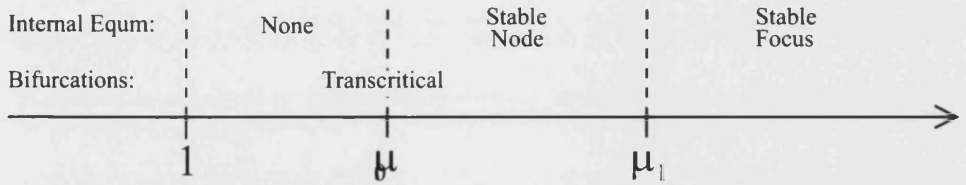

Figure 3-11: Summary of the behaviour of the internal equilibrium for the gynodioecy model with high selfing as μ increases, under the assumption that a hermaphrodite only population is viable ($b > 1$) and does not exhibit critical depensation ($s \geq 1/(b-1)$.)

Global Behaviour

The model has a different range of global behaviours for $0 < s < 1/(b-1)$ and $s \geq 1/(b-1)$ indicating that whether or not the underlying hermaphrodite species exhibits an Allee effect has significant consequences for the stability of gynodioecious populations

Path of the Stable Manifold of $(\hat{u}^-, 0)$

When $0 < s < 1/(b-1)$ and $p > p_{\text{crit}}$ the equilibrium $(\hat{u}^-, 0)$ is always unstable, and while $\mu \in [1, \mu_{\text{max}})$ it attracts a unique orbit in the first quadrant. This stable manifold, denoted $W_s^+(\hat{u}^-, 0)$, has a great deal of influence on global model behaviour. Here its trajectory is examined in detail. Fix b, p and s so that $p > p_{\text{crit}}$ and $0 < s < 1/(b-1)$

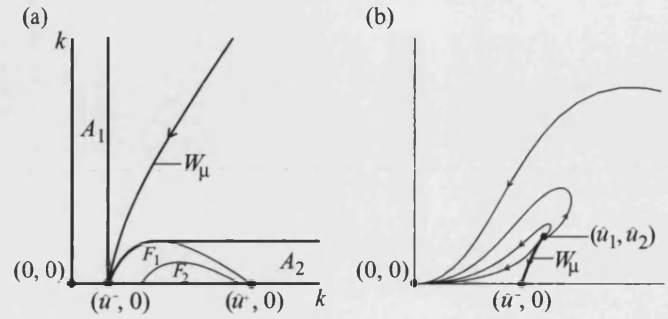

Figure 3-12: The path of the stable manifold of $(\hat{u}^-, 0)$. (a) For $\mu \in [1, \mu_1)$ the stable manifold cannot enter A_1 or A_2. (b) For μ near $\mu_{\max}$ the stable manifold originates at the unstable node $(\hat{u_1}, \hat{u_2})$.

define the following regions

$$F_1 = \{(x, y) \in \triangle_1 \mid y \leq f_1(x)\},$$
$$F_2 = \{(x, y) \in \triangle_1 \mid y \leq f_2(x)\}.$$

It should be borne in mind that F_1 is independent of μ while F_2 is not. Since b, p and s are fixed write the gynodioecy model

$$\frac{du_1}{dt} = f(u_1, u_2),$$
$$\frac{du_2}{dt} = g(u_1, u_2; \mu),$$

and denote $W_s^+(\hat{u}^-, 0)$ by W_μ in both cases to emphasize the dependence on μ.

The behaviour of W_μ near either end of the range $[1, \mu_{\max})$ is readily discerned. If $\mu \in [1, \mu_1)$ then F_2 is a strict subset of F_1 so that the regions

$$A_1 = \{(x, y) \in \mathbb{R}^2_+ \mid x \leq \hat{u}^-\},$$
$$A_2 = F_1 \cup \left\{(x, y) \in \mathbb{R}^2_+ \mid x \geq \frac{\sqrt{bp} - bs}{bp},\ y \leq \frac{sb - 2\sqrt{bp} + p(b-1)}{bp}\right\},$$

are both forward invariant sets. A_2 is invariant because

$$\left(\frac{\sqrt{bp}-bs}{bp}, \frac{sb-2\sqrt{bp}+p(b-1)}{bp}\right)$$

is the point at which the nullcline f_1 attains it's maximum. The reverse time orbit $o^-(w_1,w_2)$ of a point $(w_1,w_2) \in W_\mu$ cannot enter A_1 or A_2 and so must include points outside the forward invariant set $\triangle_k$ for any $k > 1$. So for low μ the manifold W_μ divides $\triangle_k$ in to two forward invariant regions. At the other end of the range, when $\mu = \mu_{\max}$ the equilibrium $(\hat{u}^-, 0)$ undergoes a transcritical bifurcation, as the internal equilibrium leaves the first quadrant. Consequently there is a heteroclinic orbit between $(\hat{u}^-, 0)$ and the internal equilibrium $(\hat{u_1}, \hat{u_2})$ for $\mu \in (\mu_{\max}-\delta, \mu_{\max}+\delta)$ for some $\delta > 0$. While $\mu \in (\mu_{\max}-\delta, \mu_{\max})$ the heteroclinic orbit which is W_μ connects the node $(\hat{u_1}, \hat{u_2})$ with the saddle $(\hat{u}^-, 0)$. For μ near $\mu_{\max}$ the saddle no longer divides $\triangle_k$ in two.

The behaviour of W_μ for intermediate values of μ is now addressed.

Claim 2. *For $\mu \in [1, \mu_{\max})$, if $W_\mu \cap F_1 \neq \emptyset$ then $W_\mu \subset \triangle_1$, otherwise W_μ contains points outside $\triangle_k$ for all $k > 1$.*

Proof. Consider $o^-(w_1,w_2)$ for $(w_1,w_2) \in W_\mu \backslash F_1$, if this orbit enters F_1 it does so perpendicular to the hermaphrodite axis. Define a region A whose boundary consists of: The trajectory of W_μ between $(\hat{u}^-, 0)$ and the point (x_0, y_0) of first intersection of $o^-(w_1,w_2)$ with ∂F_1; The perpendicular between (x_0, y_0) and $(x_0, 0)$; and the interval of the hermaphrodite axis between $(\hat{u}^-, 0)$ and $(x_0, 0)$. The region A is backward invariant.

If $o^-(w_1,w_2)$ does not enter F_1 then, since solutions are constrained to travel to the right indefinitely in backward time, it eventually leaves $\triangle_k$ for all $k > 1$. □

Note that since W_μ can only enter F_1 vertically from above it must do so within F_2 and so $W_\mu \cap F_2 \backslash F_1 \neq \emptyset$. Define the set

$$A_k = \triangle_k \backslash \{(x,y) \in \mathbb{R}^2_+ \mid x > \hat{u}^+ + y\},$$

for all $k > 1$. If $W_\mu \cap F_1 = \emptyset$ then W_μ contains points outside $A_k \subset \triangle_k$, so W_μ intersects the boundary of A_k at a unique point $(\xi(w_\mu), w_\mu)$ with

$$\xi(y) = \begin{cases} \hat{u}^+ + y & \text{if } y < (k-\hat{u}^+)/2 \\ k - y & \text{if } y \geq (k-\hat{u}^+)/2 \end{cases}$$

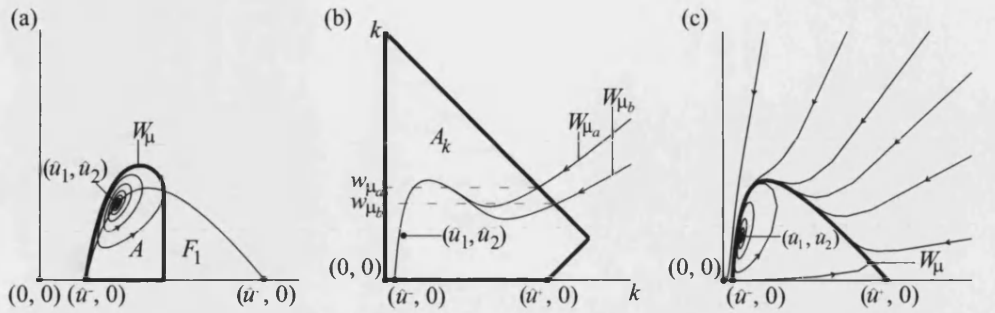

Figure 3-13: (a) If the stable manifold of $(\hat{u}^-, 0)$ enters F_1 it cannot leave $\triangle_k$. The region A is backward invariant. (b) If the stable manifold leaves A_k it is constrained to do so at a point $(\xi(w_\mu), w_\mu)$, where w_μ is monotonically decreasing with μ. In the figure $\mu_b > \mu_a$. (c) A heteroclinic orbit between between $(\hat{u}^+, 0)$ and $(\hat{u}^-, 0)$ obtains momentarily for the critical parameter value $\mu = \mu_h$.

The point is unique since f does not change sign on the relevant section of the boundary of A_k. As with W_μ the subscript emphasizes the dependency of w_μ on μ. In the following the existence of a value w_μ is taken to be synonymous with the existence of the point of intersection $(\xi(w_\mu), w_\mu)$.

Claim 3. *If $w_{\mu_a} > 0$ exists, then for $\mu_b \in (\mu_a, \mu_a + \delta_a)$ for some $\delta_a > 0$, w_{μ_b} also exists and $w_{\mu_b} < w_{\mu_a}$.*

Proof. Suppose $\xi(\mu_a) \leq \hat{u}^-$ then because of the limiting behaviour of f_1 and f_2 there exists some $\epsilon > 0$ so that the open ball $B_\epsilon(\xi(\mu_a), \mu_a)$ does not intersect $F_1 \cup F_2$. Since W_μ depends continuous on μ, there exists some $\delta_a > 0$ so that if $\mu_b \in (\mu_a - \delta_a, \mu_a + \delta_a)$ then W_{μ_b} enters $B_\epsilon(\xi(\mu_a), \mu_a)$. Since $B_\epsilon(\xi(\mu_a), \mu_a) \cap (F_1 \cup F_2) = \emptyset$, W_{μ_b} must intersect the boundary of $\triangle_k$ within $B_\epsilon(\xi(\mu_a), \mu_a)$.

Now suppose $\xi(\mu_a) > \hat{u}^-$ then there exists $\epsilon > 0$ so that $B_\epsilon(\xi(\mu_a), \mu_a)$ is entirely to the right of the perpendicular through $(\hat{u}^+, 0)$. Again there exists some $\delta_a > 0$ so W_{μ_b} enters $B_\epsilon(\xi(\mu_a), \mu_a)$ for $\mu_b \in (\mu_a - \delta_a, \mu_a + \delta_a)$. It is then impossible for W_{μ_b} to enter F_1 so that w_{μ_b} must exist.

Now given $\mu_a < \mu_b$ and that w_{μ_a} and w_{μ_b} exist, it remains to show that $w_{\mu_b} < w_{\mu_a}$. Define $X = \{x \mid (x, y) \in (W_\mu \backslash F_1) \text{ for some } y\}$. It is clear that $h_\mu : X \to \mathbb{R}$, with

$$h_\mu(x) = w, \text{ where } (x, w) \in W_\mu \backslash F_1,$$

is a well defined continuously differentiable function. The limiting gradient of $h_\mu(x)$ as $x \downarrow \hat{u}^-$ is the same as the gradient of the contracting eigenspace for $(\hat{u}^-, 0)$ which is given by

$$\frac{1-\hat{u}^-}{\hat{u}^-}\left(\frac{\hat{u}^-((b-1)p-bs-2bp\hat{u}^-)}{1+s+p\hat{u}^-}+1-\frac{\mu bp\hat{u}^-(1-\hat{u}^-)}{1+p\hat{u}^-}\right),$$

and is decreasing with μ, so that by continuity $h_{\mu_a}(x) > h_{\mu_b}(x)$ for $x \in (\hat{u}^-, \hat{u}^- + \delta)$ for some δ. Suppose that $h_{\mu_a}(x_0) = h_{\mu_b}(x_0)$ for some $x_0 \geq \hat{u}^- + \delta$ then $g(x_0, h_{\mu_a}(x_0); \mu_a) \geq g(x_0, h_{\mu_a}(x_0); \mu_b)$ which is impossible, so that $h_{\mu_a}(x) > h_{\mu_b}(x)$ for all $x > \hat{u}^-$ and as a consequence h_{μ_b} intersects the boundary of A_k a point $(\xi(w_{\mu_b}), w_{\mu_b})$ with $w_{\mu_b} < w_{\mu_a}$. □

So while the point $(\xi(w_\mu), w_\mu)$ exists w_μ is strictly decreasing with μ. A contradiction results if w_μ is assumed to exist for all $\mu \in [1, \mu_{\max})$ since in this case a heteroclinic orbit between $(\hat{u}^-, 0)$ and $(\hat{u}_1, \hat{u}_2)$ cannot occur. Consequently $w_\mu \to 0^+$ as $\mu \to \mu_h^-$, and a heteroclinic orbit between $(\hat{u}^-, 0)$ and $(\hat{u}^+, 0)$ is established when $\mu = \mu_h$.

Hopf Bifurcation and Periodic Behaviour

In the discussion of the internal equilibrium above, it was established that if $0 < s < 1/(b-1)$ the trace of the Jacobian vanishes at $\mu = \mu_2$. The Andronov-Hopf bifurcation theorem (Perko 1991, p317) establishes that at such a point the equilibrium either absorbs an unstable limit cycle (sub-critical Hopf bifurcation) or emits a stable limit cycle (super-critical Hopf bifurcation). To examine the criticality of the Hopf bifurcation in the gynodioecy model some transformations must be performed on (3.3.1). The equilibrium $(\hat{u}_1, \hat{u}_2, \mu_2)$ is translated to the origin with the substitutions $u_1^* = u_1 - \hat{u}_1$, $u_2^* = u_2 - \hat{u}_2$ and $\mu^* = \mu - \mu_2$,

$$\frac{du_1^*}{dt} = f(u_1^*, u_2^*) = (u_1^* + \hat{u}_1)\left(\frac{b(s+p(u_1^*+\hat{u}_1))(1-u_1^*-u_2^*-\hat{u}_1-\hat{u}_2)}{1+s+p(u_1^*+\hat{u}_1)} - 1\right),$$
$$\frac{du_2^*}{dt} = g(u_1^*, u_2^*) = (u_2^* + \hat{u}_2)\left(\frac{(\mu^*+\mu_2)bp(u_1^*+\hat{u}_1)(1-u_1^*-u_2^*-\hat{u}_1-\hat{u}_2)}{1+p(u_1^*+\hat{u}_1)} - 1\right).$$

Let $\hat{J} = (j_{ij})$ denote the Jacobian evaluated at $(0,0,0)$. It can be shown that $a = j_{11} = -j_{22}$, $b = -j_{12}$ and $c = j_{21}$ are always positive. Define the linear transformation

$$P = \frac{1}{\sqrt{c^2 + bc}} \begin{pmatrix} a & \sqrt{bc - a^2} \\ c & 0 \end{pmatrix},$$

then

$$P^{-1}\hat{J}P = \begin{pmatrix} 0 & \omega \\ -\omega & 0 \end{pmatrix},$$

which is the real block diagonal form of $\hat{J}$ since $\pm\omega i$ are eigenvalues of $\hat{J}$, where $\omega = \det \hat{J} = \sqrt{bc - a^2} > 0$. Now change variables to

$$\begin{pmatrix} x \\ y \end{pmatrix} = P^{-1} \begin{pmatrix} u_1^* \\ u_2^* \end{pmatrix},$$

so that the resulting system

$$\begin{pmatrix} \dot{x} \\ \dot{y} \end{pmatrix} = P^{-1} \begin{pmatrix} f(u_1^*, u_2^*) \\ g(u_1^*, u_2^*) \end{pmatrix} = \begin{pmatrix} F(x,y) \\ G(x,y) \end{pmatrix}, \tag{3.3.8}$$

is in an amenable form for analysing the criticality of the Hopf bifurcation (Marsden & McCracken 1976, pp 104-134) c.f. Perko (1991, pp 314-323).

For a system which exhibits a periodic orbit Γ through a point $\mathbf{x}_0$, and for a plane Σ through $\mathbf{x}_0$ perpendicular to Γ there exists a Poincaré or first-return map $P : \Sigma_0 \to \Sigma$ such that $P(\mathbf{x})$ is the first point at which the forward orbit of $\mathbf{x}$ intersects Σ for $\mathbf{x} \in \Sigma_0 \subset \Sigma$. Since the linearization of (3.3.8) has the appropriate real block diagonal form, Σ can be chosen as the ray $\{(x,0) \mid x \geq 0\}$. Define the displacement map $V : \Sigma \times \mathbb{R} \to \mathbb{R}$ by

$$V(x, \mu^*) = P(x, \mu^*) - x,$$

where P is the Poincaré map for (3.3.8) with bifurcation parameter μ^*. It is clear that

$$V(0) = \frac{dV}{dx}(0,0) = 0,$$

since $0 \in \Sigma$ is the stationary point of (3.3.8) which undergoes a hopf bifurcation. In fact it can be shown that $V'(0) = 0$ and $V''(0) = 0$ and that the criticality of the hopf bifurcation is distinguished by the sign of $V'''(0)$ (Unless this too is zero, which is the

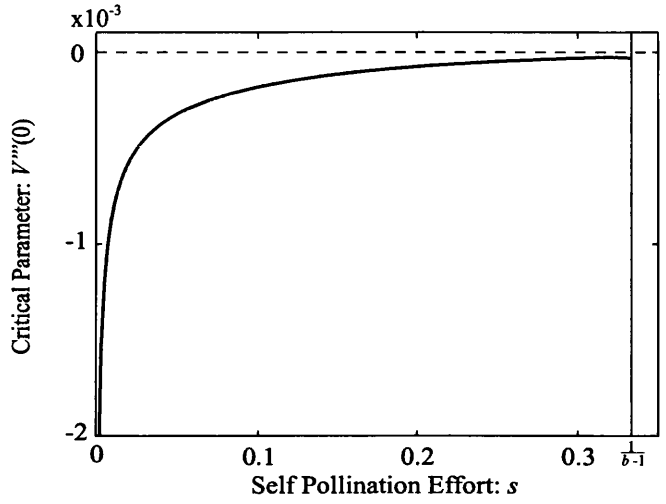

Figure 3-14: The precise behaviour of a hopf bifurcation depends upon the sign of the critical value $V'''(0)$, which depends on the models non-linear terms at the bifurcation point. For the gynodioecy model with selfing $V'''(0) < 0$ for $s \in (0, 1/(b-1))$, indicating that the hopf bifurcation is always super-critical so that a stable limit cycle is present in the model for $\mu \in (\mu_2, \mu_2 + \epsilon)$. In fact the limit cycle persists until the heteroclinic orbit between $(\hat{u}^-, 0)$ and $(\hat{u}^+, 0)$ is formed. Parameters $b = 4$ and $p = 4$ were used in the figure, $V'''(0)$ behaves similarly for all $p > p_{\text{crit}}$.

case if more than one periodic orbits are emitted or absorbed at $\mu^* = 0$.). For (3.3.8) the critical value is computed

$$V'''(0) = \frac{3\pi}{4\omega}\left(F_{xxx} + F_{xyy} + G_{xxy} + G_{yyy}\right) + \frac{3\pi}{4\omega^2}\left(-(F_{xx} - F_{yy})F_{xy} + (G_{xx} + G_{yy})G_{xy} + F_{xx}G_{xx} + F_{yy}G_{yy}\right).$$

The behaviour of the critical value is plotted in (3-14) it is negative for all $s \in (0, 1/(b-1))$ with fixed b and p, indicating that the hopf bifurcation in the gynodioecy model with selfing is super-critical.

Model Summary (Low Selfing)

When self-pollination is low ($0 < s < 1/(b-1)$) the underlying hermaphrodite population has a critical depensation threshold. This has a significant effect on the range of dynamics the gynodioecy model can exhibit. In this section global model behaviour

is deduced and summarized under the assumption that the parameters b and p are such that a hermaphrodite only population is viable, that is $p > p_{\text{crit}}$. For $p \leq p_{\text{crit}}$ global behaviour is readily deduced, since $\triangle_k$ contains only one stable equilibrium $(0,0)$. Regardless of the value of μ the ω-limit sets of all points in $\triangle_k$ contain only $(0,0)$, save in the particular case when $p = p_{\text{crit}}$ where the ω-limit set of all points in $\{(x,0) \mid x \geq \hat{u}^+ = \hat{u}^-\}$ contains only $(\hat{u}^+,0)$.

Females Cannot Invade For $\mu \leq \mu_0$ the stable manifold of $(\hat{u}^-,0)$ divides $\triangle_k$ into two non-trivial forward invariant sets both of which contain a single stable equilibrium on their boundary (see Figure 3-12(a)). These invariant sets therefore form the basins of attraction for the equilibria $(0,0)$ and $(\hat{u}^+,0)$. The asymptotic stability of $(\hat{u}^+,0)$ indicates that females certainly cannot invade a hermaphrodite population at carrying capacity. In fact females can only have a significant impact on the fate of the hermaphrodite population if they arrive in very substantial numbers, in which case their presence can drive the hermaphrodite population below its depensation threshold and to extinction. However, limitations on seed migration and the need for a substantial female population elsewhere to fund this influx, should mitigate this possibility in all practical cases. Sample solutions of the model in this case are presented in Figure 3-7(a).

Stable Coexistence For $\mu \in (\mu_0, \mu_2]$ a stable internal equilibrium $(\hat{u}_1, \hat{u}_1)$ is present in the model. The hermaphrodite carrying capacity equilibrium $(\hat{u}^+,0)$ is now unstable and attracts only orbits along the u_1-axis. The stable manifold of $(\hat{u}^-,0)$ continues to divide $\triangle_k$ into two forward invariant sets, one of which contains the origin and the other contains $(\hat{u}^+,0)$ and $(\hat{u}_1,\hat{u}_1)$. The latter set contains no periodic orbits since this would conflict with the super-criticality of the model's only Hopf bifurcation at $\mu = \mu_2$. A heteroclinic orbit connects $(\hat{u}^+,0)$ and $(\hat{u}_1,\hat{u}_1)$, indicating that if females are introduced to a hermaphrodite population at carrying capacity the result is a stable equilibrium gynodioecious population. The stable equilibrium is under-damped for $\mu \in (\mu_0, \mu_1]$, sample solutions are presented in Figure 3-7(b). The equilibrium is over-damped for $\mu \in (\mu_1, \mu_2]$ and female invasion results in transient damped oscillations between hermaphrodite and female success before equilibrium is achieved, sample solutions are presented in 3-7(c).

Limit Cycles At $\mu = \mu_2$ the model undergoes a super-critical Hopf bifurcation and a stable limit cycle is emitted. If this limit cycle undergoes no bifurcation itself then it cannot persist beyond $\mu = \mu_h$ after which a heteroclinic orbit between $(\hat{u}_1, \hat{u}_1)$ and $(\hat{u}^-, 0)$ is established. Numerical solutions indicate that this is indeed the case and the model exhibits a single stable limit cycle for $\mu \in (\mu_2, \mu_h]$. The stable manifold of $(\hat{u}^-, 0)$ divides $\triangle_k$ into basins of attraction for the origin and the limit cycle. Females can invade hermaphrodite populations from small numbers for $\mu \in (\mu_2, \mu_h)$ and the result is gynodioecious population that is stable but cycles between intervals of female and hermaphrodite success. These cycles become increasingly wild as μ approaches μ_h, hermaphrodite numbers always exceed $\hat{u}^-$ but female numbers become arbitrarily small. It is possible to argue that such small female populations would be stochastically eradicated leaving the hermaphrodite population to recover. However, for μ near μ_h the limit cycle spends much of its time near the unstable manifold of $(\hat{u}^-, 0)$ and stochastic variation, and in particular variation which increases female numbers, could move the population into the extinction region. This sensitivity to small perturbations is at its height when $\mu = \mu_h$ at which point female invasion could still theoretically result in stable cyclic coexistence, depending upon initial numbers, but in reality small fluctuations in numbers will ensure that the population either dies out or returns to a hermaphrodite only state. Sample solutions are presented in 3-7(d).

Females Cause Extinction For $\mu > \mu_h$ either there is no internal equilibrium ($\mu \geq \mu_{\max}$) or if there is the stable manifold of $(\hat{u}^-, 0)$ originates there and so no longer divides $\triangle_k$ in two. $\triangle_k$ is a forward invariant set containing no limit cycles, and a single stable equilibrium at the origin. Consequently all forward orbits, bar possibly $W_s^+(\hat{u}^-, 0)$ and those on the u_1 axis attracted to $(\hat{u}^+, 0)$, terminate at the origin. Female invasion invariably ends in population extinction. The mechanism is the same as for the gynodioecy model without selfing: the initial competitive advantage of females causes pollen shortage which drives extinction. For a species with low selfing the shortage of outcrossed pollen is not sufficiently balanced by the availability of self-produced pollen and the population cannot persist. Sample solutions are presented for $\mu \in (\mu_h, \mu_{\max})$ in Figure 3-7(e) and for $\mu \geq \mu_{\max}$ in Figure 3-7(f).

Model Summary (High Selfing)

When self-pollination is sufficiently high ($s \geq 1/(b-1)$) the underlying hermaphrodite population does not suffer from critical depensation. A small hermaphrodite population can establish from arbitrarily small numbers, as a consequence the origin in the gynodioecy model is unstable. A straightforward consequence of this is that the gynodioecy model cannot exhibit the extinction dynamics that are found in the case of low or no self-pollination. A less intuitive consequence is that the model also fails to exhibit limit cycles and all gynodioecious populations limit towards stable equilibrium coexistence.

Females Cannot Invade If $\mu \leq \mu_0$ then $\triangle_k$ contains only one stable equilibrium $(\hat{u}^+, 0)$ which is on the boundary and so globally attracting on $\triangle_k$. Females cannot persist regardless of their initial abundance and a hermaphrodite population of any size is invulnerable to invasion. Sample solutions are presented in Figure 3-8(a).

Stable Coexistence If $\mu > \mu_0$ then $\triangle_k$ contains a stable globally attracting internal equilibrium. Any gynodioecious population will limit towards stable coexistence, sample solutions in Figure 3-8(b). Transient damped oscillations occur $\mu > \mu_1$, sample solutions in Figure 3-8(c).

The transitions in model behaviour and the behaviour of the critical parameters values μ_0, μ_1, μ_2, μ_h, μ_3 and $\mu_{\max}$ in (s, μ)-parameter space are illustrated in Figure 3-15.

Discussion

Classical sex-ratio theory demands that female individuals will only persist in hermaphrodite populations if they attain in excess of twice the reproductive success of hermaphrodites (Charnov 1982, pp 10-11). Here two significant exceptions to Mendelian inheritance have been modelled. For a sexual population in which male-sterility is caused by a non-nuclear mutation, the two-fold advantage of females is not required. Non-nuclear genes are inherited solely through the maternal line, so any increase in reproductive success associated with the mutation should favour it spreading. For a pseudogamous apomictic population all genes are inherited solely through the maternal

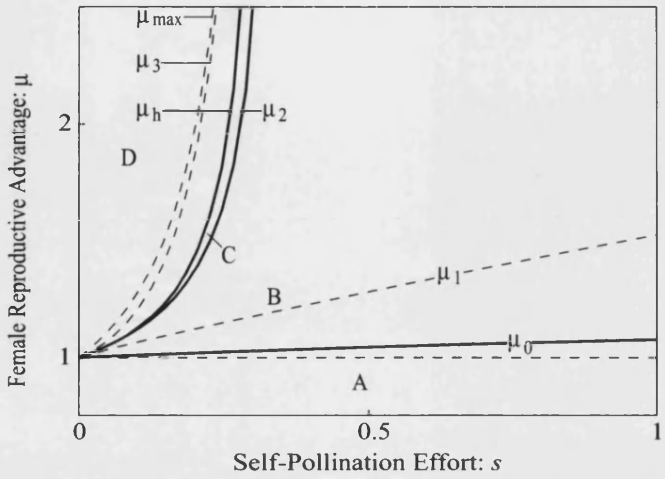

Figure 3-15: (s, μ)-parameter space for the gynodioecy model with selfing is separated into four regions of distinct model behaviour: A - Female invasion is impossible for $\mu \leq \mu_0$; B - Invasion results in a stable coexistence of females and hermaphrodites for $\mu \in (\mu, \mu_2]$; C - Invasion results in cyclic coexistence for $\mu \in (\mu_2, \mu_h)$; D - invasion results in extinction for $\mu > \mu_h$.

line and so the male-sterility mutation need not be non-nuclear in order to be favoured.

The model presented here confirms these predictions. In the absence of selfing any increase in seed production in females translates directly into improved reproductive success and permits the male-sterility mutation to spread. If hermaphrodites are capable of self-pollination then they enjoy a baseline reproductive success in the absence of outcrossed pollen. Females are deprived of that baseline and so the male-sterility mutation will only spread if the increased reproductive success derived from increased seed production exceeds that which is lost. In the model the threshold reproductive advantage for females to invade is strictly positive ($\mu_0 - 1 > 0$) and increases with the level of self-pollination in hermaphrodites. The presence of this threshold is, however, a consequence of the particular choice of functional response to pollen availability. Since with a Holling type I response, for example, there would be no pollen limitation on either hermaphrodites or females at the point of invasion.

The long term consequences of female invasion depend upon both the increased seed production of females and the level of self-pollination in hermaphrodites. In the absence of self-pollination, the introduction of females has only one possible outcome, regardless

of the size of the female reproductive advantage the population is driven extinct. For very low levels of self-pollination ($s < 1/(b-1)$) female reproductive advantage dictates model behaviour: Stable equilibrium coexistence if the advantage is small ($\mu \in (\mu_0, \mu_2]$); Limit cycles of alternating hermaphrodite and female success for intermediate values ($\mu \in (\mu_2, \mu_h]$) which as the reproductive advantage gets larger grow so wild in their oscillations that a real system would be vulnerable to stochastic eradication of either females or else the whole population; Finally for large reproductive advantages ($\mu > \mu_h$) the extinction dynamics of the model under the self-incompatibility assumption is recaptured. For greater levels of self pollination ($s \geq 1/(b-1)$) female invasion always results in stable equilibrium coexistence, although for very high female reproductive advantage there are large oscillations in the transient dynamics.

The gynodioecy model illustrates that selfing could have a central role in the coexistence of female and hermaphrodite conspecifics. This proposition applied to sexual populations seems to lack sophistication for two reasons. The first is the widespread prevalence of self-incompatibility and its likely presence in ancestral angiosperms. The second is the fitness consequences of bearing the male-sterility mutation. A CMS gene can propagate without conferring an overall fitness advantage on the carrier. If coexistence results, the gynodioecious population is less numerous than the hermaphrodite-only population that preceded it and females are less successful than hermaphrodites at passing genes into the next generation. As Charnov (1982, p 12) points out there is clearly an antagonism here between the interests of the CMS gene and the interests of other nuclear genes. The consequences of this conflict has been the evolution of nuclear fertility restoration genes, which suppress the effects of the male-sterility mutation (Schnable & Wise 1998). Clearly restoration genes would mitigate the disastrous consequences predicted by the model of CMS mutations occurring in self-incompatible hermaphrodite populations. In commercial crop breeding females lines carrying CMS genes and male or hermaphrodite lines carrying complementary fertility restorer genes are maintained in what are described as CMS systems so that male-fertile hybrids can be produced efficiently. It is not clear however that naturally occurring CMS systems promote gynodioecious coexistence, since the density independent fitness advantage of carrying the restorer gene would be expected to result in fixation. However, in a metapopulation context with several pairs of complementary CMS and fertility restoring genes a kind of fugitive coexistence can be demonstrated (Pannell 1997). CMS systems raise an evolutionary question regarding the circumstances in which fertility restoration genes might spread. If the results of the gynodioecy model with self-incompatibility

are accepted for populations prior to the evolution of fertility restoration, then the conditions for fertility restoration to have a selective advantage, that is the presence of CMS genes in the population, are highly unstable (the population is being driven extinct.) Instead of sustained conditions under which fertility restoring mutations can spread there are periods of neutral selective pressure punctuated by intermittent bursts as novel male-sterility mutations rip through whole populations causing extinction. There are therefore theoretical grounds for supposing that mechanisms promoting gynodioecious coexistence may have existed prior to the evolution of CMS systems, if indeed these can be shown to be the primary mechanism today.

In conclusion there is potentially a theoretical role for selfing in explaining gynodioecy in sexual species. The level of self-compatibility need not be high in order to open a window within parameter space in which coexistence occurs. This is consistent with the observation that self-fertility may be strategically retained at low levels by a variety of mechanisms in facultatively outcrossing species (Willson & Burley 1983, pp 37-40). A degree of protection from CMS mutations may be counted among the other advantages that low levels of selfing might accrue (the loss of critical depensation discussed in section 3.2 for example.) In at least partially self-compatible species the possibility of gynodioecious coexistence could pre-date the evolution of fertility restoration genes, with the selfing mechanism providing a background of sustained coexistence on which fertility restoration genes first gain a selective advantage.

For populations of pseudogamous apomicts the conclusion that selfing may promote gynodioecy is not strongly supported or rejected by available data. Smith (1963) identified a single male-sterile individual in a small sample of aposporous *Potentilla tabernaemontani.* As was discussed in section 1.3, in the case of pseudogamous apospory it is likely that most species are polyploid and self-compatible. In which case significant advantages may be derived from not exporting pollen, since (at least in the absence of sexual con-specifics) it has no reproductive value when dispersed to non-relatives. Aposporous blackberry species (*Rubus*) are an example of a pseudogamous species that deliberately conserves pollen (Nybom 1985). For pseudogamous apomicts there is no direct fitness disadvantage to male-sterility, since all offspring of both females and hermaphrodites inherit their genome solely from their mother. Noirot et al. (1997) advance an argument that if a proportion of pollen is retained for selfing and a proportion dispersed, then for a given trade off between male and female resource allocation there will be an evolutionarily stable balance of investment. They dismiss a priori the possibility of pseudogamous self-incompatibility, because of its vulnerability to invasion.

The non-spatial gynodioecy model would seem to support their assumption.

This section concludes with the observation that in obligately out-crossing sexual or asexual species, where self-incompatibility is absolute, the non-spatial model presented here provides no insight into the maintenance of gynodioecy.

3.4 SEXUAL-ASEXUAL

The case of inter-pollinating sexual and asexual conspecifics discussed in chapter 1 section 1.3 can be treated with a restriction of the general model (3.1.10) to two classes of conspecifics. The model derived here will assume sexuals and asexuals are physiologically very similar, so that there is no appreciable difference in competitiveness for establishment and survival. The distinction between sexuals and asexuals will be confined to their reproductive mode. Sexuals are assumed diploid, self-incompatible and hermaphrodite and asexuals are assumed to have have arisen by a single dominant mutation which confers parthenogenicity to egg cells but not polar nuclei, so that normal differentiation endosperm requires pollination. Asexuals are thus diploid, self-incompatible pseudogamous apomicts. Families in which apomicts are commonly pseudogamous include Rosaceae and Gramineae, moreover many taxa within these families contain sexual and asexual relatives and those from Gramineae often exhibit geographic parthenogenesis (Bierzychudek 1987).

Since normal male meiosis in pseudogamous apomicts is very rare (Nogler 1984), male function is assumed to be partially degenerate. Hence only a fraction of fertilization of sexual eggs by asexual pollen produce viable offspring. Degenerate partially reduced pollen would be the likely result of interrupted meioses which are commonly observed in apomicts (Nogler 1984). Such pollen may be missing chromosomes or carry corrupted or over-represented genes. By contrast all pollen whether sexual or asexual is assumed capable of fertilizing the endosperm of asexuals. Nogler (1984) observes that pollen with a more or less reduced capability to germinate appears to be sufficient to fertilize polar nuclei. The assumed arrangement is also plausible if, rather than partially reduced, a proportion of asexual pollen is unreduced. Progeny of sexuals formed with unreduced asexual pollen may be triploid and also have sub-optimal endosperm balance (2m:2p instead of 2m:1p), either of which may result in inviable seed (Vinkenoog et al. 2002). Endosperm of asexuals may achieve optimal 2m:1p endosperm balance when pollinated by unreduced pollen if one of the generative nuclei produced by the pollen fuses with the two maternal (unreduced) polar nuclei (a 2n + 2n maternal

contribution and a 2n paternal contribution). Endosperm of asexuals may also achieve optimal 2m:1p endosperm balance when pollinated by reduced pollen if both of the generative nuclei produced by the pollen fuse with the two maternal (unreduced) polar nuclei (to give a 2n + 2n maternal contribution and an n + n paternal contribution). Evidence for the latter is provided by selfing experiments on the tetraploid buttercup *Ranunculus auricomus* in which the majority (69%) of endosperm are double fertilized (Rutishauser, 1954, cited in (Nogler 1984)).

As was discussed in Chapter 1 section 1.3 the widespread existence of sexual species implies a cost to asexuality that balances the 1.5-fold cost of sex. Here such a cost is incorporated as an advantage to sexuality, in particular sexually produced seeds have a greater chance of survival than asexually produced seeds. It will be assumed for simplicity that functional pollen carries a single allele at the locus that determines reproductive mode. As a consequence all asexuals sired on sexuals will be heterozygotes. It is parsimonious to assume the original mutation was first expressed in a heterozygous individual, and since all asexuals are clones of that individual or of subsequent backcrosses with the sexual line all asexuals must likewise be heterozygous. It is assumed therefore that precisely half of all functional pollen from asexuals carries the mutant allele that confers apomixis.

The population size of sexuals is denoted u_1 and that of asexuals u_2. It is assumed that sexuals and asexuals compete for existence within the same niche and are identically competitive so that

$$A = \begin{pmatrix} 1 & 1 \\ 1 & 1 \end{pmatrix}.$$

Species specific pollen production is parameterized by p and pollination is a prerequisite of both sexual and asexual seed production so the pollination matrix is given by

$$P = \begin{pmatrix} p & p \\ p & p \end{pmatrix}.$$

Both sexuals and asexuals are assumed self-incompatible, and so no self-fertilization occurs. Sexual offspring are produced by sexuals pollinated by sexuals and by half of all asexually fertilized eggs of sexuals. However, only a proportion $\nu \in [0,1]$ of seed fertilized by asexual pollen is viable. Species specific seed production is parameterized by b, sexually produced seed has improved chance of survival specified by the modifying

parameter $\mu \geq 1$. The sexual recruitment matrix is therefore

$$B_1 = (b_{ij1}) = \begin{pmatrix} \mu b & \mu b\nu/2 \\ 0 & 0 \end{pmatrix}.$$

Asexual offspring are produced by asexuals receiving pollen from any source and also by half of all asexually fertilized eggs of sexuals, so that the asexual recruitment matrix is therefore

$$B_2 = (b_{ij2}) = \begin{pmatrix} 0 & \mu b\nu/2 \\ b & b \end{pmatrix}.$$

The resulting model is

$$\begin{aligned} \frac{du_1}{dt} &= \frac{\mu bp(u_1 + \frac{\nu}{2}u_2)u_1}{(1 + p(u_1 + u_2))}(1 - u_1 - u_2) - u_1, \\ \frac{du_2}{dt} &= \frac{bp(u_1 + u_2 + \mu\frac{\nu}{2}u_1)u_2}{1 + p(u_1 + u_2)}(1 - u_1 - u_2) - u_2. \end{aligned} \tag{3.4.1}$$

Biologically reasonable solutions of (3.4.1) exist for all $t \in [0, \infty)$, since the system is readily demonstrated invariant on any compact set $\triangle_k = \{(x_1, x_2) | \ 0 \leq x_1 \leq k - x_2, \ 0 \leq x_2 \leq k - x_1\}$ with $k > 1$.

Behaviour of Nullclines

$\dot{u}_1 = 0$ is satisfied by $u_1 = 0$ and for $\nu \in (0, 1]$ by

$$u_2 = f_1^{\pm}(u_1) = \frac{\mu\nu b - 2}{2\mu\nu b} - \frac{\nu + 2}{2\nu}u_1 \pm \sqrt{\left(\frac{\mu\nu b - 2}{2\mu\nu b} - \frac{\nu + 2}{2\nu}u_1\right)^2 + \frac{2}{\nu}\left(-u_1^2 + \frac{\mu b - 1}{\mu b}u_1 - \frac{1}{\mu bp}\right)}.$$

The components of $f_1^{\pm}$ that can pass through $\triangle_k$ are defined while

$$u_1 > \frac{\nu}{2 - \nu}\left[-\frac{2 + \mu\nu b}{\mu\nu b} + \sqrt{\frac{8(p + 1)}{\mu\nu bp}}\right].$$

It is worth noting that $f_1^{\pm}$ intersects the asexual axis for

$$\nu \geq \frac{2(p + 2) + 4\sqrt{p + 1}}{\mu bp}.$$

This only occurs for $\nu \in [0,1]$ if $p \geq p_{\text{inv}}$ where

$$p_{\text{inv}} = \frac{8\mu b}{(\mu b - 2)^2}.$$

This threshold must be met, therefore, before there is a possibility of sexuals invading an asexual population. The criteria that μ and ν must meet to permit sexuals invasion are discussed in the analysis of the boundary equilibria below. When $\nu = 0$, sexuals are coupled to asexuals only through competition. In this case the non-axial nullcline has the following familiar form

$$u_2 = f_1^0(u_1) = -u_1 + \frac{\mu b - 1}{\mu b} - \frac{1}{\mu b p u_1},$$

(cf. the non-axial hermaphrodite nullcline in the gynodioecy model without selfing.) $\dot{u}_2 = 0$ is satisfied by $u_2 = 0$ and for $\nu \in [0,1]$ by

$$f_2^{\pm}(u_1) = \frac{b-1}{2b} - \frac{4+\mu\nu}{4}u_1 \pm \sqrt{\left(\frac{b-1}{2b} - \frac{4+\mu\nu}{4}u_1\right)^2 - \left(\frac{\mu\nu+2}{2}u_1^2 + \left(\frac{1}{b} - \frac{\nu\mu+2}{2}\right)u_1 + \frac{1}{bp}\right)}.$$

f_2 is always defined for $u_1 \geq 0$.

Note that when $\nu = 1$, $\mu = 2$ the non-axial nullclines precisely overlap. This is the special case of high asexual pollen quality when all sexual-asexual crosses are viable and when the cost of sex is exactly met by the survival advantage of sexually produced seed.

Behaviour of Boundary Equilibria

The model has a maximum of five equilibria on the boundary of $\triangle_k$. The origin is an equilibrium. There are two possible non-trivial equilibria on the sexual axis. By restricting (3.4.1) to $u_2 = 0$, it is clear that these equilibria must be $(\hat{u}_1^-, 0)$ and $(\hat{u}_1^+, 0)$ where

$$\hat{u}_1^{\pm} = \frac{\mu b - 1}{2\mu b} \pm \sqrt{\left(\frac{\mu b - 1}{2\mu b}\right)^2 - \frac{1}{\mu b p}},$$

which are the non-trivial equilibria of the sexual species model given in (3.2.2) with modified birth rate μb. Similarly by restricting (3.4.1) to $u_1 = 0$ it is clear that there are two possible non-trivial equilibria on the asexual axis given by $(0, \hat{u}_2^-)$ and $(0, \hat{u}_2^+)$ where $\hat{u}_2^\pm = \hat{u}^\pm$ precisely the non-trivial equilibria of the sexual species model (3.2.2).

The origin has Jacobian

$$J(0,0) = \begin{pmatrix} -1 & 0 \\ 0 & -1 \end{pmatrix},$$

and is always a stable node.

The non-trivia equilibria $(\hat{u}_1^\pm, 0)$ exist for $p \geq p^s_{\text{crit}} = 4\mu b/(\mu b - 1)^2$ and when they exist their Jacobians are

$$J(\hat{u}_1^\pm, 0) = \begin{pmatrix} \left(\dfrac{(\mu b - 1)p - 2\mu b p \hat{u}_1^\pm}{1 + p\hat{u}_1^\pm}\right)\hat{u}_1^\pm & \left(\dfrac{(\mu\nu b - 2)p - \mu b p(\nu + 2)\hat{u}_1^\pm}{2(1 + p\hat{u}_1^\pm)}\right)\hat{u}_1^\pm \\ 0 & \dfrac{bp(2 + \mu\nu)\hat{u}_1^\pm(1 - \hat{u}_1^\pm)}{2(1 + p\hat{u}_1^\pm)} - 1 \end{pmatrix}.$$

The eigenvalues of $(\hat{u}_1^\pm, 0)$ are thus

$$\lambda_1^\pm = \left(\frac{(\mu b - 1)p - 2\mu b p \hat{u}_1^\pm}{1 + p\hat{u}_1^\pm}\right)\hat{u}_1^\pm,$$
$$\lambda_2^\pm = \frac{bp(2 + \mu\nu)\hat{u}_1^\pm(1 - \hat{u}_1^\pm)}{2(1 + p\hat{u}^\pm)} - 1,$$

The eigenvalues $\lambda_1^\pm$ have associated eigenvectors along the sexual axis. $\lambda_1^\pm$ is negative for

$$\hat{u}_1^\pm > \frac{\mu b - 1}{2\mu b},$$

this always holds for $\hat{u}_1^+$ and always fails for $\hat{u}_1^-$. So that $(\hat{u}_1^+, 0)$ always has one negative eigenvalue and $(\hat{u}_1^-, 0)$ always has a positive one. For $p = p^s_{\text{crit}}$, $(\hat{u}_1^-, 0) = (\hat{u}_1^+, 0)$ and this equilibrium, which has a zero eigenvalue, is always unstable since $\omega^+(x, 0) = \{0\}$ for all $x < \hat{u}^-$.

The eigenvalue $\lambda_2^\pm$ is negative if and only if the greater solution $\check{u}_1^+$ of $f_2(x) = 0$ is strictly less than $\hat{u}_1^+$ or what is algebraically equivalent: the lesser solution $\check{u}_1^-$ is

strictly greater than $\hat{u}_1^-$. Since

$$\breve{u}_1^{\pm} = \frac{b(\mu\nu+2)-1}{2} \pm \sqrt{\left(\frac{b(\mu\nu+2)-1}{2}\right)^2 - \frac{2}{bp(\mu\nu+2)}},$$

it is immediate that the condition holds when $\mu > \mu_1$ where

$$\mu_1 = \frac{2}{2-\nu}.$$

In this case $(\hat{u}_1^-, 0)$ is an unstable saddle and $(\hat{u}_1^+, 0)$ is a stable node. When $\mu = \mu_1$, both equilibria have zero eigenvalues and neither attract orbits from the interior of $\triangle_k$, so both are unstable. If $\mu < \mu_1$ then $(\hat{u}_1^-, 0)$ is an unstable node and $(\hat{u}_1^+, 0)$ is an unstable saddle. In summary

$$(\hat{u}_1^-, 0) \begin{cases} \text{is unstable} & \text{if } p = p^s_{\text{crit}}. \\ \text{is unstable (saddle)} & \text{if } p > p^s_{\text{crit}} \text{ and } \mu > \mu_1. \\ \text{is unstable (node)} & \text{if } p > p^s_{\text{crit}}, \text{ and } \mu \leq \mu_1. \end{cases}$$

and

$$(\hat{u}_1^+, 0) \begin{cases} \text{is unstable} & \text{if } p = p^s_{\text{crit}}. \\ \text{is stable (node)} & \text{if } p > p^s_{\text{crit}} \text{ and } \mu > \mu_1. \\ \text{is unstable (saddle)} & \text{if } p > p^s_{\text{crit}}, \text{ and } \mu \leq \mu_1. \end{cases}$$

The non-trivia equilibria $(0, \hat{u}_2^{\pm})$ exist for $p \geq p^a_{\text{crit}} = p_{\text{crit}}$ where p_{crit} is given in (3.2.3), when they exist their Jacobians are

$$J(0, \hat{u}_2^{\pm}) = \begin{pmatrix} \dfrac{\mu\nu bp\hat{u}_2^{\pm}(1-\hat{u}_2^{\pm})}{2(1+p\hat{u}_2^{\pm})} - 1 & 0 \\ \left(\dfrac{(b(2+\mu\nu)-2)p - bp(4+\mu\nu)\hat{u}_2^{\pm}}{2(1+p\hat{u}_2^{\pm})}\right)\hat{u}_2^{\pm} & \left(\dfrac{bp(1-2\hat{u}_2^{\pm})-p}{1+p\hat{u}_2^{\pm}}\right)\hat{u}_2^{\pm} \end{pmatrix}.$$

The eigenvalues of $(0, \hat{u}_2^{\pm})$ are thus

$$\sigma_1^{\pm} = \left(\frac{bp(1-2\hat{u}_2^{\pm}) - p}{1 + p\hat{u}_2^{\pm}}\right)\hat{u}_2^{\pm},$$
$$\sigma_2^{\pm} = \frac{\mu\nu bp\hat{u}_2^{\pm}(1-\hat{u}_2^{\pm})}{2(1+p\hat{u}_2^{\pm})} - 1,$$

The eigenvalues $\sigma_1^{\pm}$ have associated eigenvectors along the asexual axis. $\sigma_1^{\pm}$ is negative for

$$\hat{u}_2^{\pm} > \frac{b-1}{2b},$$

this always holds for $\hat{u}_2^{+}$ and always fails for $\hat{u}_2^{-}$. So that $(0, \hat{u}_2^{+})$ always has one negative eigenvalue and $(0, \hat{u}_2^{-})$ always has a positive one. For $p = p_{\text{crit}}$, $(0, \hat{u}_2^{-}) = (0, \hat{u}_2^{+})$ and this equilibrium, which has a zero eigenvalue, is always unstable since $\omega^{+}(0, x) = \{0\}$ for all $x < \hat{u}^{-}$.

The eigenvalue $\sigma_2^{\pm}$ is negative if and only if $f_1^{\pm}(0)$ are complex or $f_1^{+}(0) < \hat{u}_2^{+}$ or what is algebraically equivalent: $f_1^{-}(0) > \hat{u}_2^{-}$. That is when $\mu < \mu_2$ where

$$\mu_2 = \frac{2}{\nu}.$$

In this case $(0, \hat{u}_2^{-})$ is an unstable saddle and $(0, \hat{u}_2^{+})$ is a stable node. When $\mu = \mu_2$, both equilibria have zero eigenvalues and neither attract orbits from the interior of Δ_k, so both are unstable. If $\mu > \mu_2$ then $(0, \hat{u}_2^{-})$ is an unstable node and $(0, \hat{u}_2^{+})$ is an unstable saddle. In summary

$$(0, \hat{u}_2^{-}) \begin{cases} \text{is unstable} & \text{if } p = p_{\text{crit}}. \\ \text{is unstable (saddle)} & \text{if } p > p_{\text{crit}} \text{ and } \mu < \mu_2. \\ \text{is unstable (node)} & \text{if } p > p_{\text{crit}}, \text{ and } \mu \geq \mu_2. \end{cases}$$

and

$$(0, \hat{u}_2^{+}) \begin{cases} \text{is unstable} & \text{if } p = p_{\text{crit}}. \\ \text{is stable (node)} & \text{if } p > p_{\text{crit}} \text{ and } \mu < \mu_2. \\ \text{is unstable (saddle)} & \text{if } p > p_{\text{crit}}, \text{ and } \mu \geq \mu_2. \end{cases}$$

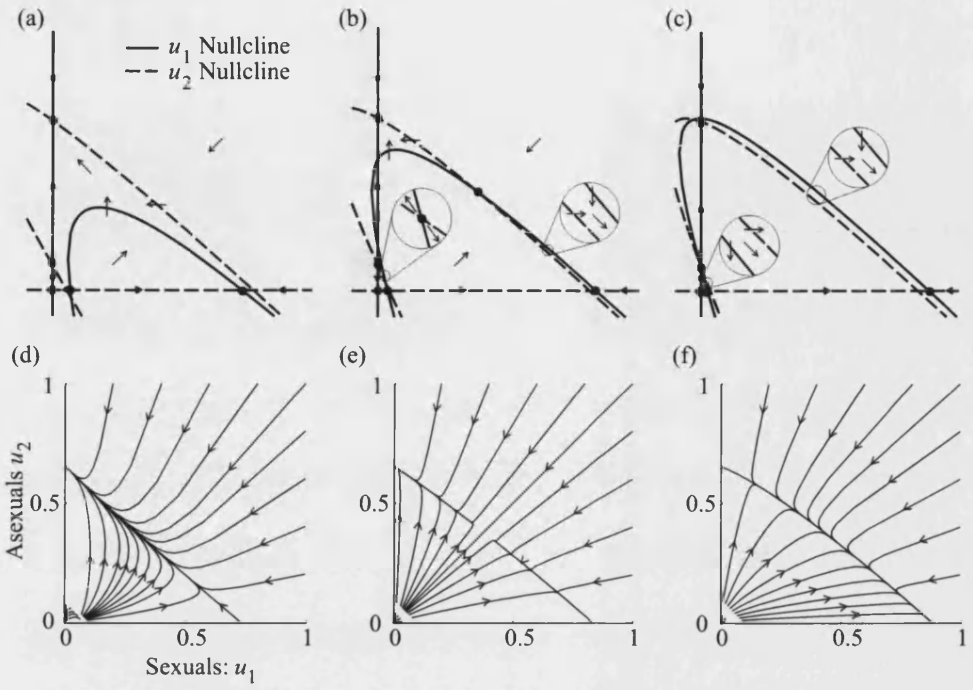

Figure 3-16: Nullclines and sample solutions for for the sexual-asexual model when both sexual and asexual populations are viable independently ($p > p_{\text{crit}} \geq p^a_{\text{crit}}$). Parameters $b = 4$, $p = 4$, $\nu = 0.75$ with (a) and (d) $\mu = 1.25$, (b) and (e) $\mu = 2$, (c) and (f) $\mu = 2.75$.

It is clear that $\mu_1 < \mu_2$ so that at most one of the single conspecific carrying equilibria $(\hat{u}_1^+, 0)$ and $(0, \hat{u}_2^+)$ may be unstable for any given parameter regime.

Behaviour of Internal Equilibrium

Internal equilibria occur when both $(\hat{u}_1^+, 0)$ and $(0, \hat{u}_2^+)$ are stable, that is for $\mu \in (\mu_1, \mu_2)$. First note that internal equilibria lie on $u_2 = \alpha u_1$ where

$$\alpha = \frac{\mu(2-\nu) - 2}{2 - \mu\nu},$$

since per capita growth rates of sexuals and asexuals are equal on this line. Thus from either $f_1^{\pm}$ or $f_2^{\pm}$ internal equilibria occur at $(\tilde{u}_1^{\pm}, \tilde{u}_2^{\pm})$ where

$$\begin{aligned} \tilde{u}_1^{\pm} &= (2-\mu\nu)\left[\frac{\gamma_1}{2} \pm \sqrt{\left(\frac{\gamma_1}{2}\right)^2 - \gamma_0}\right], \\ \tilde{u}_2^{\pm} &= (\mu(2-\nu)-2)\left[\frac{\gamma_1}{2} \pm \sqrt{\left(\frac{\gamma_1}{2}\right)^2 - \gamma_0}\right], \end{aligned} \tag{3.4.2}$$

where

$$\begin{aligned} \gamma_1 &= \frac{2}{\mu b(\mu\nu^2 + 2(\nu-2))} + \frac{1}{2\mu(1-\nu)}, \\ \gamma_0 &= \frac{1}{\mu^2 bp(\nu-1)(\mu\nu^2 + 2(\nu-2))}. \end{aligned}$$

To establish the stability of the internal equilibria first consider the determinant of $\tilde{J}^{\pm}$ the Jacobian evaluated at $(\tilde{u}_1^{\pm}, \tilde{u}_2^{\pm})$. If the total population size at the internal equilibria is given by $\tilde{w}^{\pm} = \tilde{u}_1^{\pm} + \tilde{u}_2^{\pm}$ then

$$\det \tilde{J}^{\pm} = \frac{\mu b p^2 \tilde{u}_1^{\pm} \tilde{u}_2^{\pm}(1-\tilde{w}^{\pm})}{1+p\tilde{w}^{\pm}} \left[(2\tilde{w}^{\pm}-1)(\mu b\nu^2 + 2b(\nu-2)) + 4(\nu-1)\right].$$

It can be established from the behaviour of the nullclines or otherwise that $\tilde{w}^{\pm} \in (0,1)$ (c.f. gynodioecy model section 3.3,) so that the sign of $\det \tilde{J}^{\pm}$ is determined by the sign of the square bracketed expression. Now from (3.4.2)

$$\tilde{w}^- < \frac{2(1-\nu)}{\mu b\nu^2 + 2b(\nu-2)} + \frac{1}{2} < \tilde{w}^+,$$

and it follows that $\det \tilde{J}^+ < 0$ and $\det \tilde{J}^- > 0$. Consequently $(\tilde{u}_1^+, \tilde{u}_2^+)$ is always an unstable saddle. Since per capita growth rates are equal on $u_2 = \alpha u_1$ it follows that the line is invariant and both a stable manifold of $(\tilde{u}_1^+, \tilde{u}_2^+)$ and an unstable manifold of $(\tilde{u}_1^-, \tilde{u}_2^-)$. Since $\det \tilde{J}^- > 0$ and $(\tilde{u}_1^-, \tilde{u}_2^-)$ has an unstable manifold it must necessarily be an unstable node.

Global Behaviour

When both sexual-only populations and asexual-only populations have stable carrying equilibria ($p > p^a_{\text{crit}} \geq p^s_{\text{crit}}$) two categories of global behaviour may be distinguished:

Bistability: all mixed populations either go extinct or regardless of their compositions eventually become uniform for the same reproductive mode, whether this is sexual or asexual reproduction is determined by the stability of the boundary equilibria; Tristability: some initial populations mixed for reproductive mode will limit towards solely sexual reproduction, others will limit towards asexual reproduction, small populations go extinct.

When $\mu \leq \mu_1$ there are two stable equilibria in $\triangle_k$, the origin and $(0, \hat{u}_2^+)$. The stable manifold W_2^s of $(0, \hat{u}_2^-)$ can be demonstrated to originate at $(\hat{u}_1^-, 0)$, since it is the only unstable node in the backward invariant rectangle $R = [0, \hat{x}] \times [0, f_1^+(\hat{x})]$ where $\hat{x}$ is the maximum attained by f_1^+ in the first quadrant. Thus W_2^s divides $\triangle_k$ into basins of attraction for $(0, \hat{u}_2^+)$ and the origin. The model exhibits bistability with asexual reproduction fixing in all large enough mixed initial populations.

When $\mu \geq \mu_2$ there are two stable equilibria in $\triangle_k$, the origin and $(\hat{u}_1^+, 0)$. The stable manifold W_1^s of $(\hat{u}_1^-, 0)$ can be demonstrated to originate at $(0, \hat{u}_1^-)$, since it is the only unstable node in the backward invariant rectangle $R = [0, \check{u}_1^-] \times [0, \hat{u}_2^-]$. Thus W_1^s divides $\triangle_k$ into basins of attraction for $(\hat{u}_1^+, 0)$ and the origin. The model exhibits bistability with sexual reproduction fixing in all large enough mixed initial populations.

Tristability results for $\mu \in (\mu_1, \mu_2)$ when both $(\hat{u}_1^+, 0)$ and $(0, \hat{u}_2^+)$ and the origin are locally stable. The stable manifold W_2^s of $(0, \hat{u}_2^-)$ and W_1^s of $(\hat{u}_1^-, 0)$ both originate at $(\tilde{u}_1^-, \tilde{u}_2^-)$. To see this define

$$A = \{(x, y) | 0 \leq x \leq \tilde{u}_1^-,\ f_2^-(x) \leq y \leq \min\{\hat{u}_2^-, f_1^-(x)\}\}$$
$$B = \{(x, y) | \tilde{u}_1^- \leq x \leq \hat{u}_1^-,\ f_1^-(x) \leq y \leq f_2^-(x)\}$$

and observe that A is backward invariant and must contain W_2^s and B is backward invariant and must contain W_1^s. Thus $W_1^s \cup W_1^s$ divides $\triangle_k$ into regions of survival and extinction. The stable manifold of $(\tilde{u}_1^+, \tilde{u}_2^+)$ which was shown to be given by

$$\tilde{W}^s = \{(x, \alpha x) | x > \tilde{u}_1^-\}$$

further subdivides the region of survival into basins of attraction for $(\hat{u}_1^+, 0)$ and $(0, \hat{u}_2^+)$. For large enough mixed initial populations in which the ratio of asexuals to sexuals exceeds α, asexual reproduction will fix, otherwise sexual reproduction will fix.

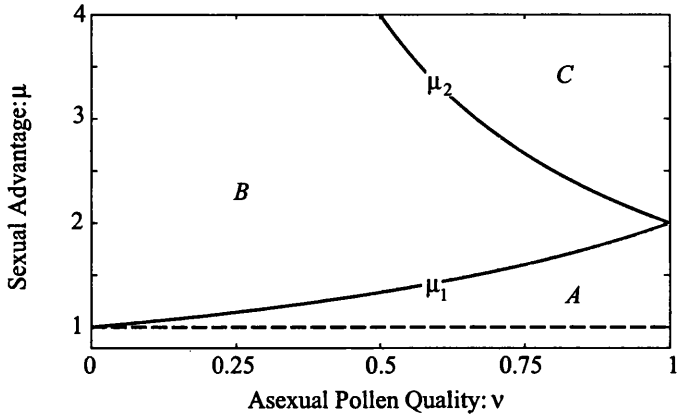

Figure 3-17: (ν, μ)-parameter space for the sexual-asexual model is divided into three regions: A - Region of bistability: Pseudogamous apomixis becomes fixed in all large enough initially mixed populations; B - Region of tristability: For large enough mixed initial populations in which the ratio of pseudogams to sexuals exceeds α, pseudogamous apomixis will fix, otherwise sexual reproduction will fix; C - Region of bistability: sexual reproduction becomes fixed in all large enough initially mixed populations

Model Behaviour

Because pollen and seed production parameters p and b are assumed species specific and do not differ between sexuals and asexuals, the qualitative behaviour of the model is dictated entirely by the advantage to sexually produced seed μ and the quality of asexually produced pollen ν. Parameters p and b determine only the extent of the Allee effect experienced by the whole population and rates of total population growth or decline.

Weak Advantage to Sex When $\mu \leq 2$ asexuals generally have the upper hand. If $\mu \leq \mu_1$ if pseudogamous apomicts are introduced into sexual population there numbers will increase and the asexual reproductive mode will spread to fixation. If $\mu > \mu_1$ sexual populations are stable to the arrival small numbers of apomicts, but sexuals will not persist in mixed populations in which the proportion of asexuals is more than

$$\beta = \frac{\mu(2-\nu)-2}{2\mu(1-\nu)} \leq \frac{1}{2}.$$

Strong Advantage to Sex When $\mu > 2$ sexual reproduction will fix in mixed populations in which the proportion of sexuals is more than β and if $\mu > \mu_2$ sexuals can invade pseudogamous apomictic populations.

Pollen is required for seed production in both sexuals and pseudogamous apomicts, which results in pollen limitation for both types and consequently the model exhibits a strong Allee effect causing the extinction of small mixed or monomorphic populations.

Figure 3-17 illustrates the regions of (ν, μ)-parameter space in which bistability and tristability occur.

Discussion

As discussed in section 1.3 the evolution of sex has received a lot of theoretical attention. As has the evolution of apomixis where sexual reproduction is believed to be the ancestral state (Mogie 1992). For hermaphrodite species in general it is possible that the transition to parthenogenesis does not entirely disable male-function. In animal parthenogens it is rare for retained male function to have any capacity for spreading parthenogenesis (Lynch 1984). However, it is hypothesized that for flowering plant species this need not be the case (Mogie 1992). The model presented here treats populations mixed for sexual and asexual reproductive mode in which asexuals produce functional pollen and are therefore able to sire offspring on sexuals.

Previous treatments of sexual and asexual relatives have in general considered autonomous apomicts and have not incorporated the pollination process explicitly (Joshi & Moody 1995, Joshi & Moody 1998, Britton & Mogie 2001). Pollen was necessarily assumed not to be limiting and as a consequence population size has no effect on the selective pressure on the asexual gene, a population genetic approach was therefore suitable. In these models partial degeneracy of asexual male-function results in the appearance of parameter regimes in which both reproductive modes are stable as resident. In the model developed here both sexual and asexual populations are pollen limited, because asexuals are assumed pseudogamous. This extension to pseudogamy necessitates additional assumptions about the response of asexuals to pollen. It is reasonable to suppose that the quality of male genetic material required to produce a functional endosperm is somewhat less than that which is required to produce a viable embryo and potentially reproductive progeny. A high proportion of genes are inactive in the endosperm and may well therefore be superfluous. It might be conjectured that

an endosperm formed with partially reduced pollen in which some genes are missing, corrupted or over represented may still function normally. In any case it is clear that in the majority of studied pseudogamous species a partially degenerate male-function is tolerated (Nogler 1984). Intriguingly assuming pseudogamous apomicts are ambivalent to the quality of pollen they receive results in a model with a very similar qualitative structure to the model of Britton & Mogie (2001) for autonomous apomicts. In particular the expressions for model bifurcation values μ_1 and μ_2 are identical and so parameter space is divided into precisely the same regions.

The principle result of assuming poor asexual male-function is that for biologically realistic values of μ and ν both sexuals and asexuals are stable as resident. Experiments conducted by Kelley et al. (1988) on grass species indicate that the advantages of being sexually produced when developing in close proximity to your maternal parent amount to increased viability of about 43%. Taking $\mu = 1.43$ if less than 60% of asexual pollen can form viable offspring with sexuals, then both sexuals and asexuals are stable as resident. This presents a partial explanation for the geographic parthenogenesis discussed in Chapter 1 Section 1.3 which does not invoke niche differentiation. If, by historical accident, populations of sexual and asexual relatives come to occupy distinct patches, then rare migration events between populations will not result in the spread of one or other type. This does not, however, go any way towards explaining the particular patterns of geographic parthenogenesis that are regularly observed in which asexuals tend to have a greater range (Bierzychudek 1987). Nor can it explain why sexuals and asexuals of some species appear to coexist over much of there range.

A distinction should be acknowledged between the assumptions concerning asexual male function made in this model and those made in previously published models. Joshi & Moody (1995) (see also (Joshi & Moody 1998)) assume that in addition to producing a proportion of poor pollen quality asexuals also produce less pollen. The distinction is potentially significant since reduced pollen production in asexuals restricts the number of sexual seeds rendered inviable due to fertilization by poor quality pollen. Replacing the assumption of poor quality pollen with that of reduced pollen production can readily be accommodated within the inter-pollinating conspecifics framework by adjusting the inter-pollination and reproduction matrices as follows

$$P = \begin{pmatrix} p & \nu p \\ p & p \end{pmatrix}, \quad B_1 = \begin{pmatrix} \mu b & b/2 \\ 0 & 0 \end{pmatrix}, \quad B_2 = \begin{pmatrix} 0 & b/2 \\ b & b \end{pmatrix},$$

that is by transferring the poor male function parameter from the reproductive rate of sexuals to the pollination rate of sexuals by asexuals. The behaviour of the model under this alteration is qualitatively unchanged, in particular the stability analysis of the boundary equilibria is the same with the exception that the stability condition for $(0, \hat{u}_2^+)$ is adjusted to

$$\mu < \mu_2^* = \frac{2p\nu\hat{u}_2^+ + 2}{bp\nu(\hat{u}_2^+ - (\hat{u}_2^+)^2)}.$$

The same condition ensures that $(0, \hat{u}_2^-)$ is a saddle point. It is straight-forward to show that $\nu \in [0, 1]$ implies $\mu_2^* \leq \mu_2$, indicating that assuming lowered pollen production rather than poor pollen quality in asexuals favours sexuals, in that it reduces the threshold sexual advantage required for sexuals to displace asexuals. The criteria for asexuals to displace sexuals are unaltered, as might have been conjectured, since when they are rare asexuals will be pollinated mainly by sexuals and so asexual male-function degenerate or otherwise will be unimportant.

3.5 DISCUSSION

The models developed in this chapter to address the ecological interaction of inter-pollinating conspecifics were applied specifically to gynodioecious and sexual-asexual populations. Each model was given a plausible genetic derivation, however the resulting models differ significantly from population genetic models models previously developed to treat similar phenomena. In particular the gynodioecy model may be compared with the treatment of (Charlesworth & Ganders 1979) and the sexual-asexual model with the treatment of a dominant allele for asexuality discussed by (Joshi & Moody 1995). These are both typical population genetical approaches to modelling the fate of a single gene and result in one-dimensional models describing gene frequency. Any change in gene frequency must be assumed independent of population size or growth rate which is not modelled. However, if population size is affected significantly by the genetic composition of the population, size dependent effects like the Allee effect exhibited by the sexual hermaphrodite conspecific class in the above models, can affect gene frequency. In particular the gynodioecy model illustrates that there may in fact be a strong interaction between population size and the success of one or other phenotype. The gynodioecy models of Charlesworth & Ganders (1979) suppose that the frequency dependent advantage of females falls as their numbers increase, as a result they predict a male-sterility gene should be held in equilibrium. In the gynodioecy model with selfing

(3.3) the specific mechanism of pollen-limitation determines the frequency dependence of the female reproductive advantage. The result of imposing this particular mechanism is that the frequency of a gene for male-sterility can be held in stable equilibrium but may instead oscillate in frequency as a direct consequence of the interaction between population size and the success of each reproductive mode. Although the assumptions of the model presented here are somewhat at variance with the models of Charlesworth & Ganders (1979), it is clear that, since one-dimensional ordinary differential equations are incapable of exhibiting oscillations, a population genetical approach would not have illuminated this possibility.

The primary intention of developing a framework for modelling inter-pollinating conspecifics is to explore issues in the evolution of flowering plant sexual diversity. It is worth noting that the resulting models are in some case suitable for other species and other more general problems. The phenomena of pseudogamy or sperm-dependent parthenogenesis is not confined to flowering plants but also occurs in animal species like enchytraeid worms. Schley et al. (2004) treat the interaction of a sexual species of hermaphrodite enchytraeid worms with a pseudogamous subspecies who do not produce mature sperm themselves and whose reproduction depends on mating with sexual individuals. Although the derivation differs, the behaviour of the gynodioecy model with self-incompatibility matches the extinction predicted by Schley et al.'s (2004) model in the absence of competitive differences. Schley et al. (2004) show that coexistence and cyclic behaviour may occur if sexuals and pseudogams differ in competitive ability or in ability to exploit resources. Certain species of enchytraeids are self-compatible (DorzsaFarkas 1995) and so the results of the pseudogamy model with selfing presented are relevant and suggest that self-fertilization amongst sexual enchytraeids provides a further mechanism for explaining the coexistence of sexual and pseudogamous forms.

The way in which producing or not producing pollen is rewarded in the gynodioecy model bears a striking resemblance to the payoffs in the prisoners dilemma. An evolutionary game commonly used to investigate the very general problem of the evolution of cooperation between non-relatives (Axelrod 1984). In the prisoners dilemma, two players decide independently whether to cooperate or defect and receive points according to what the opponent choose. Typically defecting while your opponent cooperates achieves the highest score, followed by cooperating while your opponent cooperates, followed by defecting while your opponent defects with the lowest score for cooperating while your opponent defects. Opinion varies on whether these inequalities must be strict or not. Research into the prisoners dilemma tends to focus on strategies for play-

ers who repeatedly encounter one another. A particularly successful strategy known as 'tit for tat' involves simply choosing the move that your opponent made on the previous encounter. Axelrod (1984) champions the argument that this strategy has repeatedly evolved both in biological and sociological situations. Although the structure of the gynodioecy model with self-incompatibility interpreted from the perspective of cytoplasmic alleles is similar: Producing pollen is an altruistic or cooperative behaviour since it does not promote inheritance of cytoplasmic alleles; cytoplasm is obviously incapable of employing strategies beyond always-cooperate and always-defect. In this respect the the gynodioecy model with self-incompatibility introduces very little new to the discussion: the always-defect-from-producing-pollen strategy of females will always displace the always-cooperate strategy of hermaphrodites, with the peculiarity that defectors cannot persist once hermaphrodites have been excluded. The introduction of selfing disrupts the traditional order of the payoffs: it is now more rewarding to cooperate if your opponent defects than it is to defect, since cooperators derive reproductive success from retaining some of the social resource (in this case pollen) for themselves. This introduces density dependence: both cooperators and defectors prosper when rare and suffer when ubiquitous. Although strictly this arrangement of payoffs is outside the scope of the prisoners dilemma it not so unusual in nature. Greig & Travisano (2004) conduct experiments with strains of a yeast *Saccharomyces cerevisiae* that vary in their ability to produce the enzyme invertase which permits external digestion of sucrose. Since the enzyme is secreted externally non-producers have the potential to survive in colonies of producers. Plainly producers derive a personal advantage from producing the enzyme and accordingly it is observed that if non-producer have a fitness advantage only when there is an abundance of producers in a population (Greig & Travisano 2004). Supposing that yeast reproduction is limited by a Holling type II function response to enzyme availability will yield the gynodioecy model with selfing.

The models in this chapter assume spatial uniformity and panmixia, which equate to seed and pollen dispersal that is uniform over the habitat of the population. In the following chapter the assumption of spatial uniformity will be relaxed so that questions of range expansion and non-uniform population distributions can be considered.

CHAPTER 4

Reaction-Diffusion Models

In this chapter the non-spatial models of chapter 3 are extended by revoking the panmixia assumption and the incorporation of explicit spatial domain. Reaction-diffusion models are historically the most popular, and mathematically the best understood way of making this extension. Reaction-diffusion models have been applied extensively to ecological questions of biological invasion (Skellam 1951, Lewis & Kareiva 1993, Shigesada & Kawasaki 1997, Owen & Lewis 2001) and the spread of genetic mutations within populations (Kolmogoroff et al. 1937, Fisher 1937) as well as having many chemical, biochemical and biomedical applications (Murray 1989*b*).

Diffusion will be isotropic and the only process driving population spread, corresponding to dispersal of seed by wind which blows equally often in all directions, or by animals which have no preferred direction of migration. An assumption central to the treatment given here will be that cross pollination occurs only between individuals at the same site. So that by assumption the distance that pollen is dispersed is negligible compared with seed dispersal. Such an arrangement might, for example, corresponding to short-range insect pollination.

4.1 SEXUAL SPECIES

Consider the population size of the sexually reproducing hermaphrodite population introduced in chapter 3 section 3.2. Suppose that the size of the population at a point $x \in \Omega \subseteq \mathbb{R}^2$ at time t is given by $u(x,t)$. Cross pollination is assumed to take place only between individuals at x so that the local population dynamics are governed by the same equation as 3.2.5

$$f(u(x,t)) = \frac{b(s+pu(x,t))u(x,t)(1-u(x,t))}{1+s+pu(x,t)} - u(x,t), \tag{4.1.1}$$

where $p > p_{\text{crit}}$ (p_{crit} given in (3.2.7)) so that the non-spatial dynamics include a stable carrying capacity $\hat{u}^+$ and may include a positive critical depensation threshold $\hat{u}^-$. The parameter s, the self-pollination effort, will be zero for self-incompatible species. The reaction-diffusion model is given by

$$\frac{\partial u}{\partial t} = f(u) + D\Delta u, \tag{4.1.2}$$

where D the diffusion coefficient has dimension $(\text{metres})^2/\text{generation}$. Although the parameter D can be omitted by rescaling space, it is retained here in anticipation of the following sections in which different conspecific classes may have different dispersal rates. When $s \geq 1/(b-1)$ 4.1.2 is described as monostable, because only one spatially uniform solution is stable as an equilibrium of the kinetic equations (that is $du/dt = f(u)$ see chapter 3 section 3.2) namely $u = \hat{u}^+$. For $s < 1/(b-1)$ 4.1.2 is described as bistable since both $u = 0$ and $u = \hat{u}^+$ are stable as equilibria of the kinetic equations.

Travelling Wave Solutions

A suitable question to ask of model 4.1.2 is how a population, established over some region of space, expands its range. For simplicity the initial population is assumed radially symmetric so that

$$\Delta u = \frac{\partial^2 u}{\partial r^2} + \frac{1}{r}\frac{\partial u}{\partial r},$$

and the initial extent is sufficiently large ($r \gg 0$) that the second term can be ignored. Only one spatial dimension need therefore be considered and by convention it is denoted by x. It has long been known that parabolic PDEs with suitable nonlinear inhomogeneities can exhibit travelling wave solutions, that is solutions where a fixed wave profile moves through space (Kolmogoroff et al. 1937, Fisher 1937). Such solutions are examined by taking a frame of reference moving with the wave and looking for solutions which asymptote towards roots of f. Thus solutions obey

$$u(x,t) = u(x+ct) = u(z),$$

if the wave travels to the left at a speed c and

$$u(z) \to \alpha \text{ as } z \to \infty,$$
$$u(z) \to \beta \text{ as } z \to -\infty,$$

for α, β roots of f. Substituting the travelling wave coordinate into 4.1.2 gives

$$D\frac{d^2u}{dz^2} - c\frac{du}{dz} + f(u) = 0. \tag{4.1.3}$$

So solutions of 4.1.2 of the desired form correspond with heteroclinic (or homoclinic) orbits between equilibria of the system

$$\begin{aligned} \frac{du}{dz} &= v, \\ \frac{dv}{dz} &= \frac{cv - f(u)}{D}. \end{aligned} \tag{4.1.4}$$

The equilibria of 4.1.4 are $(0,0)$, $(\hat{u}^-,0)$ and $(\hat{u}^+,0)$ where $\hat{u}^\pm$ are given in chapter 3 section 3.2. The stability of the equilibrium $(\alpha,0)$ is determined by examining the Jacobian

$$J(\alpha,0) = \begin{pmatrix} 0 & 1 \\ -f'(\alpha)/D & c/D \end{pmatrix}.$$

Eigenvalues are given by

$$\lambda^\pm = \frac{c \pm \sqrt{c^2 - f'(\alpha)}}{2D}.$$

In the bistable case ($s < 1/(b-1)$) the origin is a saddle point since

$$f'(0) = \frac{(b-1)s - 1}{s+1} < 0,$$

and if $c > 0$ then the gradient of the stable manifold through $(0,0)$ is negative and that of the unstable manifold is positive, the situation is reversed for $c < 0$.

In the monostable case ($s \geq 1/(b-1)$) the stability of $(0,0)$ is determined by c and, the origin is

a stable node for $c < -\sqrt{Df'(0)}$,
a stable focus for $-2\sqrt{Df'(0)} < c < 0$,
an unstable focus for $0 < c < 2\sqrt{Df'(0)}$,
an unstable node for $c > \sqrt{Df'(0)}$.

While it is a stable node the gradient of both the main and side manifolds is negative through $(0,0)$. While it is an unstable node their gradients are positive. Since solutions are only biologically relevant for $u > 0$, the equilibrium $(\hat{u}^-,0)$ need be considered only if $s < 1/(b-1)$, in which case it follows a similar pattern to $(0,0)$ when $s \geq 1/(b-1)$,

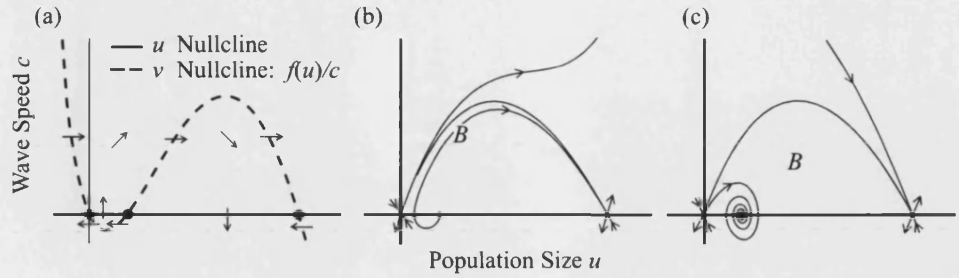

Figure 4-1: Travelling wave solutions of 4.1.2 correspond to heteroclinic orbits in the system 4.1.4, which can be found by phase plane analysis. The above figures illustrate the low self-pollination case ($s < 1/(b-1)$) with parameters $b = 3.5$, $p = 3.5$, $s = 0.1$ and $D = 0.2$. (a) Nullclines of 4.1.4 for a positive travelling wave speed $c_1 = 0.2638$, for which wave speed a unique heteroclinic orbit exists connecting $(0,0)$ and $(\hat{u}^+,0)$. The behaviour of the unstable manifold of $(0,0)$ and the stable manifold of $(\hat{u}^+,0)$ are shown in (b) for $c_1 < c < c_0$ ($c = 0.3$) and in (c) for $\bar{c}_0 < c < c_1$ ($c = -0.1$) together with the heteroclinic connection which occurs when $c = c_1$. In both (b) and (c) B is the region enclosed by the heteroclinic orbit and the u-axis.

with node behaviour exchanged for focus behaviour at the thresholds determined by

$$c^2 = 4Df'(\hat{u}^-) = \frac{4D\hat{u}^-((b-1)p - bs - 2bp\hat{u}^-)}{1+s+p\hat{u}^-}.$$

The $\hat{u}^+$ equilibrium is always a saddle since $f'(\hat{u}^+) < 0$ for all $p > p_{\text{crit}}$, the stable manifold has negative gradient and the unstable manifold has positive gradient through $(\hat{u}^+,0)$. The nullclines of 4.1.4 are illustrated in Figure 4-1(a) for a positive wave speed c and $s < 1/(b-1)$.

Systems like 4.1.4 are treated by Hadeler & Rothe (1975) and Aronson & Weinberger (1975), both provide a standard argument for the existence of a value $c_0 \geq 2\sqrt{Df'(\alpha)}$ such that for $c \geq c_0$ a heteroclinic orbit exists between a node $(\alpha,0)$ and a saddle $(\beta,0)$. Thus for given parameters b, $p > p_{\text{crit}}$ and $s < 1/(b-1)$ there exists a heteroclinic orbit between $(\hat{u}^-,0)$ and $(\hat{u}^+,0)$ for all $c \geq c_0$ for some $c_0 \geq c^* = 2\sqrt{Df'(\hat{u}^-)}$. Similarly there exists a heteroclinic orbit between $(0,0)$ and $(\hat{u}^-,0)$ for all $c \leq \bar{c}_0 \leq -c^*$. A travelling wave solution corresponding to a heteroclinic connection between $(\hat{u}^-,0)$ and $(\hat{u}^+,0)$ which develops from the initial data

$$u(x,0) = \begin{cases} \hat{u}^- & \text{if } x < 15 \\ \hat{u}^+ & \text{if } x \geq 15 \end{cases},$$

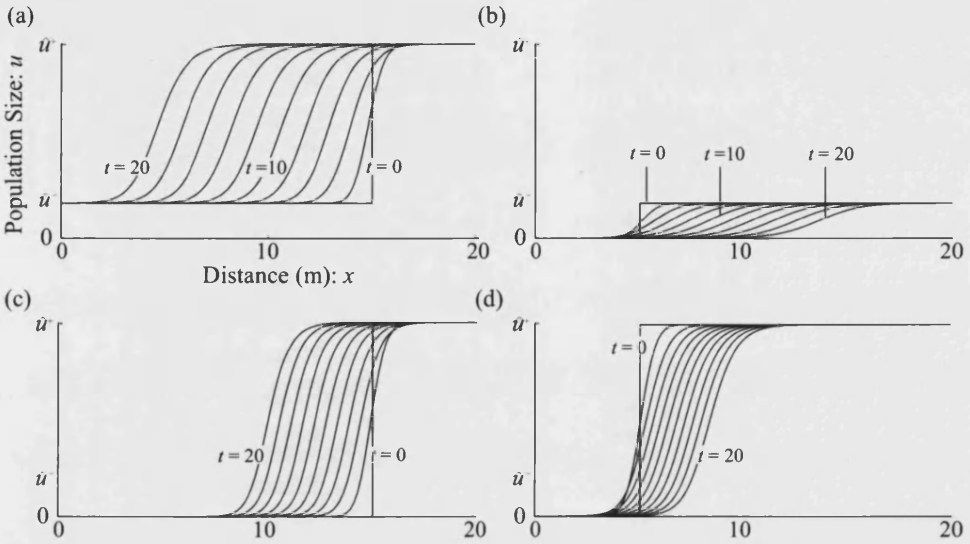

Figure 4-2: Travelling wave solution exhibited by the reaction-diffusion system for a sexual population with self-pollination 4.1.2. For (a)-(c) parameters are $b = 3.5$, $p = 3.5$, $s = 0.1$ and $D = 0.2$. (a) A comparatively fast travelling wave can be found connecting $\hat{u}^-$ and $\hat{u}^+$, the wave speed after 20 generations is $c = 0.5962$ close to the minimum wave speed $c_0 = 0.5846$. (b) Similarly a fast wave can be found connecting $\hat{u}^-$ and 0, the wave speed after 20 generations is $c = -0.5604$ close to $\bar{c}_0 = c^* = -0.5780$. (c) A slower monotone travelling wave occurs connecting 0 with $\hat{u}^+$ corresponding to range expansion of an established population, the wave speed after 20 generations is $c = 0.2631$ close to $c_1 = 0.2828$. (d) The monotone travelling wave solution connecting 0 with $\hat{u}^+$ travels to the right if $p_{\text{crit}} < p < p_{\text{stat}}$ corresponding to a retreating population. In (d) parameters are $b = 4$, $p = 1.8$, $s = 0$ and $D = 0.2$, wave speed after 20 generations is $c = -0.1870$ close to $c_1 = -0.1890$. Numerical solutions calculated by the method of lines with Neumann (zero-flux) boundary conditions on the spatial interval [0,20]. Wave speed determined by recording when $u(x,t)$ exceeded $u_{\min} = 0.001$.

is shown in Figure 4-2(a). A travelling wave solution corresponding to a heteroclinic connection between $(0,0)$ and $(\hat{u}^-,0)$ which develops from initial data

$$u(x,0) = \begin{cases} 0 & \text{if } x < 5 \\ \hat{u}^- & \text{if } x \geq 5 \end{cases},$$

is shown in Figure 4-2(b).

Note that if f is concave down on the interval $[\alpha,\beta]$ then the heteroclinic orbit exists for all $c \geq c_0 = 2\sqrt{Df'(\alpha)}$ and travelling waves are described as 'pulled waves' (Hadeler & Rothe 1975) because minimum wave speed is dictated by linear growth at the leading edge of the wave. f given by 4.1.1 is concave down on $[\hat{u}^-,\hat{u}^+]$ if $\tilde{u} < \hat{u}^-$ where $\tilde{u}$ satisfies $f''(u) = 0$ and is therefore given by

$$\tilde{u} = \frac{\sqrt[3]{(s+1)(s+1+p)} - (s+1)}{p}.$$

This is only the case for p near p_{crit} as can be seen in Figure 4-3(a), where c_0 and c^* coincide for low p. Waves that are not pulled are described as 'pushed' (Hadeler & Rothe 1975), since a higher growth rate occurs somewhere behind the wave front and the progress of the wave is driven by the overspill of these individuals. If $s \geq 1/(b-1)$ there exists a heteroclinic orbit between $(0,0)$ and $(\hat{u}^+,0)$ for all $c \geq c_0$ for some $c_0 \geq 2\sqrt{Df'(0)}$. In this case f is concave down (hence $c_0 = 2\sqrt{Df'(0)}$) when there is no depensation, which occurs when self-pollination is the predominant mode of pollination $p < s(s+1)$, (see chapter 3 section 3.2 and Figure 3-3).

If $s < 1/(b-1)$ then for c just less than c_0 the backward orbit of the stable manifold of $(\hat{u}^+,0)$, for which $u > 0$, crosses the u-axis near $(\hat{u}^-,0)$ (See Figure 4-1(b)). Also for c just greater than $\bar{c}_0$ the forward orbit of the unstable manifold of $(0,0)$, for which $u > 0$, crosses the u-axis near $(\hat{u}^-,0)$ and does not reach $(\hat{u}^+,0)$, therefore the backward orbit of the stable manifold of $(\hat{u}^+,0)$ for which $u > 0$ cannot cross u-axis and is constrained to enter the positive quadrant with some strictly positive value of v (See Figure 4-1(c)). So since solutions of 4.1.4 vary continuously with c there must exist a wave speed c_1 for which a heteroclinic orbit exists between $(0,0)$ and $(\hat{u}^+,0)$ with $\bar{c}_0 \leq c_1 \leq c_0$. Hadeler & Rothe (1975) go on to show that c_1 is unique. If B is the region enclosed by the u-axis and the heteroclinic orbit, then for all $c > c_1$ the stable manifold of $(\hat{u}^+,0)$ for which $u > 0$ is contained in B and cannot leave, and the unstable manifold of $(0,0)$ is outside B and cannot enter it, for $c < c_1$ the reverse is

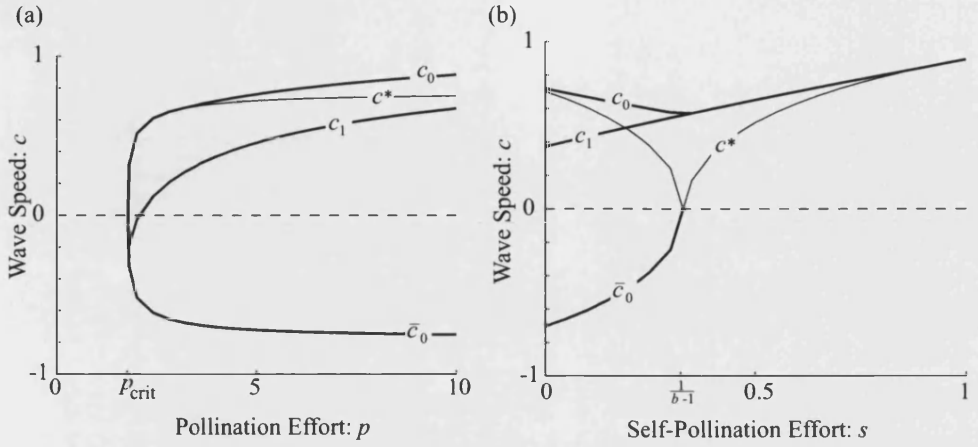

Figure 4-3: How wave speeds c_0, $\bar{c}_0$ and c_1 obtained from the phase plane analysis of 4.1.4 vary with parameters. (a) As pollination effort p increases both c_0 and c_1 increase, c_0 diverges from c^* and c_1 which is negative for small p converges to c_0. $\bar{c}_0$ coincides with or is very close to $-c^*$. Parameters $b = 4$, $s = 0$, $D = 0.2$. (b) As self-pollination effort s increases c_0 and c_1 converge at $s = 1/(b-1)$ when 0 and $\hat{u}^-$ coincide. Parameters $b = 4$, $p = 4$, $D = 0.2$.

true and so in neither case can a heteroclinic connection exist. The travelling wave corresponding to the heteroclinic connection between $(0,0)$ and $(\hat{u}^+,0)$ is always a pushed wave because critical depensation ensures a negative population growth rate at the wave front. A travelling wave solution corresponding to the heteroclinic connection between $(0,0)$ with $(\hat{u}^+,0)$ which develops from initial data

$$u(x,0) = \begin{cases} 0 & \text{if } x < 15 \\ \hat{u}^+ & \text{if } x \geq 15 \end{cases},$$

is shown in Figure 4-2(c).

How c_0, $\bar{c}_0$ and c_1 vary with parameters was obtained by numerical analysis of phase planes and is plotted together with $\pm c^*$ in Figure 4-3(a) for varying p, and in Figure 4-3(b) for varying s. Notice that $c_1 = 0$ for some value $p = p_{\text{stat}}$ corresponding to a steady state solution of 4.1.2 in which $\lim_{z\to\infty} u(z) = \hat{u}^+$, $\lim_{z\to-\infty} u(z) = 0$. p_{stat} is the threshold separating population advance from population retreat. Population

retreat is shown in Figure 4-2(d), the travelling wave develops from initial data

$$u(x,0) = \begin{cases} 0 & \text{if } x < 5 \\ \hat{u}^+ & \text{if } x \geq 5 \end{cases}$$

An implicit expression for p_{stat} is obtained with the following standard argument. Set $c = 0$ in 4.1.3, multiply by du/dz and integrate over $z \in (-\infty, \infty)$

$$\frac{D}{2}\left[\left(\frac{du}{dz}\right)^2\right]_{-\infty}^{\infty} = \int_{-\infty}^{\infty} f(u)\frac{du}{dz}dz,$$

so that since $\lim_{z\to\pm\infty} u'(z) = 0$

$$\int_0^{\hat{u}^+} f(u)du = 0.$$

Figure 4-4 illustrates the region $p_{\text{crit}} < p < p_{\text{stat}}$ for which spatially uniform populations can persist, but populations with compact initial data retreat. Note this region occupies only a thin sliver of parameter space and is independent of D, indicating that diffusion only heightens the risk of extinction for populations with already very low reproductive rates p and b.

Discussion

The reaction-diffusion model predicts that a self-incompatible sexual species is capable of spreading to colonize suitable contiguous habitat, so long as it is initially established over a small, but not negligibly small, region. A population initially confined to a glacial refuge, for example, would be expected to expand its range as climate improves and suitable territory opens up. In the vanguard of an advancing front population density is low and the strong Allee effect in the kinetic equations yields a negative per-capita growth. The colonization process is instead driven by migration of an abundance of seed from the established population behind the front. Non-local seed dispersal is therefore an integral part of range expansion in a self-incompatible sexual species. This mode of colonization requires habitat to be more or less contiguous: sufficient seed may not propagate beyond habitat disturbances such as roads, waterways or competing species to enable continuing spread. Self-incompatible sexual species could therefore be more readily contained than autonomous apomictic or vegetatively

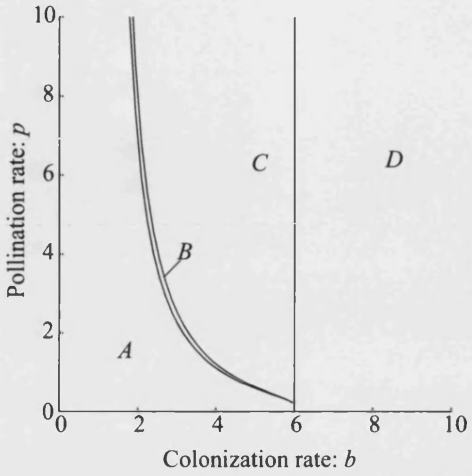

Figure 4-4: For the reaction-diffusion system 4.1.2 (b,p)-parameter space includes a slender region of parameter space for which $p_{\text{crit}} < p < p_{\text{stat}}$ in which diffusion may drive population retreat, this region is labelled B. For region A no non-trivial spatially uniform steady states exist. Regions C and D distinguish when critical depensation occurs in the non-spatial dynamics, in both cases diffusion drives range expansion for established populations

propagating species. Long-range seed dispersal is also impractical for self-incompatible sexual species since regardless of habitat suitability rare migrants in new territories will enjoy little pollination and consequently little reproductive success.

As self-fertilization is introduced ($s > 0$) and gradually increased the strong Allee effect in the model is eroded and is lost for $s \geq 1/(b-1)$. Although per-capita growth is always positive when sufficient self fertilization takes place, migration can still be the dominant process underlying range expansion. When the growth of small populations in the wave front dominates range expansion the asymptotic wavespeed is $c^* = 2\sqrt{Df'(0)}$. Figure 4-3(b) shows, however, that even when $s > 1/(b-1)$ the invasion wavespeed c_0 is greater than c^*, indicating that the wave is still pulled and migration dominates wave speed. This will be the case while the model retains a weak Allee effect and $f'(0) \neq \sup\{f'(x)|x \in [0,\infty)\}$. For self-compatible sexual species three cases should be distinguished. If self-pollination is very rare ($s < 1/(b-1)$) model predictions qualitatively match the self-incompatible case: range expansion is only possible for an established population into contiguous habitat and long-range dispersal is unprofitable. If self-pollination is a little more common ($s \geq 1/(b-1)$) but considerably more effort

is put into cross pollination, then range expansion is still driven by migration of seed from the established population behind the front. However, long-range dispersal is now beneficial, because populations can establish from an arbitrarily small size. As such small habitat disturbances will slow but not prevent continuing spread. If the majority of pollen produced is retained for selfing ($p < s(s+1)$) all depensatory effects are removed. Consequently long-range dispersal is profitable and range expansion of established populations is driven by the growth of small outlying sub-populations at the very edge of the wave front.

It is worth observing that the model suggests that seed dispersal range (governed by D) is subject to two countervailing selective pressures. Increased dispersal range increases how rapidly an established population's range can expand. Within an expanding population it is advantageous to disperse seeds beyond the established population where competition is lower. However, increased dispersal range increases the threshold population size that can become established, since dispersal acts to deplete local populations and may drive local population size below the strong Allee effect threshold. Within a small population it is therefore advantageous for offspring to remain close to their natal population where more pollen will be available when they reach sexual maturity. Conceivably sexual species might specialize into rapid colonizers suited to spreading across large contiguous territories and slow colonizers suited to establishing in difficult-to-reach habitats.

4.2 GYNODIOECY

The gynodioecy model of chapter 3 section 3.3 is extended to a reaction-diffusion system in much the same way as the sexual species model above. The size of the hermaphrodite population at x at time t is $u_1(x,t)$, the size of the female population is $u_2(x,t)$. Cross-pollination is again assumed to occur only between individuals at the same spatial location. The kinetic terms for hermaphrodites and females respectively are

$$f(u_1(x,t),u_2(x,t)) = \frac{b(s+pu_1(x,t))u_1(x,t)(1-u_1(x,t)-u_2(x,t))}{1+s+pu_1(x,t)} - u_1(x,t),$$
$$g(u_1(x,t),u_2(x,t)) = \frac{\mu bpu_1(x,t)u_2(x,t)(1-u_1(x,t)-u_2(x,t))}{1+pu_1(x,t)} - u_2(x,t).$$

The reaction-diffusion system is given by

$$\frac{\partial u_1}{\partial t} = f(u_1, u_2) + D_1 \Delta u_1,$$
$$\frac{\partial u_2}{\partial t} = g(u_1, u_2) + D_2 \Delta u_2,$$

where D_1 and D_2 specify the possibly different diffusion coefficients of hermaphrodites and females respectively. Although both conspecifics are of the same species and physiologically very similar, the modifications arising from a male-sterility mutation could potentially alter the dispersal profile of females. For example, if female seed differs in mean size or weight from hermaphrodite seed and dispersal is anemochorous, hydrochorous or autochorous (wind, water or physical expulsion) then mean dispersal distances may differ. Differences in size or weight might arise from the assumed differences in resource allocation between hermaphrodites and females, if the increased fecundity of females results from better provisioned seeds with increased viability. Koelewijn & van Damme (2005) demonstrate differences in mean seed size between hermaphrodites and females in *Plantago coronopus*; these effects play a role in the fitness advantage of females. Alternatively in endozoochorous or epizoochorous (internal or external animal dispersal) species, the redistribution of resources in the female may modify mean fruit size or weight with the result that it is more or less readily dispersed by the animal.

Travelling Wave Solutions

Of primary interest is the invasion of females into hermaphrodite populations. Again the problem is treated only in one spatial dimension. Travelling wave solutions moving to the left are sought in which the hermaphrodite only equilibrium is replaced by another of the kinetic equations' equilibria, so that

$$\begin{pmatrix} u_1(z) \\ u_2(z) \end{pmatrix} \to \begin{pmatrix} \tilde{u}_1 \\ \tilde{u}_2 \end{pmatrix} \text{as} z \to \infty,$$
$$\begin{pmatrix} u_1(z) \\ u_2(z) \end{pmatrix} \to \begin{pmatrix} \hat{u}^+ \\ 0 \end{pmatrix} \text{as} z \to -\infty,$$

where $(\tilde{u}_1, \tilde{u}_2)$ may be the extinct equilibrium $(0, 0)$ or when selfing is introduced the internal coexistence equilibrium $(\hat{u}_1, \hat{u}_2)$. The equilibrium behind the wave is described as the invading equilibrium. Looking for solutions of the form $(u_1(x,t), u_2(x,t)) =$

$(u_1(x+ct), u_2(x+ct))$ results in the ordinary differential equation system

$$\begin{aligned} D_1\frac{d^2u_1}{dt^2} - c\frac{du_1}{dt} + f(u_1,u_2) = 0, \\ D_2\frac{d^2u_2}{dt^2} - c\frac{du_2}{dt} + g(u_1,u_2) = 0. \end{aligned} \tag{4.2.1}$$

Proving the existence of a heteroclinic connection between two equilibria in a coupled system of second order ordinary differential equations such as this is very involved, but has been done in the case where f and g determine a predator prey interaction with the invading equilibrium stable and internal (Dunbar 1983, Dunbar 1984). The problem is simplified a little if the travelling wave profiles $u(z)$ and $v(z)$ are monotone, but in most cases examined here they will not be. Linear stability analysis of the $(\hat{u}^+, 0, 0, 0)$ equilibrium of 4.2.1 is profitable since it yields a condition on minimum wave-speed for biologically realistic invasions. The linearization of this system about the equilibrium written as a first order system is

$$\begin{aligned} \frac{du_1}{dt} &= v_1, \\ \frac{dv_1}{dt} &= \frac{cv_1 - \hat{f}_{u_1}u_1 - \hat{f}_{u_2}u_2}{D_1}, \\ \frac{du_2}{dt} &= v_2, \\ \frac{dv_2}{dt} &= \frac{cv_2 - \hat{g}_{u_1}u_1 - \hat{g}_{u_2}u_2}{D_2}, \end{aligned} \tag{4.2.2}$$

where

$$\hat{f}_x = \frac{\partial f}{\partial x}(\hat{u}^+, 0) \text{ and } \hat{g}_x = \frac{\partial g}{\partial x}(\hat{u}^+, 0).$$

Consulting chapter 3 section 3.3 it is clear that $\hat{g}_{u_1} = 0$ so that the characteristic equation of 4.2.2 is

$$\begin{vmatrix} -\lambda & 1 & 0 & 0 \\ 0 & \frac{c\lambda - \hat{f}_{u_1}}{D_1\lambda} - \lambda & -\frac{\hat{u_1}}{D_1} & 0 \\ 0 & 0 & -\lambda & 1 \\ 0 & 0 & -\frac{\hat{g}_{u_2}}{D_2} & \frac{c}{D_2} - \lambda \end{vmatrix} = 0,$$

that is

$$(D_1\lambda^2 - c\lambda + \hat{f}_{u_1})(D_2\lambda^2 - c\lambda + \hat{g}_{u_2}) = 0.$$

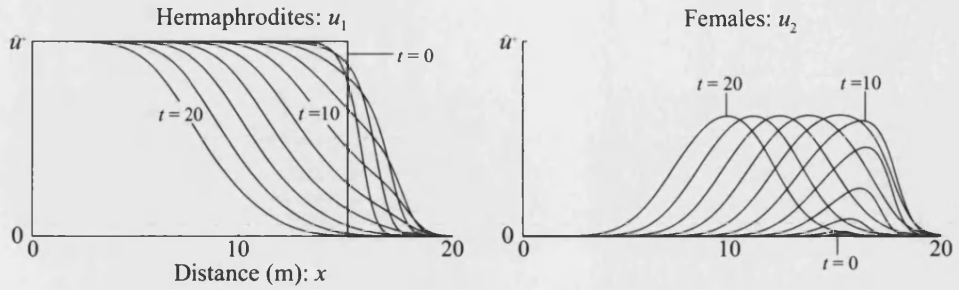

Figure 4-5: A travelling wave solution of the gynodioecy reaction-diffusion model with self-incompatible hermaphrodites. As the wave passes the hermaphrodite population is driven extinct locally. After 20 generations the wave speed is $c = 0.6301$ close to the necessary minimum $c_{\text{inv}} = 0.6325$. Model parameters $b = 4$, $p = 4$, $\mu = 1.5$, $D_1 = D_2 = 0.2$ and parameters for initial female data $\epsilon = 0.01$, $\sigma = 0.5$. Numerical solutions calculated by the method of lines with Neumann (zero-flux) boundary conditions on the spatial interval [0,20].

yielding eigenvalues

$$\lambda_1^{\pm} = \frac{c \pm \sqrt{c^2 - 4D_1\hat{f}_{u_1}}}{2D_1},$$

with corresponding eigenvectors $e_1^{\pm} = (1, 2\lambda_1^{\pm}, 0, 0)$ and

$$\lambda_2^{\pm} = \frac{c \pm \sqrt{c^2 - 4D_2\hat{g}_{u_2}}}{2D_2},$$

with corresponding eigenvectors $e_2^{\pm} = (0, 0, 1, 2\lambda_2^{\pm})$. Since $\hat{g}_{u_2} > 0$ it is necessary for $c \geq c_{\text{inv}} = 2\sqrt{D_2\hat{g}_{u_2}}$ in order that female density is always non-negative. Since the region $\triangle_k = \{(x_1, x_2) |\ 0 \leq x_1 \leq k - x_2,\ 0 \leq x_2 \leq k - x_1\}$ with $k > 1$ is invariant under the kinetic equations, it follows that it will be invariant under 4.2.1 (Smoller 1983, pp192-212). Since initial data will always be chosen in $\triangle_1$ only travelling waves with $c \geq c_{\text{inv}}$ should be anticipated.

Self-Incompatible Hermaphrodites

When $s = 0$ there is no uniform steady state with $u, v > 0$ and since female invasion results in extinction in the diffusionless equations, numerical solutions are examined

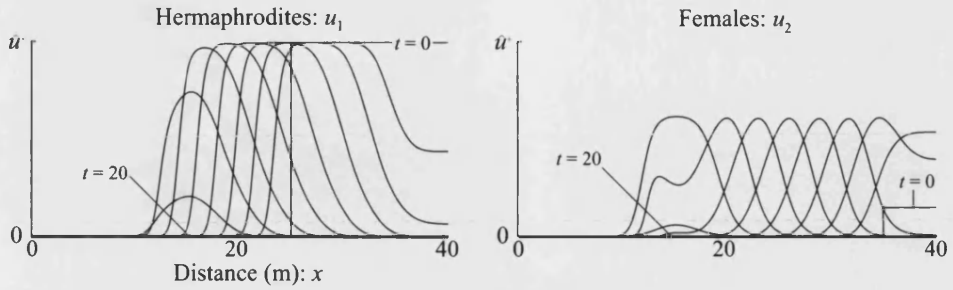

Figure 4-6: In the gynodioecy reaction-diffusion model with self-incompatible hermaphrodites, when diffusion coefficients are similar the female invasion front can catch up with the hermaphrodite establishment front resulting in global extinction for both conspecifics. Parameters $b = 4$, $p = 4$, $\mu = 1.5$, $D_1 = D_2 = 0.2$.

for travelling waves with

$$\begin{pmatrix} u_1(z) \\ u_2(z) \end{pmatrix} \to \begin{pmatrix} \hat{u}^+ \\ 0 \end{pmatrix} \text{ as } z \to -\infty.$$

Figure 4-5 shows a numerical solution developing from initial data

$$u_1(x,0) = \begin{cases} \hat{u}^+ & \text{if } x < 15 \\ 0 & \text{if } x \geq 15 \end{cases},$$
$$u_2(x,0) = \frac{\epsilon}{\sqrt{2\pi}\sigma} \exp\left(-\frac{(x-15)^2}{\sigma^2}\right).$$

In fact, the realized travelling wave rapidly achieves a wave speed very close to c_{inv}, suggesting that it is a pulled wave driven by the initial success of females at the leading edge of the wave. Owen & Lewis (2001) note that is is commonly found that multi-species waves travel at the minimum possible speed, but that this is not the case for some parameter regimes in competition models (Hosono 1998).

If both conspecifics have similar diffusion coefficients the pulled invasion wave of the females will tend to be faster than the pushed establishment wave of the hermaphrodites. So that if the male-sterility mutation first arises away from the hermaphrodite boundary the invasion front will catch up with the establishment front. When the hermaphrodite front is reached its progress is halted and females surround the remaining hermaphrodites and drive them extinct. Figure 4-6 illustrates this sce-

nario with $D_1 = D_2$ and initial data

$$u_1(x,0) = \begin{cases} 0 & \text{if } x < 25 \\ \hat{u}^+ & \text{if } x \geq 25 \end{cases},$$
$$u_2(x,0) = \begin{cases} 0 & \text{if } x < 35 \\ 0.1 & \text{if } x \geq 35 \end{cases}.$$

The ratio of diffusion coefficients determines the consequence of a male-sterility mutation arising in a spatially distributed self-incompatible hermaphrodite species. In general for $D_1/D_2 \approx 1$ the result is extinction as depicted in Figure 4-6. If, however, D_1/D_2 is sufficiently high the female front will not reach the hermaphrodite front and a type of fugitive coexistence will be achieved. This might arise if, for example, the male-sterility mutation caused female fruit to become too large or unpalatable to the animal disperser, drastically limiting female dispersal.

Self-Compatible Hermaphrodites

When $s > 0$ the spatially uniform gynodioecy model can include an internal stable attractor. In particular when $s < 1/(b-1)$ an internal equilibrium $(\hat{u}_1, \hat{u}_2)$ exists for $\mu > \mu_0$ and is stable while $\mu < \mu_2$ at which point a stable limit cycle is emitted which persists while $\mu_2 < \mu < \mu_h$. For $\mu > \mu_h$ there is no internal stable attractor. While $s \geq 1/(b-1)$ the internal equilibrium is stable when it exists for all $\mu > \mu_0$. Figure 4-7(a),(b) and (c) show numerical solutions developing from initial data

$$u_1(x,0) = \begin{cases} \hat{u}^+ & \text{if } x < 45 \\ \hat{u}_1 & \text{if } x \geq 45 \end{cases},$$
$$u_2(x,0) = \begin{cases} 0 & \text{if } x < 45 \\ \hat{u}_2 & \text{if } x \geq 45 \end{cases},$$

for different values of μ corresponding with different local behaviours of the internal equilibrium $(\hat{u}_1, \hat{u}_2)$. In (a) and (b) the internal equilibrium is stable: monotone waves result when the equilibrium is a node and non-monotone waves result when it is a focus. The invasion profile in these cases is similar to that observed in predator-prey models with self-limiting prey populations (Dunbar 1983, Dunbar 1984, Murray 1989*a*). In (c) the internal equilibrium is unstable but the tail of the wave appears, initially at least, to feature damped oscillations returning to the equilibrium. In Figure 4-7(d) numerical

solutions develop from

$$u_1(x,0) = \begin{cases} \hat{u}^+ & \text{if } x < 45 \\ \hat{u}_1 & \text{if } x \geq 45 \end{cases},$$
$$u_2(x,0) = \frac{\epsilon}{\sqrt{2\pi}\sigma} \exp\left(-\frac{(x-15)^2}{\sigma^2}\right),$$

and an extinction wave results similar to that observed for $s = 0$ in Figure 4-5.

When $\mu \in (\mu_2, \mu_h)$ as in Figure 4-7(c) the kinetic equations feature a limit cycle and the coexistence equilibrium is unstable. A similar invasion problem has been considered in predator-prey systems when the predator response to prey follows an increasing saturating functional response (Sherratt et al. 1995, Sherratt 2001) and also arises in certain unrealistic parameter regimes in cell-proliferation models (Sherratt 1993, Sherratt 1994*a*). In these cases extensive numerical simulations have found that a travelling wave front propagates at a speed close to c_{inv} driven by the linearized growth of the invader at the leading edge of the wave, the tail of the front oscillates and decays exponentially to the unstable equilibrium. As the wave passes it perturbs the unstable equilibrium and spatiotemporal oscillations result. These oscillations may be regular or irregular (chaotic), they are not part of the invasive wave and spread with their own characteristic speed. Figure 4-8 shows irregular waves developing in the wake of female invasion in the gynodioecy model. Whether regular or irregular waves occur in the wake of the invasion depends upon the stability of the oscillatory travelling waves, or wave-trains, as solutions of the reaction-diffusion system. Figure 4-9 shows that irregular oscillations also arise following a perturbation of the $(\hat{u}_1,\hat{u}_2)$ steady state with boundary conditions

$$\mathbf{u}(0,t) = (\hat{u}_1, \hat{u}_2) \text{ and } \frac{\partial \mathbf{u}}{\partial x}(l,t) = 0.$$

Such circumstances are often more conducive to stable waves-train solutions (J. Sherratt, *Pers. Comm.*) Figure 4-9(a) shows oscillations initiated with a discontinuous random initial perturbation; (b) shows oscillations initiated with the continuous perturbation

$$u_1(x,0) = \epsilon \tan^{-1}(\alpha(x - x_0)) \exp(\alpha(x - x_0)).$$

It is not known how to analyse the stability of such wave-train solutions directly, but progress can be made near the hopf-bifurcation if $D_1 = D_2$, when solution behaviour

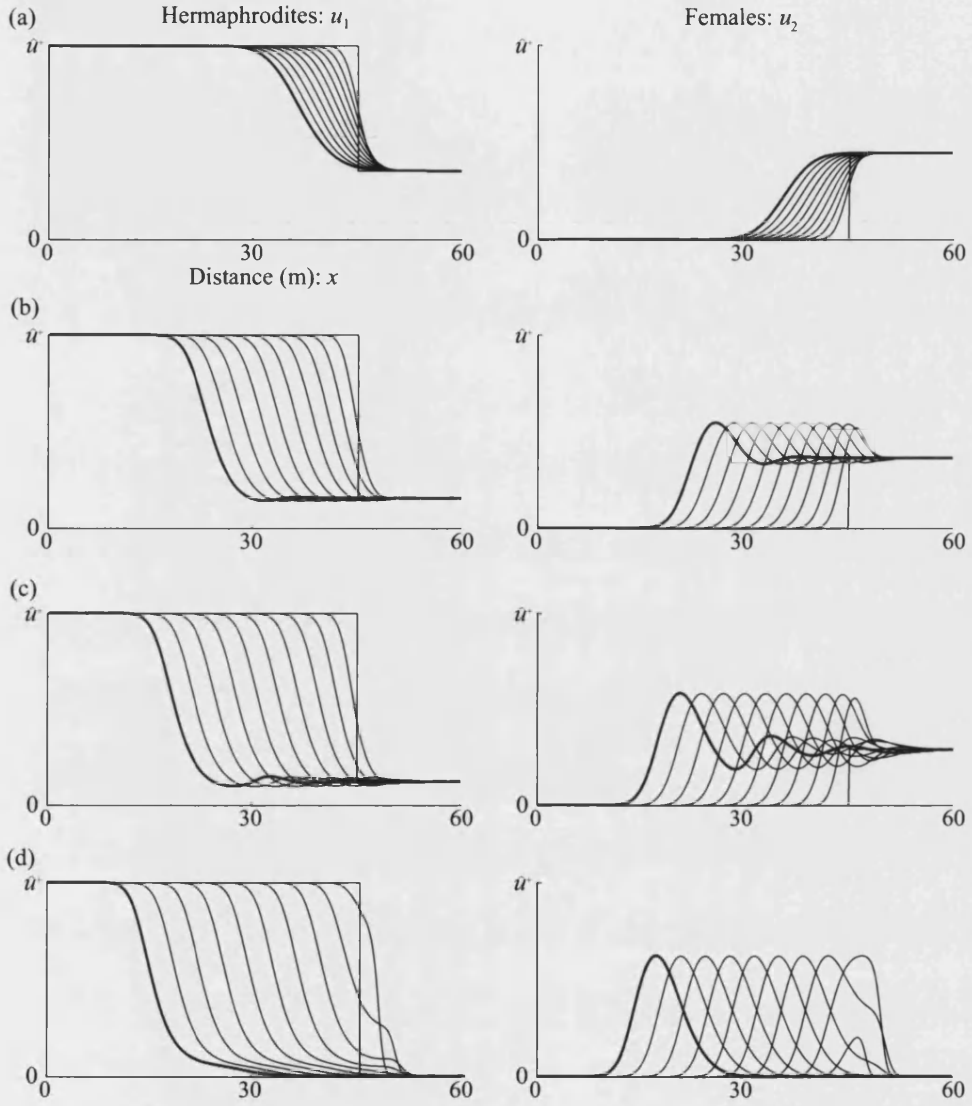

Figure 4-7: Travelling wave solutions for the reaction-diffusion gynodioecy model with selfing connect the hermaphrodite only steady-state $(\hat{u}^+, 0)$ with an internal stable attractor in (a), (b) and (c) or with the extinction steady-state $(0, 0)$ in (d). Parameters $b = 4$, $p = 4$, $s = 0.2$, $D_1 = D_2 = 0.2$. (a) $\mu = 1.1$ internal steady-state is attracting node, wave-speed after 60 generations is $c = 0.2511$ close to the necessary minimum speed $c_{\text{inv}} = 0.2594$. (b) $\mu = 1.3$ internal steady-state is attracting focus, wave-speed after 60 generations is $c = 0.4690$ and $c_{\text{inv}} = 0.4617$. (c) $\mu = 1.4$ internal stable limit cycle, wave-speed after 60 generations is $c = 0.5463$ and $c_{\text{inv}} = 0.5360$. (d) $\mu = 1.5$ no internal stable set, wave-speed after 60 generations is $c = 0.6139$ and $c_{\text{inv}} = 0.6060$.

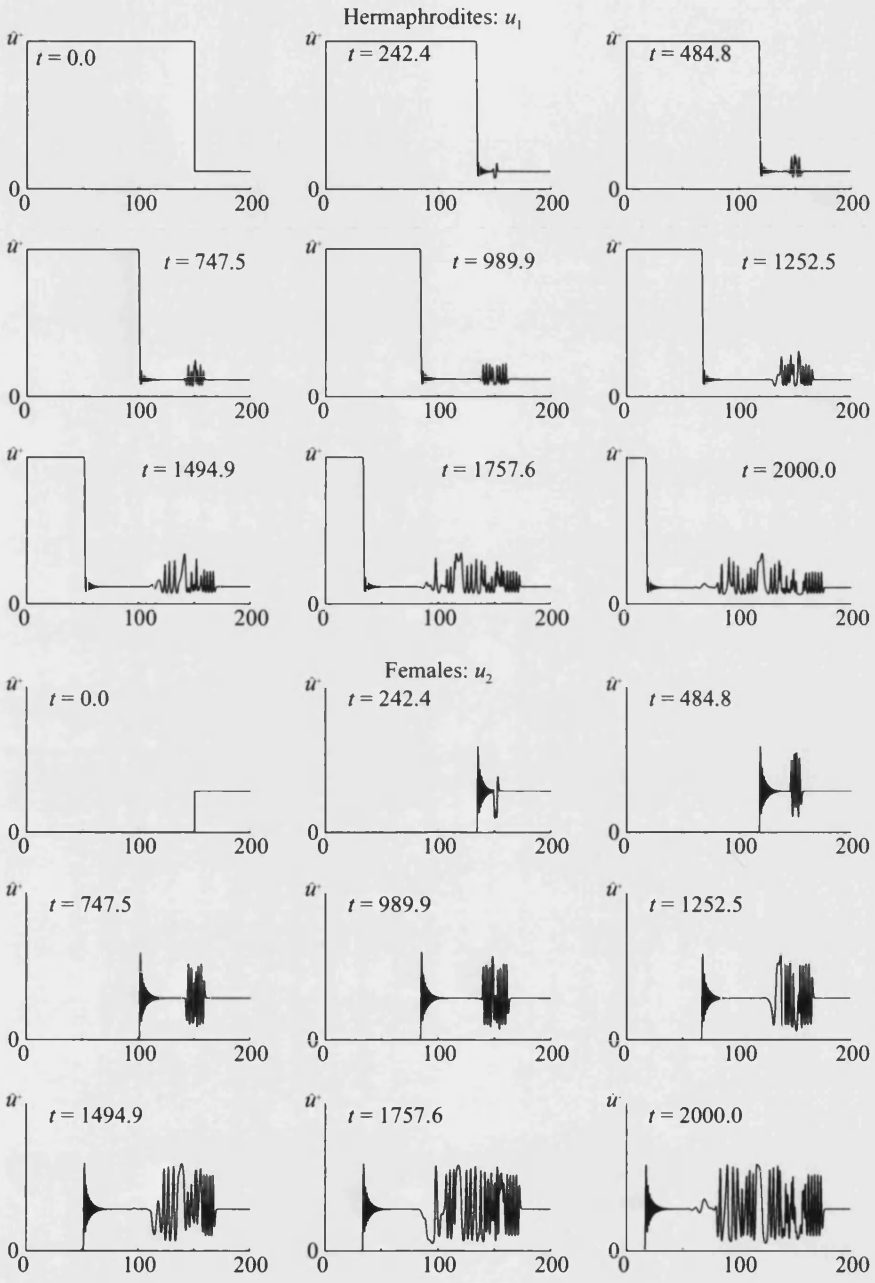

Figure 4-8: The irregular wake of travelling wave solutions connecting the hermaphrodite only equilibrium with the internal stable limit cycle. Parameters $b = 4$, $p = 4$, $s = 0.2$, $\mu = 1.42$

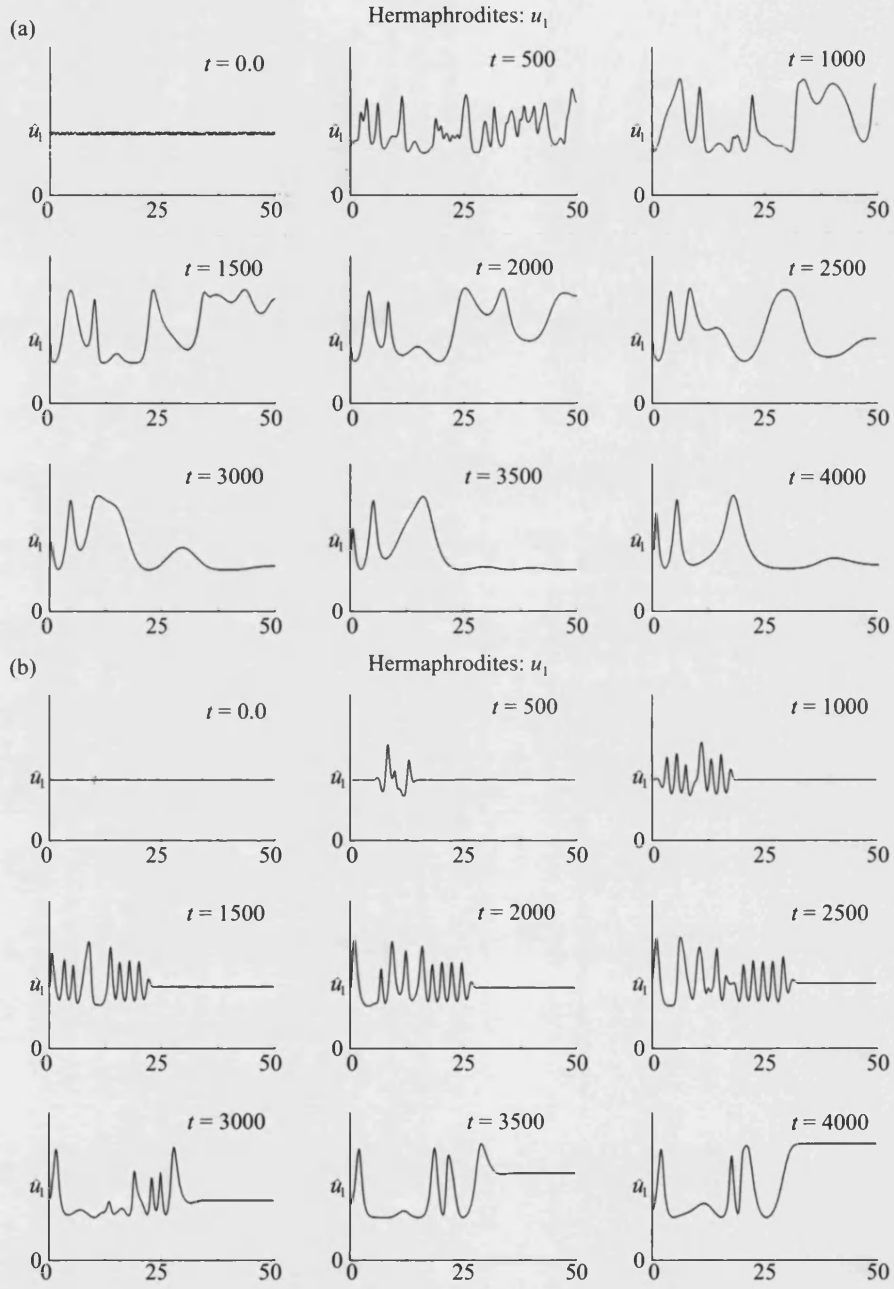

Figure 4-9: Irregular oscillations arising directly from perturbations of the unstable steady state ($\hat{u}_1$,$\hat{u}_2$). (a) Discontinuous random initial perturbation. (b) Continuous perturbation ($\epsilon = 0.05$, $\alpha = 5.0$ and $x_0 = 10$). Parameters $b = 4$, $p = 4$, $s = 0.2$, $\mu = 1.4$

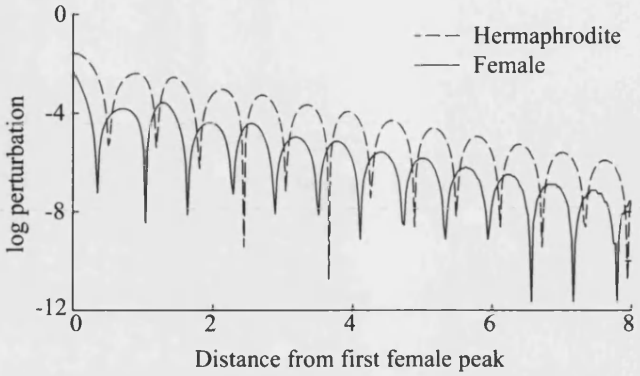

Figure 4-10: The exponential oscillating decay in the tail of the invasion wave depicted in Figure 4-8, plotted are $\ln \|u_1 - \hat{u}_1\|$ and $\ln \|u_2 - \hat{u}_2\|$ for $t = 500$ in the region to the right of the first female peak. Linear regression on maxima gives the rate of decay for hermaphrodites as -0.5814 and for females -0.5474. The period of oscillation is roughly 1.2414 for hermaphrodites, 1.2706 for females.

in the vicinity of the unstable equilibrium is well approximated by a λ-ω system of reaction-diffusion equations. λ-ω systems are the prototype reaction-diffusion system with oscillatory kinetics and in one dimension appear

$$\begin{aligned} v_t &= \lambda(r)v - \omega(r)w + v_{xx}, \\ w_t &= \omega(r)v + \lambda(r)w + w_{xx}, \end{aligned} \tag{4.2.3}$$

where $r = \sqrt{v^2 + w^2}$. Kopell & Howard (1973) show that λ-ω systems have one parameter families of spatiotemporal periodic solutions known as wave-train solutions which can be written explicitly as

$$\begin{aligned} v &= r_0 \cos(\omega(r_0)t \pm \sqrt{\lambda(r_0)}x), \\ w &= r_0 \sin(\omega(r_0)t \pm \sqrt{\lambda(r_0)}x), \end{aligned}$$

where the parameter, r_0, is the amplitude of the waves. Wave-train solutions are stable if

$$4\lambda r_0 \left[1 + \left(\frac{\omega'(r_0)}{\lambda'(r_0)}\right)^2\right] + r_0\lambda'(r_0) \leq 0.$$

To make use of these results Sherratt (1994*b*) considers a λ-ω system with

$$\lambda(r) = \lambda_0 + \lambda_1 r^2,$$
$$\omega(r) = \omega_0 + \omega_1 r^2,$$

For $\lambda_0, \lambda_1 > 0$ the kinetics have a single unstable equilibrium at $(0,0)$ surrounded by a stable limit cycle, providing a qualitative match with the unstable internal equilibrium of some predator-prey kinetics (Sherratt et al. 1995, Sherratt 2001). Confining 4.2.3 to the half-line $\mathbb{R}^-$, a perturbation may be applied to the unstable steady state $(0,0)$ that mimics the perturbation caused by the passing of the invading wave in invasion problem. Sherratt (1994*b*) considers monotone exponentially decaying perturbations and Sherratt (1998) considers an exponentially decaying oscillating perturbation and in both cases determines that wave-train solutions evolve with amplitude

$$r_0 = \sqrt{\frac{2\lambda_0}{\omega_1^2}\left(\sqrt{\lambda_1^2+\omega_1^2} - \lambda_1\right)},$$

from which the stability criterion

$$\frac{|\omega_1|}{\lambda_1} < 1.0714... \tag{4.2.4}$$

is deduced. In fact Sherratt (1998) also improves the similarity with the invasion problem by augmenting 4.2.3 with an advection term that incorporates the notion that the perturbation applied by the invasion is moving.

The stability of the wave-train solutions for the gynodioecy model can be investigated by the same method when the kinetics are sufficiently close to the Hopf bifurcation that they are well approximated by a λ-ω system of the form treated by Sherratt (1994*b*). Figure 4-10 illustrates the oscillating exponential decay of the numerical solutions in Figure 4-8 in the tail of the invasion wave. To parameterize the λ-ω system 4.2.1 must be reduced to the to appropriate form. As with the analysis of the stability of the Hopf bifurcation in the kinetics in chapter 3, the equilibrium $(\hat{u}_1, \hat{u}_2, \mu_2)$ is translated to the origin with the substitutions $u_1^* = u_1 - \hat{u}_1$, $u_2^* = u_2 - \hat{u}_2$ and $\mu^* = \mu - \mu_2$. Let $\hat{J}(\mu^*) = (j_{ij}(\mu^*))$ denote the Jacobian evaluated at $(0,0,\mu^*)$, then ω_0 and λ_0 may

be taken

$$\lambda_0(\mu^*) = \frac{\mu^*}{2}\frac{\partial \mathrm{tr}\hat{J}}{\partial \mu^*}(0),$$
$$\omega_0 = \det \hat{J}(0),$$

so that defining the linear transformation

$$P = \begin{pmatrix} j_{11}(0) & -\omega_0 \\ j_{21}(0) & 0 \end{pmatrix},$$

and the linear change of variables

$$\begin{pmatrix} v \\ w \end{pmatrix} = P^{-1}\begin{pmatrix} u_1^* \\ u_2^* \end{pmatrix},$$

the gynodioecy model at the Hopf bifurcation point can be expressed

$$\begin{pmatrix} \dot{v} \\ \dot{w} \end{pmatrix} = P^{-1}\begin{pmatrix} f(u_1^*, u_2^*) \\ g(u_1^*, u_2^*) \end{pmatrix} + \begin{pmatrix} v_{xx} \\ w_{xx} \end{pmatrix} = \begin{pmatrix} -\omega_0 w + F(x,y) + v_{xx} \\ \omega_0 v + G(x,y) + w_{xx} \end{pmatrix}. \quad (4.2.5)$$

The nonlinear terms F and G determine λ_1 and ω_1 according to the following standard formulae (Guckenheimer & Holmes 1983, Sherratt 2001) in terms of second and third order partial derivatives

$$\begin{aligned}
\lambda_1 =& \frac{-1}{16}\left[F_{vvv} + F_{vww} + G_{vvw} + G_{www}\right] \\
&+ \frac{1}{16\omega_0}\left[F_{vv}G_{vv} - F_{ww}G_{ww} - F_{vw}(F_{vv} + F_{ww}) + G_{vw}(G_{vv} + G_{ww})\right], \\
\omega_1 =& \frac{1}{16}\left[G_{vvv} + G_{vww} - F_{vvw} - F_{www}\right] \\
&+ \frac{1}{48\omega_0}\left[F_{vv}(G_{vw} - F_{ww}) + G_{ww}(F_{vw} - G_{vv}) - 3F_{ww}(G_{vw} + F_{ww})\right. \\
&\left. -3G_{vv}(F_{vw} + G_{vv}) - 2(F_{vv} + F_{ww} - G_{vw})^2 - 2(G_{vv} + G_{ww} - F_{vw})^2\right].
\end{aligned}$$

The stability condition 4.2.4 was tested on the set $(1, 40] \times (p_{\mathrm{crit}}, 40] \times (0, 1/(b-1))$ in (b, p, s)-parameter space on which it is seen to vary continuously and fail everywhere. This result is consistent with the irregular wake seen in Figure 4-8 and the irregular oscillations in Figure 4-9.

Diffusion Driven Instability

Diffusion driven or Turing instability (Turing 1952) describes the situation when a stable steady state of the reaction kinetics is unstable as a spatially uniform steady state of the reaction-diffusion system. Such a possibility arises in two-species system when an increase in one species promotes the growth of both species and an increase of the other species inhibits the growth of both species, such a system is described as a pure activator-inhibitor system. Intuitively the gynodioecy system with selfing has the potential for this arrangement since hermaphrodites produce a resource whose availability limits growth of both conspecifics and the presence of competing females is detrimental to the growth of both species. However, an increase in hermaphrodites also increases intra-specific competition and so can inhibit growth of both conspecifics particularly when the hermaphrodite population is already large and pollen is abundant. The gynodioecy system with selfing is a pure activator-inhibitor system when a stable internal equilibrium is determined by the intersection of the f_2 nullcline with the f_1 nullcline to the left of it maximal point (see for example chapter 3 Figure 3-6(c).) This applies when

$$\mu \in \begin{cases} (\mu_t, \mu_2) & \text{if } s < 1/(b-1) \\ (\mu_t, \infty) & \text{if } s \geq 1/(b-1) \end{cases},$$

where

$$\mu_t = \frac{p + (1-s)\sqrt{bp}}{p + (1-s)\sqrt{bp} - bs}.$$

It is readily demonstrated for $s < 1/(b-1)$ that $\mu_2 \geq \mu_t$ with equality when $p = p_{\text{crit}}$.

Potential Turing instability of the uniform steady state $(\hat{u}_1, \hat{u}_2)$ occurs if

$$\det(\hat{J} - \lambda D) = 0,$$

has one or more positive real roots, where $\hat{J}$ is the Jacobian of $(\hat{u}_1, \hat{u}_2)$ and

$$D = \begin{pmatrix} D_1 & 0 \\ 0 & D_2 \end{pmatrix},$$

(see for example Murray (1989*b*, pp 82-90).) This is the case for $D_1/D_2 = \delta < \delta_{\text{crit}}$

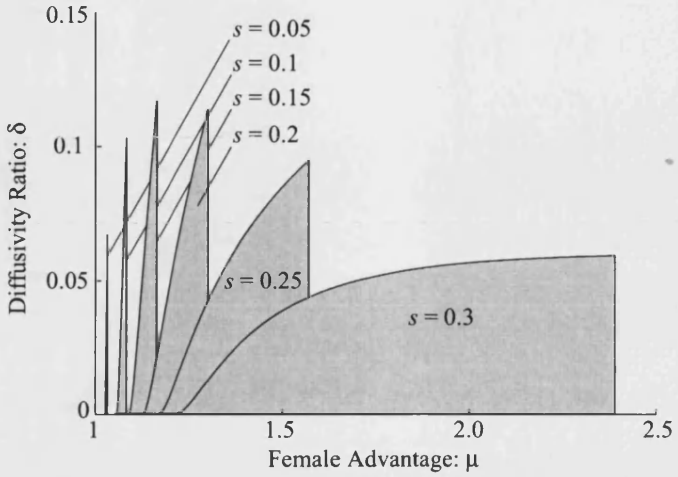

Figure 4-11: When $\mu \in (\mu_t, \mu_d)$ the gynodioecy model with selfing is potentially Turing unstable if $D_1/D_2 = \delta < \delta_{\text{crit}}$. Grey regions indicate where this is the case for various levels of selfing. Parameters $b = 4$, $p = 4$.

where $\delta_{\text{crit}} < 1$ is the lesser root of

$$\delta^2 + 2\delta\left(\frac{2\hat{f}_{u_2}\hat{g}_{u_1}}{\hat{g}_{u_2}^2} - \frac{\hat{f}_{u_1}}{\hat{g}_{u_2}}\right) + \left(\frac{f_{u_1}}{g_{u_2}}\right)^2 = 0.$$

Figure 4-11 illustrates how δ_{crit} varies with μ on (μ_t, μ_2) for several values of s. For $\delta < \delta_{\text{crit}}$ the reaction-diffusion system will exhibit Turing instability and small non-uniform perturbations of the steady state $(\hat{u}_1, \hat{u}_2)$ will grow if for at least one wavenumber k of the linearized system $k^2 \in (\lambda^-, \lambda^+)$ where

$$\lambda^{\pm} = \frac{\hat{f}_{u_1} + \delta\hat{g}_{u_2}}{2} \pm \sqrt{\left(\frac{\hat{f}_{u_1} + \delta\hat{g}_{u_2}}{2}\right)^2 - \frac{\det(\hat{J})}{D_1 D_2}}.$$

The wavenumbers of 4.2.1 linearized about $(\hat{u}_1, \hat{u}_2)$ are determined by boundary conditions (or lack thereof) imposed on the system. On an infinite domain with the requirement that u_1, u_2 are bounded every $k > 0$ is a wavenumber (Murray 1989*b*, p 90). In this case potential Turing instability coincides with Turing instability and for $\delta < \delta_{\text{crit}}$ and any non-uniform perturbation will grow. For a finite domain Ω with

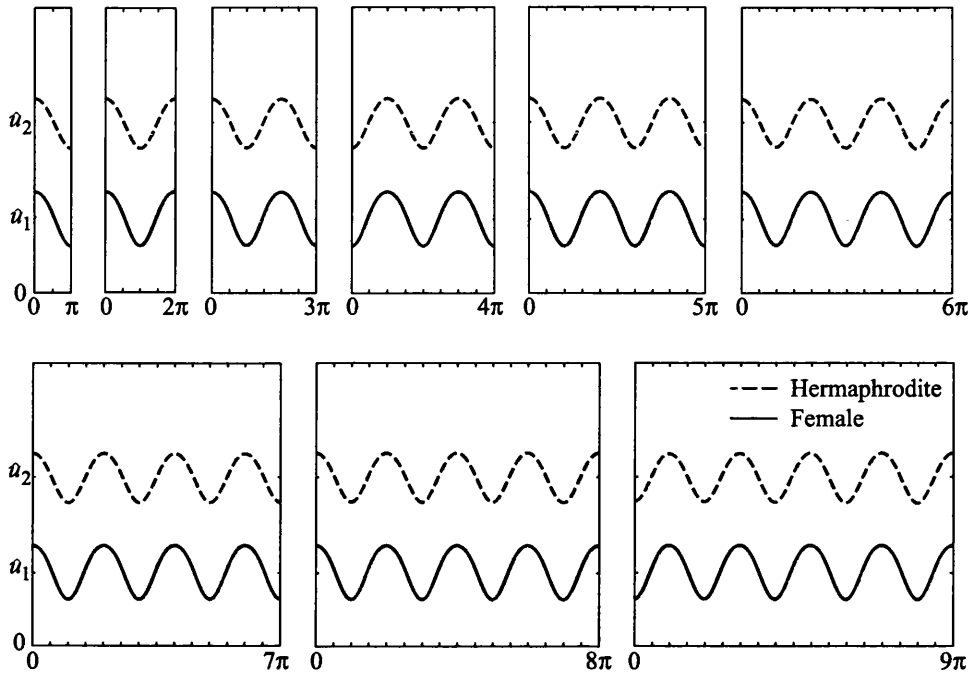

Figure 4-12: When the gynodioecy model exhibits Turing instability ($\mu_t < \mu \leq \mu_2$, $\delta > \delta_{\text{crit}}$) spatial patterns result when the spatially uniform equilibrium $(\hat{u}_1, \hat{u}_2)$ is perturbed. Successive wavenumbers become unstable as the domain size gets larger (Illustrated are wavenumbers one to nine). Parameters $b = 4$, $p = 4$, $s = 0.2$, $\mu = 1.3$, $D_1 = 0.01$, $D_2 = 0.1$.

zero-flux boundary conditions

$$\nabla \begin{pmatrix} u_1 \\ u_2 \end{pmatrix} .\mathbf{n} = 0 \text{ on } \partial\Omega,$$

solutions of the linearized system

$$\mathbf{w}_t = \hat{J}\mathbf{w} + D\Delta\mathbf{w},$$

look like

$$\mathbf{w}(x,t) = \sum_i A_i e^{\sigma t} W_i(\mathbf{x}),$$

where W_i are spatial eigenfunctions satisfying

$$\Delta W_i = -k_i^2 W_i.$$

For the domain $[0, l] \subseteq \mathbb{R}$ eigenfunctions are $W_0 = 1$ and $W_n(x) = \cos(n\pi x/l)$ with corresponding wavenumbers $k_n = n\pi/l$. When $\delta < \delta_{\text{crit}}$ domain size is, therefore, crucial to stability. If $l \leq \pi/\sqrt{\lambda^+}$ there are no wavenumbers with $k_n^2 \in (\lambda^-, \lambda^+)$ and hence no instability. As l increases successive wavenumbers become unstable and the following hold

The 1st spatial mode is unstable when $\frac{\pi}{\sqrt{\lambda^+}} < l < \frac{\pi}{\sqrt{\lambda^-}}$,
The 2nd spatial mode is unstable when $\frac{2\pi}{\sqrt{\lambda^+}} < l < \frac{2\pi}{\sqrt{\lambda^-}}$,
The 3rd spatial mode is unstable when $\frac{3\pi}{\sqrt{\lambda^+}} < l < \frac{3\pi}{\sqrt{\lambda^-}}$,
etc...

For many l more than one spatial mode will be unstable, in this case the n-th spatial mode will be the fastest growing where n minimizes

$$|k_n^2 - \lambda_{\min}|,$$

and where

$$\lambda_{\min} = \frac{\lambda^- + \lambda^+}{2} = \frac{\hat{f}_{u_1} + \delta \hat{g}_{u_2}}{2}.$$

Figure 4-12 illustrates the spatial pattern at equilibrium resulting from the instability of successive spatial modes as l increases. Note that the phase of hermaphrodites and females is synchronized, this is characteristic of pure-activator inhibitor systems. The spatial pattern in each case is one of two possible non-uniform equilibria, either $u_1(0) > \hat{u}_1$ and $u_2(0) > \hat{u}_2$ or $u_1(0) < \hat{u}_1$ and $u_2(0) < \hat{u}_2$. The pattern selected by the system is highly sensitive to the form of the initial perturbation away from the uniform steady state.

When $\mu_t < \mu < \mu_2$ and females disperse seed significantly further than hermaphrodites $D_2/D_1 > \delta_{\text{crit}}$ the gynodioecy model with selfing is potentially Turing unstable and can adopt a spatially heterogenous equilibrium. In the resulting spatial pattern, total population density oscillates with a regular spatial period.

Discussion

The reaction-diffusion gynodioecy model without selfing inherits the extinction dynamics exhibited by the kinetic equations. Females initially confined to a small region of space disperse seed to neighbouring hermaphrodite populations and further local invasions are initiated. The resulting invasion wave features neighbouring populations in various stages of the extinction dynamics. Because no internal equilibria occur in the kinetics stable coexistence of uniform or spatially heterogenous populations is impossible. If hermaphrodites disperse significantly more rapidly than females a form of fugitive coexistence is possible with hermaphrodites advancing into virgin territory at one edge while retreating from female dominated locations at the other. In such a circumstance the female population presents the hermaphrodite populations with an absolute barrier to the empty habitat behind the invasion wave. This is an artifact of the deterministic nature of the model. In a discrete stochastic model, hermaphrodites would occasionally persist in small numbers behind the wave, possibly permitting recolonization and yielding a more complicated pattern of non-equilibrium coexistence. There is however, little, if any, evidence that hermaphrodites and females disperse at significantly different rates.

When selfing amongst hermaphrodites is introduced, a variety of model behaviours are possible in the kinetic equations and many more emerge as a consequence of the spatial distribution of populations. Broadly, when the kinetic equation include a stable attractor ($\mu \in (\mu_0, \mu_h]$), coexistence results when a small number of females are introduced into a hermaphrodite population. In the absence of an internal attractor population extinction dynamics similar to the self-incompatible case result. Coexistence may take the form of a spatially uniform steady state or a spatially heterogenous steady state, or exclusively temporal oscillations or spatio-temporal oscillations. Although regular spatio-temporal oscillations or wave-train solutions exist, they are unstable and spatio-temporal chaos is observed, for example, in the wake of invasion when $(\hat{u}_1, \hat{u}_2)$ is unstable (see Figure 4-8). All of these behaviours arise within quite a narrow band of parameter space ($\mu_0 < \mu \leq \mu_h$) making it difficult to give general predictions for what might be observed in natural populations. On the other hand the range of behaviour of the model make it a powerful tool for explaining a wide range of phenomena that might be empirically observed.

The behaviour of the gynodioecy reaction-diffusion model with selfing has many parallels with predator-prey models when prey are self-limiting (Murray 1989*a*, Sherratt

2001) and when prey experience an Allee effect (Owen & Lewis 2001, Petrovskii et al. 2005), despite no formal equivalence of the reaction kinetics. In particular, waves in which the coexistence steady-state displaces the steady state featuring exclusively the self-sustaining type are found in numerical solutions when the coexistence steady-state is stable. Contrasts arise when the internal equilibrium is unstable. When a stable limit cycle exists, an invasion wave can perturb the internal equilibrium resulting in irregular spatiotemporal heterogeneity, but the regular spatiotemporal plane-waves found in predator-prey systems are seemingly never observed. As was discussed in chapter 3 the gynodioecy model with selfing characterization of host-exploiter dynamics fits a number of biological scenarios and it would be interesting to know whether host-exploiter reaction-diffusion systems can ever admit stable plane-wave solutions.

4.3 SEXUAL-ASEXUAL

The sexual-asexual model introduced in chapter 3 section 3.4 is extended to a reaction-diffusion system. The size of the sexually reproducing population at x at time t is $u_1(x,t)$, the size of the pseudogamous apomictic population is $u_2(x,t)$. Cross-pollination is again assumed to occur only between individuals at the same spatial location. The kinetic terms for sexuals and asexuals respectively are

$$f(u_1(x,t),u_2(x,t)) = \frac{\mu bp(u_1(x,t)+\frac{\nu}{2}u_2(x,t))u_1(x,t)}{1+p(u_1(x,t)+u_2(x,t))}(1-u_1(x,t)-u_2(x,t))-u_1(x,t),$$

$$g(u_1(x,t),u_2(x,t)) = \frac{bp((1+\frac{\mu\nu}{2})u_1(x,t)+u_2(x,t))u_2(x,t)}{1+p(u_1(x,t)+u_2(x,t))}(1-u_1(x,t)-u_2(x,t)) - u_2(x,t).$$

The reaction-diffusion system is given by

$$\begin{aligned}\frac{\partial u_1}{\partial t} &= f(u_1,u_2)+D_1\Delta u_1,\\ \frac{\partial u_2}{\partial t} &= g(u_1,u_2)+D_2\Delta u_2,\end{aligned} \tag{4.3.1}$$

where D_1 and D_2 specify possibly different diffusion coefficients for sexuals and apomicts. There is evidence that differing selective pressures on sexual and apomictic conspecifics can act to modify dispersal strategies. O'Connell & Eckert (2001) describe differences in the dispersal range of wind dispersed diaspores for sexual and asexual conspecifics in *Antennaria parlinii*, asexually produced seed has a lower settling veloc-

ity and so might be expected to disperse further. Although *Antennaria parlinii* are diplosporous and non-pseudogamous and the pollen requirement of pseudogams may make overly rapid dispersal mal-adaptive. The necessity of describing conspecific populations with separate equations makes the consideration of differing diffusion rates possible in a way that was unavailable to comparable population genetic models (Britton & Mogie 2001, Carrillo 2002).

Travelling Wave Solutions

Attention is focussed on travelling wave solutions that evolve from initial data describing adjacent pure populations of sexuals and asexuals at their respective carrying capacities. This initial configuration could hypothetically arise following an ice age. If, due to a greater tolerance for extreme conditions, apomicts become established in newly opened territories beyond the habitat boundaries of the sexual population. Initially geographically separate sexual and apomictic populations will be pure, but as climate improves the potential range of sexuals overlaps the established apomictic population and the boundary may become dynamic. Consider then that initially a pure sexual population is established within a circular region representing a glacial refuge and an apomictic population is established in an annulus beyond the perimeter. As before the problem is reduced to a single spatial dimension by considering only radial distance x and assuming the boundary between the populations is sufficiently far away from the centre of the refuge that $\Delta u_i \approx \partial u_i/\partial x$. In each of the figures in this section the initial data is taken as

$$u_1(x,0) = \begin{cases} \hat{u}_1^+ & \text{if } x < 30 \\ 0 & \text{if } x \geq 30 \end{cases},$$

$$u_2(x,0) = \begin{cases} 0 & \text{if } x < 30 \\ \hat{u}_2^+ & \text{if } x \geq 30 \end{cases}.$$

Travelling waves moving either right or left are sought in the moving frame $z = x+ct$

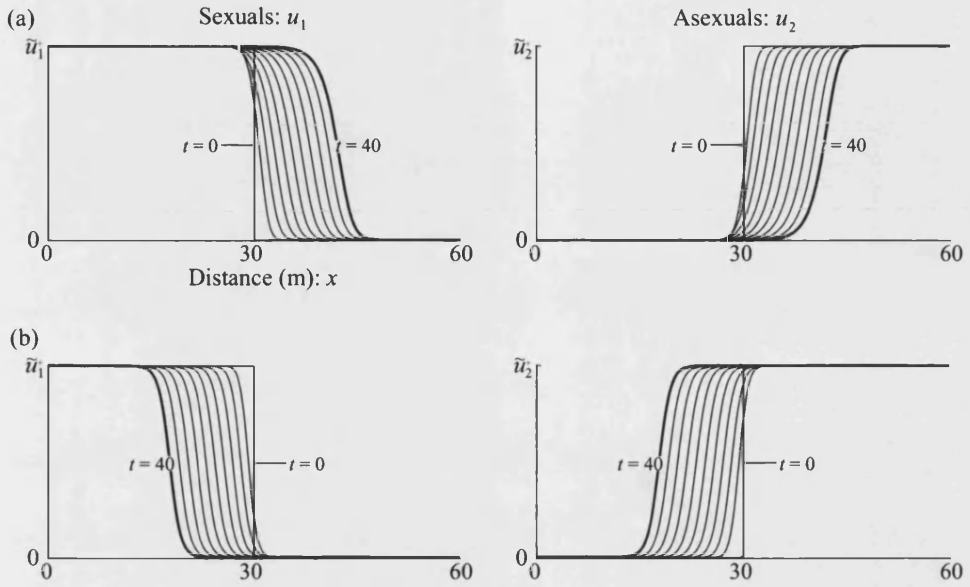

Figure 4-13: Travelling wave solutions for the sexual-asexual model connect the sexual only steady state $(\hat{u}_1^+, 0)$ with the asexual only steady state $(0, \hat{u}_2^+)$. (a) Asexual only steady state is unstable and sexual range expands. Plot takes $\mu = 3.0$, $\nu = 0.75$ and gives wave speed $c_{\text{obs}} = 0.3509$ at $t = 40$, greater than the necessary minimum wave speed from linear analysis $c_{\text{sex}} = 0.3162$. (b) Sexual only steady state is unstable and asexual range expands. Plot takes $\mu = 1.15$, $\nu = 0.5$ and gives wave speed $c_{\text{obs}} = 0.3427$ at $t = 40$, greater than the necessary minimum wave speed from linear analysis $c_{\text{asex}} = 0.3093$. Parameters $b = 4$, $p = 4$, $D_1 = D_2 = 0.2$.

with

$$\begin{aligned} \begin{pmatrix} u_1(z) \\ u_2(z) \end{pmatrix} &\to \begin{pmatrix} 0 \\ \hat{u}_2^+ \end{pmatrix} \text{as} z \to \infty, \\ \begin{pmatrix} u_1(z) \\ u_2(z) \end{pmatrix} &\to \begin{pmatrix} \hat{u}_1^+ \\ 0 \end{pmatrix} \text{as} z \to -\infty, \end{aligned} \tag{4.3.2}$$

Monostability In the cases that either $(\hat{u}_1^+, 0)$ or $(0, \hat{u}_2^+)$ are unstable equilibria of the kinetic equations travelling waves of asexual or sexual range expansion (respectively) are expected. A similar linear analysis to that conducted for the gynodioecy model

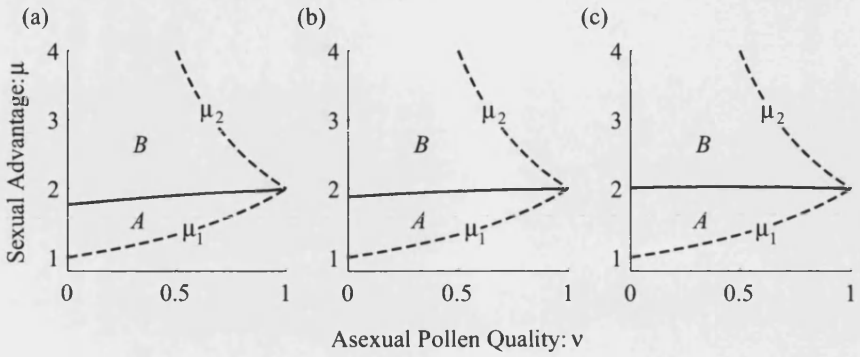

Figure 4-14: At boundaries between sexual and asexual populations parameters either favour sexual or asexual range expansion. In region A below the solid curve asexual range expansion is predicted. In region B above the solid curve sexual range expansion is predicted. Parameters $b = 4$, $p = 4$. (a) $D_1 = 0.4$, $D_2 = 0.2$. (a) $D_1 = 0.2$, $D_2 = 0.2$. (a) $D_1 = 0.2$, $D_2 = 0.4$.

above reveals necessary minimum wave speeds. In the case $(0, \hat{u}_2^+)$ is unstable the minimum speed of sexual range expansion is $c_{\text{sex}} = 2\sqrt{D\hat{f}_{u_1}}$ where

$$\hat{f}_{u_1} = \frac{\partial f}{\partial u_1}(0, \hat{u}_2^+),$$

is given as the top left element of $J(0, \hat{u}_2^+)$ in chapter 3 Section 3.4. Note that linear analysis gives a lower bound for the wave speed because $\hat{f}_{u_1} > 0$ when $(0, \hat{u}_2^+)$ is unstable. However it is not the case that

$$\frac{\partial f}{\partial u_1}(0, \hat{u}_2^+) \geq \frac{\partial f}{\partial u_1}(u, v),$$

for all $u, v \in [0, \infty)$ and so the asymptotic wave speed need not equal the necessary minimum speed. Figure 4-13(a) illustrates sexual range expansion. In the case that $(\hat{u}_1^+, 0)$ is unstable the minimum speed of asexual range expansion is $c_{\text{asex}} = 2\sqrt{D\hat{g}_{u_2}}$ where

$$\hat{g}_{u_2} = \frac{\partial g}{\partial u_2}(\hat{u}^+, 0),$$

is given as the bottom right element of $J(\hat{u}_1^+, 0)$ in chapter 3 Section 3.4. Figure 4-13(b) illustrates asexual range expansion.

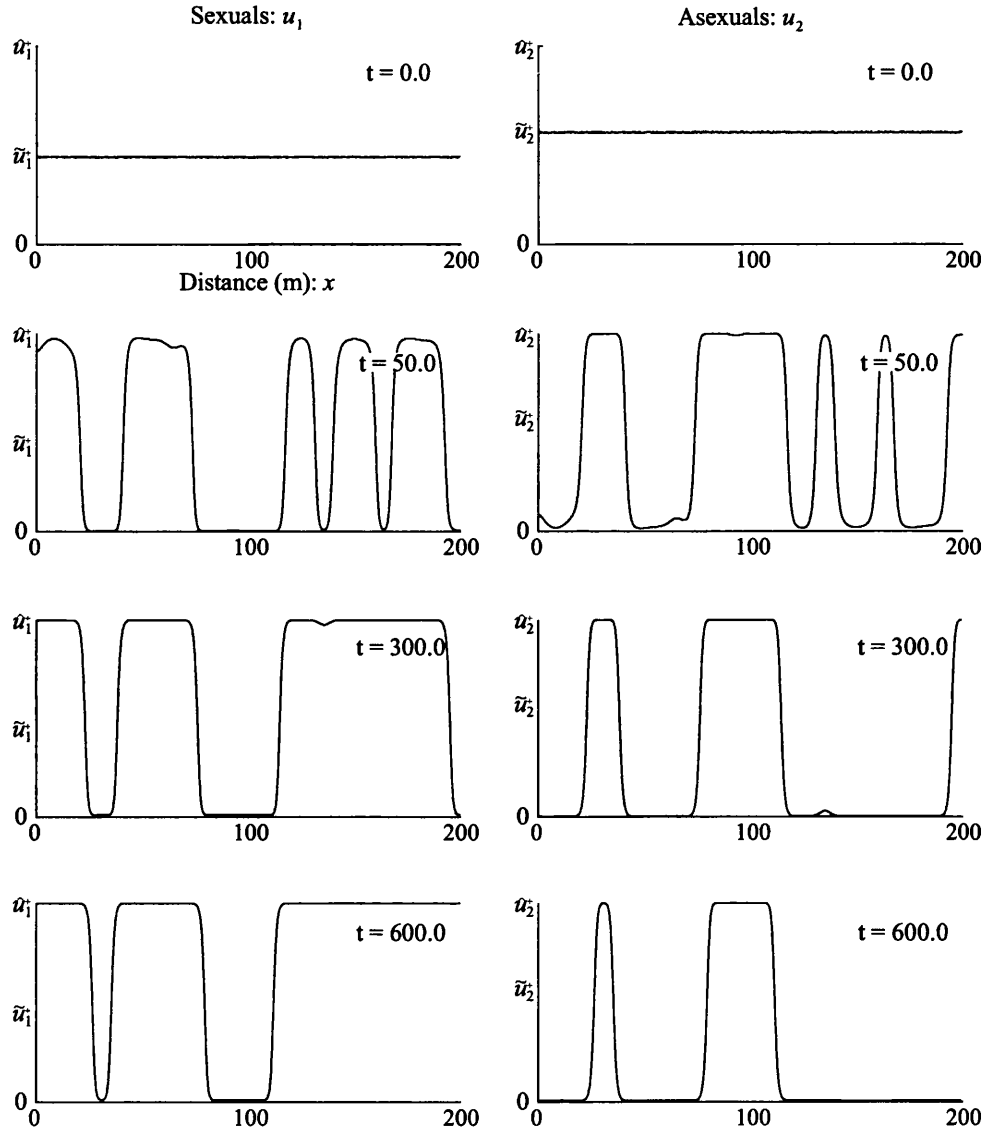

Figure 4-15: Following a perturbation of the unstable internal equilibrium $(\tilde{u}_1^+, \tilde{u}_2^+)$ domains of sexual and asexual dominance are rapidly established. Subsequent range expansion of the reproductive mode favoured at the boundary of these domains can be very slow. Parameters $b = 4$, $p = 4$, $\mu = 2.0$, $\nu = 0.5$, $D_1 = D_2 = 0.2$.

Bistability When neither $(\hat{u}^+, 0)$ or $(0, \hat{u}_2^+)$ are unstable, the direction of any range expansion travelling wave that develops depends not on the success of the invading conspecific when it is rare at the wavefront, but on the interaction of conspecifics over the whole boundary. For any continuous monotone travelling wave satisfying (4.3.2) there exists a point $x_b(t)$ such that

$$\frac{u_1(x_b,t)}{u_2(x_b,t)} = \frac{2-\mu\nu}{\mu(2-\nu)-2} = \alpha.$$

That is $(u_1(x_b,t), u_2(x_b,t))$ is a point on the linear invariant manifold of the kinetic equations connecting $(0,0)$ with $(\tilde{u}_1^{\pm}, \tilde{u}_2^{\pm})$. Defining $w = u_1 + u_2$ and $p = u_1/w$ notice

$$\begin{aligned}\frac{\partial p}{\partial t} &= \frac{1}{w}\frac{\partial u_1}{\partial t} - \frac{p}{w}\frac{\partial w}{\partial t}, \\ &= \frac{1}{w}\left((1-p)f - pg + (1-p)D_1\frac{\partial^2 u_1}{\partial x^2} - pD_1\frac{\partial^2 u_1}{\partial x^2}\right).\end{aligned}$$

At $x_b(t)$ per-capita growth is the same for both conspecifics so that $u_2 f - u_1 g = 0$, consequently any change in the proportion of sexuals and apomicts at this point results only from diffusion. It is natural, therefore, to consider $x_b(t)$ as demarking the boundary between the sexual and asexual populations and to specify the wavespeed of range expansion as dx_b/dt. By seeking parameters that minimize $|dx_b/dt|$, (μ, ν)-parameter space can be divided into a region of sexual range expansion, where wavespeed is positive, and a region of asexual range expansion where wavespeed is negative. Figures 4-14(a)-(c) illustrate this division for fixed reproductive parameters b and p. In (a) $D_1 > D_2$ and sexual range expansion occurs over a slightly wider region of parameter space than when $D_1 = D_2$. Similarly in (c) $D_2 > D_1$ and asexual range expansion occurs over a slightly wider region. It is clear then, that the relative diffusivity of the reproductive modes can prove decisive in determining which conspecific class fixes at boundaries, particularly when $\mu \approx 2$.

The numerical simulations in this section have concentrated on competition at the boundary between established sexual and asexual populations. This focus was motivated by the general observation of distinct sexual and asexual ranges in natural populations. It is interesting to consider briefly whether initial conditions of this sort are artificial. In fact distinct sexual and asexual ranges emerge very rapidly from more generic initial conditions. Figure 4-15 shows domains dominated by one or other conspecific becoming established following a small random perturbation of the unstable

internal equilibrium $(\tilde{u}_1^+, \tilde{u}_2^+)$. The establishment of sexual and asexual clumps may occur on a timescale significantly faster than that of any subsequent range expansion. In more than one spatial dimension the wavespeed of range expansion at boundaries between clumps will depend not only on model parameters but also on curvature of the boundary.

Discussion

The sexual-asexual reaction-diffusion model indicates that in natural populations mixed for sexual and pseudogamous apomicts strong autocorrelation of reproductive modes is expected. Moreover, range expansion of the conspecific that dominates at the boundaries can be very slow for realistic parameters ($\mu = 1.41$ (Kelley et al. 1988), $\nu < 1$ (Mogie 1992)). Britton & Mogie (2001) demonstrate that boundaries between competing sexual and autonomous asexual populations may move arbitrarily slowly. The sexual-asexual model in this section augments this result, showing that it also applies to competing pollen-limited sexual and pseudogamous apomictic populations.

The introduction of an explicit pollination process made it necessary to treat sexual and asexual populations with separate equations. This ecological approach made it possible, however, to consider the effect of reproductive modes having differing diffusivities, or seed dispersal ranges. Increasing the seed dispersal range of one conspecific slightly boosts its competitiveness at boundaries, increasing the range of parameters which result in range expansion. It is possible that intra-specific competition between reproductive modes creates a selective pressure to disperse further. This prediction should, however, be tempered by a consideration of whether increased dispersal favours each reproductive mode in isolation (see comments in section 4.1), since they will be isolated from one another over most of their range.

Some species mixed for sexual and asexual reproductive mode coexist rather more intimately than is seen in the model here. Verduijn et al. (2004) report sexual and asexual dandelions within metres of each other on opposing sizes of dykes in the Netherlands. Verduijn et al. (2004) propose that small and delicately balanced differences in environment within adjacent habitats favour dominance of one or other reproductive mode. The model presented here would suggest that it is likely that such habitat specialization is necessary when sexuals and asexuals are found in intermingled populations.

4.4 DISCUSSION

Reaction-diffusion models have provided a means of extending the non-spatial models of chapter 3 to consider populations on a continuous spatial domain. This enterprise has revealed mechanisms whereby populations subject to a strong Allee effect can spread. It has shown that when gynodioecious coexistence is maintained because hermaphrodites are self-compatible, coexistence does not imply that a uniform ratio of female and hermaphrodites will be found throughout the population. A variety of complex spatial and spatio-temporal patterns can be generated just from the ecological interaction of the reproductive modes. It has shown too that the inability of sexual and asexual conspecifics to coexist locally results in monomorphic patches which establish very rapidly but can spread very slowly.

Whilst a reaction-diffusion treatment is a traditional extension to non-spatial or spatially homogeneous population dynamics, application of the approach to plant populations attracts the following caveats. The conclusion that populations diffuse through space may be derived from the assumption that all individuals in a population move randomly, examining the probability distribution for how far an individual moves and assuming that population size is large enough to reflect this probability distribution (Okubo 1980, Murray 1989*a*). An alternative derivation supposes that individuals succumb to a pressure to migrate proportional to the local gradient of density and in an opposite direction to that gradient (Murray 1989*a*). Both derivations treat mobile populations, but in general individual plants are static and population spread results from the mobility of the reproductive propagules, the seeds. Seeds dispersed to regions of low population density experience minimal establishment competition, whereas those dispersed into regions of high density experience extreme establishment competition. As a result a plant species may be expected to spread from areas where it is already established into suitable uncolonized areas nearby. This constitutes a phenomenological analogy with diffusion, where a strict mechanistic derivation is inadmissable. The analogy is sometimes misguided. Consider, for example, a real plant population completely sterilized by a pathogen, supposing a constant death rate, the spatial distribution will remain the same as population size decays to zero, by contrast a diffusion model would predict that the species would continue to spread as it decays. The validity of the application of reaction-diffusion models to plant populations relies on the phenomenological match between the observed way plant species spread and the mathematical mechanism for spread that diffusion provides. This match is not, however, always a good one.

The fundamental solution of the diffusion equation implies that population spread and hence seed dispersal should follow a gaussian probability distribution. Many studies into seed dispersal have concluded that the distribution is rarely gaussian and may well have non-zero moments of 4th or higher order which signal the presence or absence of long distance dispersal events (Richards 1986, pp 192-194). The models of this chapter then should be viewed as a worthwhile first treatment, which ought to illuminate some of the sorts of behaviour that is possible for the populations of chapter 3 to exhibit when placed in a spatially extended context.

As mentioned in the introduction to this chapter reaction-diffusion modelling has a long history as a technique for adding spatial structure to non-spatial state-variable models without revising the local kinetics. More recently a number of other approaches have become popular. Reaction-dispersal or integro-differential models are a continuous space alternative that allow the exploration of more realistic dispersal functions. Unlike reaction-diffusion models certain choices of dispersal kernel can produce accelerating or decelerating wave solutions (Kot et al. 2004). Coupled map lattice models (Hassell et al. 1991) introduce a regular discrete spatial structure, populations are located at the points of a lattice and interact with neighbouring populations through migration. Coupled map lattice models can behave similarly to reaction-diffusion model or can exhibit complex spatio-temporal patterns. Introducing space into state-variable models is somewhat of an ad-hoc procedure. Since the non-spatial kinetics assume panmixia the resulting model will always have two spatial scales: The scale of the introduced spatial dimension in which the distance between interacting populations is scrupulously respected and a local scale on which distance is ignored. The relationship between these scales is often not formally justified. For example, in the models of this chapter seed dispersal has been treated on the explicit spatial scale and pollen dispersal and competition have been treated only on the local scale, yet in natural populations each of these processes would have its own characteristic scale and seed dispersal would not necessarily be the longest. In view of these considerations the next chapter will start the modelling process afresh so that space can be incorporated on the scale of the individual.

PART III

Individual-Based Approaches

INTRODUCTION

The motivation for individual-based modelling (IBM) in ecology is the desire to reflect more accurately the reality that populations and ecosystems consist of individuals with complex behavioural patterns and interactions. The aspiration of the approach is that selecting the appropriate level of detail to model individual behaviour will result in the emergence of realistic population scale phenomena (DeAngelis et al. 1994, Judson 1994). The level of detail included in an IBM varies from the simple discrete nature of individuals and the stochasticity this introduces in real population demography, to complex simulations informed by real geographic and census information, incorporating all sorts of physiological and demographic parameters. Examples of the latter are the EpiSim model developed to explore epidemic scenarios in real cities (Barrett et al. 2005) and the numerous simulators used for forestry planning all over the world. The disparity in approaches arises from the variety of academic disciplines and commercial and governmental organizations from which individual-based modelers come.

Grimm (1999) identifies the motivations of modelers as either 'pragmatic': An IBM approach is required to incorporate a particular feature of an ecosystem; or 'paradigmatic': A new approach is necessary to address the failure of population-based models to account for ecological phenomena. Grimm (1999) acknowledges that the two motivations may be interdependent and that is certainly the case for the work in this report. Arguably the most important feature of plant communities at the level of abstraction that is under consideration here is the discreteness of individuals and their static nature. These practical considerations will be addressed forthwith. It was concluded from the models of chapter 3 that pollen limited hermaphrodite species require a level of self-fertility in order to establish from very small frequencies. This conclusion was overturned in part in chapter 4 when the small populations are outliers of an abundant established population, but the conclusion for isolated populations is still at odds with regularly reported invasions of sexual species. Similarly it was concluded in chapters 3 and 4 that in the absence of self-fertilization hermaphrodite populations are vulnerable in various circumstances to invasion by females with an arbitrarily small reproductive advantage and that this invasion precipitates population extinction. These conclusions provoke the 'paradigmatic' shift in focus from population to individual in the following models in the following pages.

The work in this part of the report will avoid the temptation to incorporate a

high level of biological detail and pursue instead more general theoretical principles that arise from considering flowering plants as discrete and spatially distributed. The level of abstraction chosen means that, as with the reaction-diffusion models, a rich framework historically developed for physical science applications can be employed. Interacting particle systems have been used classically for modelling magnetic bodies (the well known Ising model) and inhomogeneous chemical reactions. Typically the mathematical structure of these systems is too deep to make rapid analytical progress with the full system and, particularly with ecological applications, it is common to treat models with a combination of simulation and approximation. In this respect many innovative techniques have arisen for analysing simulation results and obtaining approximations in the pursuit of ecological understanding.

It is worth discussing briefly the terms that arise in the literature for related modelling approaches, some of which are essentially the same. An interacting particle system (IPS) is a stochastic process in continuous time taking place on the nodes of a (finite dimensional) integer lattice. The same spatial discretization occurs in cellular automata, which in their original guise were deterministic (von Neumann 1966) but ecological models usually use a stochastic version referred to as probabilistic cellular automata. Artificial ecologies (Rand & Wilson 1995) are a generalization of probabilistic cellular automata in which simultaneous events occur. Either of these systems may be discrete or continuous in time. In the case of discrete time the updating procedure may be specified as synchronous or asynchronous. So in full: a continuous-time probabilistic cellular automaton or artificial ecology is an IPS. A lattice-based spatial ecology (Iwasa 2000) usually refers to the same thing.

CHAPTER 5

Interacting Particle System Models

In this chapter interacting particle system (IPS) models will be introduced for the inter-pollinating conspecific phenomena introduced in chapter 1 and modelled with a population-based approaches in chapters 3 and 4. The shift of emphasis of scale will necessitate re-evaluation of the mechanics of interaction. In particular processes of intra-specific interactions, namely: competition, cross-pollination and seed dispersal, will appear at first to be treated quite differently in the new framework. These processes will cease to be modelled as interactions between an individual and the rest of the population and instead be treated as pair-wise interactions between neighbouring individuals.

The models of this chapter will be stochastic where previous chapters have been deterministic. Thus random variability will be introduced into all model processes which, it may be argued, better reflects ecological reality. But it should be remarked that variability in natural populations derives from a complicated interaction of genetic and environmental factors which do not affect members of a population independently. Related individuals will share genetic effects and proximal individuals will share environmental effects. These correlations are not to be included in the model. Mathematically, stochasticity complicates the analysis of the models and rather than rigorously pursuing basic properties of the models, a combination of simulation and approximation techniques will be used to illuminate ecologically important model behaviour.

Space in an IPS model is discrete and intimately related to the discreteness of individuals themselves. One spatial unit is the area required for one individual to develop and achieve its reproductive potential. Though this unit is in many respects natural, the model will assume that these units are regularly spaced and are occupied by a single individual. This results in all of an individual's neighbours being at a fixed distance and, should they all be of the same type, indistinguishable in their competitive and cooperative effects.

Species will be assumed self-incompatible in the models of this chapter. This is a

simplification, but it is motivated by the desire to highlight the effect of incorporating discrete local interactions. Several phenomena that emerge in the IPS models of this chapter in the absence of self-fertilization bare a striking similarity to phenomena in non-spatial models with self-fertilization. Self-incompatibility is assumed then in the spirit of eliminating competing explanations for model behaviour. The general derivation of the inter-pollinating conspecifics IPS will, however, include self-pollination terms in order to illustrate the flexibility of the approach.

This chapter will introduce the notation necessary for assembling IPS models. The derivation of a general inter-pollination conspecifics model will then be supplied. Analysis will proceed through simulation and approximation. Details of the simulation techniques and the derivation of two approximation techniques: mean field and hydrodynamic limit, will follow the general model derivation. The three example models treated in chapters 3 and 4, the sexual species mode, the gynodioecy model and the sexual-asexual model will be translated into the IPS framework and analysed.

5.1 DERIVATION

Interaction Particle System Preliminaries

Let $\mathbb{Z}^2$ be the two-dimensional integer lattice, and suppose that the positions of plants in a population occur at sites on the lattice. A single site is either occupied by a single individual or unoccupied, so let the state of each site be an element from finite set of states $\mathcal{S} = \{A, B, C, ...\}$, where A is unoccupied and the other states denote occupancy by different conspecific classes. At time t the configuration of the IPS is denoted ξ_t and is a map $\mathbb{Z}^2 \mapsto S$, so that the state of site $x \in \mathbb{Z}^2$ at time t is $\xi_t(x)$. The dynamics of the population consists of changes between states that are either independent of or dependent on the system configuration. Independent changes occur at a constant rate irrespective of system configuration. Dependent processes depend only on the states of sites in a finite local neighbourhood of the site changing state. This neighbourhood, the set of sites influencing state change at x, is denoted $\mathcal{N}(x)$. The size of the neighbourhood is assumed independent of x and is denoted $z = |\mathcal{N}(x)|$. The neighbourhood is often specified by:

$$\mathcal{N}(x) = \{y \in \mathbb{Z}^2 | 0 < \|y - x\|_p \leq r\}, \tag{5.1.1}$$

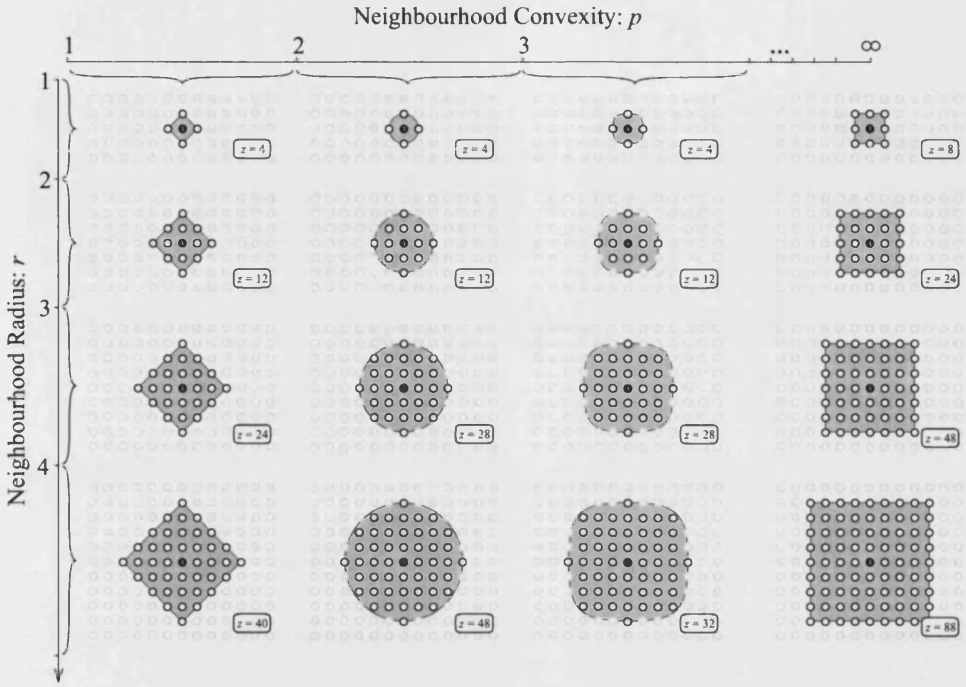

Figure 5-1: Examples of (r, p)-neighbourhoods on $\mathbb{Z}^2$ acheivable with definition (5.1.1)

with $r \geq 1$ and $1 \leq p \leq \infty$ (Krone 2004). So for example the von Neumann four site neighbourhood $\mathcal{N}_4$ commonly used in two dimensional cellular automata, is recovered with $r = 1$, $p = 1$; the Moore eight site neighbourhood $\mathcal{N}_8$ with $r = 1$, $p = \infty$. Some further examples are given in Figure 5-1. Other interesting regular geometries are not covered in this definition but can be accommodated on $\mathbb{Z}^2$. When a site is a member of its own neighbourhood, the zero lower bound should be non-strict. This neighbourhood arises in game-theoretic applications when individuals can play with themselves. For a triangular three site geometry the neighbourhood can be given by:

$$\mathcal{N}_3(x) = \{y \in \mathbb{Z}^2 | (0 < |y - x| \leq 1) \wedge ((x_1 \in 2\mathbb{Z} \wedge x_2 \leq y_2) \vee (x_1 \notin 2\mathbb{Z} \wedge x_2 \geq y_2))\}.$$

For a hexagonal six site geometry the neighbourhood can be given by:

$$\mathcal{N}_6(x) = \{y \in \mathbb{Z}^2 | (0 < |y - x| \leq 1) \wedge ((y_1 - x_1)(y_2 - x_2) \geq 0)\}.$$

See Figure 5-2 for an illustration of $\mathcal{N}_3$ and $\mathcal{N}_6$.

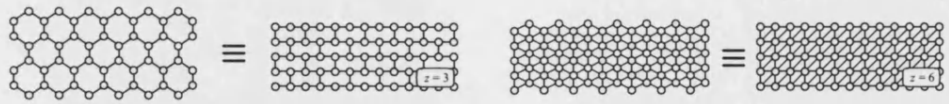

Figure 5-2: Examples of non (r,p)-neighbourhoods that are nonetheless regular and acheivable on $\mathbb{Z}^2$.

Two types of state change dynamics are identified: Flip dynamics involve a state change at a single site; Exchange dynamics involve two particles exchanging sites. Since the models here concern a sessile species, the former will be used exclusively except in the discussion of hydrodynamic limit models, where introducing the latter is an indispensable requirement. In describing flip rates that are dependent on the configuration of the local neighbourhood of a site x, it is economical to denote the number of state σ sites in the neighbourhood of a site x by:

$$n_\sigma(x,\xi) = |\{y \in \mathcal{N}(x) | \xi(y) = \sigma\}|.$$

So for example if a site occupied by a state-B individual tries to colonize neighbouring empty sites at a constant rate b/z, the birth rate onto an empty site x is:

$$c_{AB}(x,\xi) = b n_B(x,\xi).$$

Here the AB subscript denotes that this is the rate that A sites become B sites.

The bulk of the notation for this section is in common with Krone's (2004) introduction to IPS and hydrodynamic limits.

Pollination and Colonization Timescale Separation

Before deriving models for inter-pollinating conspecifics, some careful thought must go into how pollination and subsequent seed production combine to produce colonization events. Suppose an obligate sexual is pollinated by a neighbour, sets seed and disperses this seed to neighbouring sites. In empty sites the seed may germinate and develop into a reproductive individual, the conspecific class of the individual depending on both the female parent and the pollen donor. Hence when pollen origin is taken into account a sexual colonization process involves triplets of sites: pollen donor, seed producer and empty site. The evaluation of the rate of colonization of a given empty site by a

given conspecific class depends not only on seed producers in its neighbourhood, but also on the pollen producers in their neighbourhoods. This is not an insurmountable problem for the IPS framework and could be incorporated, but an attractive alternative is available which is ecologically motivated and keeps interactions pair-wise.

In most flowering plant species the length of time that grains of pollen are active is very short with respect to the life expectancy of individuals. Pollen in some grasses survives as little as 30 minutes after being released from the anther (Richards 1986)[p 55]. Similarly it is clear from the number of seeds that many sexual flowering plant species produce that colonization events are usually rare compared with pollination events. In a population at equilibrium, for example, one colonization event per individual will maintain the population. In a growing population colonization events will be more frequent but it is nonetheless true that in natural populations vast numbers of seeds fail to germinate because of predation, disease or unsuitable conditions (Harper 1977, pp 111-147). In short it is argued that pollination and pollen expiry occur frequently within a reproductive season and by contrast colonization and death events are rare. It might be assumed therefore that these processes effectively take place on different times scales: rapid pollination and slow colonization. Mechanistically this assumption should be interpreted in the following way: Throughout a reproductive season a sexual flowering plant with female function is continually maturing seeds, and the paternity of a given seed depends on whose pollen was available at a certain point in the seed's development. So following the arrival of pollen at a site occupied by a sexual, a window of opportunity is assumed to exist in which some of the sexual's seed is fertilized. The window opens with the arrival of pollen and closes when all remaining pollen unused in fertilization has become inactive. If pollen producers are common in the sexual's neighbourhood many such fertilization windows will occur during the season. Suppose that the small proportion of that season's seeds that germinate contains a small random selection of fertilized seed irrespective of the point in the season that the seed matured. Since seeds destined for germination are rare, very few pollination events will result in colonization events and so the requisite separation of timescales is achieved. For convenience it will be necessary to assume that the fortunate seeds destined for germination are dispersed immediately upon fertilization and within the pollination window. In reality the various mechanisms of seed dispersal in nature do not fit this assumption very well: Seed is usually retained and dispersed in batches, in fruit, burrs or otherwise, late in the season. Note that this process does treat the distribution of paternity amongst pollen producing neighbours of a sexual individual sensibly. The

distribution of paternity amongst neighbours is a consequence of how often the pollen from each neighbour is brought into the sexual's site. Hence the frequency of seeds sired on the sexual by a particular conspecific class will reflect the frequency of each class in the sexual's neighbourhood.

Why timescale separation is preferable to a triplet process will become more apparent in the second order moment-closure approximation models of the following chapter, where the pair-wise nature of interaction obviates additional assumptions which make unreasonable claims about independence. This will be discussed further in chapter 6.

General Inter-pollinating Conspecifics IPS

In order to realize the processes of pollination and colonization on separate timescales as discussed above, it is necessary to introduce sub-states of the site states $\mathcal{S}$ introduced already. In generality every conspecific class may be pollinated by any other conspecific class, so different sub-states representing the current availability at an occupied site of pollen from each different conspecific class are required. For simplicity it is assumed that if pollen is present at a site at a given time then it is from a single source, and that between expiry of pollen from one source and arrival of pollen from another the occupied site is in a pollen-free or unpollinated state. Thus for N conspecific classes each state $\sigma \in \mathcal{S}$ has $N+1$ sub-states: σ_0 - unpollinated, and σ_i - pollen available from class i for $i \in \{1, \ldots, N\}$. The total collection of all $N \times (N+1)+1$ sub-states including the empty state A is denoted $\mathcal{S}_0$. So in general an inter-pollinating conspecifics IPS will be completely determined by specifying the flip rates between states in $\mathcal{S}_0$. The flip dynamics will specify four different types of events, two on a fast timescale: pollination, pollen expiry, and two on a slow timescale: colonization and death.

Pollination flip rates Since individuals can be pollinated by at most one conspecific class at any one time, pollination events only ever flip the unpollinated sub-state of a state into one of its pollinated sub-states. The flip rate for a pollination event is given by:

$$c_{\sigma_0^i \sigma_j^i}(x, \xi) = \frac{p_{ij}}{\epsilon z} \sum_{k=0}^{N} n_{\sigma_k^j}(x, \xi) + s_i,$$

where $\sigma^i, \sigma^j \in \mathcal{S} \setminus \{A\}$ are occupied states and the superscript denotes conspecific class, so: $\sigma^1 = B$, $\sigma^2 = C$, ... p_{ij} is an entry in the pollination matrix P, (recall from

chapter 3 section 3.1 that p_{ij} specifies the pollen production and dispersal effort of class j experienced by conspecifics of class i.) Here though pollen is dispersed amongst z neighbours and so the rate is adjusted accordingly. s_i is the rate at which conspecifics of class i self-pollinate, this rate will be assumed zero in the models pursued in this chapter. $\epsilon > 0$ is small and has been introduced to parameterize the separation of timescales.

Pollen expiry flip rates The window of opportunity for the pollen available at an occupied site to fertilize seed that is destined to germinate closes when all the pollen in the site becomes inactive. This process is termed pollen expiry and did not require consideration in chapter 3 because the functional response to pollen availability was chosen explicitly. As with the death rate in the non-spatial derivation, pollen-expiry is assumed to occur at a species specific rate. It should be noted, however, that although all conspecific classes belong to the same species, they are distinguished by their reproductive mode which could plausibly affect pollen longevity and thus confound this assumption. The constant rate at which pollen expires can be set to $1/\epsilon$ by scaling the entries in P accordingly, therefore the flip rate for a pollen expiry event is given by:

$$c_{\sigma_i\sigma_0}(x,\xi) = \frac{1}{\epsilon}.$$

Colonization flip rates Whilst pollen is available in an occupied site colonization of neighbouring empty sites can take place. Should colonization occur, the empty site will become occupied by an unpollinated individual belonging to a conspecific class determined by the state and sub-state of the colonizing site. The state and sub-state is specified by the female and male parents of the seed that arrives in the empty site. The flip rate for a colonization event is given by:

$$c_{A\sigma_0^k} = \sum_{i=1}^{N}\sum_{j=1}^{N}\frac{b_{ijk}}{z}n_{\sigma_j^i}(x,\xi) + \frac{c_k}{z}\sum_{j=0}^{N}n_{\sigma_j^k}(x,\xi),$$

where b_{ijk} is an entry in the reproductive array B, (recall from chapter 3 section 3.1 that b_{ijk} specifies the class k seed production and dispersal effort of class i individuals pollinated by class j individuals.) c_k is then vegetative colonization rate of conspecific class k, this will be assumed zero in the models in this chapter. As with pollination, colonization effort is now distributed amongst z neighbours.

Death flip rates As in the non-spatial derivation of chapter 3 the death rate is assumed constant across all conspecific classes inferring that an occupied site's pollination sub-state is irrelevant to the death process. Time may be scaled so that the flip rate for a death event can be considered unitary, so:

$$c_{\sigma_i A} = 1,$$

for all $\sigma \in \mathcal{S} \setminus \{A\}$, $i \in \{0, \ldots, N\}$.

An inter-pollinating conspecifics IPS is therefore completely determined by specifying the number of conspecific classes N, the pollination matrix P and the reproduction array B. Notice that in contrast with the derivation in chapter 3 it is no longer necessary to specify the inter-conspecific competition matrix A. This is because competition is now implicit in the lattice structure of the particle system. Competition is implied between adjacent sites since they cannot colonize each other and, at least for certain neighbourhood geometries, they compete for empty sites to colonize. Although this has the drawback that competition coefficients cannot vary, it neatly reduces the number of processes operating in the system and is perfectly adequate for this report since all coefficients are assumed unitary in the chosen applications.

5.2 ANALYSIS TOOLS

Simulation

The only analysis of fully-fledged interacting particle systems in this report will be by means of simulation. Simulations will take place on finite square lattices of size L by which it is meant that the lattice consists of $L \times L$ sites. Generally a lattice size of $L = 100$ will be used; For small neighbourhood sizes this is comfortably large enough for IPS behaviour to be largely deterministic and predictable (Rand & Wilson 1995). In some circumstances a reduced lattice size of $L = 50$ will be used to improve computational efficiency. The neighbourhoods of boundary sites are wrapped around from north to south and from east to west, so that the IPS effectively takes place on a torus. This is preferable to alternative methods of completing neighbourhoods which invariably introduce inequalities between the treatment of boundary and interior sites, which may induce artificial 'edge' effects. Although the extent of a real population's habitat is finite and so such 'edge' effects may be of real significance, they will not be treated

in this report which will instead concentrate on the core behaviour of the system.

Time is discretized into units of length Δt. For a configuration of this lattice ξ the time until an event at site x is an exponential random variable with rate specified by the flip rates above. To implement this in a discrete time simulation an approximation must be made that the probability of an event with flip rate $c(x, \xi_t)$ occurring at a site x during the interval $(t, t + \Delta t]$ is:

$$\frac{c(x, \xi)}{1 - e^{-\lambda \Delta t}},$$

where λ is the sum of the rates of all the possible flips that could occur at site x given ξ. This approximation amounts to the assuming that Δt is small enough that more than one type of event cannot occur at site x during the interval $(t, t + \Delta t]$. So for example the probability that a colonization event followed by a death event occurs in the same site during the interval is assumed negligible. In practice the maximum probability of more than one event occurring can be evaluated in advance and Δt can be controlled to keep this small. For the simulations in this chapter this probability is less than 10^{-5}. Since the time step is kept small $\Delta t \approx 0.01$, it has proved worthwhile to implement some optimization procedures in the simulation code. Briefly: The probabilities of each possible flip at a site x are stored between time steps and only re-evaluated should the state at x or at $y \in \mathcal{N}(x)$ change. A description of a similar optimization for simulation of the well known cellular automaton model Bak's sand-pile can be found in Walter & Worsch (2004).

As the timescale parameter ϵ becomes very small, the simulation procedure outlined above becomes very slow. However, in the limit $\epsilon \to 0$ the distribution of times spent in each pollination sub-state approaches an equilibrium for any given configuration of neighbouring states. This equilibrium can be evaluated for a given occupied site x in state σ by modelling the rates of change of the probability of being each sub-state P_i. If the site is unpollinated at time t then it becomes pollinated during the interval $(t, t + \Delta t)$ with probability:

$$\sum_{i=1}^{N} c_{\sigma_0 \sigma_i}(x, \xi) \Delta t + O(\Delta t^2).$$

If the site is pollinated then the probability it remains pollinated is:

$$(1 - \Delta t) + O(\Delta t^2).$$

Thus the probability P_i that site x is in state σ_i at time $t + \Delta t$ with $i \geq 1$ is given by:

$$P_i(t + \Delta t) = c_{\sigma_0\sigma_i}(x, \xi)\Delta t P_0(t) + (1 - \Delta t)P_i(t).$$

With P_0 recovered by:

$$P_0 = 1 - \sum_{i=1}^{N} P_i.$$

In the limit $\Delta t \to 0$ a linear system of ODEs is obtained:

$$\frac{dP_i}{dt} = c_{\sigma_0\sigma_i}(x, \xi)P_0(t) - P_i(t). \tag{5.2.1}$$

If $c_{\sigma_0\sigma_i} = 0$ for any i then the i-th equation should be omitted since the σ_i state can never arise in the IPS (unless it is pathologically introduced in the system's initial configuration.) The resulting system:

$$\dot{\mathbf{P}} = \mathbf{c} - C\mathbf{P},$$

where:

$$C = \begin{pmatrix} c_{\sigma_0\sigma_1} + 1 & c_{\sigma_0\sigma_1} & \cdots & c_{\sigma_0\sigma_1} \\ c_{\sigma_0\sigma_2} & c_{\sigma_0\sigma_i} + 1 & \cdots & c_{\sigma_0\sigma_2} \\ \vdots & & \ddots & \vdots \\ c_{\sigma_0\sigma_N} & c_{\sigma_0\sigma_N} & \cdots & c_{\sigma_0\sigma_N} + 1 \end{pmatrix} \quad \text{and} \quad \mathbf{c} = \begin{pmatrix} c_{\sigma_0\sigma_1} \\ c_{\sigma_0\sigma_2} \\ \vdots \\ c_{\sigma_0\sigma_N} \end{pmatrix}$$

has a unique asymptotically stable equilibrium $\hat{\mathbf{P}} = C^{-1}\mathbf{c}$, that is:

$$\hat{\mathbf{P}} = \frac{\mathbf{c}}{1 + \sum_{i=1}^{N} c_{\sigma_0\sigma_i}}. \tag{5.2.2}$$

To simulate the inter-pollinating conspecifics IPS in the limit of large timescale separation ($\epsilon \to 0$) the sub-state of a site in state σ can be drawn from the distribution $\hat{\mathbf{P}}$ at each time step and the simulation need only evaluate the ensuing colonization-death dynamics. Such simulations will be described as employing equilibrium pollination dynamics. It is somewhat satisfying that the probability distribution $\hat{\mathbf{P}}$ looks very much like a localized version of the multi-species Holling Type II functional response selected for phenomenological reasons in chapter 3.

Mean Field Approximation

The mean field approximation is a deterministic first order moment closure approximation of the dynamics of population densities in the IPS. As will become clear the assumptions of the approximation ignore the spatial structure of the lattice and so the mean field is best employed not as a predictor of IPS behaviour but as a benchmark of the underlying population dynamics. In this way the mean field can help to distinguish the extent to which the behaviour of simulations depend on the discrete spatial nature and local interaction dynamics of the IPS.

For each state $\sigma \in \mathcal{S}_0$ define a probability measure $\rho_\sigma(t) : \xi_t \to [0,1]$ where $\rho_\sigma(t)$ evaluates the probability that a randomly selected site of the IPS is in state σ at time t. ρ_σ can also be considered as the density of sites in state σ. Similarly for $\sigma, \sigma' \in \mathcal{S}_0$ define a probability measure $q_{\sigma/\sigma'}(t) : \xi_t \to [0,1]$ where $q_{\sigma/\sigma'}(t)$ evaluates the probability that a randomly selected site in state σ' has a randomly selected neighbour in state σ. $q_{\sigma/\sigma'}$ is sometimes called the local or environs density of state σ with respect to state σ' (Matsuda et al. 1992). By definition the density and environs density satisfy:

$$\sum_{\sigma \in \mathcal{S}_0} \rho_\sigma = 1, \tag{5.2.3a}$$

$$\sum_{\sigma \in \mathcal{S}_0} q_{\sigma/\sigma'} = 1. \tag{5.2.3b}$$

The way in which ρ_σ develops with time is, of course, governed by the four types of flip dynamics set out above. Since the flip rates are exponential random variables a deterministic system describing the expected change in ρ_σ is readily composed. Consider, for example, the density of unpollinated sites in state σ^i denoted $\rho_{\sigma_0^i}$. The effect of the pollination process is to decrease this density at a per-capita expected rate proportional to p_{ij}/ϵ and the probability that a neighbouring site is in state σ^j summed over all states $\sigma^j \in \mathcal{S} \setminus \{A\}$ plus the rate of self-pollination s_i. With the above notation, the probability that a randomly selected neighbour of a state σ_0^i site is in state σ^j is:

$$\sum_{k=0}^{N} q_{\sigma_k^j/\sigma_0^i}.$$

So the rate at which $\rho_{\sigma_0^i}$ decreases due to σ_0^i sites becoming pollinated is:

$$\rho_{\sigma_0^i}\left(\sum_{j=1}^{N}\frac{p_{ij}}{\epsilon}\sum_{k=0}^{N}q_{\sigma_k^j/\sigma_0^i}+s_i\right).$$

Pollen expiry at pollinated state σ^i sites increases the density of σ_0^i at a rate:

$$\frac{1}{\epsilon}\sum_{j=1}N\rho_{\sigma_j^i}.$$

Colonization events also increase the density of state σ_0^i sites. The rate of increase is proportional to the density of empty sites ρ_A and the sum over σ^j and k of the product of the rate at which σ_k^j sites produce seeds of class i, b_{jki} and the probability of empty sites having σ_k^j neighbours plus the product of the vegetative propagation rate c_i and the probability of empty sites having σ^i neighbours. So the rate of change of $\rho_{\sigma_0^i}$ due to colonization is:

$$\rho_A\left(\sum_{j=1}^{N}\sum_{k=1}^{N}b_{jki}q_{\sigma_k^j/A}+c_i\sum_{k=0}^{N}q_{\sigma_k^i/A}\right).$$

Finally death events decrease $\rho_{\sigma_0^i}$ at unit per-capita rate. The way in which the density of unpollinated sites develops is shown below together with a similarly derived equation for pollinated sites.

$$\begin{aligned}\epsilon\frac{d\rho_{\sigma_0^i}}{dt}= &\underbrace{-\rho_{\sigma_0^i}\left(\sum_{j=1}^{N}p_{ij}\sum_{k=0}^{N}q_{\sigma_k^j/\sigma_0^i}+s_i\right)}_{\text{pollination}} \underbrace{+\sum_{j=1}^{N}\rho_{\sigma_j^i}}_{\text{pollen expiry}}\\ &+\epsilon\Big[\underbrace{\rho_A\left(\sum_{j=1}^{N}\sum_{k=1}^{N}b_{jki}q_{\sigma_k^j/A}+c_i\sum_{k=0}^{N}q_{\sigma_k^i/A}\right)}_{\text{colonization}} \underbrace{-\rho_{\sigma_0^i}}_{\text{death}}\Big],\end{aligned} \tag{5.2.4}$$

$$\epsilon\frac{d\rho_{\sigma_j^i}}{dt}=\left(p_{ij}\sum_{k=0}^{N}q_{\sigma_k^j/\sigma_0^i}+s_i\right)\rho_{\sigma_0^i}-\rho_{\sigma_j^i}+\epsilon\Big[-\rho_{\sigma_j^i}\Big].$$

Note that no colonization term appears in the second equation and that the pollination

and pollen expiry terms in the equations complement each other. An equation for ρ_A can be recovered via (5.2.3). The deterministic equations (5.2.4) accurately describe the expected behaviour of the IPS. They do not however, form a closed system. The mean field approximation consists of assuming that the neighbourhood of every site of the IPS has an identical constitution which reflects the density of states in the system as a whole. This assumption provides:

$$q_{\sigma/\sigma'} = \rho_\sigma. \tag{5.2.5}$$

The mean field assumption is satisfied in the limit $\mathcal{N}(x) \to \mathbb{Z}^2$ for all sites x. Whether the assumption is interpreted as homogenizing neighbourhoods or making them infinitely large, it is clear that the spatial structure of the IPS must be lost. In the former case the potential for different states to develop different expected neighbourhood compositions is removed. In the latter case the collection of sites becomes well-mixed and mass-action arguments may be applied.

Hydrodynamic Limit Approximation

Hydrodynamic limit approximation is the name given to a number of rigorous methods for extracting deterministic continuum limits from IPS that include both flip and exchange dynamics. A large body of probability literature exists concerning the existence of and convergence to these limits under various different assumptions on the dynamics. Here the IPS with flip dynamics described above is modified by the addition of some exchange dynamics. The form of the exchange dynamics will be chosen to conform to the pre-requisites of a useful generic result presented by Krone (2004) by means of which a hydrodynamic limit with linear diffusion is obtained.

It is important to remark that with the introduction of exchange dynamics the application of this model to sessile flowering plant species becomes very dubious indeed. It will be assumed that sites will be exchanging states with their nearest neighbours on a very rapid timescale. The value of pursuing this approximation, however, lies not in the realism of the assumptions, but in what the procedure says about the implicit assumptions made in the reaction-diffusion models of chapter 4.

At present the IPS process ξ_t takes place on $\mathbb{Z}^2$. To obtain a hydrodynamic limit it

is necessary to consider the scaled process denoted ξ_t^k taking place on a scaled lattice:

$$\mathbb{Z}_k^2 = \{x/k |\ x \in \mathbb{Z}^2\}.$$

On the scaled lattice the space between sites is $1/k$. In the limit $k \to \infty$ the scaled lattice approaches the continuum $\mathbb{R}^2$. Neighbourhoods must also be rescaled so that the flip dynamics on the lattice are effectively the same only viewed on a different scale. There is no change in how individual sites interact with neighbouring sites on the rescaled lattice. To the rescaled process is added some fast stirring. In general a stirring process involves exchange dynamics: Two sites x and y on the scaled lattice exchange their states at a rate $p(x,y)$. Here $p(x,y)$ is chosen so that only nearest neighbours can exchange sites:

$$p(x,y) = \begin{cases} 0.25, & \text{if } |x-y| = 1/k, \\ 0, & \text{else.} \end{cases}$$

Thus $p(x,y)$ has a finite range and is translation invariant. In a fast stirring process the rate of exchange is increased by some factor. For the purpose of extracting a hydrodynamic limit this factor is chosen as k^2. So that the more the lattice shrinks as k increases, the more frequently sites exchange state with their nearest neighbours. With these exchange dynamics the behaviour of the particle densities ρ_σ, $\sigma \in \mathcal{S}_l$ can be shown to converge probabilistically to a deterministic limit which is described by a reaction-diffusion equation. Krone (2004) provides this result (the notation of which has been modified suitably):

Theorem (Hydrodynamic Limit). *Suppose the particle flip dynamics on $\mathbb{Z}^2$ are translation invariant and of finite range. Let the exchange dynamics be given by fast (k^2) symmetric nearest neighbour stirring. Then the scaled process ξ_t^k with initial configuration distributed according to product measure with $\mathbb{P}(\xi_0^k(x) = \sigma) = g_\sigma(x)$ for $\sigma \in \mathcal{S}_0$, has hydrodynamic limit $\rho(x,t) = (\rho_A(x,t), \rho_{B_0}(x,t), \rho_{B_1}(x,t), \dots)$, where $\rho_\sigma(x,t)$ is the bounded solution of*

$$\frac{\partial \rho_\sigma}{\partial t} = \Delta \rho_\sigma + f_\sigma(\rho),$$
$$\rho_\sigma(x,0) = g_\sigma(x).$$

The reaction term is given by

$$f_\sigma(\rho) = \sum_{\sigma' \neq \sigma} \langle c_{\sigma'\sigma}(0,\xi)\mathbf{1}_{(\xi(0)=\sigma')}\rangle_\rho - \sum_{\sigma \neq \sigma'} \langle c_{\sigma\sigma'}(0,\xi)\mathbf{1}_{(\xi(0)=\sigma)}\rangle_\rho.$$

Here $\rho = (\rho_A, \rho_{B_0}, \rho_{B_1}, \dots)$ and $\langle \dots \rangle_\rho$ denotes expected value under product measure (i.e. independent sites) in which state σ has density ρ_σ.

It is straight forward to evaluate the expectations that appear in f_σ since they are to be determined as if sites on ξ_t are independent. Thus:

$$\langle n_\sigma(0,\xi)\rangle_\rho = z\rho_\sigma(\xi),$$

and it follows that:

$$\begin{aligned} f_{\sigma^i} = \; & \underbrace{+\rho_A\left(\sum_{j=1}^{N}\sum_{k=1}^{N} b_{jki}\rho_{\sigma_k^j} + c_i\sum_{k=0}^{N}\rho_{\sigma_k^i}\right)}_{\text{colonization}} \quad \underbrace{+\frac{1}{\epsilon}\sum_{j=1}^{N}\rho_{\sigma_j^i}}_{\text{pollen expiry}} \\ & \underbrace{-\rho_{\sigma_0^i}\left(\sum_{j=1}^{N}\frac{p_{ij}}{\epsilon}\sum_{k=0}^{N}\rho_{\sigma_k^j} + s_i\right)}_{\text{pollination}} \quad \underbrace{-\rho_{\sigma_0^i}}_{\text{death}}, \end{aligned} \tag{5.2.6}$$

$$f_{\sigma_j^i} = \left(\frac{p_{ij}}{\epsilon}\sum_{k=0}^{N}\rho_{\sigma_k^j} + s_i\right)\rho_{\sigma_0^i} - \frac{1}{\epsilon}\rho_{\sigma_j^i} - \rho_{\sigma_j^i},$$

which are readily identified as the terms from the mean field approximation. So the hydrodynamic limit obtained by introducing fast stirring results in a reaction-diffusion approximation with linear diffusion and local dynamics obeying the mean-field approximation. It is perhaps not surprising that stirring validates the mean field assumption locally. Intuitively individuals exchange sites so regularly that there can be no divergence in expected neighbourhood composition for different states.

5.3 SEXUAL SPECIES

A self-incompatibility sexual species IPS is extracted from flip rates given in 5.1.3 by choosing the same parameter values as the corresponding non-spatial model developed in chapter 3 3.2. There is a single conspecific class ($N = 1$) denoted by state B and only one source of pollen, so B has two sub-states one unpollinated and one pollinated. The set of states is $\mathcal{S}_0 = \{A, B_0, B_1\}$. There is no self-fertilization or vegetative propagation, so $s_1 = 0$ and $c_1 = 0$; and the subscripts are dropped on the pollination and reproductive rates for notational simplicity. The resulting flip rates are:

$$\begin{aligned} c_{B_0B_1}(x,\xi) &= \frac{p}{z\epsilon}(n_{B_0}(x,\xi) + n_{B_1}(x,\xi)), \\ c_{B_1B_0}(x,\xi) &= \frac{1}{\epsilon}, \\ c_{AB_0}(x,\xi) &= \frac{b}{z}n_{B_1}(x,\xi), \\ c_{B_0A}(x,\xi) &= c_{B_1A}(x,\xi) = 1. \end{aligned} \tag{5.3.1}$$

To elaborate: Occupied sites provide pollen to their unpollinated neighbours at a rate $p/z\epsilon$. Occupied pollinated sites become unpollinated as pollen expires at rate $1/\epsilon$. Occupied pollinated sites disperse seed to neighbouring empty sites at rate b/z. Both types of occupied site are vacated at a constant unit death rate.

Simulations

Simulations were run on a $L = 100$ lattice to determine the behaviour of sexual species IPS. Figures 5-3(a)-(d) show the growth of a population with neighbourhood size $z = 4$ ($r = 1, p = 1$) from a small initial population of five occupied sites in a cross configuration. Figures 5-4(a)-(d) show a similar pattern when pollination and colonization timescales are asymptotically separated ($\epsilon \to 0$). The requirement of cross-pollination and the restriction of colonization to neighbouring sites causes the population to grow as a self-regulating cluster composed of a mosaic of empty, unpollinated and pollinated sites. Occupied sites whose neighbourhoods are empty or full of other occupied sites have zero colonization rate. Colonization rate is maximized at sites with intermediately occupied neighbourhoods. Such sites are generally found around the boundary of the clustered population where pollen flow from the interior promotes the rapid colonization of empty sites beyond the boundary. Behind the boundary population density

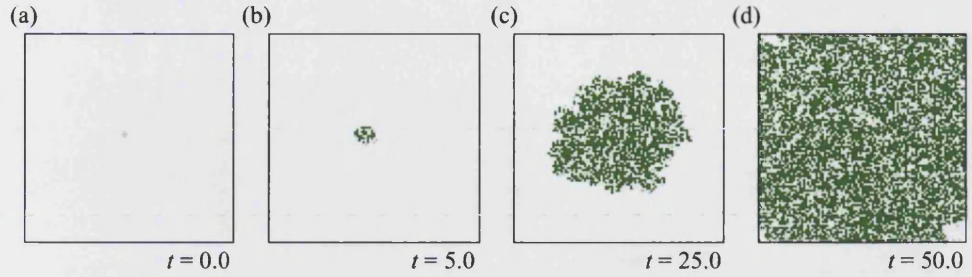

Figure 5-3: Typical growth pattern of the IPS sexual species model initiated with a small clump of five neighbouring cells. The lattice $\mathbb{Z}^2$ is represented by a grid of square cells. Sites are coloured: White if empty; Light green if occupied and unpollinated and dark green if pollinated. Parameters $b = 6$, $p = 6$, $z = 4$ $(r = 1, p = 1)$, $\epsilon = 0.05$.

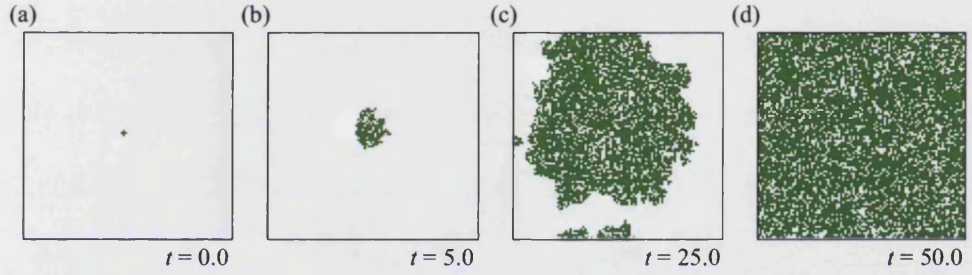

Figure 5-4: Typical growth pattern of the IPS sexual species model if the pollination process is assumed to equilibrate between colonization and death events. Parameters $b = 6$, $p = 6$, $z = 4$ $(r = 1, p = 1)$.

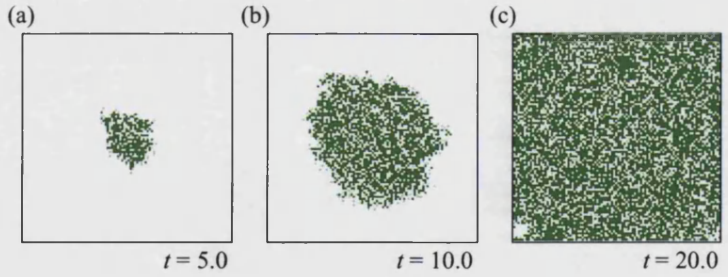

Figure 5-5: Typical growth pattern of the IPS sexual species model if the pollination process is assumed to equilibrate between colonization and death events. Parameters $b = 6$, $p = 6$, $z = 24$ $(r = 2, p = \infty)$.

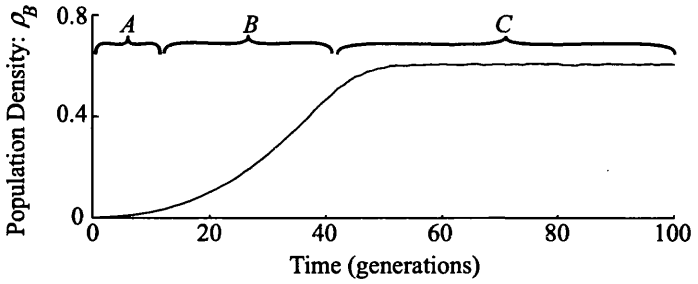

Figure 5-6: An establishing population on a finite lattice has three growth phases: A - Before a distinction exists between interior and exterior ($t \in [0, 10)$) growth is nearly linear ($\rho_B(t) \propto t^{1.3966}$ from least-squares regression). B - Once the population has established a clustered pattern ($t \in [10, 40)$), growth is close to parabolic ($\rho_B(t) \propto t^{2.1992}$). C - As the uninvaded space on the finite lattice is exhausted population density levels off rapidly. On the infinite lattice phase C would not arise and growth would be expected to continue parabolically. Plot is an average of five simulations on an $L = 100$ lattice with model parameters: $b = 6$, $p = 6$, $z = 4$ ($r = 1, p = 1$), $\epsilon = 0.05$.

is close to a local carrying equilibrium with an expectation of unitary reproductive success. However, because of the small neighbourhood size stochastic fluctuations in a given individual's neighbourhood composition can be profound: A previously overcrowded individual can be left isolated in very short space of time. Consequently the concepts of boundary and interior are vague on the IPS, as they are in real populations.

Three phases of growth can be identified in a population that establishes in a finite territory from initially small numbers. Figure 5-6 illustrates that initial growth is nearly linear until the population has an appreciable clustered pattern, subsequent growth is approximately parabolic until uninvaded space on the lattice is exhausted and population density rapidly levels off. The time until the equilibrium is reached is therefore explicitly dependent on the size of the lattice. On an infinite lattice, the original context of the IPS, such an invasion scenario corresponds to an initial configuration of regularly spaced small populations. Figures 5-5(a)-(c) show the growth of a population with a much larger neighbourhood size $z = 24$ ($r = 2, p = \infty$). The boundary is appreciably more diffuse and the interior more homogenous; population growth is also significantly faster. The larger neighbourhood provides greater access both to empty sites and to pollen hence reducing competition and enhancing the mutual benefits of cross-pollination. Notice that population growth is also somewhat quicker when the pollination equilibrium (5.2.2) is used (Figure 5-4). This occurs because newly

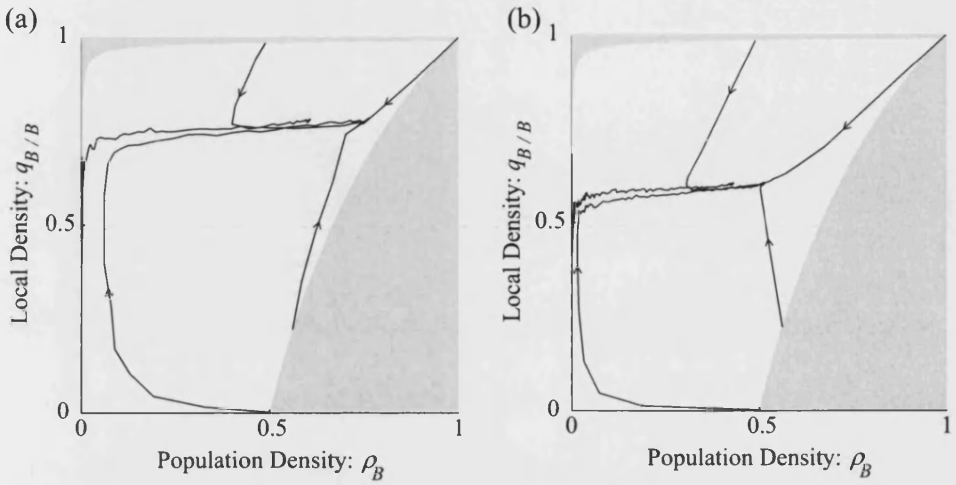

Figure 5-7: Population dynamics of the sexual species IPS in $(\rho_B, q_{B/B})$ phase space developing from various initial configurations on a $L = 100$ lattice. Grey regions indicate the constraints on $q_{B/B}$ on a finite lattice.(a) Plots are the average of five trials run for 120 generations with parameters $b = 6$, $p = 6$, $z = 4$ $(r = 1, p = 1)$, $\epsilon = 0.05$. (b) Plots are the average of 25 trials run for 200 generations using the pollination equilibrium (5.2.2) and parameters $b = 4$, $p = 4$, $z = 4$ $(r = 1, p = 1)$.

occupied sites are initially unpollinated and when $\epsilon > 0$ their expected probability of pollination grows from zero. In the limit of small ϵ newly occupied sites with neighbours immediately have a non-zero expected probability of being pollinated and thus spend a larger proportion of their life time capable of colonization.

In view of the clustered nature of the population dynamics Figure 5-7 illustrates the courses of simulations with different initial configurations in $(\rho_B, q_{B/B})$ space. Observe that regardless of initial configuration the simulations converge rapidly to a manifold across the centre of this space. This manifold corresponds to what might be described as the regular growth of clustered populations at a local equilibrium in the interior of the cluster and growing at the boundary. The grey regions in Figure 5-7 indicate the lower and upper bounds of achievable values for $q_{B/B}$, which are dependent on neighbourhood geometry and simulation size. For $z = 4$ $(r = 1, p = 1)$ the population configuration with maximal local density arises when the population occupies a square or nearly square block of the lattice. For a population size of n^2 individuals this

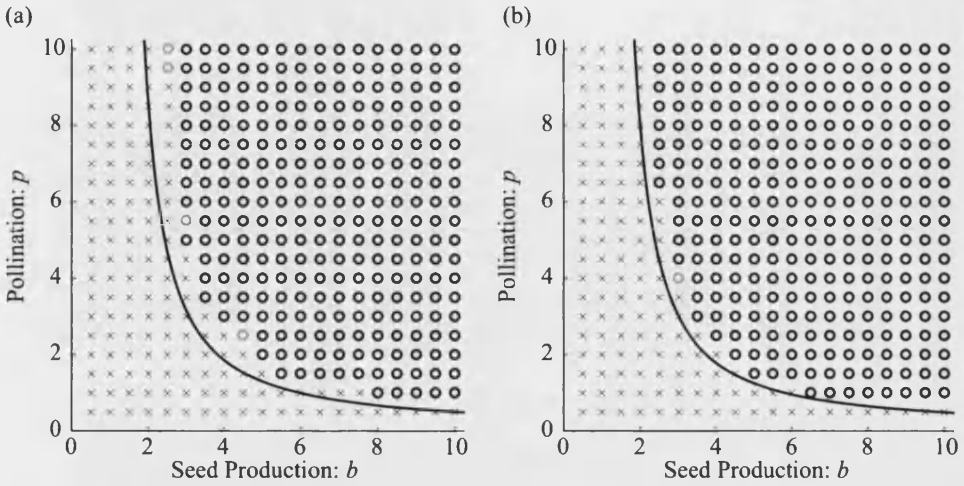

Figure 5-8: (b, p) parameter space for the sexual species IPS with $z = 8$ $(r = 1, p = \infty)$. (a) With pollen dynamics $\epsilon = 0.05$. (b) Using pollination equilibrium (5.2.2). Black circles indicate that a population will usually establish from an initial configuration of twelve neighbouring occupied sites. Light grey circles indicate that establishment is unusual but that large initial populations persist for at least 200 generations. Crosses indicate that populations rarely survive. The plotted line gives p_{crit} for the mean field approximation: $p > p_{\text{crit}}$ implies that the mean field has a locally attracting non-trivial equilibrium.

configuration gives:

$$q_{B/B} = \frac{8 + 12(n-2) + 4(n-2)^2}{zn^2} = 1 - \frac{1}{n} = 1 - \frac{1}{L\sqrt{\rho_B}}.$$

For non square population sizes this is a slight over-estimate, since proportionally more individuals are located on the boundary. In the limit of large lattice size this upper bound becomes unitary. The population configuration with minimal local density is achieved by adding or removing individuals from a checkerboard configuration. Beyond $\rho_B = 0.5$ every additional individual adds local density thus:

$$q_{B/B} = \frac{16n}{z(L^2 + 2n)} = 2 - \frac{1}{\rho_B}.$$

Figure 5-8 indicates the range of reproductive parameters b and p for which populations survive with $z = 8$ $(r = 1, p = \infty)$. Simulations were conducted both for

initially small populations $\rho_B = 0.0005$ and for initially large overcrowded populations $\rho_B = 1.0$. What is revealed is that if b and p are sufficient for maintenance of a large population they are also sufficient for establishment of a small population. Of course for a small population the initial configuration of occupied sites is all-important. Crucially individuals must be neighbours. The role of initial configuration is explored in more detail in the next section. Large populations may also face certain extinction, consider a checker board configuration with $z = 4$ $(r = 1, p = 1)$. However, this is an artifact of the regular neighbourhood geometry and not a pressing concern for real populations.

Small Cluster Dynamics

The simulations indicate that sexual species can become established from very small initial numbers so long as some of the initial individuals are neighbours. To examine this requirement in more detail it is necessary to focus on the dynamics of specific small configurations in the time leading up to the first colonization or death event. During this time the configuration can be assumed constant and the consequent probability that this first slow event will be either a colonization or a death event can be determined. If the probability that the first event will be colonization exceeds 0.5 this can be taken as an indication that population survival is likely.

Assume that for a given an initial configuration ξ_0 of the IPS all occupied sites are unpollinated. Define measures $Q_i : \xi_0 \to \mathbb{Z}^+$ for $i \in \{0, \ldots, z-1\}$ such that Q_i evaluates the number of empty sites with occupied neighbours which themselves have i occupied neighbouring sites. The expected probability of pollination of such sites is denoted q_i and will develop according to:

$$\epsilon \frac{dq_i}{dt} = \frac{ip}{z}(1 - q_i) - q_i,$$

which has explicit solution:

$$q_i(t) = \frac{ip}{z + ip}\left(1 - \exp(-\frac{(ip + z)t}{z\epsilon})\right),$$

when $q_i(0) = 0$. The rate at which slow events occur can therefore be specified as:

$$\lambda(t) = \frac{b}{z}\sum_{i=0}^{z-1} Q_i q_i(t) + N,$$

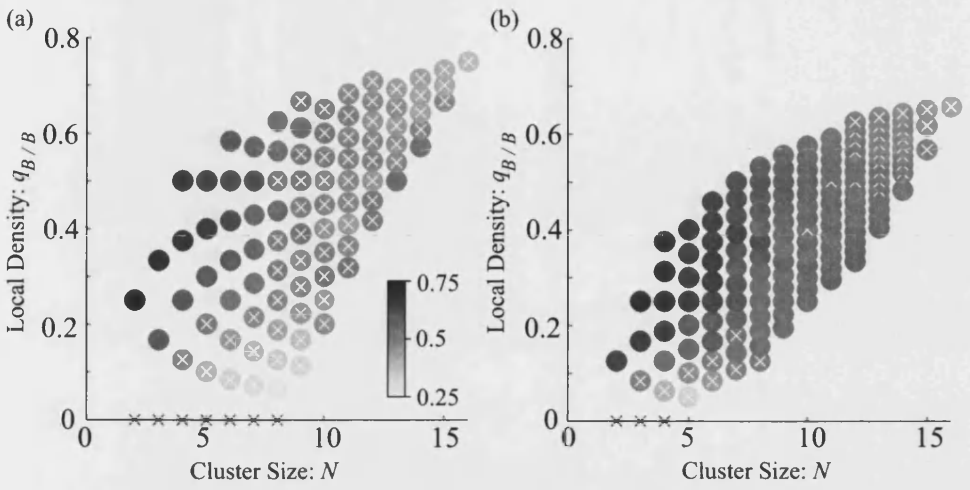

Figure 5-9: Probability that the first slow event will be a colonization for specific cluster configurations. Every configuration possible within a 4×4 block of sites is plotted as a circle in $(N, q_{B/B})$ - space; the shade of each circle indicates probability of colonization. Crosses indicate configurations for which a death is the more likely first slow event. (a) Neighbourhood size: $z = 4$ $(r = 1, p = 1)$. (b) Neighbourhood size: $z = 8$ $(r = 1, p = \infty)$. Parameters $b = 5$, $p = 5$, $\epsilon = 0.05$.

where N gives the total number of occupied cells which is also the death rate for the configuration as a whole. The expected time until one slow event occurs is denoted t_1 and must satisfy:

$$\int_0^{t_1} \lambda(t)dt = 1.$$

The probability that the first event is a colonization is $\mathbb{P}_c$ is then given by:

$$\mathbb{P}_c = 1 - \frac{N}{\bar{\lambda}} = 1 - Nt_1,$$

where $\bar{\lambda} = 1/t_1$ is the temporal average of $\lambda(t)$ on $[0, t_1)$.

Figure 5-9 illustrates how the probability that the first slow event is a colonization varies with cluster size and the local density $q_{B/B}$ experienced by the individuals in the cluster. The clusters with the highest chance of developing into established populations are small with high local density. Notice, however, in Figure 5-9(b) the advantage for larger clusters of having a lower neighbourhood density. Figure 5-10 shows the configurations with the top five highest probabilities of the first slow event being colonization.

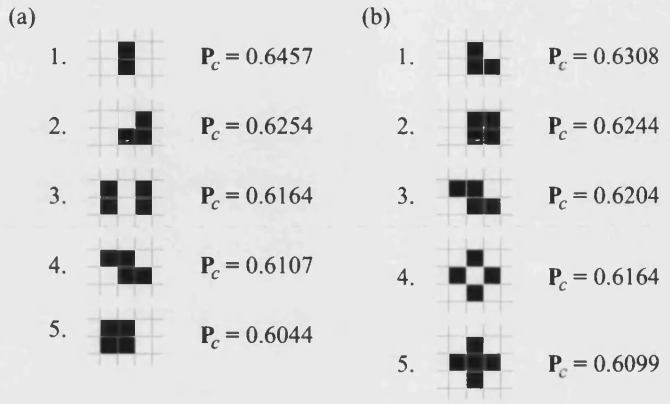

Figure 5-10: Top five configurations of small clusters with highest probability of first slow event being a colonization. (a) Neighbourhood size: $z = 4$ $(r = 1, p = 1)$. (b) Neighbourhood size: $z = 8$ $(r = 1, p = \infty)$. Parameters $b = 5$, $p = 5$, $\epsilon = 0.05$.

In fact the configurations shown are representatives of equivalence classes containing configurations which are equivalent up to rotation, translation and any other transformation which preserves number of occupied neighbouring sites each occupied site has. For example, the class of configurations represented by 5-10(a)2 also includes a row of three cells, since both configurations have two sites with one neighbour and one site with two. In both cases ($z = 4$ and $z = 8$) the configuration with the highest probability of colonization is very small, pointing toward the conclusion that the deterministic thresholds for successful population establishment are more or less $N > 1$, $q_{B/B} > 0$. Thus in the IPS sexual species model the only phenomena akin to the strong Allee effect found in the non-spatial model is that populations of isolated individuals are not viable. It should be pointed out that although small clusters have a high expectation to grow, they are far more vulnerable to stochastic extinction than larger clusters. The point being made here is that *deterministic* barriers to establishment that are predicted by non-spatial models appear to be absent in the IPS model.

Mean Field Approximation

By inserting the appropriate parameters into the general state density equations (5.2.4) and closing moments with (5.2.5) the following mean field approximation is obtained:

$$\begin{aligned}\epsilon\frac{d\rho_{B_0}}{dt} &= -p(\rho_{B_0}+\rho_{B_1})\rho_{B_0}+\rho_{B_1}+\epsilon\left[b\rho_{B_1}(1-\rho_{B_0}-\rho_{B_1})-\rho_{B_0}\right],\\ \epsilon\frac{d\rho_{B_1}}{dt} &= p(\rho_{B_0}+\rho_{B_1})\rho_{B_0}-\rho_{B_1}+\epsilon\left[-\rho_{B_1}\right].\end{aligned} \tag{5.3.2}$$

This system is invariant on $\triangle_1$ as defined in chapter 3:

$$\triangle_1 = \{(x_1,x_2)|\ 0\le x_1\le 1-x_2,\ 0\le x_2\le 1-x_1\},$$

which in this case is the region of validity for the variables since they express probabilities. The system has a trivial equilibrium and up to two non-trivial equilibria $(\hat{\rho}^{\pm}_{B_0},\hat{\rho}^{\pm}_{B_1})$ as follows:

$$\begin{aligned}\hat{\rho}^{\pm}_{B_0} &= \frac{(1+\epsilon)\left[p(b+1)\pm\sqrt{p^2(b^2+1)-2pb(p+2(1+\epsilon))}\right]}{2pb(p+1+\epsilon)},\\ \hat{\rho}^{\pm}_{B_1} &= \frac{p(b-1)-2(1+\epsilon)\pm\sqrt{p^2(b^2+1)-2pb(p+2(1+\epsilon))}}{2b(p+1+\epsilon)}.\end{aligned} \tag{5.3.3}$$

It follows that the equilibrium density for the conspecific class as a whole is:

$$\hat{\rho}^{\pm}_{B} = \frac{b-1}{2b}\pm\sqrt{\frac{(b-1)^2}{4b^2}-\frac{1+\epsilon}{bp}}. \tag{5.3.4}$$

The non-trivial equilibria therefore exist for $p\ge p_{\text{crit}}$ where:

$$p_{\text{crit}} = \frac{4b(1+\epsilon)}{(b-1)^2}. \tag{5.3.5}$$

The stability of the equilibria is readily extracted from the Jacobian. The Jacobian at the origin is given by:

$$J(0,0) = \frac{1}{\epsilon}\begin{pmatrix}-\epsilon & 1+\epsilon b\\ 0 & -(1+\epsilon)\end{pmatrix},$$

indicating that the origin is always stable. The Jacobian of the non-trivial equilibria is:

$$J(\hat{\rho}^{\pm}_{B_0}, \hat{\rho}^{\pm}_{B_1}) = \frac{1}{\epsilon}\begin{pmatrix} -2p\hat{\rho}^{\pm}_{B_0} - (p+\epsilon b)\hat{\rho}^{\pm}_{B_1} - \epsilon & -(p+\epsilon b)\hat{\rho}^{\pm}_{B_0} - 2\epsilon b\hat{\rho}^{\pm}_{B_1} + 1 + \epsilon b \\ p(2\hat{\rho}^{\pm}_{B_0} + \hat{\rho}^{\pm}_{B_0}) & p\hat{\rho}^{\pm}_{B_0} - (1+\epsilon) \end{pmatrix}.$$

Clearly $\mathrm{tr}J < 0$ so that stability is determined by $\det J$ which is neatly expressible in terms of $\hat{\rho}^{\pm}_B$:

$$\det J = 2pb\epsilon\hat{\rho}^{\pm}_B\left(\hat{\rho}^{\pm}_B - \frac{b-1}{2b}\right).$$

So that $(\hat{\rho}^{+}_{B_0}, \hat{\rho}^{+}_{B_1})$ is stable and locally attracting and $(\hat{\rho}^{-}_{B_0}, \hat{\rho}^{-}_{B_1})$ is an unstable saddle. Thus the mean field approximation predicts a strong Allee effect with population survival slightly dependent on the initial proportions of pollinated and unpollinated individuals. A dependence that disappears in the limit of large ϵ.

Aggregated Mean Field

Intuitively in the limit of small ϵ the pollination dynamics are expected to equilibrate between colonization and death events. This intuition was behind the derivation of the pollination equilibrium (5.2.2). It can be formalized for the mean field approximation (5.3.2). A quasi-equilibrium may be derived for the pollination dynamics on the fast time scale and then an outer asymptotic expansion taken around that quasi-equilibrium. The first term of this expansion which can be expressed in terms of the 'aggregated' variable $\rho_B = \rho_{B_0} + \rho_{B_1}$ then provides an approximation for the full dynamics, the accuracy of which depends on how small ϵ is. This is a standard perturbation method; it has previously been applied to the population dynamics of fast migrating species (Auger & Poggiale 1996, Auger & de la Parra Bravo 2000).

Fast Equilibria Define a fast timescale $\tau = t/\epsilon$, and the aggregated variable $\rho_B = \rho_{B_0} + \rho_{B_1}$. The fast dynamics are obtained by rescaling to the fast timescale and neglecting terms of order ϵ:

$$\frac{d\rho_{B_0}}{d\tau} = -p(\rho_{B_0} + \rho_{B_1})\rho_{B_0} + \rho_{B_1},$$
$$\frac{d\rho_{B_1}}{d\tau} = p(\rho_{B_0} + \rho_{B_1})\rho_{B_0} - \rho_{B_1},$$

This system contains only expressions for pollination and pollen expiry and notice:

$$\frac{d\rho_B}{d\tau} = \frac{d\rho_{B_0}}{d\tau} + \frac{d\rho_{B_1}}{d\tau} = 0,$$

As might be expected there is no change in site occupancy on this timescale and so the equations in (5.3.6) are not linearly independent and:

$$\frac{d\rho_{B_1}}{d\tau} = p\rho_B(\rho_B - \rho_{B_1}) - \rho_{B_1}, \tag{5.3.6}$$

is sufficient to describe the dynamics. The system (5.3.6) has a unique equilibrium:

$$\tilde{\rho}_{B_1} = \frac{p\rho_B^2}{1+\rho_B}. \tag{5.3.7}$$

which is easily checked to be globally asymptotically stable on the interval $[0, \rho_B]$. Thus pollination follows a Holling Type II functional response. The uniqueness of (5.3.7) guarantees that their is no branch switching between quasi-equilibria in the full model (5.3.2) that would be overlooked in the aggregated dynamics.

Aggregated Dynamics The first term of the outer asymptotic expansion of (5.3.2) about (5.3.7) gives:

$$\frac{d\rho_B}{dt} = b\frac{p\rho_B^2}{1+\rho_B}(1-\rho_B) - \rho_B. \tag{5.3.8}$$

The aggregated dynamics are instantly recognizable as the non spatial sexual-species model of chapter 3 3.2. Note, however, that the here ρ_B specifies a probability of occupancy on a lattice and is therefore constrained on the interval $[0, 1]$, by contrast the variable u in (3.2.1) was a rescaled population size.

By comparing the equilibria (3.2.2) and bifurcation point (3.2.3) of the aggregated dynamics with those of the timescale separated dynamics (5.3.4) and (5.3.5), the effect of the small parameter ϵ can be examined. To wit ϵ slightly lowers the size of the carrying equilibrium and slightly raises the threshold equilibrium which concomitantly raises the threshold pollen production level p_{crit} which must be exceeded for population viability. This is in line with observations from simulations that reproductive parameters can be slightly lower when the pollination equilibrium is used (see Figure 5-3.)

Figure 5-11 compares population growth predicted by the mean field approximation

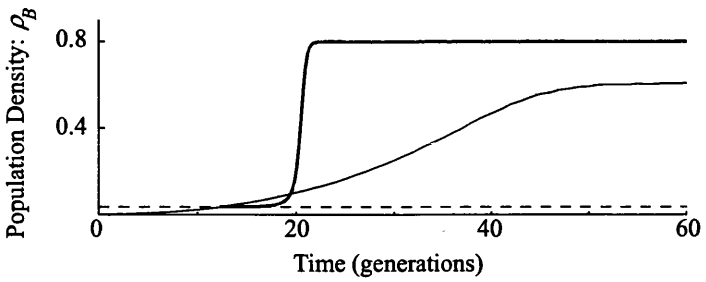

Figure 5-11: Comparison between mean field (bold curve) and simulation for the predicted growth of an establishing population. Note that the mean field has a strong Allee effect and predicts populations smaller than the threshold $\hat{\rho}_B^-$ indicated by the dashed line will decay. Consequently the comparison was initiated when the simulated population first exceeded this threshold. Plot is an average of five simulations on an $L = 100$ lattice with model parameters: $b = 6$, $p = 6$, $z = 4$ ($r = 1, p = 1$), $\epsilon = 0.05$.

5.3.2 and that observed in simulations. Such a comparison is only possible for populations which initially exceed the strong Allee effect threshold $\hat{\rho}_B^-$. For such a population mean field growth is initially exponential and soon overtakes the parabolic growth of the simulation. The mean field also predicts an equilibrium which is substantially higher than seen in simulations.

Hydrodynamic Limit

The hydrodynamic limit model obtained by adding a fast stirring process to the sexual species IPS is given by:

$$\begin{aligned} \frac{\partial \rho_{B_0}}{\partial t} &= f(\rho_{B_0}, \rho_{B_1}) + \Delta\rho_{B_0}, \\ \frac{\partial \rho_{B_1}}{\partial t} &= g(\rho_{B_0}, \rho_{B_1}) + \Delta\rho_{B_1}, \end{aligned} \tag{5.3.9}$$

where

$$\begin{aligned} f(\rho_{B_0}, \rho_{B_1}) &= -\frac{p}{\epsilon}(\rho_{B_0} + \rho_{B_1})\rho_{B_0} + \frac{\rho_{B_1}}{\epsilon} + b\rho_{B_1}(1 - \rho_{B_0} - \rho_{B_1}) - \rho_{B_0}, \\ g(\rho_{B_0}, \rho_{B_1}) &= \frac{p}{\epsilon}(\rho_{B_0} + \rho_{B_1})\rho_{B_0} - \frac{\rho_{B_1}}{\epsilon} - \rho_{B_1}. \end{aligned}$$

As with the mean field approximation, the aggregation of variables technique can be applied to (5.3.9) and results in:

$$\frac{\partial \rho_B}{\partial t} = b\frac{p\rho_B^2}{1+\rho_B}(1-\rho_B) - \rho_B + \Delta\rho_B, \tag{5.3.10}$$

which is immediately identified as the single species reaction-diffusion model of chapter 4 section 4.1.

Discussion

From simulations and examining the dynamics of local clusters, the behaviour of the sexual species IPS has been shown to differ significantly from the corresponding non-spatial model in chapter 3 and the continuum reaction-diffusion model of chapter 4. The novel behaviours arise because of the discrete nature of individuals and the local neighbourhood structure that develops in an IPS model. The models of chapter 3 and 4 have been shown to arise from continuum limits of the IPS in which the discreteness of individuals is lost and neighbourhood structure is either assumed away, as in the mean field, or 'washed-out' by a fast stirring process, as in the hydrodynamic limit.

Specifically the IPS model does not exhibit the strong Allee effect that arises in the population based models. Very small populations with sufficient reproductive rates and in which some individuals are neighbours are more likely to grow than to decay, and such a population is expected to colonize a finite lattice of any given size. By contrast the mean field approximation requires that initial population density exceed a positive threshold determined by the reproductive rates, so in effect larger lattices require larger initial populations in order to meet this threshold. The mean field does a reasonable job of identifying when a carrying equilibrium is present in the IPS (Figure 5-8.) It does a much worse job of predicting the rate of population growth and the size of the carrying equilibrium (Figure 5-11.) In both cases the explanation is that the mean field fails to recognize that occupied sites compete to colonize only neighbouring empty sites. For small clustered populations the mean field greatly under-estimates this competition and predicts rapid (exponential) growth. The mean field similarly over estimates the availability of empty sites at equilibrium because it ignores the fact that some empty sites are themselves clustered and hence unavailable for colonization. Consequently the mean field estimate for the carrying equilibrium improves in accuracy for higher reproductive rates. This is a more general observation, it is also the case,

for example, with the basic contact process (Iwasa 2000).

The hydrodynamic limit approximation similarly fails to capture IPS behaviour. Since the equilibria of the mean field are uniform steady states of the hydrodynamic limit, it inherits the strong Allee effect not seen in the IPS and the over-estimates the carrying equilibrium . In fact the diffusion in the hydrodynamic limit enhances the Allee effect, since a local population above the threshold may fall as individuals diffuse into surrounding territory. For populations established over part of a territory the strong Allee effect slows range expansion and in fact diffusion can drive population retreat (Figure 4-4.) Range expansion is slow (parabolic) in the IPS model too, but for very different reasons. In the hydrodynamic limit the strong Allee effect means that range expansion is 'pushed', that is: driven by migration rather than local growth. By contrast, in the IPS model, population growth is fastest at the population boundary, where neighbouring empty sites are in greatest abundance. Recall of course, that migration of individuals did not occur in the original formulation of the IPS and had to be introduced in order for the hydrodynamic limit to be extracted. As was mentioned in the discussion of chapter 4, the static nature of individuals means that deriving a reaction-diffusion model from mechanisms in plant ecology is awkward. Constructing the hydrodynamic limit has highlighted more precisely where a mechanistic derivation breaks down.

5.4 GYNODIOECY

The gynodioecy model has two conspecific classes, so three states are required for an IPS model $\mathcal{S} = \{A, B, C\}$, where state B denotes hermaphrodites and state C denotes females. According to the general derivation a total of seven sub-states are therefore required $\mathcal{S}_0 = \{A, B_0, B_1, B_2, C_0, C_1, C_2\}$. However, since the two subscript indicates pollination by class two individuals, that is females, states B_2 and C_2 will never arise unless they are artificially introduced. These two sub-states are therefore excluded from the model. Recall from chapter 3 section 3.3 that the interaction rates in the gynodioecy model without selfing are specified by the following pollination matrix and reproductive array:

$$P = \begin{pmatrix} p & 0 \\ p & 0 \end{pmatrix}, \quad B_1 = (b_{ij1}) = \begin{pmatrix} b & 0 \\ 0 & 0 \end{pmatrix}, \quad B_2 = (b_{ij2}) = \begin{pmatrix} 0 & 0 \\ \mu b & 0 \end{pmatrix}.$$

The resulting flip rates are:

$$\begin{aligned}
c_{B_0B_1}(x,\xi) &= \frac{p}{z\epsilon}(n_{B_0}(x,\xi)+n_{B_1}(x,\xi)),\\
c_{C_0C_1}(x,\xi) &= \frac{p}{z\epsilon}(n_{B_0}(x,\xi)+n_{B_1}(x,\xi)),\\
c_{B_1B_0}(x,\xi) &= c_{C_1C_0}(x,\xi) = \frac{1}{\epsilon},\\
c_{AB_0}(x,\xi) &= \frac{b}{z}n_{B_1}(x,\xi),\\
c_{AC_0}(x,\xi) &= \frac{\mu b}{z}n_{C_1}(x,\xi),\\
c_{B_0A}(x,\xi) &= c_{B_1A}(x,\xi) = 1,\\
c_{C_0A}(x,\xi) &= c_{C_1A}(x,\xi) = 1.
\end{aligned} \tag{5.4.1}$$

Hermaphrodites pollinate their unpollinated hermaphrodite and female neighbours at rate $p/z\epsilon$. Pollinated sites of both classes become unpollinated at rate $1/\epsilon$. Pollinated sites colonize empty neighbouring sites at rate b/z for hermaphrodites and $\mu b/z$ for females. All occupied site types become empty at unit death rate.

Simulations

The gynodioecy model without selfing was simulated on an $L = 100$ lattice. Reproductive rates $b = 4$, $p = 4$ were chosen so that a hermaphrodite only population would be viable and the pollination equilibrium 5.2.2 was used in the calculation of flip rates. Figures 5-12(a)-(c) illustrate how model behaviour differs as μ varies. Females depend on the local proximity of hermaphrodites to reproduce. If pollen is available in sufficient quantities females will locally out compete hermaphrodites by means of their higher fecundity. For given reproductive parameters females rarely survive if $\mu < \mu_0 \approx 1.5$. For higher μ a single female mutant can initiate an invasion. In Figure 5-12(a) where μ only just exceeds the invasion threshold female numbers increase very slowly. Females are accommodated in the population without greatly disrupting the hermaphrodite population or disturbing the carrying capacity of the population. Females are generally observed on the edges of small temporary clearings which they are unable to colonize because of the absence of pollen. These clearings are quickly recolonized by hermaphrodites. For $\mu = 1.75$ the effect is small and clearing are only marginally larger than those created stochastically elsewhere. For larger μ these clearings become more distinctive. Figure 5-12(b) shows that for intermediate

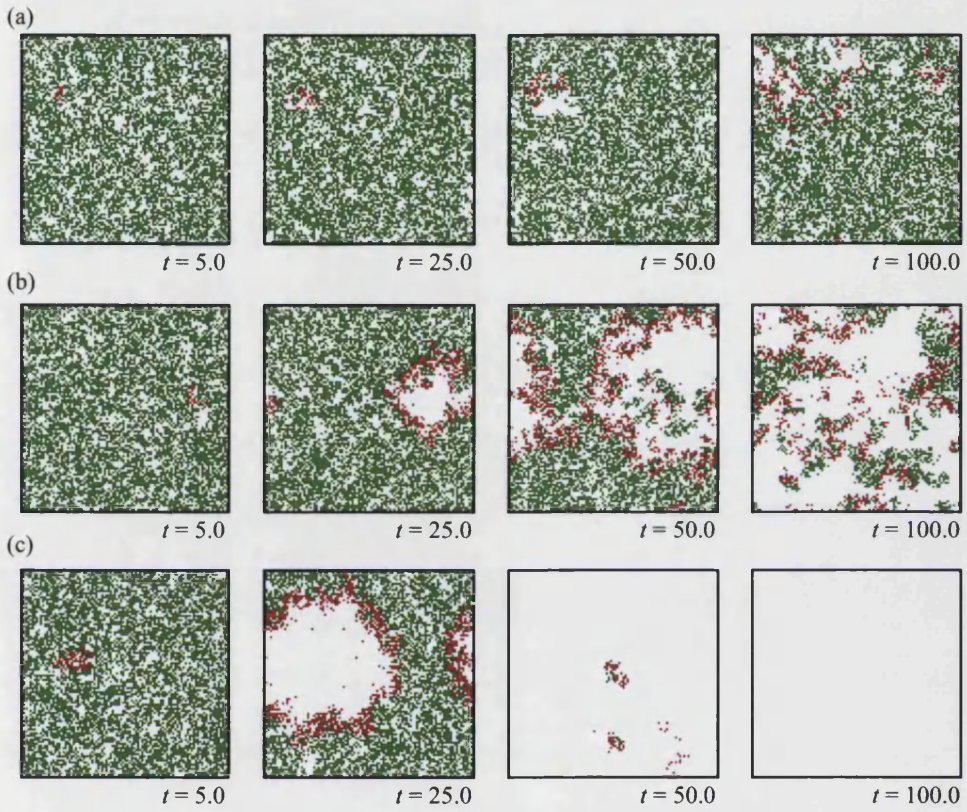

Figure 5-12: Typical simulations of the gynodioecy model without selfing on an $L = 100$ lattice using pollination equilibrium 5.2.2. A single female was introduced to a hermaphrodite population at carrying capacity at time $t = 0.0$. Sites are coloured: White if empty; Green if occupied by a hermaphrodite and red if occupied by a female. Parameters $b = 4$, $p = 4$, $z = 8$ ($r = 1$,$p = \infty$). (a) $\mu = 1.75$. (b) $\mu = 2.75$. (c) $\mu = 3.75$.

values of μ the female population on the boundary of the clearing is not impervious to hermaphrodites who eventually recolonize the cleared area. The female population, initially concentric around the point of introduction, is disrupted by these break-away hermaphrodite populations and population dynamics become erratic: Veering alternately between high hermaphrodite success and high female success. For large μ the female population at the edge of the clearing is effectively impervious to hermaphrodites and hermaphrodite numbers swiftly diminish as they are overrun. This often results in population extinction however, because female numbers fall rapidly too. Small numbers of hermaphrodites occasionally persist and can recolonize the lattice. Note that the extinction shown in 5-12(c) is in part an artifact of the finite lattice size, since the hermaphrodite population becomes encircled by females. Female populations have also been observed to overrun hermaphrodites advancing into empty territory by catching up and overtaking the front.

Figures 5-13(a)-(e) show the population trajectories of simulations, again on an $L = 100$ lattice with neighbourhood size $z = 8$ ($r = 1$,$p = \infty$). In Figure 5-13(a) where $\mu = 1.25$, various initial configurations converge on a hermaphrodite only carrying equilibrium, indicating that this system state has a wide basin of attraction. Figures 5-13(b)-(e) show mixed populations persisting for a long time. Note that in Figure 5-13(b) where $\mu = 1.75$, the system settled to a similar proportion of hermaphrodites and female on each run regardless of initial conditions. However, for Figure 5-13(c) where $\mu = 2.25$ and (d) where $\mu = 2.75$ the mixed populations alternate between hermaphrodite and female success. These irregular oscillations, averaged over 25 runs in the plots, are not readily apparent, although the increasingly cyclic behaviour is noticeable in the transience dynamics. In Figure 5-13(e) where $\mu = 3.25$, the whole population may die out, or as was discussed above hermaphrodites may escape extinction and recolonize the lattice.

Broadly the IPS gynodioecy model suggests three potential outcomes to the scenario of a male-sterility mutation arising in a hermaphrodite population: No invasion - bearers of the mutation do not experience improved reproductive success and the mutation is lost from the population; Coexistence - hermaphrodites and females coexist, either in stable proportions or with alternating phases of success; Extinction - the rapid invasion of females results in pollen shortage and the extinction of either females or both types. For given reproductive parameters model behaviour switches at threshold values of μ. Neighbourhood size is also crucially important in determining these thresholds. Larger neighbourhoods generally provide females with greater access to

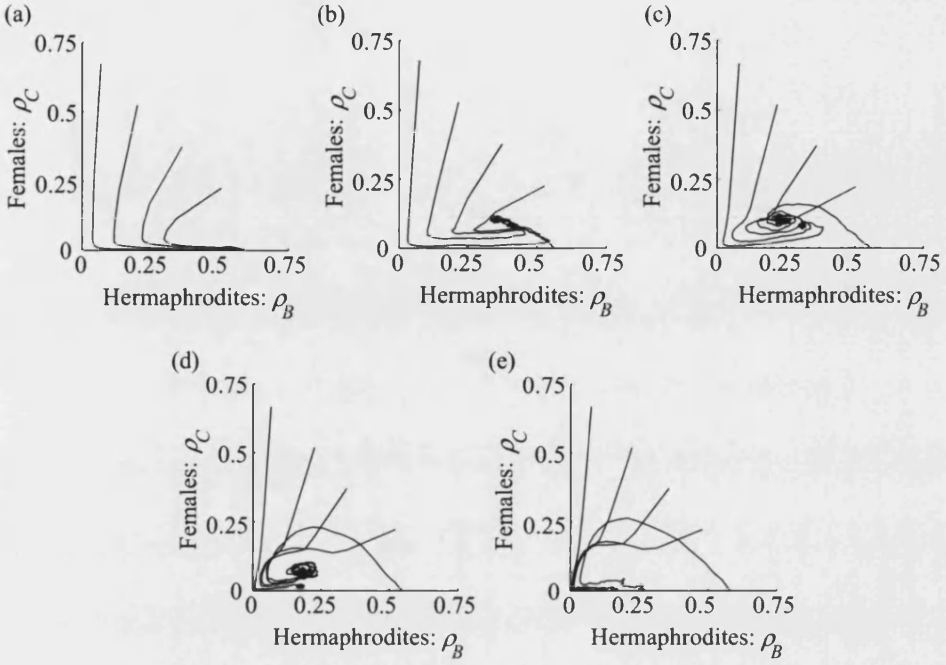

Figure 5-13: Population trajectories for simulations of the gynodioecy model without selfing on an $L = 100$ lattice with various initial configurations. Plots are averages of 25 runs of 200 generations. Parameters $b = 4$, $p = 4$, $z = 8$ ($r = 1$,$p = \infty$). (a) $\mu = 1.25$. (b) $\mu = 1.75$. (c) $\mu = 2.25$. (d) $\mu = 2.75$. (e) $\mu = 3.25$.

pollen. Figure 5-14 illustrates how the thresholds for different model behaviour change with neighbourhood size.

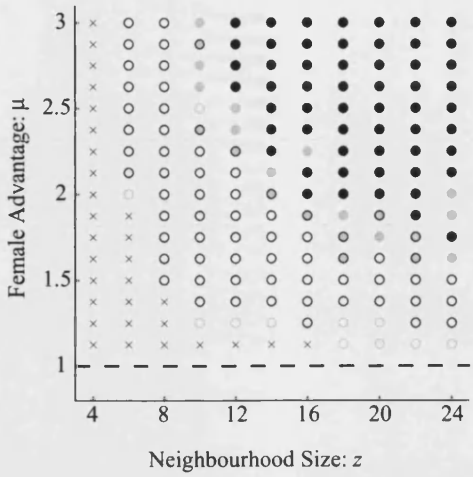

Figure 5-14: (z,μ)-parameter space for simulation of the IPS gynodioecy model without selfing. The introduction of 10 females, randomly distributed but adjacent to extant hermaphrodites was simulated on an $L = 50$ lattice with five replicates. Crosses indicate invasion always failed and no female were present at $t = 200$. Circles indicate some invasion success: Black outlines indicate females still present at $t = 200$ (or population extinct) in at least four of five trials; Grey outlines indicate fewer successful invasions; Black interiors indicate population extinct at $t = 200$ in at least four of five trials; Grey interiors indicate fewer extinctions; White interior indicate population still present at $t = 200$. Neighbourhood used always had at least 2-degrees of rotational symmetry, although were not always of (r,p) form. Parameters $b = 4$, $p = 4$.

Mean Field Approximation

By inserting the appropriate parameters into the general state density equations (5.2.4) and closing moments with (5.2.5) the following mean field approximation is obtained:

$$\begin{aligned}
\epsilon\frac{d\rho_{B_0}}{dt} &= -p(\rho_{B_0}+\rho_{B_1})\rho_{B_0} + \rho_{B_1} + \epsilon\left[b\rho_{B_1}\rho_A - \rho_{B_0}\right],\\
\epsilon\frac{d\rho_{B_1}}{dt} &= p(\rho_{B_0}+\rho_{B_1})\rho_{B_0} - \rho_{B_1} + \epsilon\left[-\rho_{B_1}\right],\\
\epsilon\frac{d\rho_{C_0}}{dt} &= -p(\rho_{B_0}+\rho_{B_1})\rho_{C_0} + \rho_{C_1} + \epsilon\left[\mu b\rho_{C_1}\rho_A - \rho_{C_0}\right],\\
\epsilon\frac{d\rho_{C_1}}{dt} &= p(\rho_{B_0}+\rho_{B_1})\rho_{C_0} - \rho_{C_1} + \epsilon\left[-\rho_{C_1}\right].
\end{aligned} \tag{5.4.2}$$

An aggregated model is sought directly by the same method used for the sexual species model.

Fast Equilibrium Define aggregated variables $\rho_B = \rho_{B_0} + \rho_{B_1}$ and $\rho_C = \rho_{C_0} + \rho_{C_1}$, rescaling to the fast timescale $\tau = t/\epsilon$ and neglecting $O(\epsilon)$ terms:

$$\begin{aligned} \frac{d\rho_{B_1}}{d\tau} &= p\rho_B(\rho_B - \rho_{B_1}) - \rho_{B_1}, \\ \frac{d\rho_{C_1}}{d\tau} &= p\rho_B(\rho_C - \rho_{C_1}) - \rho_{C_1}. \end{aligned} \tag{5.4.3}$$

The fast system is decoupled and the unique fast equilibrium:

$$\begin{aligned} \tilde{\rho}_{B_1} &= \frac{p\rho_B^2}{1+\rho_B}, \\ \tilde{\rho}_{C_1} &= \frac{p\rho_B\rho_C}{1+\rho_B}, \end{aligned}$$

is readily found and checked to be globally asymptotically stable on $[0, \rho_B] \times [0, \rho_C]$. The fast equilibrium in full is:

$$\tilde{\rho} = (\rho_B - \tilde{\rho}_{B_1}, \tilde{\rho}_{B_1}, \rho_C - \tilde{\rho}_{C_1}, \tilde{\rho}_{C_1}). \tag{5.4.4}$$

Aggregated Dynamics The first term of the outer asymptotic expansion of (5.4.2) about (5.4.4) gives:

$$\begin{aligned} \frac{d\rho_B}{dt} &= b\frac{p\rho_B^2}{1+\rho_B}(1 - \rho_B - \rho_C) - \rho_B. \\ \frac{d\rho_C}{dt} &= \mu b\frac{p\rho_B\rho_C}{1+\rho_B}(1 - \rho_B - \rho_C) - \rho_C. \end{aligned} \tag{5.4.5}$$

The aggregated dynamics are instantly recognizable as the non spatial gynodioecy model of chapter 3 3.3, with the aggregated densities ρ_B and ρ_C in place of the scaled population sizes u_1 and u_2.

Hydrodynamic Limit

As before the hydrodynamic limit is given by the mean-field equations with linear diffusion added. Aggregating variables leads to:

$$\begin{aligned}\frac{d\rho_B}{dt} &= b\frac{p\rho_B^2}{1+\rho_B}(1-\rho_B-\rho_C)-\rho_B+\Delta\rho_B.\\ \frac{d\rho_C}{dt} &= \mu b\frac{p\rho_B\rho_C}{1+\rho_B}(1-\rho_B-\rho_C)-\rho_C+\Delta\rho_C,\end{aligned} \tag{5.4.6}$$

the reaction-diffusion gynodioecy model of chapter 4 section 4.2 in the special case of equal unitary diffusion coefficients: $D_1 = D_2 = 1$. Different diffusion coefficients can be obtained by adjusting the rates of fast stirring, although since there was no biological justification for including the exchange dynamics in the first place there can be no reason for choosing different rates.

Discussion

The IPS gynodioecy model without selfing exhibits a range of behaviours absent from the corresponding non-spatial and continuum models of chapters 3 and 4. A male sterility mutation which conveys a seed production advantage introduced into a hermaphrodite population may be eliminated by deterministic selective pressure; or may spread, resulting in coexistence of the the two reproductive modes or in pollen shortage and population extinction. The fate of the mutation depends on the magnitude of the reproductive advantage it conveys and the size of local neighbourhoods.

In chapter 3 it was found that invasion failure and coexistence phenomena arose in a non spatial gynodioecy model if the hermaphrodites were self-compatible and thus enjoyed a greater share of pollen. Thus both conspecifics enjoyed a reproductive advantage when rare: Females producing greater numbers of seeds when pollen was abundant and hermaphrodites fertilizing a greater proportion of seed when pollen was rare. In the IPS gynodioecy model a similar arrangement of frequency dependent effects is responsible for generating remarkably similar model behaviour. In the IPS model however, hermaphrodites have no intrinsic individual advantage but instead derive what might be described as a configurational advantage which arises naturally from the short-range of interactions between individuals. Figure 5-15 illustrates that in a female invasion that results in coexistence, the contents of hermaphrodite and female neighbourhoods are

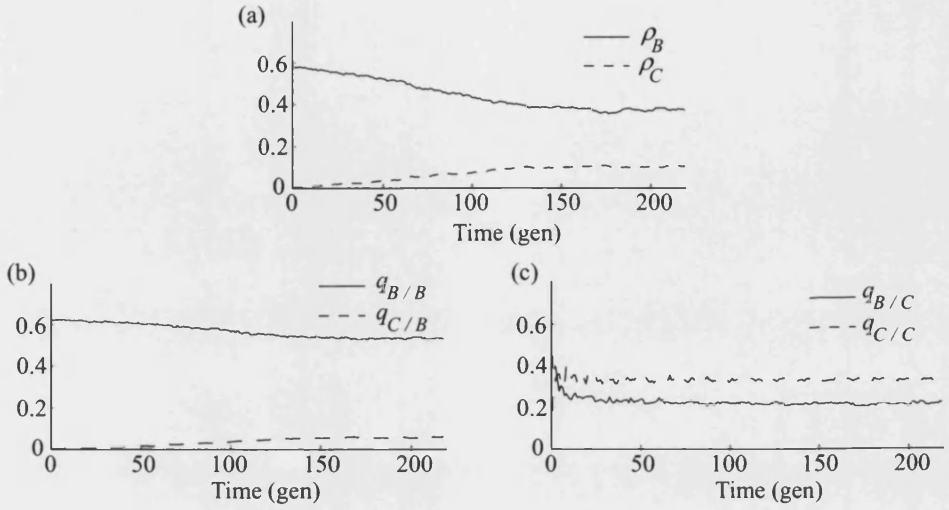

Figure 5-15: The development of neighbourhood structure in the IPS gynodioecy model without selfing. Simulation of the introduction of a single female mutant into a hermaphrodite population near carrying equilibrium, on an $L = 100$ lattice using pollination equilibrium 5.2.2. (a) - Global density of hermaphrodites and females. (b) Local density of conspecifics experienced by hermaphrodites. (c) Local density of conspecifics experienced by females. Parameters $b = 4$, $p = 4$, $\mu = 1.75$, $z = 8$ ($r = 1$,$p = \infty$).

typically quite different. At equilibrium females have a higher occupancy in their neighbourhoods and a much higher proportion of their neighbours are other females. The proportion of neighbouring sites containing hermaphrodites is appreciably lower for females so they experience a restricted access to pollen. Moreover, higher neighbourhood occupancy results in greater competition for available empty sites. The combination of these effects counterbalances the intrinsic reproductive advantage of females ($\mu > 1$) and in the case depicted in Figure 5-15 brings hermaphrodite and female reproductive success into parity. Because interactions are local, female reproductive success is subject to negative feedback: A highly reproductively successful female will fill its neighbourhood with other females, decreasing access to pollen and increasing competition for empty sites. The disadvantages females experience in individual-based discrete spatial models has previously been reported by Wilson (2000, pp 181-207). Wilson modelled a gynodioecious population on a lattice dispersing pollen and seed according to peaked (leptokurtic) dispersal kernels. The pollen and seed dispersal functions did not have to be identical for coexistence phenomena to result, suggesting that choosing

different neighbourhoods for pollen and seed dispersal in the IPS model above would not qualitatively alter model behaviour. Although given the model's sensitivity to neighbourhood size, significant quantative differences in population size and configuration would be expected. Some similar behaviour is also seen in a cellular automaton model of a chemical system studied in relation to the origins of life (Cronhjort 2000). If a 'host' autocatalytic polymer species is 'parasitized' by a rapidly multiplying species providing no catalytic support for the host species but receiving catalytic support from it, a non spatial model predicts extinction of the host. By contrast a cellular automaton model exhibits clusters of the host polymer pursued through space by a thin layer of the parasite species lining one edge of the cluster. The theoretical similarity with the gynodioecy model is striking, although the governing equations differ somewhat.

The reason the mean field approximation fails to capture most simulation behaviour is now quite apparent. Since the advantage hermaphrodites experience when rare derives from their superior neighbourhood, only if the distinct constitution of hermaphrodite and female neighbourhoods is respected will the effect emerge. The mean field, however, quashes this distinction and so suppresses the effect.

5.5 SEXUAL-ASEXUAL

The sexual-asexual model has two conspecific classes, so three states are required for an IPS model $\mathcal{S} = \{A, B, C\}$, where state B denotes sexuals and state C denotes asexual. Since both sexuals and pseudogamous asexuals are pollen producing and require pollen for reproduction all seven possible sub-states $\mathcal{S}_0 = \{A, B_0, B_1, B_2, C_0, C_1, C_2\}$ are achievable. Recall from chapter 3 section 3.4 that the interaction rates in the sexual-asexual model are specified by the following pollination matrix and reproductive array:

$$P = \begin{pmatrix} p & p \\ p & p \end{pmatrix}, \quad B_1 = (b_{ij1}) = \begin{pmatrix} \mu b & \frac{\mu\nu b}{2} \\ 0 & 0 \end{pmatrix}, \quad B_2 = (b_{ij2}) = \begin{pmatrix} 0 & \frac{\mu\nu b}{2} \\ b & b \end{pmatrix}.$$

Since pollinated asexuals produce asexual offspring at the same rate regardless of which conspecific they were pollinated by it is unnecessary to keep track of this information. Sub-states C_1 and C_2 can therefore be amalgamated and for notational convenience

the amalgamated state will be denoted C_1. The IPS flip rates are:

$$\begin{aligned}
c_{B_0B_1}(x,\xi) &= \frac{p}{z\epsilon}(n_{B_0}(x,\xi) + n_{B_1}(x,\xi) + n_{B_2}(x,\xi)),\\
c_{B_0B_2}(x,\xi) &= \frac{p}{z\epsilon}(n_{C_0}(x,\xi) + n_{C_1}(x,\xi)),\\
c_{C_0C_1}(x,\xi) &= \frac{p}{z\epsilon}(n_{B_0}(x,\xi) + n_{B_1}(x,\xi) + n_{B_2}(x,\xi) + n_{C_0}(x,\xi) + n_{C_1}(x,\xi)),\\
c_{B_1B_0}(x,\xi) &= c_{B_2B_0}(x,\xi) = c_{C_1C_0}(x,\xi) = \frac{1}{\epsilon},\\
c_{AB_0}(x,\xi) &= \frac{\mu b}{z}\left(n_{B_1}(x,\xi) + \frac{\nu}{2}n_{B_2}(x,\xi)\right),\\
c_{AC_0}(x,\xi) &= \frac{b}{z}\left(n_{C_1}(x,\xi) + \frac{\mu\nu}{2}n_{B_2}(x,\xi)\right),\\
c_{B_0A}(x,\xi) &= c_{B_1A}(x,\xi) = c_{B_2A}(x,\xi) = 1,\\
c_{C_0A}(x,\xi) &= c_{C_1A}(x,\xi) = 1.
\end{aligned} \tag{5.5.1}$$

Sexuals and asexuals both pollinate their unpollinated neighbours at rate $p/z\epsilon$. Pollinated sites of both classes become unpollinated at rate $1/\epsilon$. Sexuals pollinated by other sexuals colonize neighbouring empty sites at rate $\mu b/z$ with offspring that are unpollinated sexuals. Sexuals pollinated by asexuals colonize neighbouring empty sites at the reduced rate $\mu\nu b/z$, since only a proportion ν of seeds fertilized by asexuals are viable. Offspring have a fifty percent chance of carrying an allele conferring parthenogenicity so half are unpollinated asexuals and half are unpollinated sexuals. Asexuals pollinated by either class colonize neighbouring empty sites at rate b/z with offspring that are genetically identical to their parents and hence are themselves asexual.

Simulations

Simulations of the sexual-asexual IPS model were run on an $L = 100$ lattice using the pollination equilibrium 5.2.2. Since asexuals produce only asexual offspring and sexuals whose neighbourhoods comprise mainly other sexuals produce mainly sexual offspring, regions of the IPS dominated by one or other class tend to remain dominated by that class. Interaction between conspecific classes takes place on the boundary between these regions. Because interactions are short-range it is only the relative frequencies of sexuals and asexuals in the boundary that determines which regions spread and which contract. This is in contrast to the non-spatial model of chapter 3 section 3.4 in which the global frequency of conspecifics determines reproductive success. A

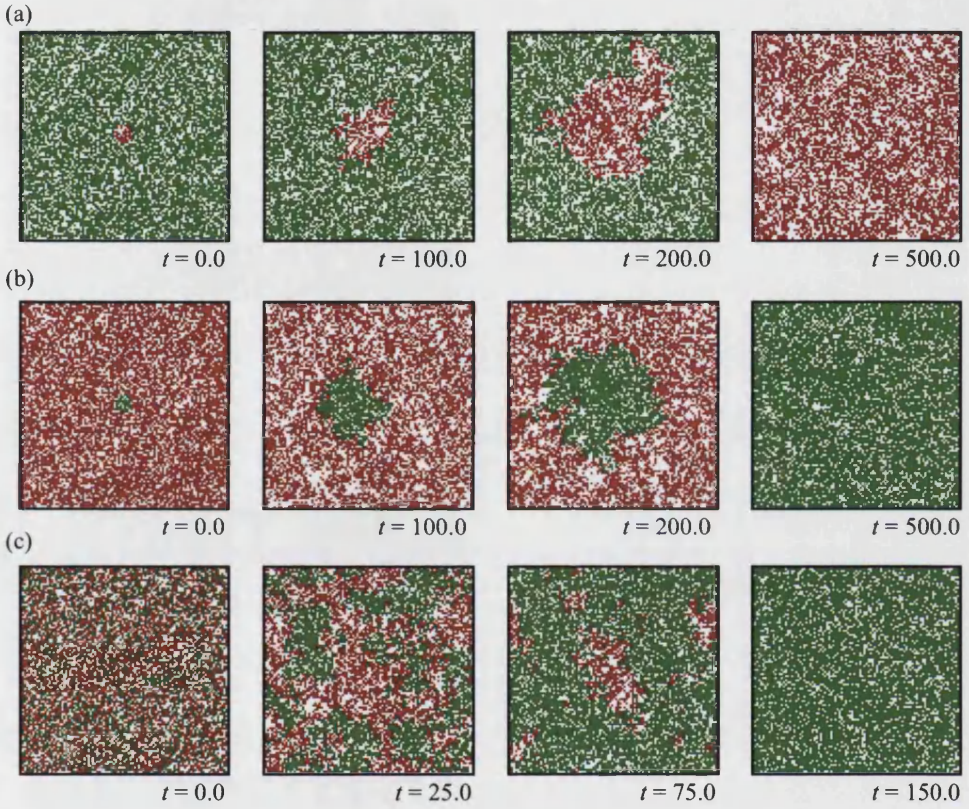

Figure 5-16: Typical interaction patterns in the sexual-asexual IPS model, simulated on and $L = 100$ lattice using the pollination equilibrium 5.2.2. Sites are coloured: White if empty; Green if occupied by a sexually and red if occupied by an asexual. Parameters $b = 4$, $p = 4$, $z = 8$, ($r = 1$,$p = \infty$). (a) $\mu = 1.25$, $\nu = 0.2$. (b) and (c) $\mu = 1.75$, $\nu = 0.5$.

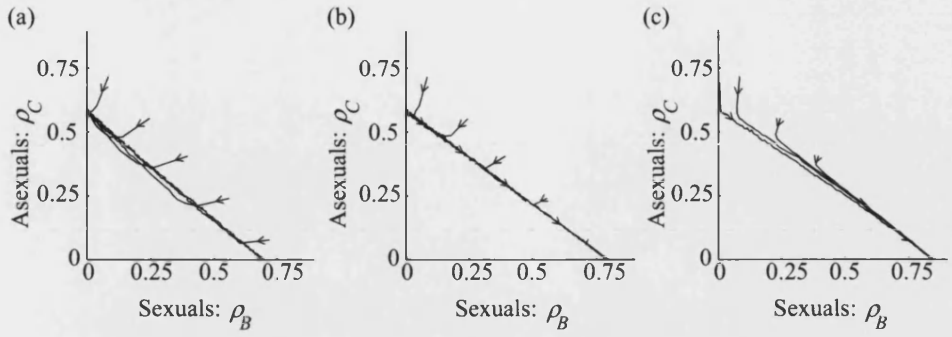

Figure 5-17: Population trajectories for simulations of the sexual-asexual IPS model on an $L = 100$ run for 500.0 generations averaged over five replicates. Parameters $b = 4$, $p = 4$, $z = 8$, ($r = 1$,$p = \infty$). (a) $\mu = 1.25$, $\nu = 0.2$. (b) $\mu = 1.75$, $\nu = 0.5$. (c) $\mu = 2.25$, $\nu = 0.8$.

consequence of this global dependency was that the model exhibited bistability over a wide region of parameter space. Figures 5-16(a)-(b) take parameters from within the region of bistability and initial frequencies that, in the non-spatial model, would see the rarer conspecific class driven extinct. In both cases, because conflict between the classes is concentrated in the boundary, the initially rare class prevails, albeit slowly. The initial clumping in Figures 5-16(a)-(b) is artificially contrived, but clumping is a generic feature of the model; Figure 5-16(c) demonstrates that an initially random distribution of conspecifics rapidly form clumps. During the formation of clumps, although a significant number of colonizations and deaths take place, the frequencies of each class remain relatively constant. Once clumps are established the boundary dynamics take over and govern the eventual predominance of one class. Note that in Figures 5-16(a)-(b) movement of the boundary between sexuals and asexuals is very slow: under 65 sites in 500 generations. Figure 5-17(a)-(c) shows the trajectories of populations with different initial frequencies converging to the same equilibrium for three sets of parameters taken from within the bistability region predicted by the mean field.

When neither conspecific class is very rare clumps will establish and the boundary interaction will determine which class prevails, irrespective of initial frequencies. Figures 5-18(a)-(b) show that there is no difference in which reproductive mode fixes when initially at least a quarter of individuals belong to either class. Although time to fixation can vary. When both conspecifics have established populations their interaction

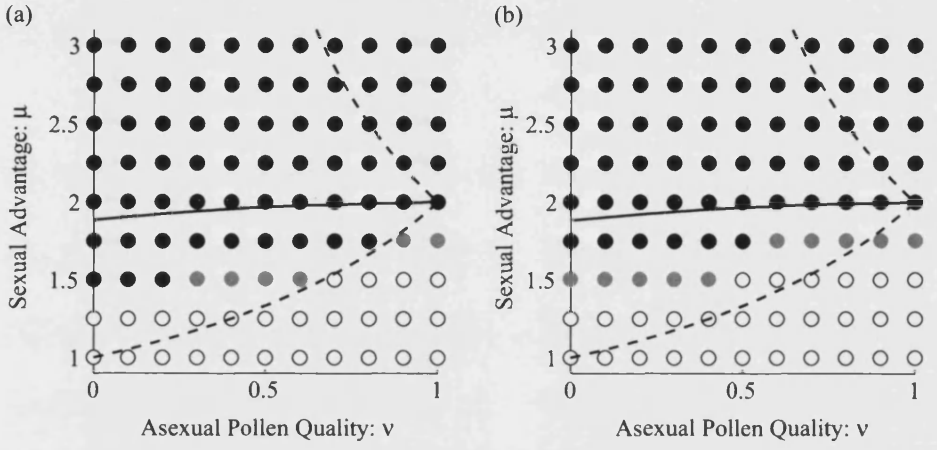

Figure 5-18: (ν, μ)-parameter space for the sexual-asexual IPS model. Simulated on an $L = 50$ lattice with five replicates and initial conditions: (a) Asexuals outnumber sexuals 3 : 1; (b) Sexuals outnumber asexuals 3 : 1. Parameters: $b = 4$, $p = 4$, $z = 8$ ($r = 1$,$p = \infty$). White circles indicate asexual reproduction fixed by $t = 200$; Black circles indicate sexual reproduction fixed by $t = 200$; Grey circles indicate neither mode fixed by $t = 200$. Dashed curves are the bifurcation curves of the non-spatial model c.f. Figure 3-17. The black curve recalls the numerically obtained curve dividing advance and retreat of the sexual front in the sexual-asexual reaction-diffusion of chapter 4 with $D_1 = D_2$.

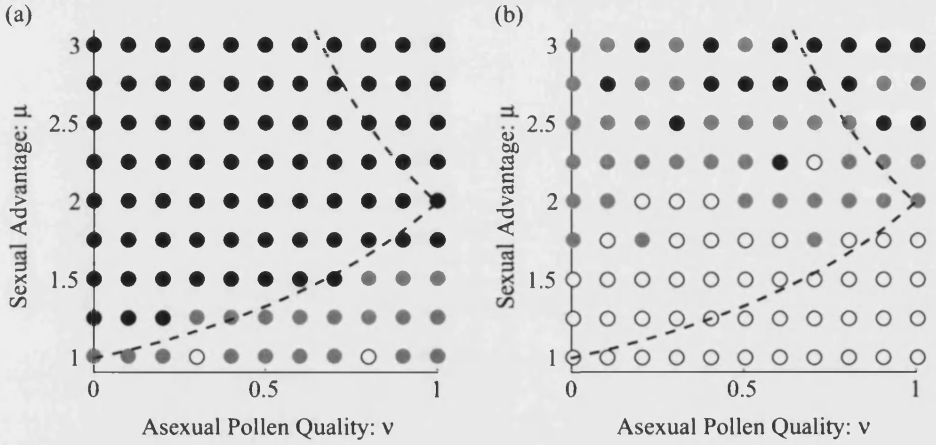

Figure 5-19: (ν, μ)-parameter space for the sexual-asexual IPS model. Simulated on an $L = 50$ lattice with five replicates and initial conditions: (a) Sexuals introduced in a 3×3 clump into a population fixed for asexual reproduction; (b) Asexuals introduced in a 3×3 clump into a population fixed for sexual reproduction. Parameters: $b = 4$, $p = 4$, $z = 8$ ($r = 1$,$p = \infty$). White circles indicate asexual reproduction fixed by $t = 200$; Black circles indicate sexual reproduction fixed by $t = 200$; Grey circles indicate neither mode fixed by $t = 200$.

is frequency independent. By contrast, when one conspecific is very rare, as might be the case for a novel reproductive mode arising through mutation, frequency becomes important. Figures 5-19(a)-(b) illustrate (ν, μ)-parameter space when the rare mode is introduced in a clump of only nine sites. In this case the neighbourhood of an individual of the rare mode is predominantly constituted of the common conspecific class. Since both modes fare poorly when there is a local abundance of the other mode a significant intrinsic advantage is required for the rare class to spread and establish a clump large enough for boundary dynamics to govern population development. Consequently the bistability of the non-spatial model is to some extent recovered.

Mean Field Approximation

By inserting the appropriate parameters into the general state density equations (5.2.4) and closing moments with (5.2.5) the following mean field approximation is obtained:

$$\begin{aligned}
\epsilon\frac{d\rho_{B_0}}{dt} &= -p(1-\rho_A)\rho_{B_0} + \rho_{B_1} + \rho_{B_2} + \epsilon\left[\mu b\left(\rho_{B_1} + \tfrac{\nu}{2}\rho_{B_2}\right)\rho_A - \rho_{B_0}\right], \\
\epsilon\frac{d\rho_{B_1}}{dt} &= p(\rho_{B_0} + \rho_{B_1} + \rho_{B_2})\rho_{B_0} - \rho_{B_1} + \epsilon\left[-\rho_{B_1}\right], \\
\epsilon\frac{d\rho_{B_2}}{dt} &= p(\rho_{C_0} + \rho_{C_1})\rho_{B_0} - \rho_{B_2} + \epsilon\left[-\rho_{B_2}\right], \\
\epsilon\frac{d\rho_{C_0}}{dt} &= -p(1-\rho_A)\rho_{C_0} + \rho_{C_1} + \epsilon\left[b\left(\rho_{C_1} + \tfrac{\mu\nu}{2}\rho_{B_2}\right)\rho_A - \rho_{C_0}\right], \\
\epsilon\frac{d\rho_{C_1}}{dt} &= p(1-\rho_A)\rho_{C_0} - \rho_{C_1} + \epsilon\left[-\rho_{C_1}\right].
\end{aligned} \tag{5.5.2}$$

An aggregated model is sought directly by the same method used for the sexual species model.

Fast Equilibrium Define aggregated variables $\rho_B = \rho_{B_0} + \rho_{B_1} + \rho_{B_2}$ and $\rho_C = \rho_{C_0} + \rho_{C_1}$, rescaling to the fast timescale $\tau = t/\epsilon$ and neglecting $O(\epsilon)$ terms:

$$\begin{aligned}
\frac{d\rho_{B_1}}{d\tau} &= p\rho_B(\rho_B - \rho_{B_1} - \rho_{B_2}) - \rho_{B_1}, \\
\frac{d\rho_{B_2}}{d\tau} &= p\rho_C(\rho_B - \rho_{B_1} - \rho_{B_2}) - \rho_{B_2}, \\
\frac{d\rho_{C_1}}{d\tau} &= p(\rho_B + \rho_C)(\rho_C - \rho_{C_1}) - \rho_{C_1}.
\end{aligned} \tag{5.5.3}$$

The fast system is decoupled. Define the density of pollinated sexual $\rho_{B_p} = \rho_{B_1} + \rho_{B_2}$ so that:

$$\frac{d\rho_{B_p}}{d\tau} = p(\rho_B + \rho_C)(\rho_B - \rho_{B_p}) - \rho_{B_p},$$

and at equilibrium:

$$\tilde{\rho}_{B_p} = \frac{p(\rho_B + \rho_C)\rho_B}{1 + \rho_B + \rho_C}.$$

From 5.5.3 $\rho_{B_1}\rho_C = \rho_{B_2}\rho_B$ so:

$$\begin{aligned}
\tilde{\rho}_{B_1} &= \frac{\rho_B}{\rho_B + \rho_C}\tilde{\rho}_{B_p} = \frac{p\rho_B^2}{1 + \rho_B + \rho_C}, \\
\tilde{\rho}_{B_2} &= \frac{\rho_C}{\rho_B + \rho_C}\tilde{\rho}_{B_p} = \frac{p\rho_C\rho_B}{1 + \rho_B + \rho_C}, \\
\tilde{\rho}_{C_1} &= \frac{p(\rho_B + \rho_C)\rho_C}{1 + \rho_B + \rho_C},
\end{aligned}$$

which is the unique and globally asymptotically stable equilibrium of 5.4.3. The fast equilibrium in full is:

$$\tilde{\rho} = (\rho_B - \tilde{\rho}_{B_1} - \tilde{\rho}_{B_2}, \tilde{\rho}_{B_1}, \tilde{\rho}_{B_2}, \rho_C - \tilde{\rho}_{C_1}, \tilde{\rho}_{C_1}). \tag{5.5.4}$$

Aggregated Dynamics The first term of the outer asymptotic expansion of (5.5.2) about (5.5.4) gives:

$$\begin{aligned}
\frac{d\rho_B}{dt} &= \mu b\frac{p(\rho_B + \frac{\nu}{2}\rho_C)\rho_B}{1 + \rho_B + \rho_C}(1 - \rho_B - \rho_C) - \rho_B, \\
\frac{d\rho_C}{dt} &= b\frac{p(\rho_C + (1 + \frac{\mu\nu}{2})\rho_B)\rho_C}{1 + \rho_B + \rho_C}(1 - \rho_B - \rho_C) - \rho_C.
\end{aligned} \tag{5.5.5}$$

The aggregated dynamics are instantly recognizable as the non spatial sexual-asexual model of chapter 3 3.4, with the aggregated densities ρ_B and ρ_C in place of the scaled population sizes u_1 and u_2.

Hydrodynamic Limit

As before the hydrodynamic limit is given by the mean-field equations with linear diffusion added. Aggregating variables leads to:

$$\begin{aligned}\frac{d\rho_B}{dt} &= \mu b\frac{p(\rho_B+\frac{\nu}{2}\rho_C)\rho_B}{1+\rho_B+\rho_C}(1-\rho_B-\rho_C)-\rho_B+\Delta\rho_B,\\ \frac{d\rho_C}{dt} &= b\frac{p(\rho_C+(1+\frac{\mu\nu}{2})\rho_B)\rho_C}{1+\rho_B+\rho_C}(1-\rho_B-\rho_C)-\rho_C+\Delta\rho_C,\end{aligned} \tag{5.5.6}$$

the reaction-diffusion sexual-asexual model of chapter 4 section 4.3 in the special case of equal unitary diffusion coefficients: $D_1 = D_2 = 1$.

Discussion

The putative loss of bistability from the sexual-asexual IPS is perhaps not unexpected, since it has been demonstrated that IPS with finite interaction ranges cannot exhibit bistability (Liggett 1978, Durrett & Levin 1994). This is because the dynamics of such a system depend only on the interaction at boundaries between regions dominated by one or other state. At these boundaries neither state predominates and neighbourhoods contains roughly equal numbers of both types. The performance of each state in the mixed boundary determines which state will spread and come to dominate globally. The initial global abundance of either state is therefore inconsequential. The argument applies to generic initial conditions for which both states have strictly positive global density. So that on an infinite lattice clumps of a significant size are certain to occur for both states. In Figure 5-19 the non-generic case of the introduction of a finite number of one state was examined. This case is interesting from an evolutionary perspective, since novel mutations arise infrequently in one individual at a time. In this case the bistability exhibited by the non-spatial model is restored.

The slow progress of the boundary between sexuals and asexuals for reasonably biologically realistic parameters is potentially an explanation for geographic parthenogenesis. Carrillo (2002) found with a cellular automaton model that sexuals and non-pseudogamous apomicts could coexist on an $L = 225$ lattice for upwards of 16000 generations, at least as long as an interglacial period. Similar long fixation times are expected in the IPS model above when parameters are close to the boundary between sexual and asexual fixation. It should be pointed out that although empirical measure-

ments estimate model parameters near this threshold ($\mu = 1.41$ (Kelley et al. 1988), $\nu < 1$ (Mogie 1992)), the behaviour of a model at or near a measure zero region of parameter space does not give a prediction that is likely to be robust across the varying life history parameters of the numerous species exhibiting geographic parthenogenesis. Nevertheless the slow movement of inter-conspecific boundaries is predicted by both continuum and discrete spatial models and this strengthens its claim as at least a strong component of the explanation.

Figure 5-18 includes the curve obtained numerically for the reaction-diffusion model in chapter 4 which separates parameters which predict advance and retreat of the sexual front. There is a good qualitative match in behaviour between simulations and the hydrodynamic limit approximation, with neither predicting bistability for the population as a whole. However, the curve does not quantatively match simulation results very closely. This is to be expected since rapid migration was absent from the simulations. Note also that the dynamics at the sexual-asexual boundary in the hydrodynamic limit are governed by the diffusion process, since:

$$\frac{\rho_B(x)}{\rho_C(x)} \approx \alpha,$$

in this region and so per capita growth of both classes is roughly equal. By contrast the dynamics at the boundary in the IPS model is governed entirely by local demographic interactions.

5.6 DISCUSSION

It is well known that discrete space models often predict behaviours absent from non-spatial state-variable models (Durrett & Levin 1994). In particular the literature abounds with discrete space models in which coexistence of competing types arises where non-spatial models predict it is impossible. Examples include: Fugitive coexistence of strong colonisers and strong competitors; Coexistence of multiple prey types, or predator types. But discrete space and local interactions should not be considered a panacea for coexistence. The modified predictions of discrete spatial models are subtly dependent on the sort of interactions between types. Durrett & Levin (1994) identify three cases: Mutualism, both species fitness is enhanced by the presence of the other; Competitive, both species can exist in isolation; Exploitative, one species can exist only in the presence of the other and has a negative effect on fitness. Coexistence between

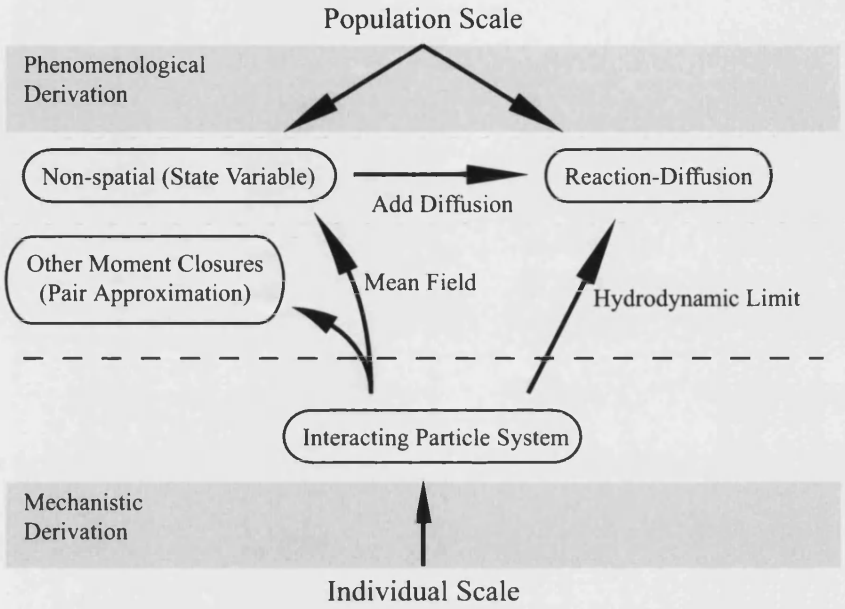

Figure 5-20: The links and correspondence between the different models derived and analysed in chapters 3, 4 and 5. For completeness higher order moment closure approximations of IPS have been included in anticipation of their introduction in chapter six.

mutualists is predicted across the board, in non-spatial, continuum and discrete spatial models. In competition models localization of interactions tends to erode the bistability found in non-spatial models. In an exploitative relationship, non-spatial models predict extinction whereas coexistence can occur in discrete space. Durrett and Levin used the simplest possible models that encapsulate these types of interaction, and in each case each species capable of persisting in isolation had a positive growth rate at low density. The inter-pollinating conspecific model approach, by contrast, produces models that, in the absence of space at least, feature strong Allee effects for monomorphic populations. Nevertheless the findings of Durrett and Levin are preserved in the cases of the competitive interaction of sexuals and asexuals and the exploitative interaction of female and hermaphrodites. Perhaps crucially the Allee effect itself is also effectively lost in the transition to discrete space.

This chapter has seen the equivalence between approximations to mechanistically derived individual-based discrete space models and the phenomenologically derived

population based models of both chapters 3 and 4. For reference Figure 5-20 illustrated these links.

CHAPTER 6

Pair Approximation

In this chapter a further approximation method applicable to IPS models is introduced. Pair approximation (PA) is a moment closure technique in the same spirit as the mean field approximation. Like the mean field, pair approximation is applicable to systems with or without exchange dynamics and does not require a particular choice of scaling. In fact pair approximation describes the general approach of approximating the behaviour of a stochastic system involving pair-wise interactions by deriving equations for the change in first *and* second moments and applying an approximation to achieve a closed system. An application of this approach to ecological IPS models was first proposed by Matsuda et al. (1992) and this choice of moment-closure approximation has since been widely used in spatial ecological applications (Iwasa et al. 1998, Satō 2000). It has proved successful in capturing aspects of simulation behaviour in IPS models missed by the mean field, particularly when the IPS features only flip dynamics (Iwasa et al. 1998) or flip dynamics and slow exchange dynamics (Harada et al. 1995). The moment closure approximation described by Matsuda et al. (1992) will be employed in this chapter and the qualitative similarities with simulation results will be highlighted.

6.1 DERIVATION

Pair Approximation Preliminaries

To use the PA approach for the IPS models presented in chapter 5, equations for the change in first and second moments are required. Equations for the development of first moments in a general inter-pollinating conspecifics model have already been derived in pursuit of the mean field approximations (5.2.4). The second moment equations describe the development of pairs of sites. To this end site-pair densities $\rho_{\sigma\sigma'}$ are defined for $\sigma, \sigma' \in S_0$, where S_0 is the set of all sub-states in the model. It is required

that

$$\rho_{\sigma\sigma'} = \rho_{\sigma'\sigma}, \tag{6.1.1a}$$

$$\sum_{\sigma\in S_0} \rho_{\sigma\sigma'} = \rho_{\sigma'}, \tag{6.1.1b}$$

so that $\rho_{\sigma\sigma'}$ is the probability for a randomly chosen pair of nearest neighbours that the first site chosen is in state σ and the chosen neighbour is in state σ'. The conditional neighbour probability $q_{\sigma/\sigma'}$ which was approximated by ρ_σ to obtain the mean field equations can now be given explicitly:

$$q_{\sigma/\sigma'} = \frac{\rho_{\sigma\sigma'}}{\rho_{\sigma'}}. \tag{6.1.2}$$

In the derivation of site-pair equations expressions will arise for the probability that the σ' cell of a $\sigma'\sigma''$ site-pair has a randomly chosen neighbour (apart from the other member of the pair) in state σ. This conditional probability is denoted $q_{\sigma/\sigma'\sigma''}$ and its precise value would depend upon the evolution of triplets, and triplet equations would depend on still higher order statistics. The PA consists in assuming all configurations of triplets are equivalent, and that:

$$q_{\sigma/\sigma'\sigma''} \approx q_{\sigma/\sigma'}. \tag{6.1.3}$$

This approximation is based on the intuition that because interactions are pair-wise the dynamic coupling between nearest neighbours are significantly more important to the behaviour of the IPS than coupling beyond the immediate neighbourhood (Matsuda et al. 1992).

General Inter-pollinating Conspecifics Pair Approximation

It is possible to derive site-pair equations for a general inter-pollinating conspecifics model with N classes. Stewart-Cox et al. (2004*b*) show how this is done in the absence of self-fertilization and vegetative reproduction processes. The resulting equations are not very illuminating because of the arsenal of notation required to identify each site-pair and the effects of flip dynamics on the pairs. It is more instructive to compose the site-pair equations as they are needed in the models examined below. This is also pragmatic because the three example models are arranged in a hierarchy of complexity

and tricks learnt from treating one model will prove useful in the assembly and analysis of the next.

Timescale Separation

The PA benefits greatly from the separation of pollination and colonization in the IPS. Since all interactions are pair-wise understanding changes in site-pairs is significantly more straight-forward. That is not to say that moment closure approximation is completely stymied by triplet processes, rather that it cannot proceed without additional definitions and assumptions. Consider the process of colonization. In the absence of timescale separation a colonization event occurs at an empty site if a neighbouring occupied site provides seed fertilized by pollen provided by one of its neighbours. Suppose sites with an occupied neighbour colonize neighbouring cells at a rate r/z. For an empty-occupied site-pair the per-capita rate at which the empty site gets colonized is the sum of two rates. The first is the rate at which the occupied site of the site-pair colonizes its empty neighbour:

$$\frac{r(z-1)}{z} q_{B/BA}.$$

There are $z-1$ neighbours of the occupied site other than the known empty site and the probability that one of these is occupied is $q_{B/BA}$. The second rate is the rate at which the empty site is colonized from outside the pair:

$$\frac{r(z-1)^2}{z} q_{BB/AB}.$$

There are $z-1$ neighbours of the empty site in the pair other than its known occupied neighbour and these neighbours have $z-1$ neighbours other than the empty site itself. The expression $q_{BB/AB}$ has been introduced to denote the probability that one of these neighbouring pairs of sites is an occupied pair. Concentrating on this second rate the neighbouring site pair probability can be broken down as follows:

$$q_{BB/AB} = \frac{\rho_{BBAB}}{\rho_{AB}} = \frac{q_{B/BAB}\rho_{BAB}}{\rho_{AB}} = q_{B/BAB}q_{B/AB},$$

extending the definitions of densities and neighbour probabilities naturally where necessary. The PA introduced above recommends that $q_{B/AB}$ be approximated by $q_{B/A}$ ignoring any longer range coupling. The same intuition might guide the approximation

of $q_{B/BAB}$ by $q_{B/B}$ with the result that:

$$q_{BB/AB} \approx q_{B/B}q_{B/A} = \frac{\rho_{BB}\rho_{AB}}{\rho_B\rho_A},$$

can now be given an approximate expression in terms of single and site-pair densities. Moment closure is therefore achievable with the extra assumption that $q_{\sigma/\sigma'\sigma''\sigma'''} \approx q_{\sigma/\sigma'}$. This seems an inexpensive assumption since information is already being ignored at ranges greater than immediate neighbourhoods but there is a problem. For many neighbourhood geometries the states of sites at either ends of a quadruplet will be far from independent, these sites may be neighbours themselves, or they may in fact be the same site. For almost any neighbourhood geometry with $z > 4$ imposed on a regular lattice, triangles of three interconnected sites occur. Thus the pollen providing neighbour of the colonizing site can be the occupied site in the empty occupied site-pair under consideration. It follows that if a neighbourhood geometry induces triangles then $q_{BB/AB}$ must be greater than $q_{BB/AA}$ or any $q_{BB/A\sigma}$ with $\sigma \neq B$. The proposed approximation violates this inequality since both expressions are approximated by $q_{B/B}q_{B/A}$. A more appropriate approximation might be devised by explicitly considering the number of triangles induced by the neighbourhood geometry. Timescale separation assumptions for pollination and colonization, however, allow these difficulties to be bypassed by splitting the triplet process into two pair-wise processes.

In defiance of these concerns, the simple approximation proposed above has attracted some success for processes involving triplet and its natural extension to longer chains of sites in applications to the prisoners' dilemma on a lattice (Nakamaru et al. 1997) (also Nakamaru et al. (1998).)

6.2 SEXUAL SPECIES

In this section a PA will be obtained for the sexual species IPS model of chapter 5 5.3. The PA will be analysed using a perturbation method which exploits the small parameter ϵ to obtain a dimensionally reduced model. This procedure and the analysis of the model obtained was first presented by Stewart-Cox et al. (2004*b*) in the context of a general PA framework for inter-pollinating conspecific IPS models and subsequently in more detail by Stewart-Cox et al. (2005*a*).

By inserting the appropriate parameters in the general state density equations (5.2.4) and applying the definition of local density in terms of site-pair densities (6.1.2)

the following single site density equations arise:

$$\begin{aligned}\epsilon\frac{d\rho_{B_0}}{dt} &= -p(\rho_{B_0B_0}+\rho_{B_0B_1})+\rho_{B_1}+\epsilon\left[b\rho_{AB_1}-\rho_{B_0}\right],\\ \epsilon\frac{d\rho_{B_1}}{dt} &= p(\rho_{B_0B_0}+\rho_{B_0B_1})-\rho_{B_1}+\epsilon\left[-\rho_{B_1}\right].\end{aligned} \tag{6.2.1}$$

These equations describe the way single site densities develop in terms of single site densities and site-pair densities. As before an equation describing the development of empty site density can be recovered by applying (5.2.3)a. Since there are three states in the sexual species model there are nine possible pairs of states (respecting order) and corresponding site-pair densities:

$$\begin{array}{ccc}\rho_{AA} & \rho_{AB_0} & \rho_{AB_1}\\ \rho_{B_0A} & \rho_{B_0B_0} & \rho_{B_0B_1}\\ \rho_{B_1A} & \rho_{B_1B_0} & \rho_{B_1B_1}\end{array}$$

Consulting (6.1.1)a the densities above the diagonal are each equal to one of the densities below. So one member of each of these pairs must be removed to make the collection of single and site-pair densities linearly independent. Also by (6.1.1)b, the sum of each of the above rows is equal to one of the single site densities so one density must be removed from each of the above rows. Making these deletions judiciously leaves ρ_{AB_0}, ρ_{AB_1} and $\rho_{B_0B_1}$, so to compose a complete set of site-pair equation the effect of the model's flip dynamics on AB_0, AB_1 and B_0B_1 pairs must be examined.

Empty-unpollinated pairs are created when: Pollen expires at the pollinated site of an AB_1 pair; The second empty site of an AA pair becomes colonized; A death occurs at the first site in a B_0B_0 or a B_1B_0 pair. The first process occurs at the per-pair pollen expiry rate $1/\epsilon$. The second process happens at a per-pair rate proportional to the number of neighbours $z-1$ (excluding the other member of the pair), the probability these neighbouring sites are pollinated $q_{B_1/AA}$ and the colonization rate b/z. The death processes happen at unit per-pair rate. The total rate at which ρ_{AB_0} increases due to these gains is therefore:

$$\frac{1}{\epsilon}\rho_{AB_1}+b\frac{z-1}{z}q_{B_1/AA}\rho_{AA}+\rho_{B_0B_0}+\rho_{B_1B_0}.$$

Empty-unpollinated pairs are lost when: The unpollinated site becomes pollinated; The empty site becomes colonized; The unpollinated site dies. The first process occurs

at a per-pair rate proportional the number of neighbours $z-1$, the probability these neighbours are either unpollinated or pollinated occupied sites $q_{B_0/AB_0} + q_{B_1/AB_1}$ and the pollination rate $p/\epsilon z$. As above the second process occurs at the per-pair rate $b(z-1)q_{B_1/AB_0}/z$. The death process happens at unit per-pair rate. The total rate at which ρ_{AB_0} decreases due to these losses is therefore:

$$\left(\frac{p}{\epsilon}\frac{z-1}{z}(q_{B_1/B_0A} + q_{B_0/B_0A}) + b\frac{z-1}{z}q_{B_1/AB_0} + 1\right)\rho_{AB_0}.$$

Similar considerations inform the composition of the rates of change for AB_1 and B_0B_1 site-pairs. The resulting site-pair equations are:

$$\begin{aligned}
\epsilon\frac{d\rho_{AB_0}}{dt} &= -p\tfrac{z-1}{z}(q_{B_1/B_0A} + q_{B_0/B_0A})\rho_{AB_0} + \rho_{AB_1} \\
&\quad + \epsilon\left[b\tfrac{z-1}{z}(q_{B_1/AA}\rho_{AA} - q_{B_1/AB_0}\rho_{AB_0}) + \rho_{B_0B_0} + \rho_{B_1B_0} - \rho_{AB_0}\right], \\
\epsilon\frac{d\rho_{AB_1}}{dt} &= p\tfrac{z-1}{z}(q_{B_1/B_0A} + q_{B_0/B_0A})\rho_{AB_0} - \rho_{AB_1} \\
&\quad + \epsilon\left[b\left(\tfrac{1}{z} + \tfrac{z-1}{z}q_{B_1/AB_1}\right)\rho_{AB_1} + \rho_{B_0B_1} + \rho_{B_1B_1} - \rho_{AB_1}\right], \\
\epsilon\frac{d\rho_{B_0B_1}}{dt} &= p\tfrac{z-1}{z}\left(q_{B_0/B_0B_0} + q_{B_1/B_0B_0}\right)\rho_{B_0B_0} - p\left(\tfrac{1}{z} + \tfrac{z-1}{z}(q_{B_0/B_0B_1} + q_{B_1/B_0B_1})\right)\rho_{B_0B_1} \\
&\quad + \rho_{B_1B_1} - \rho_{B_0B_1} + \epsilon\left[b\left(\tfrac{1}{z} + \tfrac{z-1}{z}q_{B_1/AB_1}\right)\rho_{AB_1} - 2\rho_{B_0B_1}\right].
\end{aligned} \tag{6.2.2}$$

In combination (6.2.1) and (6.2.2) describe the development of the first and second moments of the sexual species IPS model. The PA (6.1.3) can be applied to obtain a closed system which approximates the IPS model. This five-dimensional system can be simplified to a two-dimensional system in the limit of small ϵ. As with the mean field approximations of chapter 5, this simplified system describes the development of single site and site-pair densities that are sums of the sub-state densities described in the full system, these are referred to as aggregated variables. The aggregated system is obtained by considering the first term of the outer asymptotic expansion about a quasi-equilibrium found by considering only fast events.

Fast Equilibrium

Define a fast timescale $\tau = t/\epsilon$ and aggregated variables $\rho_B = \rho_{B_0} + \rho_{B_1}$ and $\rho_{B\sigma} = \rho_{B_0\sigma} + \rho_{B_1\sigma}$ for $\sigma \in \mathcal{S}_1 = \{A, B, B_0, B_1\}$. Note from (6.2.1) that it is still the case that:

$$\frac{d\rho_B}{d\tau} = \frac{d\rho_{B_0}}{d\tau} + \frac{d\rho_{B_1}}{d\tau} = O(\epsilon),$$

as with the mean field and also:

$$\frac{d\rho_{AB}}{d\tau} = \frac{d\rho_{AB_0}}{d\tau} + \frac{d\rho_{AB_1}}{d\tau} = O(\epsilon),$$
$$\frac{d\rho_{BB}}{d\tau} = \frac{d\rho_{BB_0}}{d\tau} + \frac{d\rho_{BB_1}}{d\tau} = O(\epsilon),$$

so that, as might be expected, for states $\sigma \in \{A, B\}$ neither single site densities nor site-pair densities change on the fast timescale. A system featuring only fast events is obtained by rescaling to the fast timescale and neglecting terms of order ϵ:

$$\frac{d\rho_{B_0}}{d\tau} = -p\rho_{B_0B} + \rho_{B_1}, \tag{6.2.3a}$$
$$\frac{d\rho_{B_1}}{d\tau} = p\rho_{B_0B} - \rho_{B_1}, \tag{6.2.3b}$$
$$\frac{d\rho_{AB_0}}{d\tau} = -p\tfrac{z-1}{z}q_{B/B_0}\rho_{AB_0} + \rho_{AB_1}, \tag{6.2.3c}$$
$$\frac{d\rho_{AB_1}}{d\tau} = p\tfrac{z-1}{z}q_{B/B_0}\rho_{AB_0} - \rho_{AB_1}, \tag{6.2.3d}$$
$$\frac{d\rho_{B_0B_1}}{d\tau} = p\tfrac{z-1}{z}q_{B/B_0}\rho_{B_0B_0} - p\left(\tfrac{1}{z} + \tfrac{z-1}{z}q_{B/B_0}\right)\rho_{B_0B_1} + \rho_{B_1B_1} - \rho_{B_0B_1}, \tag{6.2.3e}$$

In (6.2.3) equations (a) and (b) sum to zero, as do equations (c) and (d), so one of each must be removed to form a linearly independent system. In the resulting system:

$$\frac{d\rho_{B_0}}{d\tau} = p(\rho_{B_0} - \rho_{AB_0}) - (\rho_B - \rho_{B_0}), \tag{6.2.4a}$$
$$\frac{d\rho_{AB_0}}{d\tau} = p\tfrac{z-1}{z}(1 - q_{A/B_0})\rho_{AB_0} - (\rho_{AB} - \rho_{AB_0}), \tag{6.2.4b}$$
$$\frac{d\rho_{B_0B_1}}{d\tau} = p\tfrac{z-1}{z}(1 - q_{A/B_0})(\rho_{B_0} - \rho_{AB_0} - 2\rho_{B_0B_1}) - (2 + \tfrac{p}{z})\rho_{B_0B_1} + \rho_{BB} - \rho_{B_0} + \rho_{AB_0}. \tag{6.2.4c}$$

equations (a) and (b) form an independent system decoupled from equation (c). The variables of the independent system are constrained by the inequalities:

$$\rho_{AB_0} \leq \rho_{B_0} \leq \rho_B \text{ and } \rho_{B_0} - \rho_{BB} \leq \rho_{AB_0} \leq \rho_{AB},$$

which demand that all single and site-pair densities are positive. Thus the region of interest for this system is the parallelogram with vertices $(0,0)$, $(\rho_{BB},0)$, (ρ_{AB},ρ_{AB}) and (ρ_B,ρ_{AB}) in (ρ_{B_0},ρ_{AB_0})-space. The region of interest is invariant under the fast system. The independent system has one equilibrium $(\tilde{\rho}_{B_0},\tilde{\rho}_{AB_0})$, which is asymptotically stable over the region of interest (by virtue of being the only equilibrium in an invariant compact set) and is given by:

$$\begin{aligned}\tilde{\rho}_{B_0} &= \rho_B - \tilde{\rho}_{B_1},\\ \tilde{\rho}_{AB_0} &= \rho_B - \rho_{BB} - \tilde{\rho}_{AB_1},\end{aligned}$$

where the equilibria have been expressed in terms of $\tilde{\rho}_{B_1}$ and $\tilde{\rho}_{AB_1}$ because these quantities are required directly in the aggregated model.

$$\begin{aligned}\tilde{\rho}_{B_1} &= \frac{(p+z)\rho_B + zp\rho_{BB}}{2(p+1)} - \sqrt{\left(\frac{(p+z)\rho_B + pz\rho_{BB}}{2(p+1)}\right)^2 - \frac{pz\rho_B\rho_{BB}}{p+1}},\\ \tilde{\rho}_{AB_1} &= \frac{p+1}{p}\tilde{\rho}_{B_1} - \rho_{BB},\end{aligned} \tag{6.2.5}$$

Note that the fast equilibrium has been specified here as a function of ρ_B and ρ_{BB} which are fixed quantities on the fast timescale. The expression for $\tilde{\rho}_{B_1}$ is an increasing saturating functional response to the availability of pollen. On a lattice it is the local availability of pollen to individuals that determines the probability of being pollinated and the PA respects this. Thus the proportion of pollinated individuals in the population depends only on the local density $q_{B/B}$, that is:

$$\frac{\tilde{\rho}_{B_1}}{\rho_B} = \Pi(q_{B/B}) = \frac{p+z+zpq_{B/B}}{2(p+1)} - \sqrt{\left(\frac{p+z+pzq_{B/B}}{2(p+1)}\right)^2 - \frac{pzq_{B/B}}{p+1}}. \tag{6.2.6}$$

The function $\Pi : [0,1] \to [0,1]$ is the PA for a Holling type II response on a regular lattice with neighbourhood size z. In fact for the purposes of the models in this chapter Π is quite generic and will appear several times.

The remaining dependent system 6.2.4c can be solved in the light of (6.2.5) and

incorporated into the full fast equilibrium:

$$\tilde{\rho} = (\tilde{\rho}_{B_0}, \tilde{\rho}_{B_1}, \tilde{\rho}_{AB_0}, \tilde{\rho}_{AB_1}, \tilde{\rho}_{B_0B_1}). \tag{6.2.7}$$

As before it is vital that the fast equilibrium is unique and asymptotically attracting, so that branch-switching behaviour is absent from the original system.

Aggregated Dynamics

The first term of the outer asymptotic expansion of the original system ((6.2.1) and (6.2.2) under 6.1.3) about (6.2.7) gives the system:

$$\begin{aligned}
\frac{d\rho_{B_0}}{dt} &= b\tilde{\rho}_{AB_1} - \rho_{B_0}, \\
\frac{d\rho_{B_1}}{dt} &= -\rho_{B_1}, \\
\frac{d\rho_{AB_0}}{dt} &= \frac{b(z-1)\tilde{\rho}_{AB_1}(\rho_{AA} - \rho_{AB_0})}{z\rho_A} + \rho_{B_0} - 2\rho_{AB_0}, \\
\frac{d\rho_{AB_1}}{dt} &= -\frac{b(\rho_A + (z-1)\tilde{\rho}_{AB_1})\rho_{AB_1}}{z\rho_A} + \rho_{B_1} - 2\rho_{AB_1}, \\
\frac{d\rho_{B_0B_1}}{dt} &= \frac{b(\rho_A + (z-1)\tilde{\rho}_{AB_1})\rho_{AB_1}}{z\rho_A} - 2\rho_{B_0B_1}.
\end{aligned} \tag{6.2.8}$$

Closed equations in the aggregated variables ρ_B ad ρ_{BB} are obtained with linear combinations from (6.2.8):

$$\begin{aligned}
\frac{d\rho_B}{dt} &= b\tilde{\rho}_{AB_1} - \rho_B, \\
\frac{d\rho_{BB}}{dt} &= \frac{2b(z(\rho_B - \rho_{BB}) + 1 - 2\rho_B + \rho_{BB})\tilde{\rho}_{AB_1}}{z(1-\rho_B)} - 2\rho_{BB},
\end{aligned}$$

Thus a system is obtained which describes the population density and autocorrelation of occupied sites. All single site and site-pair densities remain non-negative so long as

$$2\rho_B - 1 \leq \rho_{BB} \leq \rho_B.$$

The region of interest Δ on the (ρ_B, ρ_{BB})-plane is therefore the triangle with vertices $(0,0)$, $(\frac{1}{2},0)$ and $(1,1)$. Taking $\dot{\rho}_B = 0$ yields the nullcline $\rho_B = 0$ outside the region of

interest and two linear nullclines given by:

$$f_B^{\pm}(\rho_B) = \frac{\rho_B}{2}\left(1 - \frac{z-2}{b(z-1)} \pm \sqrt{\left(1 - \frac{z-2}{b(z-1)}\right)^2 - \frac{4z}{bp(z-1)} - \frac{4(b-1)}{b^2(z-1)}}\right).$$

Taking $\dot{\rho}_{BB} = 0$ yields two nullclines: the first is $\rho_{BB} = 0$. The remaining nullcline is obtained by solving a cubic in ρ_B:

$$\begin{aligned} &\rho_{BB}^3 - (2(2\rho_B - 1) + K_1(1-\rho_B))\rho_{BB}^2 \\ &+((2\rho_B-1)^2 + (1-\rho_B)((2K_1 - K_2 + K_3)\rho_B - K_1 - K_3))\rho_{BB} \\ &+\rho_1(1-\rho_B)((2K_2 - K_3)\rho_1 - K_2 + K_3) = 0, \end{aligned} \tag{6.2.9}$$

where

$$K_1 = \frac{z(z-2)}{b(z-1)^2}, \quad K_2 = \frac{z(z+p)}{bp(z-1)^2}, \quad K_3 = \frac{z^2}{b^2(z-1)^3}.$$

To be valid nullclines the roots of (6.2.9) must satisfy the following condition:

$$\begin{aligned} &\rho_{BB}^2 + \left(1 - 2\rho_B + \frac{(p+z)\rho_B}{p(z-2)} + \frac{2z(1-\rho_B)}{b(z-1)(z-2)}\right)\rho_{BB} \\ &+\left(\frac{(p+z)(1-2\rho_B)}{p(z-2)} - \frac{2z(1-\rho_B)}{b(z-1)(z-2)}\right)\rho_B \geq 0. \end{aligned} \tag{6.2.10}$$

In fact all the roots of (6.2.9) are real but only one, f_{BB}, satisfies this condition. From (6.2.9) and (6.2.10) it is readily deduced that $f_{BB}(0) = 0$ and $f_{BB}(1) = 1$. Clearly then the origin is an equilibrium and whether or not f_B^+ and f_B^- intersect f_{BB} elsewhere on $[0,1]$ depends only on the gradients of these functions at the origin. Consequently up to two non-trivial equilibria may occur in $\triangle$: A stable node that attracts local orbits; and a saddle, the stable manifold of which divides $\triangle$ into basins of attraction for the non-trivial stable node and the origin. These basins can be considered survival and extinction zones. The equilibria of the aggregated dynamics can be directly computed because (6.2.9) indicates that equilibria must occur on:

$$\rho_{BB} = \frac{\rho_B((z-2)\rho_B + 1)}{z - \rho_B}. \tag{6.2.11}$$

The non-trivial equilibria are given by:

$$\hat{\rho}_B^{\pm} = \frac{1 - z\alpha^{\pm}}{2 - z - \alpha^{\pm}}, \tag{6.2.12}$$

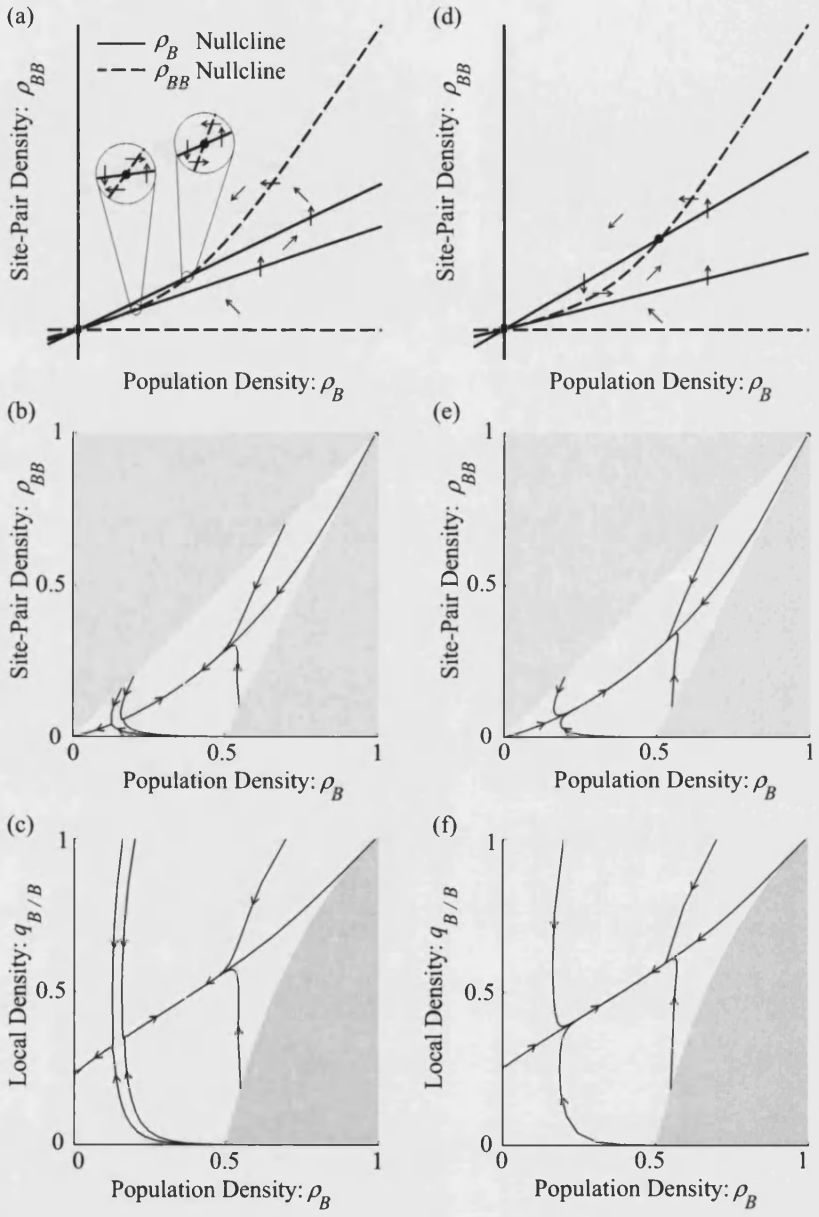

Figure 6-1: Nullclines and sample solutions of the aggregated dynamics for the PA of the sexual species IPS. Grey regions indicate the constraints on ρ_{BB} and $q_{B/B}$. Parameters $z = 4$. (a)-(c) $p = 3.7$, $b = 3.7$. (d)-(f) $p = 4.0$, $b = 4.0$.

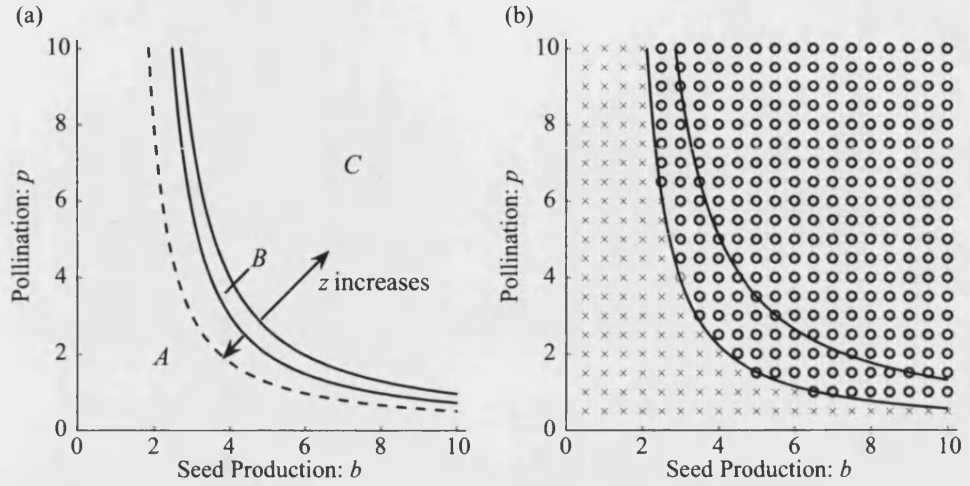

Figure 6-2: (p, b) - parameter space for the aggregated dynamics for the PA of the sexual species IPS. (a) Parameter space is divided in three regions: A - Extinction $p \leq p_{\text{crit}}$; B - Conditional survival dependent on initial conditions $p_{\text{crit}} < p \leq p_{\text{trans}}$; C - Unconditional survival $p > p_{\text{trans}}$. Neighbourhood size $z = 4$. Dashed curve recalls the mean field boundary between extinction and conditional survival. (b) Parameter space comparison between PA and simulations with neighbourhood size $z = 8$. Black circles indicate unconditional survival and grey circles indicate conditional survival in simulations. c.f. Figure 5-3.

where $\alpha^{\pm} = f_B^{\pm}(\rho_B)/\rho_B$ and so $\hat{\rho}_{BB}^{\pm} = \alpha^{\pm}\hat{\rho}_B^{\pm}$.

Nullclines and sample solution are presented in Figures 6-1(a)-(f). Sample solutions have been plotted in (ρ_B, ρ_{BB}) phase space and also in $(\rho_B, q_{B/B})$ phase space. The latter is provided for comparison with the corresponding simulation plots in Figures 5-7(a)-(b). For the PA $(\rho_B, q_{B/B})$ phase space is constrained in a similar way to the finite lattice simulations of the IPS. The local density $q_{B/B}$ must exceed $2 - 1/\rho_B$. The upper bound for $q_{B/B}$ is 1 in the PA which matches the upper bound on the IPS in the limit of large lattice size. Note that in Figures 6-1(a)-(c) two non-trivial equilibria occur in the region of interest, but for the higher reproductive parameters in Figures 6-1(d)-(f) only one appears.

For $b > z/(z-1)$ this model undergoes a saddle-node bifurcation when $f_B^+ = f_B^-$, that is when $p = p_{\text{crit}}$ where:

$$p_{\text{crit}} = \frac{4bz(z-1)}{(b(z-1)-z)^2}. \tag{6.2.13}$$

For p smaller than p_{crit} the two non-trivial equilibria disappear, and the model predicts extinction for all initial conditions. Note that $p_{\text{crit}} \to 4b/(b-1)^2$ as $z \to \infty$, which recovers the corresponding critical value in the mean field model. The model undergoes a transcritical bifurcation when $\alpha^- = 1/z$, at this point $\hat{\rho}_B^- = 0$, and the basin of attraction for $(\hat{\rho}_B^+, \hat{\rho}_{BB}^+)$ becomes the whole of $\triangle$. This occurs so long as $b > z/(z-1)$ when $p = p_{\text{trans}}$ where:

$$p_{\text{trans}} = \frac{bz^3}{(b(z-1)-z)^2}. \tag{6.2.14}$$

For $p > p_{\text{trans}}$ the model predicts survival for all initial conditions in the interior of $\triangle$ since $\hat{\rho}_B^- < 0$. It is straight forward to see that $p_{\text{crit}} < p_{\text{trans}}$ so long as $z > 2$ and that $p_{\text{trans}} \to \infty$ as $z \to \infty$. The relationships 6.2.13 and 6.2.14 divide (b,p)-parameter space into three regions: An extinction region where survival is impossible for all initial conditions; A region of survival conditional on initial conditions and a region of unconditional survival. Figure 6-2(a) illustrates parameter space for the aggregated dynamics and also indicates limiting values of p_{crit} obtained in the mean field approximation. Figure 6-2(b) superimposes the parameter space of the aggregated dynamic over that obtained by simulation in chapter 5. The loss of the strong Allee effect in the PA qualitatively matches the lack of appreciable Allee effect in simulations of the IPS. Also the PA predicts with greater accuracy than the mean field approximation when populations are viable in the IPS model. Simulations and the small cluster dynamics examined in chapter 5 suggested that if reproductive parameters are large enough for a large population to be sustained then they are also large enough for an arbitrarily small population to establish. The PA does not quite match this result, predicting instead that a strong Allee effect still operates in a non-trivial region of parameter space.

Insight into precisely why the strong Allee effect is lost in the PA can be gained by considering invasion trajectories. Direct analysis of the $(0,0)$ equilibrium by linearization is not possible, because the partial derivatives:

$$\begin{aligned}
\frac{\partial \tilde{\rho}_{AB_1}}{\partial \rho_B} &= \frac{(p+1)(pz\rho_{BB} - (p+z)\tilde{\rho}_{B_1})}{p\sqrt{((p+z)\rho_B + pz\rho_{BB})^2 - 4p(p+1)z\rho_B\rho_{BB}}}, \\
\frac{\partial \tilde{\rho}_{AB_1}}{\partial \rho_{BB}} &= \frac{(p+1)z(\rho_B - \tilde{\rho}_{B_1})}{\sqrt{((p+z)\rho_B + pz\rho_{BB})^2 - 4p(p+1)z\rho_B\rho_{BB}}} - 1,
\end{aligned}$$

are undefined at $(0,0)$. However, these derivatives are always defined for the $(\hat{\rho}_B^-, \hat{\rho}_{BB}^-)$ equilibrium, because $\hat{\rho}_{BB}^- = \alpha^- \hat{\rho}_B^-$. So linearization is possible about the origin at the

bifurcation point $p = p_{\text{trans}}$. The Jacobian J at the origin is given by:

$$J = \begin{pmatrix} b\frac{\partial \hat{\rho}_{AB_1}}{\partial \rho_B} - 1 & b\frac{\partial \hat{\rho}_{AB_1}}{\partial \rho_{BB}} \\ \frac{2b}{z}\frac{\partial \hat{\rho}_{AB_1}}{\partial \rho_B} & \frac{2b}{z}\frac{\partial \hat{\rho}_{AB_1}}{\partial \rho_B} - 2 \end{pmatrix}.$$

Since $p = p_{\text{trans}}$ is a transcritical bifurcation point: $\det J = 0$, and eigenvalues are $\lambda_0 = 0$ and $\lambda_1 = 2\text{tr}J$. The gradients g_0 and g_1 of the associated eigenvectors e_0 and e_1 are given by:

$$g_0 = \frac{1 - b\frac{\partial \hat{\rho}_{AB_1}}{\partial \rho_B}}{b\frac{\partial \hat{\rho}_{AB_1}}{\partial \rho_{BB}}} = \frac{1}{z} \quad \text{and} \quad g_1 = \frac{bz\frac{\partial \hat{\rho}_{AB_1}}{\partial \rho_B} + 4b\frac{\partial \hat{\rho}_{AB_1}}{\partial \rho_{BB}} - 5z}{bz\frac{\partial \hat{\rho}_{AB_1}}{\partial \rho_{BB}}} = \frac{-bz - 2b - 4z}{bz(z-1)}.$$

By centre manifold theory a centre manifold must pass through the origin tangent to e_0, which has a strictly positive gradient. An invasion from an arbitrarily small initial density will follow the centre manifold.

The invasion trajectory can be investigated further following the reasoning of Matsuda et al. (1992). On the verge of invasion, when population density ρ_B is very small, the neighbourhood density $q_{B/B}$ should reach a quasi-equilibrium before ρ_B changes significantly. To obtain the dynamics of $q_{B/B}$ on the verge of invasion observe that:

$$\begin{aligned} \frac{dq_{B/B}}{dt} &= \frac{1}{\rho_B}\frac{d\rho_{BB}}{dt} - \frac{q_{B/B}}{\rho_B}\frac{d\rho_B}{dt} \\ &= \frac{b(2zq_{B/A} + 2q_{A/A} - zq_{B/B})\hat{\rho}_{AB_1}}{z\rho_B} - q_{B/B}, \end{aligned}$$

and recognise that $\rho_B \approx 0$ implies that $q_{B/A} \approx 0$ and $q_{A/A} \approx 1$. It is also clear from (6.2.6) and (6.2.5) that $\hat{\rho}_{AB_1}/\rho_B$ depends only on $q_{B/B}$. The dynamics of $q_{B/B}$ when $\rho_B \approx 0$ are therefore given by:

$$\begin{aligned} \frac{dq_{B/B}}{dt} = b(2 - zq_{B/B})\Bigg[&\frac{p + z + p(z-2)q_{B/B}}{2pz} \\ &- \frac{\sqrt{(p + z + pzq_{B/B})^2 - 4p(p+1)zq_{B/B}}}{2pz}\Bigg] - q_{B/B}. \end{aligned} \tag{6.2.15}$$

Equation (6.2.15) has two equilibria in the region of interest, $q_{B/B} = 0$ and the smallest

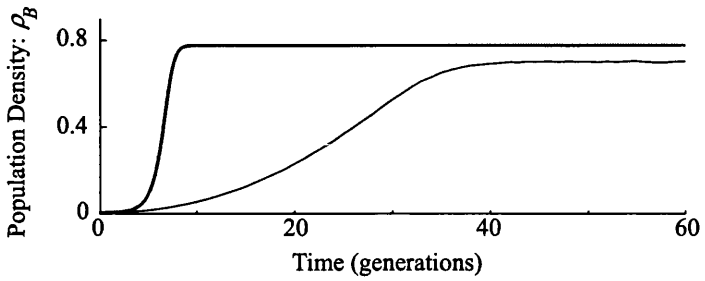

Figure 6-3: Comparison between PA (bold curve) and simulation for the predicted growth of an establishing population. Simulation plot is an average of ten simulations on an $L = 100$ lattice using the pollination equilibrium. Parameters: $b = 6$, $p = 6$, $z = 4$.

root of:

$$\begin{aligned} b^2pz^2(1-z)q_{B/B}^3 + bpz((b+1)z^3 - 4b + 3bz - 2z)q_{B/B}^2 \\ +(4b^2p(1-z^2) + bpz(4-z) + (bz+p)z^2)q_{B/B} \\ +4b^2(p+1)z - 2b(2b+z)(p+z) = 0, \end{aligned} \tag{6.2.16}$$

denoted by $\check{q}_{B/B}$ and which satisfies:

$$\check{q}_{B/B} \geq \frac{b(p-z)z - 2p(z+2)}{2pz(2-bz)} + \sqrt{\left(\frac{b(p-z)z - 2p(z+2)}{2pz(2-bz)}\right)^2 - \frac{2b(p+z)}{pz(2-bz)}}.$$

$\check{q}_{B/B}$ increases monotonically with p and $\check{q}_{B/B} = 1/z$ when $p = p_{\text{trans}}$ upholding the result obtained above with centre manifold theory ($\check{q}_{B/B}$ also increases monotonically with b and decreases monotonically with z.) The criterion for invasion from arbitrarily small numbers to be viable, is that reproductive output of pollen and seeds must be high enough that a contact rate of at least ρ_B/z is established. At this threshold of the reproductive rates the strong Allee effect disappears and the trivial equilibrium becomes unstable, so that any initial configuration of individuals with $\rho_{BB} > 0$ results in population establishment.

Discussion

The single most interesting property of the IPS model that was absent from the mean field approximation was that very small populations could become established despite

the dependence of reproduction on contact with other individuals. It is satisfying that the PA captures this feature and provides an explanation: The strong Allee effect is lost because when pollen and seed dispersal are local the contact rate between individuals ρ_{BB} scales linearly with population size. By contrast the mean field assumes $\rho_{BB} = \rho_B^2$, that the contact rate scales quadratically. It is the discrepancy in the initial order of magnitude of ρ_{BB} that permits invasion from arbitrarily small numbers in the PA when it could not occur in the mean field. But the accuracy of the PA should not be overstated, Figure 6-3 compares simulated population growth with that predicted by the PA. The simulation was initiated with a cluster of five occupied sites in a cross shape and the initial conditions for the PA extracted from this configuration:

$$\rho_B(0) = \frac{5}{L^2}, \quad \rho_{BB}(0) = \frac{4}{zL^2}.$$

Since $p > p_{\text{trans}}$ both PA and simulations predict population establishment but growth in the PA is much more rapid and the population achieves a greater density at equilibrium. Growth in the PA is not as rapid as the mean field predicts (for initial populations exceeding the Allee threshold) and equilibrium density is closer to that seen in simulations (c.f. Figure 5-11.) This relationship between mean field, PA and simulation is frequently observed (Iwasa 2000). In general the PA fits simulation better than the mean field because it acknowledges the increased competition experienced by individuals in clustered populations. This slows population growth, but the effect of clustering is underestimated (van Baalen 2000) and initial growth remains exponential rather than parabolic.

The PA identifies two phenomena not found in the mean field and present to a greater or lesser extent in simulations. The first in the region of parameter space where population survival is unconditional so long as $q_{B/B} > 0$. The second highlights the importance of spatial configuration for the survival of locally interacting populations. When survival depends on initial conditions, there is a threshold population density below which extinction is certain. Above this density survival is subject to configurational constraints: If the population is too sparse or if the population is too clustered extinction is possible for initial population densities in excess of the threshold density. This constitutes, however, a greater sensitivity to configuration than is seen in simulation of the IPS, where constraints on population survival are conjectured to be minimal ($q_{B/B} > 0$) for all reproductive parameters that yield viable populations.

The IPS models of chapter 5 and the PA in this chapter have made the simplifying

assumption that neighbourhood sizes of pollen and seed dispersal are the same. This is scarcely likely to be the case in real populations because mechanisms of dispersal will usually differ. If mechanisms do not differ, if both pollen and seed are wind dispersed as in some grasses for example, the physiological characteristics of pollen and seed, their weight and longevity, will surely result in different mean dispersal distances. Different neighbourhood sizes are straightforward to implement in simulations and have no effect on the mean field approximations, but they would present a difficulty for pair approximation. Ellner (2001) provides a solution that permits the introduction of different finite neighbourhood sizes for different processes, at the expense of increasing the complexity and the number of equations of the PA. An alternative that requires only one neighbourhood size and in fact tends to simplify the PA was considered by Stewart-Cox et al. (2005*a*). If the neighbourhood size of one process is very much greater than that of the other, it may be reasonable to consider the large neighbourhood process as an interaction with the entire lattice while the smaller neighbourhood process remains local. Stewart-Cox et al. (2005*a*) found that if pollen is dispersed everywhere on the lattice while seed is dispersed only in a local neighbourhood the resulting PA predicts a strong Allee effect for all parameters yielding viable populations. Populations grow as clusters but have no greater access to pollen than randomly dispersed populations. The likelihood of pollination scales with ρ_B^2 as in the mean field. If pollen is dispersed locally while seeds are dispersed everywhere on the lattice, the strong Allee effect again persists for all parameters. In this case populations do not grow as clusters and, although the functional response differs, the likelihood of pollination still scales with ρ_B^2 because occupied sites are much less likely to be neighbours. Stewart-Cox et al. (2005*a*) also examined models in which pollen or seed dispersal was partially local, with some remaining in a local neighbourhood and the rest dispersed everywhere on the lattice. In both the case of mixed range pollen dispersal and local seed dispersal, and local seed dispersal and mixed range pollen dispersal the strong Allee effect was found to disappear, but at a higher threshold than before. It was concluded that both pollen and seed dispersal need to be at least partially local and reproductive effort must be high for the Allee effect to be lost. This combination leads to a self-regulating clumped invasion where small populations can have sufficiently high contact rates to ensure population growth. Long range pollen and seed dispersal can be positively beneficial for larger populations allowing re-establishment if, for instance, environmental fluctuations leave a population overly clumped or overly diffuse.

6.3 GYNODIOECY

In this section a PA is obtained for the gynodioecy IPS model proposed in chapter 5 section 5.4. Again the PA will be analysed using a perturbation method which exploits the small parameter ϵ to obtain a dimensionally reduced model. This procedure and the analysis of the model obtained was first presented by Stewart-Cox et al. (2005*b*).

By inserting the appropriate parameters in the general state density equations (5.2.4) and applying the definition of local density in terms of site-pair densities (6.1.2) the following single site density equations arise:

$$\begin{aligned}
\epsilon\frac{d\rho_{B_0}}{dt} &= -p(\rho_{B_0B_0}+\rho_{B_0B_1})+\rho_{B_1}+\epsilon\left[b\rho_{AB_1}-\rho_{B_0}\right],\\
\epsilon\frac{d\rho_{B_1}}{dt} &= p(\rho_{B_0B_0}+\rho_{B_0B_1})-\rho_{B_1}+\epsilon\left[-\rho_{B_1}\right],\\
\epsilon\frac{d\rho_{C_0}}{dt} &= -p(\rho_{B_0C_0}+\rho_{B_1C_0})+\rho_{C_1}+\epsilon\left[\mu b\rho_{AC_1}-\rho_{C_0}\right],\\
\epsilon\frac{d\rho_{C_1}}{dt} &= p(\rho_{B_0C_0}+\rho_{B_1C_0})-\rho_{C_1}+\epsilon\left[-\rho_{C_1}\right].
\end{aligned} \tag{6.3.1}$$

These equations describe the way single site densities develop in terms of single site densities and site-pair densities. There are 25 possible pairs of states (respecting order) and corresponding site-pair densities:

$$\begin{array}{ccccc}
\rho_{AA} & \rho_{AB_0} & \rho_{AB_1} & \rho_{AC_0} & \rho_{AC_1}\\
\rho_{B_0A} & \rho_{B_0B_0} & \rho_{B_0B_1} & \rho_{B_0C_0} & \rho_{B_0C_1}\\
\rho_{B_1A} & \rho_{B_1B_0} & \rho_{B_1B_1} & \rho_{B_1C_0} & \rho_{B_1C_1}\\
\rho_{C_0A} & \rho_{C_0B_0} & \rho_{C_0B_1} & \rho_{C_0C_0} & \rho_{C_0C_1}\\
\rho_{C_1A} & \rho_{C_1B_0} & \rho_{C_1B_1} & \rho_{C_1C_0} & \rho_{C_1C_1}
\end{array}$$

A linearly independent set of variables includes only those above the diagonal. Equations for the development of these pair are derived along the same lines as the sexual species model. Consider for example an pollinated hermaphrodite - unpollinated female, B_1C_0 site-pair. Such site-pairs are created when: The unpollinated hermaphrodite site of a B_0C_0 site-pair becomes pollinated; Pollen expires at the female site of a B_1C_1 site-pair or the empty site of an AB_1 site-pair is colonized by a female. Following very similar reasoning to the sexual species model above the total rate at

which $\rho_{B_1C_0}$ increases due to these gains is:

$$\frac{p}{\epsilon}\frac{z-1}{z}(q_{B_0/B_0C_0}+q_{B_1/B_0C_0})\rho_{B_0C_0}+\frac{1}{\epsilon}\rho_{B_1C_1}+\mu b\frac{z-1}{z}q_{C_1/AB_1}.$$

B_1C_0 site-pairs are lost when: The unpollinated female site becomes pollinated; Pollen expires at the pollinated hermaphrodite site or either site dies. In the first case pollen comes from the hermaphrodite in the pair at rate $p/\epsilon z$ and from outside the pair at rate proportional to $p/\epsilon z$ and the number of hermaphrodite neighbours $(z-1)(q_{B_0/C_0B_0}+q_{B_1/C_0B_0})$. The total rate at which $\rho_{B_1C_0}$ decreases due to these losses is:

$$\left(\frac{p}{\epsilon}\left(\frac{1}{z}+\frac{z-1}{z}(q_{B_0/C_0B_0}+q_{B_1/C_0B_0})\right)+\frac{1}{\epsilon}+2\right)\rho_{B_1C_0}.$$

Before the site-pair equations are presented note that empty sites arise from the death of any of the four occupied states, so any site-pair with an empty site will increase in frequency as a result of these deaths at rate:

$$\rho_{\sigma B_0}+\rho_{\sigma B_1}+\rho_{\sigma C_0}+\rho_{\sigma C_1},$$

where σ is the state of the other site in the pair. This is more conveniently expressed in the following equations as:

$$\rho_\sigma-\rho_{\sigma A}.$$

The site-pair equations are:

$$\begin{aligned}
\epsilon\frac{d\rho_{AB_0}}{dt} &= -p\tfrac{z-1}{z}(q_{B_0/B_0A}+q_{B_1/B_0A})\rho_{AB_0}+\rho_{AB_1}\\
&\quad+\epsilon\left[b\tfrac{z-1}{z}\left(q_{B_1/AA}\rho_{AA}-(q_{B_1/AB_0}+\mu q_{C_1/AB_0})\rho_{AB_0}\right)+\rho_{B_0}-2\rho_{AB_0}\right],\\
\epsilon\frac{d\rho_{AB_1}}{dt} &= p\tfrac{z-1}{z}(q_{B_0/B_0A}+q_{B_1/B_0A})\rho_{AB_0}-\rho_{AB_1}\\
&\quad+\epsilon\left[-b\left(\tfrac{1}{z}+\tfrac{z-1}{z}(q_{B_1/AB_1}+\mu q_{C_1/AB_1})\right)\rho_{AB_1}+\rho_{B_1}-2\rho_{AB_1}\right],\\
\epsilon\frac{d\rho_{AC_0}}{dt} &= -p\tfrac{z-1}{z}(q_{B_0/C_0A}+q_{B_1/C_0A})\rho_{AC_0}+\rho_{AC_1}\\
&\quad+\epsilon\left[b\tfrac{z-1}{z}(\mu q_{C_1/AA}\rho_{AA}-(q_{B_1/AB_0}+\mu q_{C_1/AB_0})\rho_{AC_0})+\rho_{C_0}-2\rho_{AC_0}\right],\\
\epsilon\frac{d\rho_{AC_1}}{dt} &= p\tfrac{z-1}{z}(q_{B_0/C_0A}+q_{B_1/C_0A})\rho_{AC_0}-\rho_{AC_1}\\
&\quad+\epsilon\left[-b\left(\tfrac{\mu}{z}+(1-\tfrac{1}{z})(q_{B_1/AC_1}+\mu q_{C_1/AC_1})\right)\rho_{AC_1}+\rho_{C_1}-2\rho_{AC_1}\right],
\end{aligned}$$

$$
\begin{aligned}
\epsilon\frac{d\rho_{B_0B_1}}{dt} &= p\tfrac{z-1}{z}(q_{B_0/B_0B_0}+q_{B_1/B_0B_0})\rho_{B_0B_0}\\
&\quad -p\big(\tfrac{1}{z}+\tfrac{z-1}{z}(q_{B_0/B_0B_1}+q_{B_1/B_0B_1})\big)\rho_{B_0B_1}\\
&\quad +\rho_{B_1B_1}+\epsilon\left[b\tfrac{z-1}{z}q_{B_1/AB_1}\rho_{AB_1}-\rho_{B_0B_1}\right],\\
\epsilon\frac{d\rho_{B_0C_0}}{dt} &= -p\left(\tfrac{1}{z}+\tfrac{z-1}{z}(q_{B_0/B_0C_0}+q_{B_1/B_0C_0})\right)\rho_{B_0C_0}\\
&\quad +\rho_{B_1C_0}+\rho_{B_0C_1}-p\tfrac{z-1}{z}(q_{B_0/C_0B_0}+q_{B_1/C_0B_0})\rho_{B_0C_0}\\
&\quad +\epsilon\left[b\tfrac{z-1}{z}(q_{B_1/AC_0}\rho_{AC_0}+\mu q_{C_1/AB_0}\rho_{AB_0})-2\rho_{B_0C_0}\right],\\
\epsilon\frac{d\rho_{B_0C_1}}{dt} &= p\left(\tfrac{1}{z}+\tfrac{z-1}{z}(q_{B_0/C_0B_0}+q_{B_1/C_0B_0})\right)\rho_{B_0C_0}\\
&\quad -p\tfrac{z-1}{z}(q_{B_0/B_0C_1}+q_{B_1/B_0C_1})\rho_{B_0C_1}\\
&\quad +\rho_{B_1C_1}-\rho_{B_0C_1}+\epsilon\left[b\tfrac{z-1}{z}q_{B_1/AC_1}\rho_{AC_1}-2\rho_{B_0C_1}\right],\\
\epsilon\frac{d\rho_{B_1C_0}}{dt} &= p\tfrac{z-1}{z}(q_{B_0/B_0C_0}+q_{B_1/B_0C_0})\rho_{B_0C_0}\\
&\quad -p\left(\tfrac{1}{z}+\tfrac{z-1}{z}(q_{B_0/C_0B_1}+q_{B_1/C_0B_1})\right)\rho_{B_1C_0}\\
&\quad +\rho_{B_1C_1}-\rho_{B_1C_0}+\epsilon\left[\mu b\tfrac{z-1}{z}q_{C_1/AB_1}\rho_{AB_1}-2\rho_{B_1C_0}\right],\\
\epsilon\frac{d\rho_{B_1C_1}}{dt} &= p\tfrac{z-1}{z}(q_{B_0/B_0C_1}+q_{B_1/B_0C_1})\rho_{B_0C_1}\\
&\quad +p\left(\tfrac{1}{z}+\tfrac{z-1}{z}(q_{B_0/C_0B_1}+q_{B_1/C_0B_1})\right)\rho_{B_1C_0}\\
&\quad +\rho_{B_1C_1}-\rho_{B_1C_0}-\rho_{B_1C_1}+\epsilon\left[-2\rho_{B_1C_1}\right],\\
\epsilon\frac{d\rho_{C_0C_1}}{dt} &= p\tfrac{z-1}{z}(q_{B_0/C_0C_0}+q_{B_1/C_0C_0})\rho_{C_0C_0}\\
&\quad -p\tfrac{z-1}{z}(q_{B_0/C_0C_1}+q_{B_1/C_0C_1})\rho_{C_0C_1}\\
&\quad +\rho_{C_1C_1}-\rho_{C_0C_1}+\epsilon\left[\mu b(\tfrac{1}{z}+\tfrac{z-1}{z}q_{C_1/AC_1})\rho_{AC_1}-2\rho_{C_0C_1}\right]. \qquad (6.3.2)
\end{aligned}
$$

In combination (6.3.1) and (6.3.2) describe the development of the first and second moments of the gynodioecy IPS model. Applying the pair approximation (6.1.3) results in a closed system which approximates the IPS model. This fourteen-dimensional system can be simplified to a five-dimensional system in the limit of small ϵ. This simplified system describes the development of single site and site-pair densities that are sums of the sub-state densities described in the full system, these are referred to as aggregated variables. The aggregated system is obtained by considering the first term of the outer asymptotic expansion about a quasi-equilibrium found by considering only fast events.

Fast Equilibrium

The fast dynamics arise from considering (6.3.1) and (6.3.2) under (6.1.3) on the fast timescale $\tau = t/\epsilon$. Define aggregated variables ρ_B, $\rho_{\sigma B}$, ρ_C and $\rho_{\sigma C}$ with $\sigma \in S_1 = \{A, B_0, B_1, C_0, C_1\}$ as follows:

$$\begin{aligned}\rho_B &= \rho_{B_0} + \rho_{B_1},\\ \rho_{\sigma B} &= \rho_{\sigma B_0} + \rho_{\sigma B_1},\\ \rho_C &= \rho_{C_0} + \rho_{C_1},\\ \rho_{\sigma C} &= \rho_{\sigma C_0} + \rho_{\sigma C_1},\end{aligned}$$

and note that:

$$\begin{aligned}\dot{\rho_B} &= \dot{\rho_{AB}} = \rho_{BB} = \rho_{BC} = O(\epsilon),\\ \dot{\rho_C} &= \dot{\rho_{AC}} = \rho_{BC} = \rho_{CC} = O(\epsilon).\end{aligned} \tag{6.3.3}$$

The fast system is obtained by neglecting terms of order ϵ in the rescaled complete system. By (6.4.3) all singlet and doublet densities of empty and aggregated states are conserved on the fast timescale. On the fast timescale the system becomes uncoupled and most equations cease to be linearly independent. By applying the relationships (6.3.1), the fast-system reduces to a system of eight equations. By changing variables of the resultant system to:

$$\rho_{B_1},\ \rho_{C_1},\ \rho_{AB_1},\ \rho_{AC_1},\ \rho_{BB_1},\ \rho_{BC_1},\ \rho_{B_1C},\ \rho_{C_1C},$$

it is observed that the fast-system is decoupled into six separate systems. Of these, two are independent two dimensional systems and four are dependent one dimensional systems. The independent systems are treated first. These systems separately describe pollinated hermaphrodites and pollinated females and correlation of pollinated individuals with hermaphrodites. The fast system for hermaphrodites is:

$$\begin{aligned}\frac{d\rho_{B_1}}{d\tau} &= p\rho_{B_0B} - \rho_{B_1},\\ \frac{d\rho_{B_1B}}{d\tau} &= p\left(\tfrac{1}{z} + \tfrac{z-1}{z}q_{B/B_0}\right)\rho_{B_0B} - \rho_{B_1B}.\end{aligned} \tag{6.3.4}$$

The system is closed because:

$$\rho_{B_0B} = \rho_{BB} - \rho_{B_1B} \text{ and } q_{B/B_0} = \frac{\rho_{BB} - \rho_{B_1B}}{\rho_B - \rho_{B_1}}.$$

Since all singlet and doublet densities must be positive, the variables of (6.3.4) are constrained by the inequalities

$$\rho_{B_1B} \leq \rho_{B_1} \leq (\rho_B - \rho_{B_0B}) \text{ and } 0 \leq \rho_{B_1B} \leq \rho_{BB}.$$

Thus the region of interest for this system is the parallelogram with vertices $(0,0)$, $(\rho_B - \rho_{BB}, 0)$, (ρ_{BB}, ρ_{BB}) and (ρ_B, ρ_{BB}) in $(\rho_{B_1}, \rho_{B_1B})$-space. This region is invariant under (6.3.4). The system has one equilibrium $(\tilde{\rho}_{B_1}, \tilde{\rho}_{B_1B})$, which is globally asymptotically stable over the region of interest and is given by:

$$\begin{aligned} \tilde{\rho}_{B_1} &= \rho_B \Pi(q_{B/B}), \\ \tilde{\rho}_{B_1B} &= \frac{\rho_B \Pi(q_{B/B})}{p}. \end{aligned} \tag{6.3.5}$$

Π is the same functional response (6.2.6) found in the sexual species model above. The fast system for females is:

$$\begin{aligned} \frac{d\rho_{C_1}}{d\tau} &= p\rho_{BC_0} - \rho_{C_1}, \\ \frac{d\rho_{BC_1}}{d\tau} &= p\left(\tfrac{1}{z} + \tfrac{z-1}{z} q_{B/C_0}\right)\rho_{BC_0} - \rho_{BC_1}. \end{aligned} \tag{6.3.6}$$

In this case the region of interest is the parallelogram in $(\rho_{C_1}, \rho_{C_1B})$-space with vertices $(0,0)$, $(\rho_C - \rho_{BC}, 0)$, (ρ_{CB}, ρ_{BC}) and (ρ_B, ρ_{BC}). The system has one equilibrium $(\tilde{\rho}_{C_1}, \tilde{\rho}_{BC_1})$, which is globally asymptotically stable over the region of interest and is given by:

$$\begin{aligned} \tilde{\rho}_{C_1} &= \rho_C \Pi(q_{B/C}), \\ \tilde{\rho}_{BC_1} &= \frac{\rho_C \Pi(q_{B/C})}{p}. \end{aligned} \tag{6.3.7}$$

Notice that hermaphrodite and female pollination follows the same functional response to the local availability of pollen.

There are four fast systems dependent on (6.3.4) and (6.3.6), these treat the corre-

lations of pollinated hermaphrodites and females with other cell types:

$$\frac{d\rho_{AB_1}}{d\tau} = p(1-\tfrac{1}{z})q_{B/B_0}\rho_{AB_0} - \rho_{AB_1}, \tag{6.3.8a}$$

$$\frac{d\rho_{AC_1}}{d\tau} = p(1-\tfrac{1}{z})q_{B/C_0}\rho_{AC_0} - \rho_{AC_1}, \tag{6.3.8b}$$

$$\frac{d\rho_{B_1C}}{d\tau} = p(1-\tfrac{1}{z})q_{B/B_0}\rho_{B_0C} - \rho_{B_1C}, \tag{6.3.8c}$$

$$\frac{d\rho_{C_1C}}{d\tau} = p(1-\tfrac{1}{z})q_{B/C_0}\rho_{C_0C} - \rho_{C_1C}. \tag{6.3.8d}$$

From (a) and (c) at equilibrium:

$$\frac{\tilde{\rho}_{AB_1}}{\rho_{AB}} = \frac{\tilde{\rho}_{B_1C}}{\rho_{BC}}. \tag{6.3.9}$$

This relationship is not surprising since the probability of a hermaphrodite cell being pollinated ought to be independent of whether its non-hermaphrodite neighbours are empty or female, since neither can provide pollen. From the deduction (6.3.9) it follows that:

$$\begin{aligned}
\tilde{\rho}_{AB_1} &= \tilde{\rho}_{B_1} - \tilde{\rho}_{B_1B} - \tilde{\rho}_{B_1C} \\
&= \tilde{\rho}_{B_1} - \tilde{\rho}_{B_1B} - \frac{\rho_{BC}\tilde{\rho}_{AB_1}}{\rho_{AB}} \\
&= \frac{\rho_{AB}}{\rho_{AB}+\rho_{BC}}(\tilde{\rho}_{B_1} - \tilde{\rho}_{B_1B}) \\
&= \frac{\rho_{AB}}{\rho_{AB}+\rho_{BC}}\left(\frac{p+1}{p}\tilde{\rho}_{B_1} - \rho_{BB}\right).
\end{aligned} \tag{6.3.10}$$

Similarly from (6.3.8) (b) and (d) at equilibrium:

$$\frac{\tilde{\rho}_{AC_1}}{\rho_{AC}} = \frac{\tilde{\rho}_{C_1C}}{\rho_{CC}}, \tag{6.3.11}$$

and it follows that:

$$\tilde{\rho}_{AC_1} = \frac{\rho_{AC}}{\rho_{AC}+\rho_{CC}}\left(\frac{p+1}{p}\tilde{\rho}_{C_1} - \rho_{BC}\right). \tag{6.3.12}$$

Using the relationships (6.3.9) and (6.3.11) expressions for the fast equilibrium values $\tilde{\rho}_{B_1C}$ and $\tilde{\rho}_{C_1C}$ can also be obtained. The fast equilibrium in the fourteen original variables is denoted $\tilde{\rho}$.

Aggregated Dynamics

By summing equations that arise as in the first term of the outer asymptotic expansion of the original system ((6.3.1) and (6.3.2) under (6.1.3)) about the fast equilibrium $\tilde{\rho}$ a timescale separated system in the aggregated variables is obtained:

$$\begin{aligned}
\frac{d\rho_B}{dt} &= b\tilde{\rho}_{AB_1} - \rho_B, \\
\frac{d\rho_C}{dt} &= \mu b\tilde{\rho}_{AC_1} - \rho_C, \\
\frac{d\rho_{AB}}{dt} &= \frac{b\tilde{\rho}_{AB_1}((z-1)\rho_{AA} - \rho_A) - b(z-1)\rho_{AB}(\tilde{\rho}_{AB_1} + \mu\tilde{\rho}_{AC_1})}{z\rho_A} + \rho_B - 2\rho_{AB}, \\
\frac{d\rho_{AC}}{dt} &= \frac{\mu b\tilde{\rho}_{AC_1}((z-1)\rho_{AA} - \rho_A) - b(z-1)\rho_{AC}(\tilde{\rho}_{AB_1} + \mu\tilde{\rho}_{AC_1})}{z\rho_A} + \rho_C - 2\rho_{AC}, \\
\frac{d\rho_{BC}}{dt} &= \frac{b(z-1)(\tilde{\rho}_{AB_1}\rho_{AC} + \mu\tilde{\rho}_{AC_1}\rho_{AB})}{z\rho_A} - 2\rho_{BC},
\end{aligned} \tag{6.3.13}$$

The region of interest for the aggregated dynamics is delimited by the following inequalities:

$$\rho_B,\ \rho_C,\ \rho_{AB},\ \rho_{AC},\ \rho_{BC} \geq 0, \tag{6.3.14a}$$

$$\rho_B + \rho_C \leq 1, \tag{6.3.14b}$$

$$\rho_{AB} + \rho_{AC} \leq 1 - \rho_B - \rho_C, \tag{6.3.14c}$$

$$\rho_{AB} + \rho_{BC} \leq \rho_B, \tag{6.3.14d}$$

$$\rho_{AC} + \rho_{BC} \leq \rho_C. \tag{6.3.14e}$$

This region is readily shown to be invariant under (6.3.13).

Female Free Population

When the population is free of females, (6.3.13) reduces to the two dimensional aggregated sexual species system (6.2.9). The equilibria of (6.2.9) correspond to boundary equilibria of the gynodioecy system. If $p_{\text{crit}} < p \leq p_{\text{trans}}$ there are two such boundary

equilibria:

$$\begin{aligned}\hat{\rho}^{+} &= \left(\hat{\rho}_B^{+},\ 0,\ \hat{\rho}_B^{+} - \hat{\rho}_{BB}^{+}, 0\ ,\ 0\right),\\ \hat{\rho}^{-} &= \left(\hat{\rho}_B^{-},\ 0,\ \hat{\rho}_B^{-} - \hat{\rho}_{BB}^{-}, 0\ ,\ 0\right),\end{aligned} \tag{6.3.15}$$

and the hermaphrodite-only dynamics include a strong Allee effect. Extinction is predicted for small or poorly configured hermaphrodite populations. If $p \geq p_{\text{trans}}$ only the stable hermaphrodite carrying equilibrium $\hat{\rho}^{+}$ remains in the region of interest and the strong Allee effect is lost.

Female Invasion

Can a hermaphrodite only population at equilibrium be invaded by females? The system (6.3.13) is not differentiable at the hermaphrodite-only carrying equilibrium $\hat{\rho}^{+}$. However, stability can still investigated at $\hat{\rho}^{+}$ by considering the neighbourhood that a very small density δ of invading females would experience. Consider $q_{A/C}$ and $q_{B/C}$ the local densities of empty and hermaphrodite sites in females neighbourhoods. These densities will be non-negligible for arbitrarily small δ. The dynamics of the invaders' neighbourhood are obtained as follows:

$$\begin{aligned}\frac{dq_{A/C}}{dt} &= \frac{1}{\rho_C}\left(\frac{d\rho_{AC}}{dt} - q_{A/C}\frac{d\rho_C}{dt}\right)\\ &= \mu b\left(\frac{\rho_{AC_1}}{\rho_C}\right)\left(\frac{(z-1)\rho_{AA}}{z\rho_A} - \frac{1}{z} - q_{A/C}\right)\\ &\quad - b\left(\frac{z-1}{z}\right)\left(\frac{\rho_{AB_1} + \mu\rho_{AC_1}}{\rho_A}\right)q_{A/C} + 1 - q_{A/C},\\ \frac{dq_{B/C}}{dt} &= \frac{1}{\rho_C}\left(\frac{d\rho_{BC}}{dt} - q_{B/C}\frac{d\rho_C}{dt}\right)\\ &= \mu b\left(\frac{\rho_{AC_1}}{\rho_C}\right)\left(\frac{(z-1)\rho_{AB}}{z\rho_A} - q_{B/C}\right)\\ &\quad + b\left(\frac{z-1}{z}\right)\left(\frac{\rho_{AB_1}}{\rho_A}\right)q_{A/C} - q_{B/C},\end{aligned} \tag{6.3.16}$$

The aggregated system can be transformed to a system of the variables ρ_B, ρ_C, ρ_{AB}, $q_{A/C}$ and $q_{B/C}$. Consider the limiting system obtained from this transformation along any trajectory ($\delta \to 0$) approaching $\hat{\rho}^{+}$. This new system collapses to a two dimensional system in terms of the local densities of the invaders' neighbourhood $q_{A/C}$ and $q_{B/C}$. It describes the changes in the neighbourhood of the invaders when their numbers are

still small enough that they have a negligible effect on the established population. See Matsuda et al. (1992), Harada et al. (1995) and Iwasa et al. (1998) for other applications of this technique to PA problems. In the limit $\delta \to 0$ the system (6.3.16) becomes:

$$\begin{aligned}
\frac{dq_{A/C}}{dt} &= \mu b\left(\frac{\rho_{AC_1}}{\rho_C}\right)\left(\frac{(z-1)(1-2\hat{\rho}_B^+-\hat{\rho}_{BB}^+)}{z(1-\hat{\rho}_B^+)}-\frac{1}{z}-q_{A/C}\right)\\
&\quad - b\left(\frac{z-1}{z}\right)\left(\frac{\hat{\rho}_{AB_1}^+}{1-\hat{\rho}_B^+}\right)q_{A/C}+1-q_{A/C},\\
\frac{dq_{B/C}}{dt} &= \mu b\left(\frac{\rho_{AC_1}}{\rho_C}\right)\left(\frac{(z-1)(\hat{\rho}_B^+-\hat{\rho}_{BB}^+)}{z(1-\hat{\rho}_B^+)}-q_{B/C}\right)\\
&\quad + b\left(\frac{z-1}{z}\right)\left(\frac{\hat{\rho}_{AB_1}^+}{1-\hat{\rho}_B^+}\right)q_{A/C}-q_{B/C},
\end{aligned} \tag{6.3.17}$$

where:

$$\hat{\rho}_{AB_1}^+ = \frac{p+1}{p}\hat{\rho}_B^+\Pi(\hat{q}_{B/B}^+)-\hat{\rho}_{BB}^+.$$

and:

$$\frac{\rho_{AC_1}}{\rho_C} = \frac{q_{A/C}}{1-q_{B/C}}\left(\frac{p+1}{p}\Pi(q_{B/C})-q_{B/C}\right),$$

where Π is the functional response given in (6.2.6). Proceed by examining nullclines. $\dot{q}_{A/C}=0$ yields:

$$q_{A/C}^2 + a_1 q_{A/C} + a_0 = 0 \tag{6.3.18}$$

where:

$$\begin{aligned}
a_0 &= \frac{-2p(1-q_{B/C})}{\mu b(p+z+(z-2)pq_{B/C}-\sqrt{(p+z+zpq_{B/C})^2-4zp(p+1)q_{B/C}})},\\
a_1 &= \frac{(z-1)(1-2\hat{\rho}_B^+ + \hat{\rho}_{BB}^+ - ba_0\hat{\rho}_{AB_1}^+)}{z(1-\hat{\rho}_B^+)}-\frac{1}{z}-a_0.
\end{aligned}$$

$\dot{q}_{B/C}=0$ yields:

$$q_{A/C} = \frac{a_0 z(1-\hat{\rho}_B^+)q_{B/C}}{(z-1)(ba_0\hat{\rho}_{AB_1}^+ + \hat{\rho}_B^+ - \hat{\rho}_{BB}^+)-z(1-\hat{\rho}_B^+)q_{B/C}}. \tag{6.3.19}$$

The equilibrium of the invader neighbourhood dynamics ($\hat{q}_{A/C}$, $\hat{q}_{B/C}$) occurs where the positive root of (6.3.18) and 6.3.19 intersect. These densities can now use be used to resolve the differentiability problem at $\hat{\rho}^+$ and conduct stability analysis as normal. It

is more straight forward, however, to consider the per capita growth rate of the density of female invaders in the equilibrium neighbourhood:

$$\begin{aligned}\frac{\dot{\rho}_C}{\rho_C} &= \mu b\frac{\rho_{AC_1}}{\rho_C} - 1 \\ &= \frac{\mu b\hat{q}_{A/C}}{1-\hat{q}_{B/C}}\left(\frac{p+1}{p}R(\hat{q}_{B/C}) - \hat{q}_{B/C}\right) - 1.\end{aligned} \tag{6.3.20}$$

A positive per capita growth rate for females at the hermaphrodite equilibrium $\hat{\rho}^+$ indicates an invasion will be successful, a negative growth rate indicates the reverse. As might be expected, invasion success or failure depends strongly on the reproductive advantage μ which females enjoy through not expending resources on pollen production. Unlike the mean field, the PA indicates that μ_0, the threshold above which invasion will be successful, is now greater than 1. Figures 6-4(a) and 6-5(b) illustrates that for $\mu \in [1, \mu_0)$ invasion is not possible and, moreover, solutions are attracted to $\hat{\rho}^+$ for a wide range of initial conditions. Figure 6-6(a) illustrates how μ_0 varies with neighbourhood size z for fixed b and p. μ_0 also decreases with b and p. For very small neighbourhood sizes (≈ 3) $\mu_0 \gg 2$, so high in fact that it requires what is likely to be an unattainable efficiency in reallocating resources from male to female function. For larger neighbourhood sizes the interval $[1, \mu_0)$, in which invasion is predicted to be possible by the mean field model but impossible by the PA, shrinks. Note that $\mu_0 \to 1$ as $z \to \infty$, since the PA model (6.3.13) resolves to the mean field model (5.4.2) in this limit.

Coexistence Beyond Invasion

For $\mu > \mu_0$ the PA model exhibits a variety of behaviours absent from the mean field model. Numerical solutions (see Figures 6-4(b)-(e) and 6-4(b) and (c)) indicate that within the region of interest there is typically a maximum of one internal equilibrium:

$$\check{\rho} = (\check{\rho}_B, \check{\rho}_C, \check{\rho}_{AB}, \check{\rho}_{AC}, \check{\rho}_{BC}),$$

which is either attracting or repelling. There may also be a limit cycle surrounding $\check{\rho}$. In addition there may be a non-trivial basin of attraction for the origin if the origin is stable in the reduced hermaphrodite-only system.

By investigating the local stability of the internal equilibrium the fate of a population in which females arise can be predicted. When it exists and is stable the internal

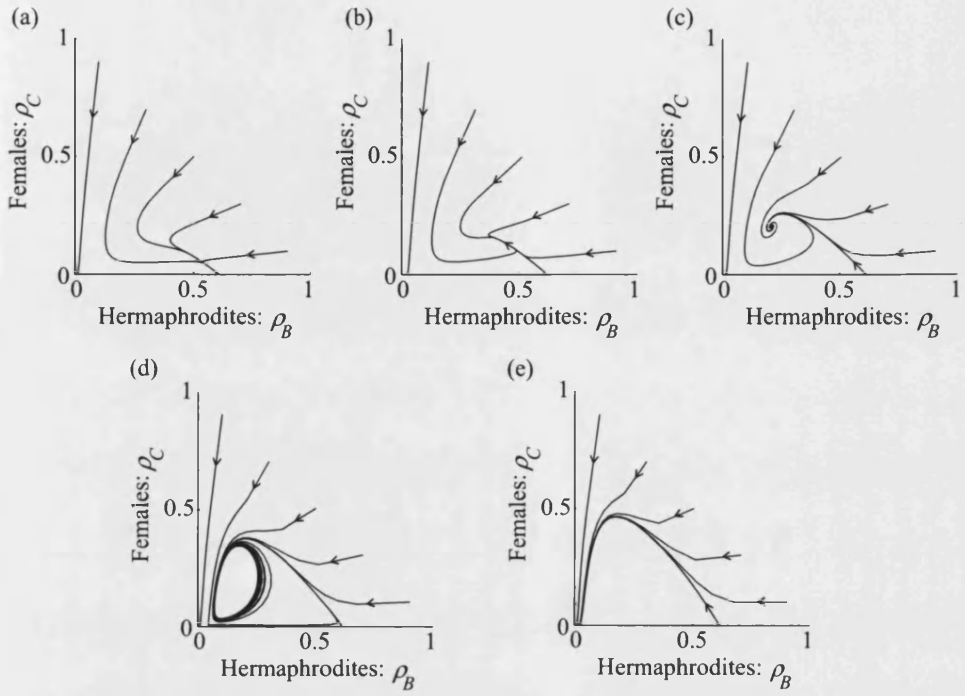

Figure 6-4: Sample solutions of the aggregated dynamics of the PA of the gynodioecy IPS when the underlying hermaphrodite-only population exhibits a strong Allee effect. Parameters $p = 4$, $b = 4$, $z = 8$. (a) $\mu = 1.05$. (b) $\mu = 1.2$. (c) $\mu = 1.5$. (d) $\mu = 2.0$. (e) $\mu = 2.6$.

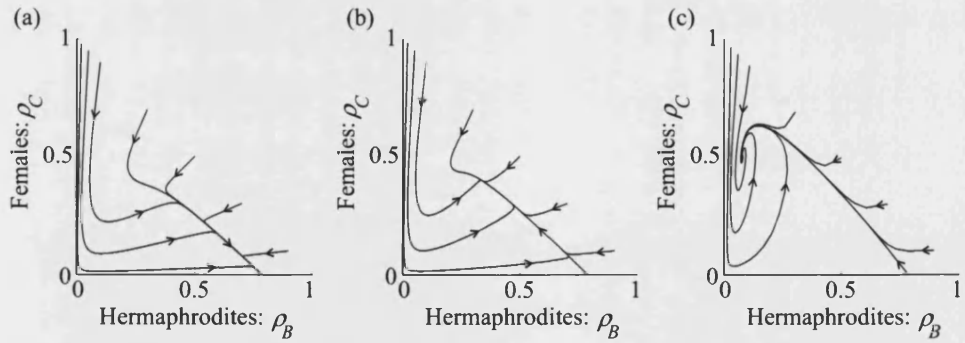

Figure 6-5: Sample solutions of the aggregated dynamics of the PA of the gynodioecy IPS when the underlying hermaphrodite-only population does not exhibit a strong Allee effect. Parameters $p = 6$, $b = 6$, $z = 8$. (a) $\mu = 1.01$. (b) $\mu = 1.2$. (a) $\mu = 2.6$

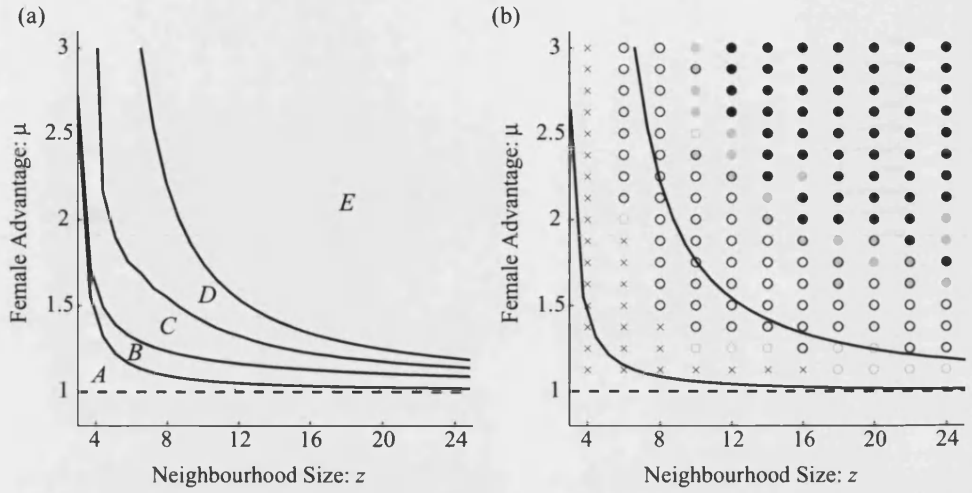

Figure 6-6: (z,μ) parameter space for the aggregated dynamics of the PA of the gynodioecy IPS. (a) Five regions of distinct model behaviours are distinguishable: A - No invasion $1 \leq \mu \leq \mu_0$. B - Internal equilibrium is a stable node $\mu_0 < \mu \leq \mu_1$. C - Internal equilibrium is a stable focus $\mu_1 < \mu \leq \mu_2$. D - Limit Cycles $\mu_2 < \mu \leq \mu_2$. E - Extinction $\mu > \mu_3$. Dashed curve recalls the mean field boundary between no invasion and extinction. Parameters $b = 4$ and $p = 4$. (b) Comparison of parameter space between PA and simulation for the gynodioecy IPS. The bifurcation curves μ_0 and μ_3 have been superimposed on the simulation outcomes in Figure 5-14. Circles indicate invasion success, filled circles indicate exploitation driven extinction.

equilibrium can readily be found with the Newton-Raphson method using the Jacobian $J(\rho_B, \rho_C, \rho_{AB}, \rho_{AC}, \rho_{BC})$ specified in Appendix A. By examining $J(\check{\rho})$ for eigenvalues as $\mu > \mu_0$ increases, different model behaviours can be distinguished and in particular when $\check{\rho}$ becomes unstable can be determined. For fixed b, p and z, let $\lambda_i(\mu)$ for $i \in \{1, \ldots, 5\}$ be the eigenvalues of $J(\check{\rho})$, where $\check{\rho}$ is the internal equilibrium of (6.3.13) for the given value of μ. Define:

$$\mu_1 = \min_{\mu > \mu_0} \{ \mu \,|\, Im(\lambda_i(\mu)) \neq 0 \text{ for some } i \}. \tag{6.3.21}$$

When $\mu_0 \leq \mu < \mu_1$ the internal equilibrium is a stable node, indicating that coexistence is possible between hermaphrodites and females. The invasion of females causes a minimum of disruption to the hermaphrodite population, although total population

density drops. This case is illustrated in Figure 6-4(b) and 6-5(b). Define:

$$\mu_2 = \min_{\mu > \mu_1} \{ \mu \mid \lambda_i(\mu) \geq 0 \text{ for some } i \}. \tag{6.3.22}$$

When $\mu_1 \leq \mu \leq \mu_2$ the internal equilibrium is a stable focus, indicating that coexistence is reached via damped oscillations. These oscillations affect total population density and engender alternating female and hermaphrodite success. When the underlying hermaphrodite-only system does not exhibit a strong Allee effect, μ_2 appears to be infinite, with the internal equilibrium remaining stable for arbitrarily large μ. Damped oscillations are illustrated in 6-4(c) and 6-5(c). If the hermaphrodite-only system does exhibit an Allee effect, μ_2 is finite and as μ increases past μ_2 the internal equilibrium becomes unstable and bifurcation to periodic solutions is observed. Periodic solutions are illustrated in Figure 6-4(d). For greater μ the attractor increases in period as the fortunes of hermaphrodites and females oscillate more wildly. When a threshold, μ_3, is reached the attractor disappears and population extinction is predicted to follow female invasion. Extinction behaviour is illustrated in Figure 6-4(e). Figure 6-6(a) illustrates how μ_0, μ_1, μ_2 and μ_3 divide (μ, z) parameter space for fixed b and p.

Stability of the Origin

The origin is stable in the reduced hermaphrodite-only system so long as $p < p_{\text{trans}}$. This stability must extend to the full gynodioecy system (6.3.13). It is straightforward to demonstrate that solutions of the full system (6.3.13) are sub-solutions of the reduced hermaphrodite-only system. This is also intuitive since, for a hermaphrodite, an empty or hermaphrodite neighbour is always preferable to a female neighbour. The presence of females reduces pollen flow and inhibits colonization. So if $p < p_{\text{trans}}$ choosing initial conditions $(\rho_B^*(0), \rho_{BB}^*(0))$ in the interior of the extinction region of the reduced system, guarantees that taking initial conditions $(\rho_B^*(0), \rho_C(0), \rho_B^*(0) - \rho_{BB}^*(0) - \rho_{BC}(0), \rho_{AC}(0), \rho_{BC}(0))$ in the full system will result in hermaphrodite extinction. If females persist beyond hermaphrodite extinction it cannot be for long, since the female-only system features only death terms. So the origin is necessarily stable and attracting to all points $(\rho_B, \rho_C, \rho_{AB}, \rho_{AC}, \rho_{BC})$ in the region of interest with $(\rho_B, \rho_B - \rho_{AB} - \rho_{BC})$ in the extinction region of the hermaphrodite-only system. Conversely the instability of the origin of the reduced hermaphrodite system for $p \geq p_{\text{trans}}$ ensures that the origin of the full system is also unstable.

μ_3 is the threshold beyond which female invasions culminate in extinction. An approximate value for μ_3 is obtained by following solutions originating near $\hat{\rho}^+$ and determining if $(\rho_B, \rho_B - \rho_{AB} - \rho_{BC})$ enters the region of extinction for the reduced system.

Although it is theoretically interesting that for $p \geq p_{\text{trans}}$ the model is incapable of exhibiting extinction dynamics similar to the mean field, bare in mind that the PA is a deterministic prediction. When μ is large the stable equilibrium approached by the gynodioecy model involves very few hermaphrodites. In practice the small number of pollen producing individuals supporting the populations' reproduction would eventually be eliminated stochastically entailing population extinction. In this sense female invasion when $\mu \gg \mu_2$ is very destabilizing and should be regarded as threatening population survival regardless of whether the reduced hermaphrodite-only system exhibits an Allee effect or not.

Discussion

Many features of the gynodioecy IPS model have been captured by the PA: Hermaphrodite populations may resist invasion by females with a strictly positive seed production advantage; Female invasion can result in gynodioecious coexistence which may be stable or may entail cycles of hermaphrodite and female success; Female invasion can result in extinction. Figure 6-6(b) compares (z,μ) parameter space determined by simulation in chapter 5 with the predictions of the PA. Only the boundary μ_0 separating the region of no invasion from that of coexistence and the boundary μ_3 between coexistence and extinction have been plotted because the distinction between oscillatory and non-oscillatory dynamics in simulations of the IPS is not clear.

The region of parameter space in which females cannot invade hermaphrodite populations is underestimated by the PA. This is consistent with the general observation that the PA underestimates the effects of competition. Invading female compete with other females in their locality not only for empty sites to colonize as hermaphrodites do, but also for pollen. Competition for pollen is indirect and arises because females in the same locality will tend to fill each other's neighbourhoods with their male-sterile offspring, lowering the frequency of hermaphrodites in female neighbourhoods and thus depleting the availability of pollen. Figure 6-7 compares successful female invasion on a finite lattice simulation with a PA of a female invasion. The population dynamics are

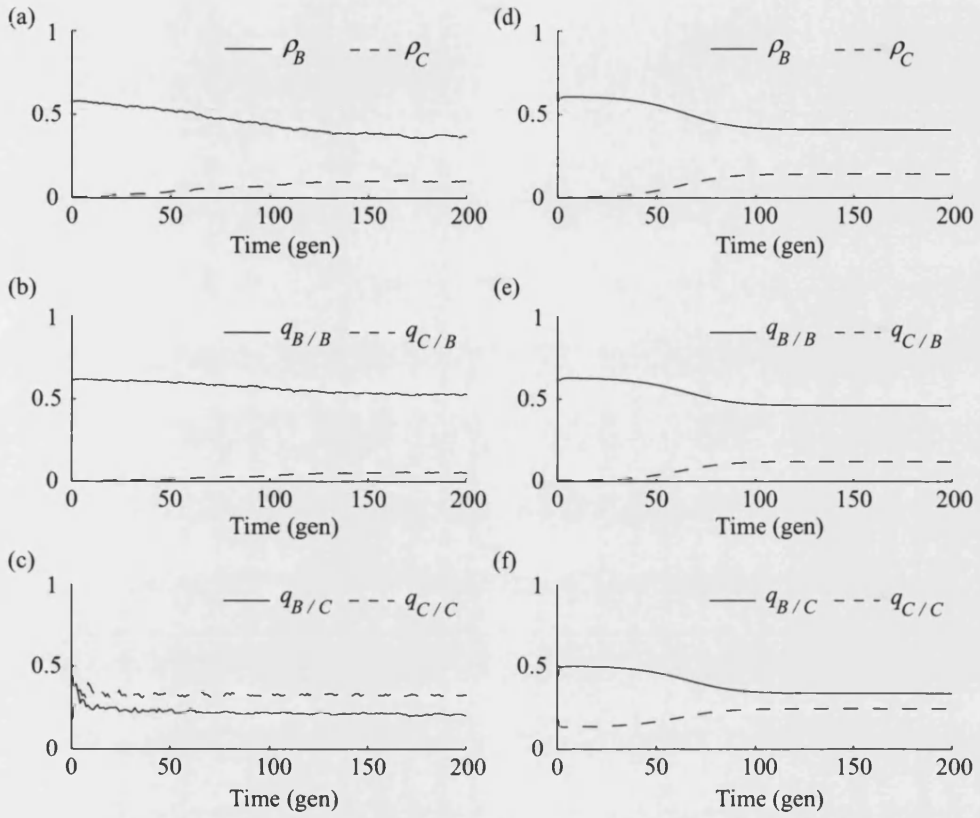

Figure 6-7: Comparison of neighbourhood composition exhibited by simulations and that predicted by PA in the gynodioecy IPS model in cases where both predict stable coexistence. (a)-(c) Average of 25 simulation runs on $L = 100$ lattice with a single female introduced at $t = 0$ into a hermaphrodite population at carrying capacity. Parameters $p = 4$, $b = 4$, $\mu = 1.75$, $z = 8$. (d)-(f) PA initialized with data from simulation initial conditions. Parameters $p = 4$, $b = 4$, $\mu = 1.18$, $z = 8$ (a) and (d) population densities. (b) and (e) local density of hermaphrodites $q_{B/B}$ and females $q_{C/B}$ in the neighbourhoods of hermaphrodites. (c) and (f) local density of hermaphrodites $q_{B/B}$ and females $q_{C/B}$ in the neighbourhoods of females.

superficially similar but the neighbourhoods invading females experience are starkly different. The PA predicts that hermaphrodites will be initially abundant in female neighbourhoods with their frequency falling in line with a global depletion of their numbers. Thus the PA predicts high availability of pollen to females. By contrast, in simulations the frequency of hermaphrodites in female neighbourhoods decreases very quickly and so invaders face limited access to pollen. The PA is quite bad at approximating the dynamics of two species IPS in which species form distinct clusters (Iwasa et al. 1998). Although simulations show that coexisting females and hermaphrodites are fairly well mixed, local seed dispersal naturally induces some clustering of conspecifics of the same type. Failure to accurately model this, albeit reasonably low, level of clustering is responsible for the PA overestimating the prospects of females.

The PA indicates that for intermediate values of μ damped oscillations and limit cycles can arise. It is difficult to identify such behaviour in simulations because of their stochastic nature. Oscillations in success of females and hermaphrodites do appear to occur, but taking population averages over numerous realizations with similar initial conditions evens out and obscures these oscillations (Figure 5-13.) Deterministic dynamics might underlie the oscillations but because the simulation is not constrained to behave similarly over the whole lattice, 'pockets' of individuals will be in different phases and a unified oscillation with a characteristic period is not observed. The aperiodic oscillations in the total population size is a result of the randomized synchrony and asynchrony of the oscillations in small parts of the system (Rand & Wilson 1995). Note that limit cycles are only predicted by the PA when the hermaphrodite-only system includes a strong Allee effect. In simulations an Allee effect is almost never observed (see Figure 5-8.) It is not clear, therefore, that the PA can be claimed to predict limit cycles in the IPS model since they arise in the PA in an artificial region of parameter space.

When the female advantage is particularly high simulations of the gynodioecy IPS model on a finite lattice result either in population extinction or in the population declining to very small numbers, female extinction and hermaphrodites recovering to recolonize the lattice. The PA also predicts two possible outcomes to invasion by highly fecund females: Extinction and coexistence with hermaphrodites becoming extremely rare. The former arises if the hermaphrodite-only system includes a strong Allee effect, otherwise the latter is predicted. It may be conjectured that the extinction phenomenon encountered in simulations is not deterministically driven because the Allee effect is absent. The PA prediction in the absence of an Allee effect is that hermaphrodites

persist in very small numbers. This is untenable in a finite stochastic model and if hermaphrodites are lost then the female population expires too.

6.4 SEXUAL-ASEXUAL

In this section a PA is obtained for the sexual-asexual IPS model proposed in chapter 5 section 5.5. Again the PA will be analysed using a perturbation method which exploits the small parameter ϵ to obtain a dimensionally reduced model.

By inserting the appropriate parameters in the general state density equations (5.2.4) and applying the definition of local density in terms of site-pair densities (6.1.2) the following single site density equations arise:

$$\begin{aligned}
\epsilon\frac{d\rho_{B_0}}{dt} =& -p(\rho_{B_0B_0}+\rho_{B_0B_1}+\rho_{B_0B_2}+\rho_{B_0C_0}+\rho_{B_0C_1})+\rho_{B_1}+\rho_{B_2}\\
&+\epsilon[\mu b\rho_{AB_1}+\mu b\tfrac{\nu}{2}\rho_{AB_2}-\rho_{B_0}],\\
\epsilon\frac{d\rho_{B_1}}{dt} =& p(\rho_{B_0B_0}+\rho_{B_0B_1}+\rho_{B_0B_2})-\rho_{B_1}-\epsilon\rho_{B_1},\\
\epsilon\frac{d\rho_{B_2}}{dt} =& p(\rho_{B_0C_0}+\rho_{B_0C_1})-\rho_{B_2}-\epsilon\rho_{B_2},\\
\epsilon\frac{d\rho_{C_0}}{dt} =& -p(\rho_{C_0B_0}+\rho_{C_0B_1}+\rho_{C_0B_2}+\rho_{C_0C_0}+\rho_{C_0C_1})+\rho_{C_1}\\
&+\epsilon[b\rho_{AC_1}+\mu b\tfrac{\nu}{2}\rho_{AB_2}-\rho_{C_0}],\\
\epsilon\frac{d\rho_{C_1}}{dt} =& p(\rho_{C_0B_0}+\rho_{C_0B_1}+\rho_{C_0B_2}+\rho_{C_0C_0}+\rho_{C_0C_1})-\rho_{C_1}-\epsilon\rho_{C_1},
\end{aligned} \tag{6.4.1}$$

There are 36 possible pairs of states (respecting order) and corresponding site-pair densities:

$$\begin{array}{cccccc}
\rho_{AA} & \rho_{AB_0} & \rho_{AB_1} & \rho_{AB_2} & \rho_{AC_0} & \rho_{AC_1}\\
\rho_{B_0A} & \rho_{B_0B_0} & \rho_{B_0B_1} & \rho_{B_0B_2} & \rho_{B_0C_0} & \rho_{B_0C_1}\\
\rho_{B_1A} & \rho_{B_1B_0} & \rho_{B_1B_1} & \rho_{B_1B_2} & \rho_{B_1C_0} & \rho_{B_1C_1}\\
\rho_{B_2A} & \rho_{B_2B_0} & \rho_{B_2B_1} & \rho_{B_2B_2} & \rho_{B_2C_0} & \rho_{B_2C_1}\\
\rho_{C_0A} & \rho_{C_0B_0} & \rho_{C_0B_1} & \rho_{C_0B_1} & \rho_{C_0C_0} & \rho_{C_0C_1}\\
\rho_{C_1A} & \rho_{C_1B_0} & \rho_{C_1B_1} & \rho_{C_1B_1} & \rho_{C_1C_0} & \rho_{C_1C_1}
\end{array}$$

A linearly independent set of variables includes only those above the diagonal. Equations for the development of these pairs are derived along the same lines as the gyn-

odioecy PA. The site-pair equations are:

$$
\begin{aligned}
\epsilon\frac{d\rho_{AB_0}}{dt} &= -p\tfrac{z-1}{z}(q_{B_0/B_0A}+q_{B_1/B_0A}+q_{B_2/B_0A}+q_{C_0/B_0A}+q_{C_1/B_0A})\rho_{AB_0}\\
&\quad +\rho_{AB_1}+\rho_{AB_2}+\epsilon[-b\tfrac{z-1}{z}(\mu q_{B_1/AB_0}+\mu\nu q_{B_2/AB_0}+q_{C_1/AB_0})\rho_{AB_0}\\
&\quad +\mu b\tfrac{z-1}{z}(q_{B_1/AA}+\tfrac{\nu}{2}q_{B_2/AA})\rho_{AA}+\rho_{B_0}-2\rho_{AB_0}],\\
\epsilon\frac{d\rho_{AB_1}}{dt} &= p\tfrac{z-1}{z}(q_{B_0/B_0A}+q_{B_1/B_0A}+q_{B_2/B_0A})\rho_{AB_0}-\rho_{AB_1}\\
&\quad +\epsilon[-b(\tfrac{\mu}{z}+\tfrac{z-1}{z}(\mu q_{B_1/AB_1}+\mu\nu q_{B_2/AB_1}+q_{C_1/AB_1}))\rho_{AB_1}\\
&\quad +\rho_{B_1}-2\rho_{AB_1}],\\
\epsilon\frac{d\rho_{AB_2}}{dt} &= p\tfrac{z-1}{z}(q_{C_0/B_0A}+q_{C_1/B_0A})\rho_{AB_0}-\rho_{AB_2}\\
&\quad +\epsilon[-b(\tfrac{\mu\nu}{2z}+\tfrac{z-1}{z}(\mu q_{B_1/AB_2}+\mu\nu q_{B_2/AB_2}+q_{C_1/AB_2}))\rho_{AB_2}\\
&\quad +\rho_{B_2}-2\rho_{AB_2}],\\
\epsilon\frac{d\rho_{AC_0}}{dt} &= -p\tfrac{z-1}{z}(q_{B_0/C_0A}+q_{B_1/C_0A}+q_{B_2/C_0A}+q_{C_0/C_0A}+q_{C_1/C_0A})\rho_{AC_0}\\
&\quad +\rho_{AC_1}+\epsilon[-b\tfrac{z-1}{z}(\mu q_{B_1/AC_0}+\mu\nu q_{B_2/AC_0}+q_{C_1/AC_0})\rho_{AC_0}\\
&\quad +b\tfrac{z-1}{z}(q_{C_1/AA}+\mu\tfrac{\nu}{2}q_{B_2/AA})\rho_{AA}+\rho_{C_0}-2\rho_{AC_0}],\\
\epsilon\frac{d\rho_{AC_1}}{dt} &= p\tfrac{z-1}{z}(q_{B_0/C_0A}+q_{B_1/C_0A}+q_{B_2/C_0A}+q_{C_0/C_0A}+q_{C_1/C_0A})\rho_{AC_0}\\
&\quad -\rho_{AC_1}+\epsilon[-b(\tfrac{1}{z}+\tfrac{z-1}{z}(\mu q_{B_1/AC_1}+\mu\nu q_{B_2/AC_1}+q_{C_1/AC_1}))\rho_{AC_1}\\
&\quad +\rho_{C_1}-2\rho_{AC_1}],\\
\epsilon\frac{d\rho_{B_0B_1}}{dt} &= -p(\tfrac{1}{z}+\tfrac{z-1}{z}(q_{B_0/B_0B_1}+q_{B_1/B_0B_1}+q_{B_2/B_0B_1}\\
&\quad +q_{C_0/B_0B_1}+q_{C_1/B_0B_1}))\rho_{B_0B_1}\\
&\quad +p(\tfrac{1}{z}+\tfrac{z-1}{z}(q_{B_0/B_0B_0}+q_{B_1/B_0B_0}+q_{B_2/B_0B_0}))\rho_{B_0B_0}+\rho_{B_1B_1}\\
&\quad +\rho_{B_2B_1}-\rho_{B_0B_1}+\epsilon[\mu b(\tfrac{1}{z}+\tfrac{z-1}{z}(q_{B_1/AB_1}+\tfrac{\nu}{2}q_{B_2/AB_1}))\rho_{AB_1}-2\rho_{B_0B_1}],\\
\epsilon\frac{d\rho_{B_0B_2}}{dt} &= -p(\tfrac{1}{z}+\tfrac{z-1}{z}(q_{B_0/B_0B_2}+q_{B_1/B_0B_2}+q_{B_2/B_0B_2}\\
&\quad +q_{C_0/B_0B_2}+q_{C_1/B_0B_2}))\rho_{B_0B_2}\\
&\quad +p\tfrac{z-1}{z}(q_{C_0/B_0B_0}+q_{C_1/B_0B_0})\rho_{B_0B_0}+\rho_{B_1B_2}+\rho_{B_2B_2}-\rho_{B_0B_2}\\
&\quad +\epsilon[\mu b(\tfrac{\nu}{2z}+\tfrac{z-1}{z}(q_{B_1/AB_2}+\tfrac{\nu}{2}q_{B_2/AB_2})\rho_{AB_2}-2\rho_{B_0B_2}],
\end{aligned}
$$

$$
\begin{aligned}
\epsilon\frac{d\rho_{B_0C_0}}{dt} &= -p(\tfrac{1}{z}+\tfrac{z-1}{z}(q_{B_0/B_0C_0}+q_{B_1/B_0C_0}+q_{B_2/B_0C_0}\\
&\quad +q_{C_0/B_0C_0}+q_{C_1/B_0C_0}))\rho_{B_0C_0}\\
&\quad -p(\tfrac{1}{z}+\tfrac{z-1}{z}(q_{B_0/C_0B_0}+q_{B_1/C_0B_0}+q_{B_2/C_0B_0}\\
&\quad +q_{C_0/C_0B_0}+q_{C_1/C_0B_0}))\rho_{B_0C_0}\\
&\quad +\rho_{B_1C_0}+\rho_{B_2C_0}+\rho_{B_0C_1}+\epsilon[b\tfrac{z-1}{z}(\mu q_{B_1/AC_0}+\mu\tfrac{\nu}{2}q_{B_2/AC_0})\rho_{AC_0}\\
&\quad +b\tfrac{z-1}{z}(q_{C_1/AB_0}+\mu\tfrac{\nu}{2}q_{B_2/AB_0})\rho_{AB_0}-2\rho_{B_0C_0}],\\
\epsilon\frac{d\rho_{B_0C_1}}{dt} &= -p(\tfrac{1}{z}+\tfrac{z-1}{z}(q_{B_0/B_0C_1}+q_{B_1/B_0C_1}+q_{B_2/B_0C_1}\\
&\quad +q_{C_0/B_0C_1}+q_{C_1/B_0C_1}))\rho_{B_0C_1}\\
&\quad +p(\tfrac{1}{z}+\tfrac{z-1}{z}(q_{B_0/C_0B_0}+q_{B_1/C_0B_0}+q_{B_2/C_0B_0}\\
&\quad +q_{C_0/C_0B_0}+q_{C_1/C_0B_0}))\rho_{B_0C_0}\\
&\quad +\rho_{B_1C_1}+\rho_{B_2C_1}-\rho_{B_0C_1}\\
&\quad +\epsilon[\mu b\tfrac{z-1}{z}(q_{B_1/AC_1}+\tfrac{\nu}{2}q_{B_2/AC_1})\rho_{AC_1}-2\rho_{B_0C_1}],\\
\epsilon\frac{d\rho_{B_1B_2}}{dt} &= +p(\tfrac{1}{z}+\tfrac{z-1}{z}(q_{B_0/B_0B_2}+q_{B_1/B_0B_2}+q_{B_2/B_0B_2}))\rho_{B_0B_2}\\
&\quad +p\tfrac{z-1}{z}(q_{C_0/B_0B_1}+q_{C_1/B_0B_1})\rho_{B_0B_1}-2\rho_{B_1B_2}-2\epsilon\rho_{B_1B_2},\\
\epsilon\frac{d\rho_{B_1C_0}}{dt} &= -p(\tfrac{1}{z}+\tfrac{z-1}{z}(q_{B_0/C_0B_1}+q_{B_1/C_0B_1}+q_{B_2/C_0B_1}\\
&\quad +q_{C_0/C_0B_1}+q_{C_1/C_0B_1}))\rho_{C_0B_1}\\
&\quad +p\tfrac{z-1}{z}(q_{B_0/B_0C_0}+q_{B_1/B_0C_0}+q_{B_2/B_0C_0})\rho_{B_0C_0}+\rho_{B_1C_1}\\
&\quad -\rho_{B_1C_0}+\epsilon[b\tfrac{z-1}{z}(q_{C_1/AB_1}+\mu\tfrac{\nu}{2}q_{B_2/AB_1})\rho_{AB_1}-2\rho_{B_1C_0}],\\
\epsilon\frac{d\rho_{B_1C_1}}{dt} &= p(\tfrac{1}{z}+\tfrac{z-1}{z}(q_{B_0/C_0B_1}+q_{B_1/C_0B_1}+q_{B_2/C_0B_1}\\
&\quad +q_{C_0/C_0B_1}+q_{C_1/C_0B_1}))\rho_{B_1C_0}\\
&\quad +p\tfrac{z-1}{z}(q_{B_0/B_0C_1}+q_{B_1/B_0C_1}+q_{B_2/B_0C_1})\rho_{B_0C_1}\\
&\quad -2\rho_{B_1C_1}-2\epsilon\rho_{B_1C_1},\\
\epsilon\frac{d\rho_{B_2C_0}}{dt} &= -p(\tfrac{1}{z}+\tfrac{z-1}{z}(q_{B_0/C_0B_2}+q_{B_1/C_0B_2}+q_{B_2/C_0B_2}\\
&\quad +q_{C_0/C_0B_2}+q_{C_1/C_0B_2}))\rho_{B_2C_0}\\
&\quad +p(\tfrac{1}{z}+\tfrac{z-1}{z}(q_{C_0/B_0C_0}+q_{C_1/B_0C_0}))\rho_{B_0C_0}+\rho_{B_2C_1}-\rho_{B_2C_0}\\
&\quad +\epsilon[-b(\tfrac{\mu\nu}{2z}+\tfrac{z-1}{z}(q_{C_1/AB_2}+\tfrac{\mu\nu}{2}q_{B_2/AB_2}))\rho_{AB_2}-2\rho_{B_2C_0}],
\end{aligned}
$$

$$\begin{aligned}
\epsilon\frac{d\rho_{B_2C_1}}{dt} &= p(\tfrac{1}{z}+\tfrac{z-1}{z}(q_{B_0/C_0B_2}+q_{B_1/C_0B_2}+q_{B_2/C_0B_2}\\
&\quad +q_{C_0/C_0B_2}+q_{C_1/C_0B_2}))\rho_{B_2C_0}\\
&\quad +p(\tfrac{1}{z}+\tfrac{z-1}{z}(q_{C_0/B_0C_1}+q_{C_1/B_0C_1}))\rho_{B_0C_1}-2\rho_{B_2C_1}-2\epsilon\rho_{B_2C_1},\\
\epsilon\frac{d\rho_{C_0C_1}}{dt} &= p(\tfrac{1}{z}+\tfrac{z-1}{z}(q_{B_0/C_0C_0}+q_{B_1/C_0C_0}+q_{B_2/C_0C_0}\\
&\quad +q_{C_0/C_0C_0}+q_{C_1/C_0C_0}))\rho_{C_0C_0}\\
&\quad -p(\tfrac{1}{z}+\tfrac{z-1}{z}(q_{B_0/C_0C_1}+q_{B_1/C_0C_1}+q_{B_2/C_0C_1}\\
&\quad +q_{C_0/C_0C_1}+q_{C_1/C_0C_1}))\rho_{C_0C_1}+\rho_{C_1C_1}-\rho_{C_0C_1}\\
&\quad +\epsilon[-b(\tfrac{1}{z}+\tfrac{z-1}{z}(q_{C_1/AC_1}+\tfrac{\mu\nu}{2}q_{B_2/AC_1}))\rho_{AC_1}-2\rho_{C_0C_1}],
\end{aligned} \tag{6.4.2}$$

In combination (6.4.1) and (6.4.2) describe the development of the first and second moments of the gynodioecy IPS model. Applying the pair approximation (6.1.3) results in a closed system which approximates the IPS model. This twenty-one-dimensional system can be simplified to a five-dimensional system in the limit of small ϵ. This simplified system describes the development of single site and site-pair densities that are sums of the sub-state densities described in the full system, these are referred to as aggregated variables. The aggregated system is obtained by considering the first term of the outer asymptotic expansion about a quasi-equilibrium found by considering only fast events.

Fast Equilibrium

The fast dynamics arise from considering (6.4.1) and (6.4.2) under (6.1.3) on the fast timescale $\tau = t/\epsilon$. Define aggregated variables ρ_B, $\rho_{\sigma B}$, ρ_C and $\rho_{\sigma C}$ with $\sigma \in S_1 = \{A, B_0, B_1, B_2, C_0, C_1\}$ as follows:

$$\begin{aligned}
\rho_B &= \rho_{B_0}+\rho_{B_1}+\rho_{B_2},\\
\rho_{\sigma B} &= \rho_{\sigma B_0}+\rho_{\sigma B_1}+\rho_{\sigma B_2},\\
\rho_C &= \rho_{C_0}+\rho_{C_1},\\
\rho_{\sigma C} &= \rho_{\sigma C_0}+\rho_{\sigma C_1},
\end{aligned}$$

and note that:

$$\begin{aligned}
\dot{\rho_B} &= \dot{\rho_{AB}} = \rho_{BB} = \rho_{BC} = O(\epsilon),\\
\dot{\rho_C} &= \dot{\rho_{AC}} = \rho_{BC} = \rho_{CC} = O(\epsilon).
\end{aligned} \tag{6.4.3}$$

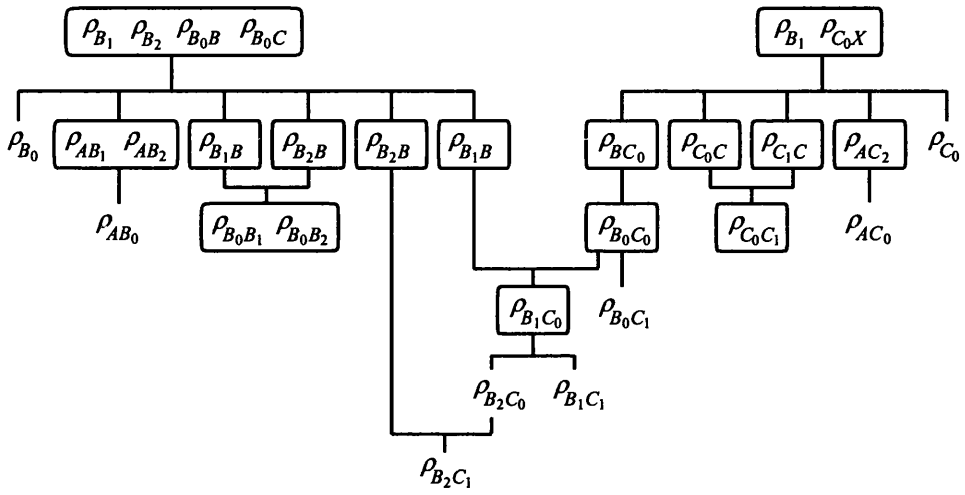

Figure 6-8: The cascade of dependencies in the fast system. Variables in boxes indicate the systems of equations describing the development of that variable on the fast timescale. Variables in the same box are interdependent and their equations must be solved simultaneously. Lines indicate the dependence of a system on variables in systems in higher rows. Un-boxed variables can be obtained by applying (6.4.1). The diagram prescribes an order in which equilibria may be sought but is by no means unique.

The fast system is obtained by neglecting terms of order ϵ in the rescaled complete system. By (6.4.3) all single site and site-pair densities of empty and aggregated states are conserved on the fast-timescale. On the fast timescale the system becomes uncoupled and most equations cease to be linearly independent. All fast equilibrium densities can be recovered by first finding equilibria for two uncoupled linearly independent systems arising from the fast system, and using these equilibria to obtain the equilibria of the remaining dependent systems. This needs to be done in an order which respects the dependencies of each system, one possible order can be lifted from the cascade of dependencies depicted in Figure 6-8. The first independent system concerns the pollination

status of sexuals and features four coupled equations:

$$\begin{aligned}
\frac{d\rho_{B_1}}{d\tau} &= p\rho_{B_0B} - \rho_{B_1},\\
\frac{d\rho_{B_2}}{d\tau} &= p\rho_{B_0C} - \rho_{B_2},\\
\frac{d\rho_{B_0B}}{d\tau} &= -p\left(\tfrac{1}{z} + \tfrac{z-1}{z}(q_{B/B_0} + q_{C/B_0})\right)\rho_{B_0B} + \rho_{BB} - \rho_{B_0B},\\
\frac{d\rho_{B_0C}}{d\tau} &= -p\left(\tfrac{1}{z} + \tfrac{z-1}{z}(q_{B/B_0} + q_{C/B_0})\right)\rho_{B_0C} + \rho_{BC} - \rho_{B_0C}.
\end{aligned} \tag{6.4.4}$$

The symmetry of this system means that behaviour is determined by the two dimensional system:

$$\begin{aligned}
\frac{d\rho_{B_p}}{d\tau} &= p\rho_{B_0X} - \rho_{B_p},\\
\frac{d\rho_{B_0X}}{d\tau} &= -p\left(\tfrac{1}{z} + \tfrac{z-1}{z}q_{X/B_0}\right)\rho_{B_0X} + \rho_{BX} - \rho_{B_0X}.
\end{aligned} \tag{6.4.5}$$

where new variables $\rho_{B_p} = \rho_{B_1} + \rho_{B_2}$, $\rho_{B_0X} = \rho_{B_0B} + \rho_{B_0C}$ and $\rho_{BX} = \rho_{BB} + \rho_{BC}$ have been introduced. Since the all singlet and doublet densities must be positive these new variables are constrained by the inequalities

$$\rho_{BX} - \rho_{B_0X} \leq \rho_{B_p} \leq \rho_B - \rho_{B_0X} \text{ and } 0 \leq \rho_{B_0X} \leq \rho_{BX}.$$

Thus the region of interest is the parallelogram with vertices $(0,0)$, $(\rho_B - \rho_{BX}, 0)$, (ρ_{BX}, ρ_{BX}) and (ρ_B, ρ_{BX}) in $(\rho_{B_p}, \rho_{B_0X})$-space. This region is invariant under (6.4.5) and contains a unique globally stable equilibrium $(\tilde{\rho}_{B_p}, \tilde{\rho}_{B_0X})$ given by:

$$\begin{aligned}
\tilde{\rho}_{B_p} &= \rho_B \Pi(q_{X/B}),\\
\tilde{\rho}_{B_0X} &= \frac{\tilde{\rho}_{B_p}}{p},
\end{aligned}$$

where Π is the functional response to local pollinators (6.2.6) introduced in the single species model and $q_{X/B}$ is consistently defined as ρ_{BX}/ρ_B. From the final two equations of (6.4.4) it is deducible that $\tilde{\rho}_{B_0B}\rho_{BC} = \tilde{\rho}_{B_0C}\rho_{BB}$ and so the equilibrium of (6.4.4) is

$$\tilde{\rho}_{B_1} = \frac{\rho_{BB}}{\rho_{BX}}\tilde{\rho}_{B_p},\ \tilde{\rho}_{B_2} = \frac{\rho_{BC}}{\rho_{BX}}\tilde{\rho}_{B_p},\ \tilde{\rho}_{B_0B} = \frac{\rho_{BB}}{\rho_{BX}}\tilde{\rho}_{B_0X},\ \tilde{\rho}_{B_0C} = \frac{\rho_{BC}}{\rho_{BX}}\tilde{\rho}_{B_0X}. \tag{6.4.6}$$

The second independent system concerns pollination of asexuals and is given by:

$$\begin{aligned} \frac{d\rho_{C_1}}{d\tau} &= p\rho_{C_0X} - \rho_{C_1}, \\ \frac{d\rho_{C_0X}}{d\tau} &= -p\left(\tfrac{1}{z} + \tfrac{z-1}{z}q_{X/C_0}\right)\rho_{C_0X} + \rho_{CX} - \rho_{C_0X}, \end{aligned} \tag{6.4.7}$$

where the new variables $\rho_{C_0X} = \rho_{C_0B} + \rho_{C_0C}$ and $\rho_{CX} = \rho_{CB} + \rho_{CC}$ have been introduced. The variables in (6.4.7) are constrained by the inequalities

$$\rho_{CX} - \rho_{C_0X} \leq \rho_{C_1} \leq \rho_C - \rho_{C_0X} \text{ and } 0 \leq \rho_{C_0X} \leq \rho_{CX}.$$

Thus the region of interest is the parallelogram with vertices $(0,0)$, $(\rho_C - \rho_{CX}, 0)$, (ρ_{CX}, ρ_{CX}) and (ρ_C, ρ_{CX}) in $(\rho_{C_1}, \rho_{C_0X})$-space. This region is invariant under (6.4.7) and contains a unique globally stable equilibrium $(\tilde{\rho}_{B_1}, \tilde{\rho}_{C_0X})$ given by:

$$\begin{aligned} \tilde{\rho}_{C_1} &= \rho_C \Pi(q_{X/C}), \\ \tilde{\rho}_{C_0X} &= \frac{\tilde{\rho}_{C_1}}{p}. \end{aligned} \tag{6.4.8}$$

Rather than the equilibrium values given in (6.4.6) and (6.4.8) the aggregated dynamics will require expressions for $\tilde{\rho}_{AB_1}$, $\tilde{\rho}_{AB_2}$ and $\tilde{\rho}_{AC_1}$. These site-pairs contain information crucial to the rate of colonization of empty cells. The variables $\tilde{\rho}_{AB_1}$ and $\tilde{\rho}_{AB_2}$ are interdependent and must be treated as a system:

$$\begin{aligned} \frac{d\rho_{AB_1}}{d\tau} &= p\tfrac{z-1}{z}q_{B/B_0}(\rho_{AB} - \rho_{AB_1} - \rho_{AB_2}) - \rho_{AB_1}, \\ \frac{d\rho_{AB_1}}{d\tau} &= p\tfrac{z-1}{z}q_{C/B_0}(\rho_{AB} - \rho_{AB_1} - \rho_{AB_2}) - \rho_{AB_1}, -\rho_{AB_2}. \end{aligned}$$

the equilibrium of which is:

$$\begin{aligned} \tilde{\rho}_{AB_1} &= \frac{(z-1)\rho_{AB}\rho_{BB}\Pi(q_{X/B})}{\rho_{BX}(z - \Pi(q_{X/B}))}, \\ \tilde{\rho}_{AB_2} &= \frac{(z-1)\rho_{AB}\rho_{BC}\Pi(q_{X/B})}{\rho_{BX}(z - \Pi(q_{X/B}))}. \end{aligned} \tag{6.4.9}$$

The variable $\tilde{\rho}_{AC_1}$ develops according to:

$$\frac{d\rho_{AC_1}}{d\tau} = p\tfrac{z-1}{z}q_{X/C_0}(\rho_{AC} - \rho_{AC_1}) - \rho_{AC_1},$$

which has has equilibrium:

$$\tilde{\rho}_{AC_1} = \frac{(z-1)\rho_{AC}\Pi(q_{X/C})}{z - \Pi(q_{X/C})}. \tag{6.4.10}$$

The complete fast equilibrium in the original variables is denoted $\tilde{\rho}$.

Aggregated Dynamics

By summing equations that arise as in the first term of the outer asymptotic expansion of the original system ((6.4.1) and (6.4.2) under (6.1.3)) about the fast equilibrium $\tilde{\rho}$ a timescale separated system in the aggregated variables is obtained:

$$\begin{aligned}
\frac{d\rho_B}{dt} &= \mu b\left(\tilde{\rho}_{AB_1} + \tfrac{\nu}{2}\tilde{\rho}_{AB_2}\right) - \rho_B,\\
\frac{d\rho_C}{dt} &= b\left(\tilde{\rho}_{AC_1} + \tfrac{\mu\nu}{2}\tilde{\rho}_{AB_2}\right) - \rho_C,\\
\frac{d\rho_{AB}}{dt} &= \frac{\mu b\left(\rho_{AB_1} + \frac{\nu}{2}\rho_{AB_2}\right)\left((z-1)\rho_{AA} - \rho_A\right)}{z\rho_A}\\
&\quad - \frac{b(z-1)\left(\mu\rho_{AB_1} + \mu\nu\rho_{AB_2} + \rho_{AC_1}\right)\rho_{AB}}{z\rho_A} + \rho_B - 2\rho_{AB},\\
\frac{d\rho_{AC}}{dt} &= \frac{b\left(\rho_{AC_1} + \frac{\mu\nu}{2}\rho_{AB_2}\right)\left((z-1)\rho_{AA} - \rho_A\right)}{z\rho_A}\\
&\quad - \frac{b(z-1)\left(\mu\rho_{AB_1} + \mu\nu\rho_{AB_2} + \rho_{AC_1}\right)\rho_{AC}}{z\rho_A} + \rho_C - 2\rho_{AC},\\
\frac{d\rho_{BC}}{dt} &= b(z-1)\frac{\mu\left(\rho_{AB_1} + \frac{\nu}{2}\rho_{AB_2}\right)\rho_{AC} + \left(\rho_{AC_1} + \frac{\mu\nu}{2}\rho_{AB_2}\right)\rho_{AB}}{z\rho_A} - 2\rho_{BC}.
\end{aligned} \tag{6.4.11}$$

The region of interest for the aggregated dynamics is delimited by the following inequalities:

$$\rho_B,\ \rho_C,\ \rho_{AB},\ \rho_{AC},\ \rho_{BC} \geq 0, \tag{6.4.12a}$$

$$\rho_B + \rho_C \leq 1, \tag{6.4.12b}$$

$$\rho_{AB} + \rho_{AC} \leq 1 - \rho_B - \rho_C, \tag{6.4.12c}$$

$$\rho_{AB} + \rho_{BC} \leq \rho_B, \tag{6.4.12d}$$

$$\rho_{AC} + \rho_{BC} \leq \rho_C. \tag{6.4.12e}$$

This region is readily shown to be invariant under (6.4.11).

Single Conspecific Populations

In the absence of asexuals the sexual-asexual model coincides with the sexual species model with the seed production parameter modified to μb. In which case the analysis is identical: Two non-trivial equilibria exist for $p \geq p^s_{\text{crit}}$ where:

$$p^s_{\text{crit}} = \frac{4\mu bz(z-1)}{(\mu b(z-1)-z)^2}.$$

Of the non-trivial equilibria only the attracting stable node equilibrium is in the region of interest if $p \geq p^s_{\text{trans}}$ where:

$$p^s_{\text{trans}} = \frac{\mu bz^3}{(\mu b(z-1)-z)^2}.$$

The sexual-only carrying equilibrium is denoted $\hat{\rho}^s = (\hat{\rho}_B, 0, \hat{\rho}_B - \hat{\rho}_{BB}, 0, 0)$.

In the absence of sexuals the model coincides precisely with the sexual species model if state C is relabelled state B. Non-trivial equilibria exist for $p \geq p^a_{\text{crit}} = p_{\text{crit}}$ only the stable one of which is in the region of interest if $p \geq p^s_{\text{trans}} = p_{\text{trans}}$. The asexual-only carrying equilibrium is denoted $\hat{\rho}^a = (0, \hat{\rho}_C, 0, \hat{\rho}_C - \hat{\rho}_{CC}, 0)$.

Asexual Invasion

The stability of the sexual-only carrying equilibrium to asexual invasion can be assessed in the same way as the stability of the hermaphrodite-only equilibrium was in the gynodioecy model. The neighbourhood composition of rare asexuals in a population of sexuals is found as the equilibrium of neighbourhood dynamic equations under the assumption of negligible asexual frequency. The per-capita rate of increase in asexuals in equilibrium neighbourhoods indicates stability.

When asexuals are rare, very few empty or sexual sites will have any in their neighbourhoods and thus $q_{C/A}$ and $q_{C/B}$ will be negligible. By contrast the the local densities of empty and sexual sites in the neighbourhoods of asexuals $q_{A/C}$ and $q_{B/C}$

will be non-negligible and they will develop according to:

$$\begin{aligned}
\frac{dq_{A/C}}{dt} =& \frac{1}{\rho_C}\left(\frac{d\rho_{AC}}{dt} - q_{A/C}\frac{d\rho_C}{dt}\right) \\
=& b\left(\frac{\rho_{AC_1} + \frac{\mu\nu}{2}\rho_{AB_2}}{\rho_C}\right)\left(\frac{(z-1)\rho_{AA}}{z\rho_A} - \frac{1}{z} - q_{A/C}\right) \\
& - \left(\frac{\mu b(z-1)\rho_{AB_1}}{z\rho_A} + 1\right) q_{A/C} + 1, \\
\frac{dq_{B/C}}{dt} =& \frac{1}{\rho_C}\left(\frac{d\rho_{BC}}{dt} - q_{B/C}\frac{d\rho_C}{dt}\right) \\
=& b\left(\frac{\rho_{AC_1} + \frac{\mu\nu}{2}\rho_{AB_2}}{\rho_C}\right)\left(\frac{(z-1)\rho_{AB}}{z\rho_A} - q_{B/C}\right) \\
& - \frac{\mu b(z-1)\rho_{AB_1}}{z\rho_A} q_{A/C} - q_{B/C},
\end{aligned} \tag{6.4.13}$$

where

$$\begin{aligned}
\frac{\rho_{AC_1}}{\rho_C} &= \frac{(z-1)\Pi(1-q_{A/C})}{z-\Pi(1-q_{A/C})} q_{A/C}, \\
\frac{\rho_{AB_2}}{\rho_C} &= \frac{(z-1)\rho_{AB}\Pi(q_{B/B})}{\rho_{BB}(z-\Pi(q_{B/B}))} q_{B/C}.
\end{aligned}$$

The neighbourhood dynamics (6.4.13) form a closed system when all other variables are evaluated at the sexual-only equilibrium $\hat{\rho}^s$. Considering nullclines $\dot{q}_{A/C} = 0$ yields:

$$\begin{aligned}
q_{B/C} =& \frac{2\rho_{BB}(z-\Pi(q_{B/B}))}{\mu\nu(z-1)\rho_{AB}\Pi(q_{B/B})} \\
& \times \left(\frac{(\mu b(z-1)q_{B_1/A} + z)q_{A/C} - z}{b((z-1)q_{A/A} - 1 - zq_{A/C})} - \frac{(z-1)\Pi(1-q_{A/C})}{z-\Pi(1-q_{A/C})} q_{A/C}\right),
\end{aligned}$$

and $\dot{q}_{B/C} = 0$ yields:

$$q_{B/C}^2 + \gamma_1 q_{B/C} + \gamma_0 = 0,$$

where

$$\begin{aligned}
\gamma_1 &= \frac{2\rho_{BB}(z-\Pi(q_{B/B}))}{\mu\nu(z-1)\rho_{AB}\Pi(q_{B/B})}\left(\frac{(z-1)\Pi(1-q_{A/C})}{z-\Pi(1-q_{A/C})} q_{A/C} + \frac{1}{b}\right) - \frac{z-1}{z} q_{B/A}, \\
\gamma_0 &= \frac{2\rho_{BB}(z-\Pi(q_{B/B}))}{\mu\nu(z-1)\rho_{AB}\Pi(q_{B/B})}\left(\frac{(z-1)^2\Pi(1-q_{A/C})}{z(z-\Pi(1-q_{A/C}))} q_{B/A} + \mu\frac{z-1}{z} q_{B_1/A}\right) q_{A/C}.
\end{aligned}$$

From these nullclines the asexual invasion neighbourhood $(\hat{q}_{A/C}, \hat{q}_{B/C})$ is readily obtained numerically. Once the equilibrium invasion neighbourhood is known the stability of $\hat{\rho}^s$ can be assessed. If asexuals with equilibrium invasion neighbourhood have a positive per-capita growth rate:

$$\frac{1}{\rho_C}\frac{d\rho_C}{dt} = b\left(\frac{\rho_{AC_1} + \frac{\mu\nu}{2}\rho_{AB_2}}{\rho_C}\right) - 1,$$

then the sexual-only equilibrium is unstable and sexual populations are vulnerable to invasion. The threshold value of μ at which stability is lost is denoted μ_1 in line with the notation of chapter 3 3.4, that is for $\mu \leq \mu_1$ the sexual-only equilibrium is unstable.

Figure 6-9(a) shows sample solutions in the (ρ_B,ρ_C) phase plane when asexual invasion of an established sexual population is possible; in this case the asexual reproductive mode becomes fixed. In Figure 6-9(c) parameters are also in the region where asexuals invasion is predicted; in this case however, the asexual reproductive mode does not fix. Figure 6-10 illustrates how μ_1 varies with ν for fixed reproductive parameters b and p, the corresponding bifurcation value of the mean field model is also provided. The PA predicts that the sexual-only equilibrium is stable over a greater region of $(\nu,\ \mu)$ parameter space. This occurs because when μ is low, rare asexuals do better if their neighbourhoods contain mostly sexuals, as is assumed in the mean field. In the PA the neighbourhoods of rare asexual contain significant numbers of other asexuals.

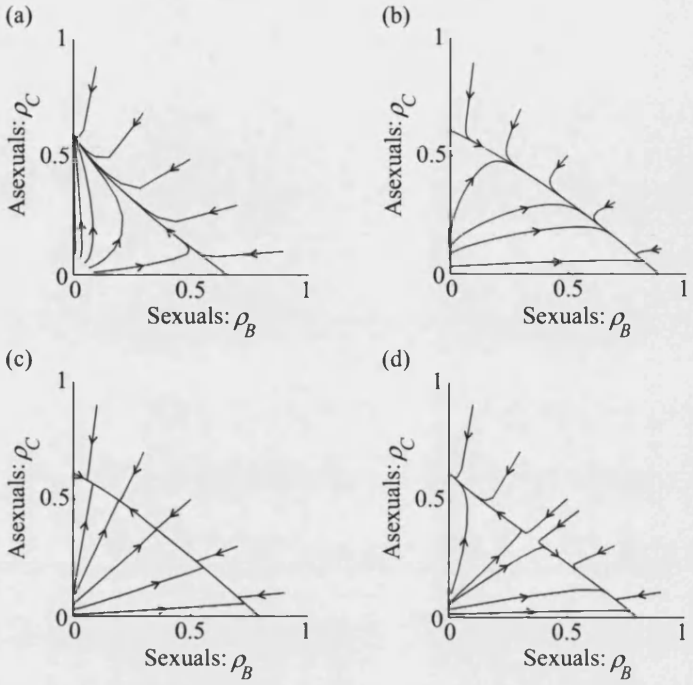

Figure 6-9: Sample solutions of the aggregated dynamics of the PA to the sexual-asexual IPS model. Parameters $p = 4$, $b = 4$. (a) $\mu = 1.1$, $\nu = 0.5$. (b) $\mu = 2.8$, $\nu = 0.5$. (c) $\mu = 1.7$, $\nu = 0.5$. (d) $\mu = 1.7$, $\nu = 0.99$.

Sexual Invasion

The stability of the asexual-only equilibrium $\hat{\rho}^a$ is assessed in precisely the same way as the sexual-only equilibrium. The neighbourhood dynamics of rare sexuals are:

$$\begin{aligned}
\frac{dq_{A/B}}{dt} =& \frac{1}{\rho_B}\left(\frac{d\rho_{AB}}{dt} - q_{A/B}\frac{d\rho_B}{dt}\right) \\
=& \mu b\left(\frac{\rho_{AB_1} + \frac{\nu}{2}\rho_{AB_2}}{\rho_B}\right)\left(\frac{(z-1)\rho_{AA}}{z\rho_A} - \frac{1}{z} - q_{A/B}\right) \\
& - \left(\frac{b(z-1)\rho_{AC_1}}{z\rho_A} + 1\right) q_{A/B} + 1, \\
\frac{dq_{C/B}}{dt} =& \frac{1}{\rho_B}\left(\frac{d\rho_{BC}}{dt} - q_{C/B}\frac{d\rho_B}{dt}\right) \\
=& \mu b\left(\frac{\rho_{AB_1} + \frac{\nu}{2}\rho_{AB_2}}{\rho_B}\right)\left(\frac{(z-1)\rho_{AC}}{z\rho_A} - q_{C/B}\right) \\
& - \frac{b(z-1)\rho_{AC_1}}{z\rho_A} q_{A/B} - q_{C/B},
\end{aligned} \tag{6.4.14}$$

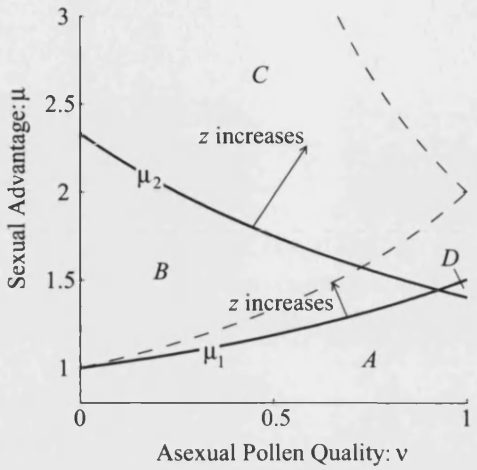

Figure 6-10: (ν,μ) parameter space for the aggregated dynamics of the PA to the sexual-asexual IPS model. Four regions of model behaviour can be distinguished: A - Asexual reproduction fixes in all mixed populations. B - Bistability: Rare reproductive mode will be eliminated. C - Sexual reproduction fixes in all mixed populations. D - Coexistence. Dashed curve recalls mean field boundaries between model behaviour. Parameters $p = 4$, $b = 4$, $z = 4$.

where

$$\frac{\rho_{AB_1}}{\rho_B} = \frac{(z-1)\Pi(1-q_{A/B})(1-q_{C/B}-q_{A/B})q_{A/B}}{(z-\Pi(1-q_{A/B}))(1-q_{A/B})},$$
$$\frac{\rho_{AB_2}}{\rho_B} = \frac{(z-1)\Pi(1-q_{A/B})q_{C/B}q_{A/B}}{(z-\Pi(1-q_{A/B}))(1-q_{A/B})}.$$

Considering nullclines $\dot{q}_{A/B} = 0$ yields:

$$q_{C/B} = \frac{(1-q_{A/B})(z-\Pi(1-q_{A/B}))((b(z-1)q_{C_1/A}+z)q_{A/B}-z)}{\mu b(z-1)(\frac{\nu}{2}-1)\Pi(1-q_{A/B})q_{A/B}((z-1)q_{A/A}-1)} - \frac{1-q_{A/B}}{\frac{\nu}{2}-1},$$

and $\dot{q}_{C/B} = 0$ yields:

$$q_{C/B}^2 + \gamma_1 q_{C/B} + \gamma_0 = 0,$$

where

$$\gamma_1 = \frac{(1-q_{A/B})(z-\Pi(1-q_{A/B}))}{\mu b(z-1)(1-\frac{\nu}{2})\Pi(1-q_{A/B})q_{A/B}} + \frac{1-q_{A/B}}{1-\frac{\nu}{2}} + \frac{z-1}{z}q_{C/A},$$

$$\gamma_0 = \frac{(1-q_{A/B})(z-\Pi(1-q_{A/B}))(b(z-1)q_{C_1/A})}{\mu bz(z-1)(1-\frac{\nu}{2})\Pi(1-q_{A/B})} + \frac{(1-q_{A/B})(z-1)q_{C/A}}{z(1-\frac{\nu}{2})}.$$

From these nullclines the asexual invasion neighbourhood $(\hat{q}_{A/C}, \hat{q}_{B/C})$ is readily obtained numerically. If sexuals with equilibrium invasion neighbourhood have a positive per-capita growth rate:

$$\frac{1}{\rho_B}\frac{d\rho_B}{dt} = \mu b\left(\frac{\rho_{AB_1} + \frac{\nu}{2}\rho_{AB_2}}{\rho_B}\right) - 1,$$

then the asexual-only equilibrium is unstable and asexual populations are vulnerable to invasion. The threshold value of μ at which stability is lost is denoted μ_2, that is for $\mu > \mu_2$ the asexual-only equilibrium is unstable.

Figure 6-9(b) gives sample solutions in (ρ_B,ρ_c) phase space when sexual invasion of an established asexual population is possible. Invasion results in fixation of the sexual reproductive mode. In Figure 6-9(c) both reproductive modes can invade each other and coexistence results. Figure 6-10 illustrates how the threshold μ_2 varies with ν for fixed reproductive parameters p and b. The pair-approximation predicts that the asexual-only equilibrium is stable over a smaller region of (ν, μ) parameter space. Asexuals are vulnerable to invasion from arbitrarily small numbers of sexuals with lower reproductive advantage μ than predicted by the mean field. A consequence of the lower value of μ_2 in the PA is that the region of bistability $\mu_1 < \mu \leq \mu_2$ is reduced. This effect was observed more markedly in simulations of the IPS model. Figure 6-9(d) shows sample solutions from the bistable region.

Discussion

Any bistability found in the sexual-asexual IPS model of chapter 5 is the result of either the finite lattice size used in simulations or the non-generic nature of the chosen initial conditions. The PA predicts a relatively wide region of bistability. Figures 6-11(a)-(d) compare the invasion thresholds predicted by the PA and the outcomes of simulations with various initial conditions. The PA assumes infinite lattice size so bistability either results because the invasion conditions are not generic or because of

some other deficiency of the approximation. Although the PA can accommodate the different neighbourhoods for different states, every individual of the same state is effectively assumed to have the same neighbourhood. Thus for a small density of invaders the stochastic variety in neighbourhoods, which in an infinite IPS ensures that some quite large clusters of invaders occur, is absent. In this respect the initial conditions assumed in PA invasions are non generic. In the PA, then, the likelihood of invasion is calculated prior to the establishment of monomorphic clusters: every individual is effectively a boundary individual. Following a successful invasion, however, the PA fails to properly capture the formation of monomorphic clusters. This arises because correlations beyond pairs are not tracked and neighbourhoods are homogenized. Consider a population consisting of two clusters, one of sexuals and the other of asexuals. In the interior of the clusters assume that individuals have on average unit reproductive success, this interior equilibrium means a proportion of interior sites are empty. Suppose this configuration is used to parameterize initial conditions for the PA. The PA supplies the probability that a randomly chosen empty site has a sexual neighbour and the probability it has an asexual neighbour but does not make a distinction between the empty sites within the sexual cluster and those in the asexual cluster. Thus it is impossible for the PA to represent monomorphic clusters. Figure 6-12 illustrates the contrast in neighbourhoods between simulations of the IPS in which monomorphic clusters form and the PA in which clusters cannot be accommodated.

The region of coexistence predicted by the PA (Figure 6-10) is almost certainly another artifact of the failure of the PA to capture the monomorphic clustering in the IPS and the dominant role boundary dynamics play in securing fixation of one or other reproductive mode. If a mixed equilibrium is to occur for some densities ρ_B and ρ_C in the IPS, the frequencies of individuals found in the boundary between monomorphic clusters must precisely match this equilibrium density. Otherwise one type will increase at the expense of the other and the boundary between clusters will tend to drift favouring the global dominance of this type. Such an equilibrium would not be structurally stable.

6.5 DISCUSSION

The modelling work in this chapter has demonstrated the useful role that moment-closure approximations can play in elucidating the ways in which the behaviour of IPS models differs from homogeneous mixing models. However, it must be borne in mind

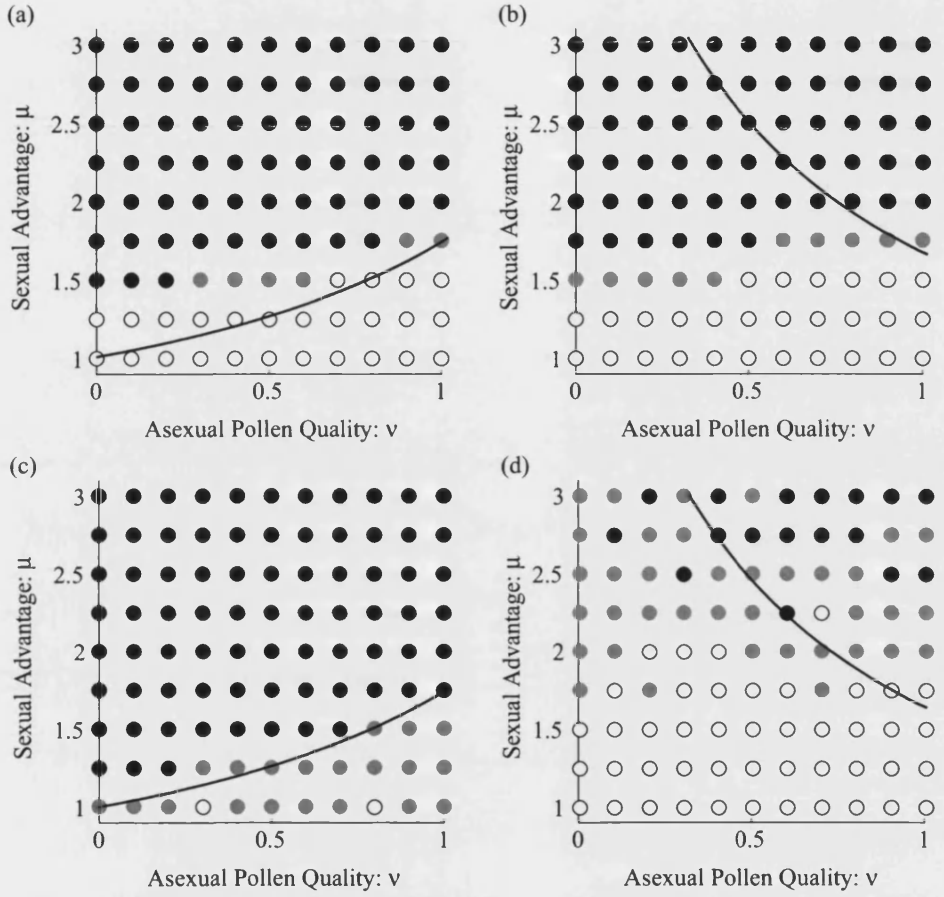

Figure 6-11: Comparison of invasion thresholds in the PA with model behaviour predicted by simulation. Simulation initial conditions: (a) Sexuals outnumber asexuals 3 : 1 in simulations with generic initial conditions. (b) Asexuals outnumber sexuals 3 : 1 in simulations with generic initial conditions. (c) Sexuals introduced in a 3×3 clump into a population fixed for asexual reproduction. (d) Asexuals introduced in a 3×3 clump into a population fixed for sexual reproduction. White circles indicate asexual reproduction fixes, black circles indicate sexual reproduction fixes and grey circles indicates population still mixed at $t = 200$. Parameters $p = 4$, $b = 4$, $z = 8$.

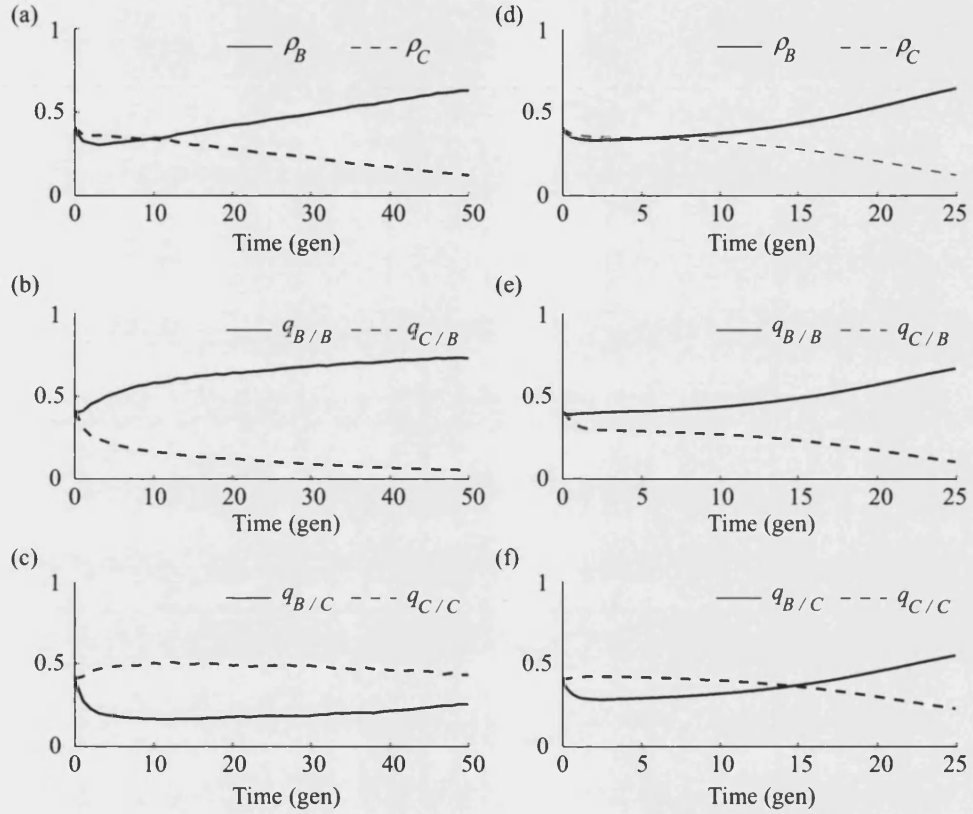

Figure 6-12: Comparison of neighbourhood composition exhibited by simulations and that predicted by PA in the sexual-asexual IPS model. (a)-(c) Average of 25 simulation runs on $L = 100$ lattice with 40% of sites initially occupied by sexuals and 40% by asexuals distributed randomly. (d)-(f) PA initialized with data from simulation initial conditions. (a) and (d) population densities. (b) and (e) local density of sexuals $q_{B/B}$ and asexuals $q_{C/B}$ in the neighbourhoods of sexuals. (c) and (f) local density of sexuals $q_{B/B}$ and asexuals $q_{C/B}$ in the neighbourhoods of asexuals. Parameters $p = 4$, $b = 4$, $\mu = 1.75$, $\nu = 0.5$, $z = 8$

that the PA derives from a heuristic argument and there is not at present rigourous underlying theory to ensure that the behaviour of the PA is any more representative of IPS behaviour than the mean field approximation. The popularity of moment closure methods results from their relative simplicity and empirical observations of an improved match with simulations. In particular the PA tends to be most accurate when the assumption that all sites of one state have the same neighbourhood composition, or at least that the distribution of neighbourhood compositions is unimodal. In the sexual-asexual models above and to a lesser extent in the gynodioecy model this assumption is a poor one, because simulations show that monomorphic clusters arise. Clustering results in the distribution of the neighbourhoods of empty sites being bi-modal because empty-sites in the interior of a cluster have neighbours only of one type.

The PA introduced here was first used, at least in an ecological context, by Matsuda et al. (1992) and is sometimes referred to as the ordinary pair-approximation. The choice of approximation to close the moment equations is by no means unique and various alternatives are available (Iwasa 2000). Improvements to the ordinary PA often exploit details specific to the model under considerations. In the epidemic model on a lattice proposed by Sato et al. (1994) susceptibles and infecteds naturally aggregate with other individuals of the same type by virtue of the inheritance of disease status from parent to offspring. The probabilities $q_{S/00}$, $q_{S/0S}$ and $q_{S/0I}$ are all estimated by the ordinary PA by $q_{S/0}$, where 0, S and I denote empty, susceptible and infected cells of the lattice respectively. Sato et al. (1994) observe that while $q_{S/0}$ is probably a good estimate for $q_{S/0I}$, as a result of the aggregation of susceptibles it is an over estimate for $q_{S/00}$ and an underestimate for $q_{S/0S}$. To incorporate this observation they propose the introduction of a discounting factor δ so that:

$$q_{S/00} \approx \delta q_{S/0}$$
$$q_{S/0S} \approx 1 - q_{I/0} - \delta q_{S/0}$$

An appropriate value of δ is estimated from the critical value for ergodicity in the basic contact process (Katori & Konno 1991). Although the same discounting factor is not appropriate in the models presented above, the principle of population clumping affecting the accuracy of the PA estimate must carry over, more so in fact because clumping is a prerequisite of colonization. It might be predicted, for example, that $q_{B_1/AB}$ should be greater than $q_{B_1/AA}$ not only because of clumped nature of the population, but because the occupied cell in the AB pair might very well be responsible for the pollinated

status of the neighbouring B_1 cell. This is the case at least when triplets in the lattice under consideration have a chance of being closed triangles. Regular lattices with neighbourhood size greater than 6 have this property: On a hexagonal lattice a third of all triplets are closed triangles.

While it is satisfying that the PAs in this chapter identify qualitative behaviours or trends present in the IPS models, it is unsettling that population growth and decline looks very different in simulation and in PA (see Figures 6-3,6-7 and 6-12.) It has been suggested by Mollison (*Pers. Comm.*) that it is erroneous to associate a PA prediction with a regular lattice, and that it is in fact an approximation of a process on a random graph with fixed degree (neighbourhood size.) Population growth on a random graph is initially exponential like the PA because there is a much smaller chance of neighbouring occupied sites sharing neighbours and hence competing for empty sites to colonize. The irregular connection of sites on a random graph makes several of the PA predictions in this chapter more plausible. For example, a small sexual population on a random graph would experience less competition for sites to colonize, but would by the same token be less likely to have numerous pollen providing neighbours. In a small population on a random graph few individuals would have more than one occupied neighbour and if this were a prerequisite for unit reproductive success then the population would decline. In the gynodioecy model on a random graph female competition for pollen would be reduced because a female's offspring would rarely be placed in adjacent sites. The threshold for female invasion would be lower. In the sexual-asexual model on a random graph monomorphic clusters would not become established and sexual and asexual individuals would see a great deal more of each other than the model predicts on a regular lattice. The greater accuracy of the pair approximation in describing the behaviour of a random graph model is appealing and assists in explaining the PA inaccuracy in describing the IPS models of chapter 5. A random graph is not, however, a spatial model and is of dubious relevance to the modelling of plant populations.

6.A JACOBIAN FOR GYNODIOECY AGGREGATED DYNAMICS

The terms of the 5×5 Jacobian for the aggregated PA of the gynodioecy IPS model (6.3.13) are given below using the following notation:

$$J_{\varsigma,\varsigma'} = \frac{\partial}{\partial \rho_{\varsigma'}} \left(\frac{d\rho_{\varsigma}}{dt} \right) \quad \text{where } \varsigma, \varsigma' \in \{B, C, AB, AC, BC\}.$$

So the complete Jacobian is given by:

$$J = \begin{pmatrix} J_{B,B} & J_{B,C} & J_{B,AB} & J_{B,AC} & J_{B,BC} \\ J_{C,B} & J_{C,C} & J_{C,AB} & J_{C,AC} & J_{C,BC} \\ J_{AB,B} & J_{AB,C} & J_{AB,AB} & J_{AB,AC} & J_{AB,BC} \\ J_{AC,B} & J_{AC,C} & J_{AC,AB} & J_{AC,AC} & J_{AC,BC} \\ J_{BC,B} & J_{BC,C} & J_{BC,AB} & J_{BC,AC} & J_{BC,BC} \end{pmatrix},$$

$$\begin{aligned} J_{B,B} &= b\frac{\partial \tilde{\rho}_{AB_1}}{\partial \rho_B} - 1, & J_{C,B} &= 0, \\ J_{B,C} &= 0, & J_{C,C} &= b\frac{\partial \tilde{\rho}_{AC_1}}{\partial \rho_C} - 1, \\ J_{B,AB} &= b\frac{\partial \tilde{\rho}_{AB_1}}{\partial \rho_{AB}}, & J_{C,AB} &= 0, \\ J_{B,AC} &= 0, & J_{C,AC} &= b\frac{\partial \tilde{\rho}_{AC_1}}{\partial \rho_{AC}}, \\ J_{B,BC} &= b\frac{\partial \tilde{\rho}_{AB_1}}{\partial \rho_{BC}}, & J_{C,BC} &= b\frac{\partial \tilde{\rho}_{AC_1}}{\partial \rho_{BC}}, \end{aligned}$$

$$
\begin{aligned}
J_{AB,B} &= b\frac{\partial\tilde{\rho}_{AB_1}}{\partial\rho_B}\left(\frac{(z-1)(\rho_{AA}-\rho_{AB})-\rho_A}{z\rho_A}\right) \\
&\quad -\frac{b(z-1)(\tilde{\rho}_{AB_1}\rho_{AC}+\mu\tilde{\rho}_{AC_1}\rho_{AB})}{z\rho_A^2}+1, \\
J_{AB,C} &= -\mu b\frac{\partial\tilde{\rho}_{AC_1}}{\partial\rho_C}\frac{(z-1)\rho_{AB}}{z\rho_A}-\frac{b(z-1)(\tilde{\rho}_{AB_1}\rho_{AC}+\mu\tilde{\rho}_{AC_1}\rho_{AB})}{z\rho_A^2}, \\
J_{AB,AB} &= \frac{b\frac{\partial\tilde{\rho}_{AB_1}}{\partial\rho_{AB}}((z-1)(\rho_{AA}-\rho_{AB})-\rho_A)-b(z-1)(2\tilde{\rho}_{AB_1}-\mu\tilde{\rho}_{AC_1})}{z\rho_A}-2, \\
J_{AB,AC} &= \frac{-b(z-1)\tilde{\rho}_{AB_1}-\mu b(z-1)\rho_{AB}\frac{\partial\tilde{\rho}_{AC_1}}{\partial\rho_{AC}}}{z\rho_A}, \\
J_{AB,BC} &= \frac{b\frac{\partial\tilde{\rho}_{AB_1}}{\partial\rho_{BC}}((z-1)\rho_{AA}-\rho_A)-b(z-1)\rho_{AB}\left(\frac{\partial\tilde{\rho}_{AB_1}}{\partial\rho_{BC}}+\mu\frac{\partial\tilde{\rho}_{AC_1}}{\partial\rho_{BC}}\right)}{z\rho_A}, \\
J_{AC,B} &= -\mu b\frac{\partial\tilde{\rho}_{AB_1}}{\partial\rho_B}\frac{(z-1)\rho_{AC}}{z\rho_A}-\frac{b(z-1)(\tilde{\rho}_{AB_1}\rho_{AC}+\mu\tilde{\rho}_{AC_1}\rho_{AB})}{z\rho_A^2}, \\
J_{AC,C} &= \mu b\frac{\partial\tilde{\rho}_{AC_1}}{\partial\rho_C}\left(\frac{(z-1)(\rho_{AA}-\rho_{AB})-\rho_A}{z\rho_A}\right) \\
&\quad -\frac{b(z-1)(\tilde{\rho}_{AB_1}\rho_{AC}+\mu\tilde{\rho}_{AC_1}\rho_{AB})}{z\rho_A^2}+1, \\
J_{AC,AB} &= \frac{-\mu b(z-1)\tilde{\rho}_{AC_1}-b(z-1)\rho_{AC}\frac{\partial\tilde{\rho}_{AB_1}}{\partial\rho_{AB}}}{z\rho_A}, \\
J_{AC,AC} &= \frac{\mu b\frac{\partial\tilde{\rho}_{AC_1}}{\partial\rho_{AC}}((z-1)(\rho_{AA}-\rho_{AB})-\rho_A)-b(z-1)(\tilde{\rho}_{AB_1}-2\mu\tilde{\rho}_{AC_1})}{z\rho_A}-2, \\
J_{AC,BC} &= \frac{\mu b\frac{\partial\tilde{\rho}_{AC_1}}{\partial\rho_{BC}}((z-1)\rho_{AA}-\rho_A)-b(z-1)\rho_{AB}\left(\frac{\partial\tilde{\rho}_{AB_1}}{\partial\rho_{BC}}+\mu\frac{\partial\tilde{\rho}_{AC_1}}{\partial\rho_{BC}}\right)}{z\rho_A},
\end{aligned}
$$

$$
\begin{aligned}
J_{BC,B} &= b\frac{\partial\tilde{\rho}_{AB_1}}{\partial\rho_B}\frac{(z-1)\rho_{AC}}{z\rho_A} - \frac{b(z-1)(\tilde{\rho}_{AB_1}\rho_{AC}+\mu\tilde{\rho}_{AC_1}\rho_{AB})}{z\rho_A^2},\\
J_{BC,C} &= \mu b\frac{\partial\tilde{\rho}_{AC_1}}{\partial\rho_C}\frac{(z-1)\rho_{AB}}{z\rho_A} - \frac{b(z-1)(\tilde{\rho}_{AB_1}\rho_{AC}+\mu\tilde{\rho}_{AC_1}\rho_{AB})}{z\rho_A^2},\\
J_{BC,AB} &= \frac{b(z-1)\left(\frac{\partial\tilde{\rho}_{AB_1}}{\partial\rho_{AB}}\rho_{AC}+\mu\tilde{\rho}_{AC_1}\right)}{z\rho_A},\\
J_{BC,AC} &= \frac{b(z-1)\left(\tilde{\rho}_{AB_1}+\mu\frac{\partial\tilde{\rho}_{AC_1}}{\partial\rho_{AC}}\rho_{AB}\right)}{z\rho_A},\\
J_{BC,BC} &= \frac{b(z-1)\left(\frac{\partial\tilde{\rho}_{AB_1}}{\partial\rho_{BC}}\tilde{\rho}_{AC}+\mu\frac{\partial\tilde{\rho}_{AC_1}}{\partial\rho_{BC}}\rho_{AB}\right)}{z\rho_A} - 2,
\end{aligned}
$$

where:

$$
\begin{aligned}
\frac{\partial\tilde{\rho}_{AB_1}}{\partial\rho_B} &= \frac{\rho_{AB}}{\rho_{AB}+\rho_{BC}}\left(\frac{p+1}{p}\frac{\partial\tilde{\rho}_{B_1}}{\partial\rho_B}\right),\\
\frac{\partial\tilde{\rho}_{AB_1}}{\partial\rho_{AB}} &= \frac{\rho_{AB}}{\rho_{AB}+\rho_{BC}}\left(\frac{p+1}{p}\frac{\partial\tilde{\rho}_{B_1}}{\partial\rho_{AB}}+1\right)+\frac{\rho_{BC}}{(\rho_{AB}+\rho_{BC})^2}\left(\frac{p+1}{p}\tilde{\rho}_{B_1}-\rho_{BB}\right),\\
\frac{\partial\tilde{\rho}_{AB_1}}{\partial\rho_{BC}} &= \frac{\rho_{AB}}{\rho_{AB}+\rho_{BC}}\left(\frac{p+1}{p}\frac{\partial\tilde{\rho}_{B_1}}{\partial\rho_{BC}}+1\right)-\frac{\rho_{AB}}{(\rho_{AB}+\rho_{BC})^2}\left(\frac{p+1}{p}\tilde{\rho}_{B_1}-\rho_{BB}\right),
\end{aligned}
$$

$$
\begin{aligned}
\frac{\partial\tilde{\rho}_{AC_1}}{\partial\rho_C} &= \frac{\rho_{AC}}{\rho_C-\rho_{BC}}\left(\frac{p+1}{p}\frac{\partial\tilde{\rho}_{C_1}}{\partial\rho_C}\right)-\frac{\rho_{AC}}{(\rho_C-\rho_{BC})^2}\left(\frac{p+1}{p}\tilde{\rho}_{C_1}-\rho_{BC}\right),\\
\frac{\partial\tilde{\rho}_{AC_1}}{\partial\rho_{AC}} &= \frac{1}{\rho_C-\rho_{BC}}\left(\frac{p+1}{p}\tilde{\rho}_{C_1}-\rho_{BC}\right),\\
\frac{\partial\tilde{\rho}_{AC_1}}{\partial\rho_{BC}} &= \frac{\rho_{ACB}}{\rho_C-\rho_{BC}}\left(\frac{p+1}{p}\frac{\partial\tilde{\rho}_{C_1}}{\partial\rho_{BC}}-1\right)+\frac{\rho_{AC}}{(\rho_C-\rho_{BC})^2}\left(\frac{p+1}{p}\tilde{\rho}_{C_1}-\rho_{BC}\right),
\end{aligned}
$$

and where:

$$\begin{aligned}
\frac{\partial \tilde{\rho}_{B_1}}{\partial \rho_B} &= \frac{zp\rho_{BB} - (p+z)\tilde{\rho}_{B_1}}{\sqrt{((p+z)\rho_B + zp\rho_{BB})^2 - 4zp(p+1)\rho_B\rho_{BB}}}, \\
\frac{\partial \tilde{\rho}_{B_1}}{\partial \rho_{AB}} = \frac{\partial \tilde{\rho}_{B_1}}{\partial \rho_{BC}} &= \frac{-zp(\rho_B + \tilde{\rho}_{B_1})}{\sqrt{((p+z)\rho_B + zp\rho_{BB})^2 - 4zp(p+1)\rho_B\rho_{BB}}}, \\
\\
\frac{\partial \tilde{\rho}_{C_1}}{\partial \rho_C} &= \frac{zp\rho_{BC} - (p+z)\tilde{\rho}_{C_1}}{\sqrt{((p+z)\rho_C + zp\rho_{BC})^2 - 4zp(p+1)\rho_C\rho_{BC}}}, \\
\frac{\partial \tilde{\rho}_{C_1}}{\partial \rho_{BC}} &= \frac{zp(\rho_C - \tilde{\rho}_{C_1})}{\sqrt{((p+z)\rho_C + zp\rho_{BC})^2 - 4zp(p+1)\rho_C\rho_{BC}}}.
\end{aligned}$$

CHAPTER 7

Summary and Discussion

This chapter will draw together the results of the example models explored in chapters 3 to 6 and examine future directions for research in spatial ecology and flowering plant reproductive diversity.

7.1 SUMMARY OF FINDINGS

Sexual Species

Intuitively small populations of self-incompatible sexual species should be expected to experience restricted growth resulting from the need to find mates. A lone self-incompatible individual cannot found a population, but how many more individuals are required before deterministic constraints are overcome? What determines the threshold and is the threshold merely a minimum population size? o Or does it prescribe other facets of population structure such as spatial configuration? This report provides partial answers to these questions. Partial in that they are circumscribed by the numerous specific assumptions introduced in model derivations. In fact the report provides answers several times over in the context of different modelling approaches.

In the non-spatial model of chapter 3 the establishment threshold is comprised only of a minimum population size determined by the reproductive effort expended in pollen and seed production. In typical flowering plant species these rates will be very high and consequently the threshold will be low. But note that the threshold is obtained as a scaled population size and determining the corresponding true population size requires multiplication by a factor involving the population carrying capacity. The threshold therefore scales linearly with population carrying capacity.

In the explicitly spatial reaction-diffusion models of chapter 4 the above factors determine threshold size for spatially uniform populations. For non-uniform populations the gradient and curvature of population boundaries of small populations are also

crucial to their establishment. In qualitatively similar models Lewis & Kareiva (1993) show that steeper gradients and tighter curvature increase rates of diffusion and inhibit the establishment of small populations.

In chapter 5 the dependence of threshold on population carrying capacity is shown to be an artifact of the contact assumptions of population-based models. Interactions between individuals are assumed rare in small populations, but this is unlikely to be the case early on in naturally occurring invasions where most individuals will be neighbours of founder members. The interacting particle system (IPS) models of chapter 5 demonstrate that, when offspring always develop near enough to their parents that they may inter-pollinate, populations are expected to establish from only a handful of neighbouring individuals. In the IPS framework it is by no means unusual for a single pair of neighbouring individuals to have better than even chance of founding a population. So it is clear that threshold is completely irrespective of the potential carrying capacity of the population, but that a (usually low) configurational threshold must be met in order that a small population establish. Being well configured involves balancing the requirements of having neighbouring pollen donors and neighbouring space to colonize. Since small populations will typically have a high ratio of boundary to interior individuals, the latter is less of a practical concern. The cause of this virtual loss of Allee effect is clarified to some extent in the second order moment-closure approximations of chapter 6. In the pair approximation the contact rate in a developing population is linearly dependent on population size, rather than parabolically dependent as the models of chapters 3 and 4 prescribe.

Self-compatible sexual species were considered in the models in chapters 3 and 4. It was demonstrated that very low levels of self-fertilization can have profound qualitative effects. If, in addition to exported pollen, an effort exceeding a value that is roughly the reciprocal of the seed production effort is put into self-fertilization, then deterministic barriers to population establishment disappear. Since seed production rates are usually high, this amounts to very little self-fertilization, which is in line with the regular observation of some breakdown of incompatibility in facultatively outcrossing species (chapter 1 section 1.2.) This analysis makes no allowance for inbreeding depression which may decrease the effectiveness of this strategy. Nonetheless it is likely that in real outcrossing populations using self-fertilization as a last resort probably overcomes the necessity for small populations to be well configured.

Gynodioecy

In gynodioecious populations females and hermaphrodites coexist. In some species hermaphrodites concentrate resources in male function and the population is functionally dioecious. Other populations, at what is believed to be a more primitive stage in the evolution of gynodioecy, feature hermaphrodites with full female function. Male-sterility is conferred either by a nuclear mutation carried on a nascent sex chromosome, or by a cytoplasmic mutation borne on non-nuclear DNA. In the latter case in a sexual species and either case in a pseudogamous apomictic species, all offspring of females will be female and a small advantage to female-function will encourage initial spread of the mutation (Charnov 1982). It is not clear from previous theoretical work what prevents the mutation spreading to fixation and driving the population extinct in the process. Richards (1986, p 318-337) points out that, as the mutation spreads, eventually female fitness will be limited by pollen availability. But in a self-incompatible population, the same might be said of hermaphrodite fitness, so this need not halt the spread of the mutation. In their population genetic models of male-sterility Charlesworth & Ganders (1979) recognize the necessity for the advantage to female function to be frequency dependent. This dependence is assumed *a priori* and it is arbitrarily assumed that the advantage disappears entirely when female frequency reaches some threshold. In the models of this report two explicit mechanisms have been examined that confer the necessary frequency dependence onto female reproductive advantage.

In the non-spatial models of chapter 3 self-compatible hermaphrodites can coexist with females because, when pollen availability is low, hermaphrodites benefit from the reproductive assurance of self-fertilization. Self-compatibility does not however ensure that female advantage will disappear before male-sterility fixes. In fact self-compatibility is the mechanism that motivates Charlesworth & Ganders's (1979) choice of frequency dependent fitness function. However, in their one dimensional population genetic framework, the rich variety of dynamics of coexistence was missed. In the two-dimensional ecological framework of chapter 3 it emerges that, depending on the magnitude of enhanced female seed production, coexistence may be achieved at a stable equilibrium frequency, which may be under- or over-damped, or coexistence may be cyclic. The reaction-diffusion models of chapter 4 illustrate that the nature of coexistence has a significant impact on the range of spatial distributions that might be observed in a gynodioecious population. If the equilibrium is over-damped then it is possible for stable spatial patterns to arise with alternating bands of high and low

population density (see Figure 4-12.) If coexistence is cyclic then invasion of females is likely to result in spatio-temporal chaos (see Figure 4-8.)

In the IPS model of chapter 5 it was determined that self-compatibility is not a pre-requisite for gynodioecy. If hermaphrodites disperse their offspring within the neighbourhood from which they obtain pollen, they accrue an advantage when pollen is scarce. Hermaphrodites will tend to have proportionally more hermaphrodites in their neighbourhoods than females will. This configurational advantage of hermaphrodites, found in a discrete spatially model, provides a level of reproductive assurance similar to that provided by self-compatibility in non-spatial and continuum models. Moreover the pair approximation analysis in chapter 6 of the IPS gynodioecy model predicts that the range of model behaviours should be strikingly similar.

Sexual and Asexual Conspecifics

It is not uncommon in flowering plant genera containing apomictic species for closely related sexually and asexually reproducing species to be sympatric. Coexistence is often patchy and it is usual for one species to have a significantly wider range than the other. Conventional explanations for geographic parthenogenesis are borrowed from studies of analogous animal systems in which parthenogens are consistently found in more extreme environments (Lynch 1984). Thus it is usually argued that the sexual and asexual sister species are adapted to different habitats, even if the species have high phenotypic similarity and inhabit patches within metres of each other (for example, *Taraxacum* species found on Dutch dykes (Verduijn et al. 2004)).

This report considers the ecological interaction of a sexual species with a closely related apomictic species that retains the need for seeds to be fertilized (pseudogamy) and retains male function, so has the ability to sire offspring on sexuals. Both species are assumed diploid and self-incompatible and so apomixis confers no advantage in the way of reproductive assurance. When sexually produced seeds have improved viability and pollen produced by apomicts is of diminished quality, territories occupied by one reproductive mode are often impervious to invasion by the other.

In the non-spatial model of chapter 3, over a wide range of parameters both asexual-only and sexual-only equilibria are stable and locally attracting, so any mixed, initially viable population will eventually become fixed for one reproductive mode. This supports the argument that sexual and asexual conspecific coexistence must be mediated

by adaptation to different habitats. However, the reaction-diffusion model of chapter 4 indicates that a spatially distributed population will tend to polarize into spatial ranges exclusively occupied by one or other reproductive mode. Boundaries between patches gradually move, but crucially they may move on a very slow timescale compared with demographic turnover. Britton & Mogie (2001) demonstrate the same behaviour in a model with non-pseudogamous apomicts and observe that this non-equilibrium form of coexistence can independently explain the geographic parthenogenesis of the dandelion in Europe, apomictic varieties of which are found further north and east than sexual varieties. Because dandelion apomicts are not pseudogamous, they enjoy reproductive assurance and have a significant colonization advantage over sexual relatives. They are thus more likely to be found further from the glacial refuges to which the species were confined during the last ice age. When the apomictic species is pseudogamous this argument does not apply, and historical accident may instead determine which reproductive mode has the wider range. Model behaviour is very similar in the discrete space IPS model of chapter 5. Generic mixed initial conditions rapidly polarize into exclusive patches of one or other reproductive mode which gradually grow or shrink in response to the success of whichever mode is favoured at the boundary.

It is clear from both of the spatial modelling approaches in this report that the maintenance of distinct sexual and asexual ranges can result simply from the ecological interaction. Lynch (1984) made a case for ecologically driven segregation on the grounds that hybrids between sexuals and asexuals would be of poor quality and so both reproductive modes would experience depressed fitness at boundaries. The models of this report indicate that such an assumption is unnecessary: sexually produced apomicts can be assumed to have greater viability than apomictically produced offspring and segregation will still emerge from the model dynamics. The results of these models harmoniously augment the argument that sexuals and asexuals are adapted to different habitats. Such arguments may still be necessary when sexual and asexual relatives are found to coexist intimately.

Behavioural Homologies

The work in this report has highlighted some interesting behavioural analogies between models with significantly different underlying dynamics. For example, both the reaction-diffusion framework and the IPS framework predict that a self-incompatible sexual species established over some region will expand its range into available virgin

territory. In the reaction-diffusion model this is in spite of a strong Allee effect conferring a negative growth rate on low density boundary populations. Range expansion is driven by the migration of an abundance of seed from the population interior where growth rates are high. By contrast in the IPS model individuals in the boundary are optimally placed to achieve high reproductive success, having access to both pollen from the interior and exterior space to colonize. The operation of very different model processes give the same qualitative behaviour. Another instance of the same homology between diffusion and local interaction is seen in the sexual-asexual models. In both the reaction-diffusion model and the IPS model randomly assorted populations rapidly become polarized into exclusive regions of one or other type. The boundaries between these regions move comparatively slowly. For the reaction-diffusion model of chapter 4 it was demonstrated that, in the region of a boundary, the per-capita growth rates of both conspecifics are very similar. The movement of boundaries is enabled by diffusion, with rate of growth and diffusivity of the populations *behind* the boundary determining the direction of movement. By contrast in the IPS model it is only the individuals at the boundary in contact with conspecifics of both reproductive modes that determine the direction of movement.

A second strong behavioural homology to emerge from this report is between self-compatibility and clumping. In chapter 3 self-compatibility, even at low levels, is shown to diminish or remove the strong Allee effect sexual species might be expected to experience. Self-incompatible sexual species can derive a similar reproductive assurance by growing in clumps. The sexual species IPS model of chapter 5 indicates that by distributing offspring locally, within pollen transfer range, the strong Allee effect incumbent on sexual species is removed in all but the smallest of populations. Whether reproductive assurance is derived from self-compatibility or clumping when male-sterility mutations arise, as in the gynodioecy models, the range of model behaviours is very similar.

Comparative Spatial Ecology

The modelling in chapters 3 to 6 of this report has been structured in such a way that rigorous pathways exist connecting each modelling approach. Thus the non-spatial models of chapter 3 emerge as a first spatial moment approximation of the IPS models of chapter 5. Similarly the reaction-diffusion models of chapter 4, introduced as a continuum extension of non-spatial models, can be developed with hydrodynamic limit

arguments from the models of chapter 5. Chapter 6 contains second-order moment closure approximations extracted from IPS models which build on the first-order closures in chapter 3. These links are illustrated in Figure 5-20.

An interconnected approach such as this is fundamental to the validity of comparisons between modelling approaches. The relationships between model parameters are respected in different modelling contexts and precise information is available about the assumptions that permit transition from one framework to another. Through understanding the impact of these assumptions, spatial ecology is not constrained to purely phenomenological comparisons with real data. It can be checked that model mechanisms match natural mechanisms. This is particularly important in light of the behavioural homologies discussed above, since very similar model behaviour can emerge via very different mechanisms.

Forging rigorous links between modelling approaches often requires involved mathematical arguments and in this respect Durrett (1995) and Krone (2004) should be particularly credited with making flexible and powerful results available to a wider theoretical audience. Rigorous comparative spatial ecology is by no means limited to the small group of modelling frameworks discussed in this report. In particular the application of different hydrodynamic limit arguments to IPS arrive at integro-differential continuum models, which can accommodate a much wider range of dispersal phenomena.

7.2 PERSPECTIVES ON FUTURE RESEARCH

Spatial Ecology

Resolving Discrepancies

The work in chapters 4, 5 and 6 of this report contributes to a growing body of evidence documenting the discrepancies between the predictions of population-based and individual-based approaches to spatial ecology (Durrett & Levin 1994, Dieckmann et al. 2000). In some cases the discrepancy is the result of unsuitable comparison (Krone 2004). But model comparisons in Durrett & Levin (1994) and in this report are disciplined in this respect and still identify significant differences. The loss of Allee effect in the sexual species IPS and the coexistence in the gynodioecy IPS are

examples of qualitative behavioural change between population- and individual-based approaches.

These different behaviours are indubitably a result of the very different ways space is built into the models. In a reaction-diffusion model the assumptions underlying the derivation of the kinetic equations carry over. Thus the population associated with a point in space is assumed large enough that population density can be treated as a continuous quantity, but nonetheless small enough that all individuals interact equally often. Diffusion is then added as the agency of interaction between adjacent populations located explicitly in continuous space. In the vast majority of ecology applications, and in the models of this report, this interaction is limited to migration of individuals or dispersal of propagules such as seeds. As a result other interactions such as competition and inter-pollination are conspicuously non-spatial components of the resulting model. The explicit treatment of space makes possible the examination of large-scale pattern such as the profile of a biological invasion or stable non-homogenous population distributions. However, the combination of non-spatial kinetics and treating population size as a continuous quantity make reaction-diffusion models inappropriate for examining very small scale pattern.

For the majority of ecological applications of IPS, and in the models of this report, each interaction process is incorporated spatially on the scale of discrete individuals and their neighbourhoods. The precise composition of an individual's neighbourhood determines its fitness. When a second-order, or higher, moment-closure approximation such as the pair approximation is extracted, space proper is discarded and what remains is some information about the composition of neighbourhoods. Moment-closures therefore help the understanding of small-scale spatial pattern, but are ambiguous about population distribution. It is inappropriate to attempt to address questions about spatial extent or population profiles with a moment-closure approximation.

The assets and liabilities outlined above for reaction-diffusion models and moment-closures of IPS models are broadly generic of population- and individual-based models. It seems clear, from this characterization at least, that the deficiencies of both approaches are complementary and greater understanding of spatial pattern and a fuller description of spatial ecology would be available to so-called third generation models (Dieckmann et al. 2000) hybridizing the two approaches. One such approach might use the ordinary differential equations model describing local configurations that a pair approximation supplies as a description of population dynamics at a point in continu-

ous space. Populations could then be linked by dispersal captured by diffusion or more generally by an integral operator. A difficulty with this approach is that ideally, each dispersal event should impact upon local configuration as well as population distribution. But the envisioned approach requires local and non-local dispersal to be treated separately, confining locally dispersed seed to its natal point in space and excluding non-locally dispersed seed from having a configurational impact where it lands. Should such difficulties be overcome new multiscale techniques will emerge which are powerful, descriptive, ecological tools and a source of insight into modelling discrepancies.

Improving Moment Approximations

The ordinary pair approximation (OPA) employed in chapter 6 enjoyed some descriptive success, but carries numerous caveats. Like the mean field, the pair approximation is not explicitly spatial and assumes that populations are spread over the entire lattice, as a consequence it is bad at predicting growth rates of small populations confined to a small region. The OPA also assumes that the average neighbourhood composition is the most common. This assumption is flawed in the case of empty cells in the sexual-asexual model. When the total population is large the distribution of neighbourhood compositions should be bimodal, since most empty cells either have only empty and sexual sites for neighbours or only empty and asexual sites. Consequently the pair-approximation for the sexual-asexual IPS is inaccurate.

Some of the common improvements to the OPA discussed in chapter 6 section 6.5 improve accuracy. However, all moment closure approximations are open to the accusation that they are really an approximate description of a process on a random contact network rather than a regular lattice. This complaint is fundamental to the approach and no amount of tinkering is likely to remove the inappropriate predictions of growth and decay. Even the most imperiously sophisticated moment closures fail to capture population growth and may in effect trade improved equilibrium prediction for worse description of transient behaviour (Raghib-Moreno 2005).

Ellner conceived of an approach to IPS approximation which focuses on the boundary between lattice regions with different population structure. The pair-edge approximation (Ellner et al. 1998) assumes that the OPA gives a good description of the equilibrium-like dynamics in the interior of a clumped population. The exterior of the clump is unpopulated. On the boundary a neighbourhood structure intermediate between interior and exterior is imposed. The resulting model approximates population

spread rate rather well and, by solving for zero spreading rate, can determine threshold population establishment parameters with increased accuracy. Iwasa (2000) reports that Ellner's method can be extended to model the movement of boundaries between two autocorrelated species. In this case each species' population is modelled in isolation by the OPA, except at the boundary where intermediate neighbourhoods are imposed. The problem that the OPA faces in dealing with empty site neighbourhoods is thus overcome and a significantly improved parameter space can be deduced. Since the boundary must move in favour of one or other species the parameter space that is obtained completely eliminates the bistable region that dominates the mean field approximation and is still retained over a significant area in the OPA.

The pair-edge approximation has two principle drawbacks. With regard to two or more interacting species, the assumption must be made that the IPS dynamics drive species into highly autocorrelated clumps. This is readily observed and deduced from the bistability of non-spatial approximations in the sexual-asexual IPS and in Iwasa et al.'s (1998) models of spiteful bacteria. But it is not clear, for example in the gynodioecy IPS, that hermaphrodites and females become sufficiently autocorrelated for the pair-edge framework to be applied. Secondly in addition to the ad-hoc choice of closure in the OPA, the pair-edge approximation requires assumptions about state frequencies at boundaries. Ellner et al. (1998) found that a 50:50 blend of interior and exterior neighbourhoods gave good results, but such a choice, although intuitive, is arbitrary and not rigorous.

Outstanding Problems in Flowering Plant Sexual Diversity

Pathways to Dioecy and Polygamy

The gynodioecy models in this report examine cytoplasmic male-sterility mutations in sexual species. In extant populations, cytoplasmic male-sterility mutation are usually found in conjunction with nuclear fertility restoration genes, as in the CMS systems widely exploited in agriculture. Cytoplasmic male-sterility alone cannot lead to dioecy, because dioecy requires gender to be determined by sex chromosomes (Richards 1986, pp 318-337). When a nuclear male-sterility mutation arises, the chromosome on which it is borne and its homologous chromosome become incipient sex chromosomes. In this case selection can act on sex-linked mutations to drive the evolution of distinct genders. The accumulation of mutations minimizing female function in hermaphrodites

would ideally be modelled on an evolutionary timescale which respected the ecological significance of the shift. The adaptive dynamics framework (Dieckman et al. 2004) provides a way to examine the root causes of selection for dioecy via the gynodioecy pathway. Moreover the technique for examining invasion in a pair approximation to an IPS can be incorporated into a discrete space extension of adaptive dynamics (see for example Le Galliard et al. (2005)), so that crucial aspects of the discrete spatial nature of plant populations need not be overlooked.

The evolutionary pathway to dioecy via monoecy, believed to be the most common route, and the route via distyly, both involve disruptive selection. Disruptive selection arises when individuals in a population dimorphic for a particular trait achieve greater reproductive success than those in a monomorphic population with an intermediate trait value. The trait hypothesized to be under disruptive selection in the case of monoecy is the proportion of flowers that are female, in distyly it is style length. Disruptive selection is the cause of sympatric speciation in the adaptive dynamics framework. There is every reason to believe this framework would be excellently suited to exploring selection for dimorphism within species.

Hitchhiking Apomixis Genes

Mutations conferring apomixis need not be confined to the genome in which they arise if male-function is undisturbed (Mogie 1992). In chapter 1 section 1.3 this was identified as likely to significantly enhance the spread of apomixis in hermaphrodite species in comparison with dioecious species. If apomixis is initially successful myriad recombinations with the genomes of sexuals will occur. The apomixis gene can potentially *hitchhike* its way through the gene pool. If the sexual reproductive mode is eventually displaced the remaining apomictic lineages might be expected to be varied and carrying the very best genetic material.

As far as the author is aware, this hitchhiking effect has not been explored mathematically. It is not know whether the rate at which the sexual mode is displaced places limitations on the quality of the resulting apomictic lineages; Or whether there are limits to the number of phenotypic niches that apomicts can achieve. An appropriate framework for examining such questions would require an explicit discrete or continuous phenotype space. The trait substitution regime of adaptive dynamics would be unsuitable in this case: an approach in which ecological and evolutionary timescales are not asymptotically separated is required. It is also potentially very important

whether population size is treated discretely or continuously. With discrete individuals a when-it's-gone-it's-gone principle will circumscribe the apomixis gene's access to some phenotypes. A continuous population size model, by contrast, would be likely to make the dubious prediction that arbitrarily rare sexual phenotypes would still be available for recombination with apomicts.

Concluding Remarks

Spatial ecology is undergoing a phase of great invention but is, to some extent, in danger of diversifying to the point where there are as many modelling frameworks as research questions. There are at present vague convergence principles which produce similar qualitative behaviour from very different raw materials. Perhaps, if better understood, these can be harnessed to provide more coherent ecological predictions. There is also a disturbing incongruence between the predictions of population- and individual-based models. In the near future the discipline faces the challenge of uniting these scales in insightful third-generation models that ameliorate the incongruence and provide access to unparalleled modelling depth and flexibility.

The formal mathematical modelling of plant breeding systems, and in particular spatial modelling of these systems, is at an early stage. There are many evolutionary questions and theoretical conundrums unique to plant species which would benefit from rigorous treatment. There is still much to be learnt about dealing with the special requirements plants impose on modelling assumptions.

Bibliography

Adams, S., Vinkenoog, R., Speilman, M., Dickinson, H. G. & Scott, R. J. (2000), 'Parent-of-origin effects on seed development in *Arabidopsis thaliana* require DNA methylation', *Development* **127**, 2493–2502.

Allee, W. C., Emerson, A. E., Park, O., Park, T. & Schmidt, K. P. (1949), *Principles of Animal Ecology*, W.B. Saunders Company.

Aronson, D. G. & Weinberger, H. F. (1975), 'Nonlinear diffusion in population genetics, combustion, and nerver pulse propagation', *Partial differential equations and related topics* **446**, 5–49.

Asker, S. E. & Jerling, L. (1992), *Apomixis in Plants*, CRC Press.

Auger, P. & de la Parra Bravo, R. (2000), 'Methods of aggregation of variables in population dynamics', *C.R. Acad. Sci. Paris, Sciences de la vie Life Sciences* **323**, 665–674.

Auger, P. & Poggiale, J.-C. (1996), 'Emergence of population growth models: fast migration and slow growth', *Journal of Theretical Biology* **182**, 99–108.

Axelrod, R. (1984), *The Evolution of Cooperation*, Basic Books.

Barlow, D. P. (1993), 'Methylation and imprinting: from host defense to gene regulation?', *Science* **260**, 309–310.

Barrett, C. L., Eubank, S. G. & Smith, J. P. (2005), 'If smallpox stikes portland...', *Scientific American* **292**(3), 54–61.

Barrett, S. C. H. (2002*a*), 'The evolution of plant sexual diversity', *Nature Reviews Genetics* **3**, 274–283.

Barrett, S. C. H. (2002*b*), 'Sexual interference of the floral kind', *Heredity* **88**(2), 154–9.

Bateman, A. J. (19952), 'Self-incompatibility syatems in angiosperms. i. theory', *Heredity* **6**, 285–310.

Bell, G. (1982), *The masterpiece of nature: The evolution and gentics of sexuyality*, Applied Biology Series, Croom Helm.

Bertin, R. I. (1993), 'Incidence of monoecy and dichogamy in relation to self-fertilization in angiosperms', *American Journal of Botany* **80**(5), 557–560.

Bertin, R. I. & Newman, C. M. (1993), 'Dichogamy in angiosperms', *Bot Rev* **59**, 112–152.

Bierzychudek, P. (1987), Patterns in plant parthenogenesis, *in* S. C. Stearns, ed., 'The evolution of sex and its consequences', Vol. 55 of *Experientia Supplementum*, Birkhauser Verlag, pp. 197–216.

Britton, N. F. & Mogie, M. (2001), 'Poor male function favours the coexistence of sexual and asexual relatives', *Ecology Letters* **4**, 116–121.

Carrillo, C. (2002), Mathematical models for the coexistence of sexual and asexual conspecifics, Phd, University of Bath, Departmet of Mathematical Sciences.

Charlesworth, B. (1980), 'The cost of sex in relation to mating system', *Journal of Theoretical Biology* **84**, 655–671.

Charlesworth, D. & Ganders, F. R. (1979), 'The population genetics of gynodioecy with cytoplasmic-genic male sterility', *Heredity* **43**, 213–18.

Charnov, E. (1979), 'Simultaneous hermaphroditism and sexual selection', *Proceedings of the National Academy of Sciences USA* **76**(5), 2480–2484.

Charnov, E. L. (1982), *Sex Allocation*, number 18 *in* 'Monographs in population biology', Princeton University Press.

Crane, P. R., Friis, E. M. & Pederson, K. F. (1995), 'The origin and early diversification of angiosperms', *Nature* **374**(2), 27–33.

Cronhjort, M. B. (2000), The interplay between reaction and diffusion, *in* U. Dieckmann, R. Law & Metz, eds, 'The Geometry of Ecological Interactions', Cambridge Studies in Adaptive Dynamics, Cambridge University Press, chapter 9, pp. 151–169.

Darlington, C. D. (1958), *The evolution of genetic systems*, 2nd edn, Oliver and Boyd.

Dawkins, R. (1976), *The Selfish Gene*, Oxford University Press.

DeAngelis, D. L., Rose, K. A. & Huston, M. A. (1994), Individual oriented approaches to modeling ecological populations and communities, *in* S. A. Levin, ed., 'Frontiers in Mathematical Biology', Springer, pp. 390–410.

Dieckman, U., Doebeli, M., Metz, J. A. J. & Tautz, D., eds (2004), *Adaptive Speciation*, number 3 *in* 'Cambridge Studies in Adaptive Dynamics', Cambridge University Press.

Dieckmann, U., Law, R. & Metz, J. A. J., eds (2000), *The Geometry of Ecological Interactions*, Cambridge Studies in Adaptive Dynamics, Cambridge University Press.

DorzsaFarkas, K. (1995), 'Self-fertilization: An adaptive strategy in widespread enchytraeids', *European Journal of Soil Biology* **31**(4), 207–215.

Dunbar, S. R. (1983), 'Travelling wave solutions of diffusive lotka-volterra equations', *Journal of Mathematical Biology* **17**, 11–32.

Dunbar, S. R. (1984), 'Travelling wave solutions of diffusive lotka-volterra equations: a heteroclinic connection in $\mathbb{R}^4$', *Transactions of the American Mathematical Society* **268**, 557–594.

Durrett, R. (1995), *Ten Lectures on Particle Systems*, Vol. 1608 of *Lecture Notes in Mathematics*, Springer.

Durrett, R. & Levin, S. (1994), 'The importance of being discrete (and spatial)', *Theoretical Population Biology* **46**, 363–394.

Ellner, S. P. (2001), 'Pair approximation for lattice models with multiple interaction scales', *Journal of Theorectical Biology* **210**, 435–447.

Ellner, S. P., Sasaki, A., Haraguchi, Y. & Matsuda, H. (1998), 'Speed of invasion in lattice population models: pair-edge approximation', *J. Math. Biol.* **36**, 469–484.

Felsenstein, J. (1988), Sex and the evolution of recombination, *in* R. E. Michod & B. R. Levin, eds, 'The evolution of sex: An examiniation of current ideas', Sinauer Associates, chapter 5, pp. 74–86.

Fisher, R. A. (1930), *The genetical theory of natural selection*, Clarendon Press.

Fisher, R. A. (1937), 'The wave of advance of an advantageous gene', *Annals of Eugenics* **7**, 353–369.

Friedman, W. E. & Floyd, S. K. (2001), 'Perspective: The origin of flowering plants and their reproductive biology', *Evolution* **55**(2), 217–231.

Friedman, W. E. & Williams, J. H. (2004), 'Developmental evolution of the sexual process in ancient flowering plant lineages', *The Plant Cell* **16**, S119–S132.

Green, R. F. & Noakes, D. L. G. (1995), 'Is a little bit of sex as good as a lot', *Journal of Theoretical Biology* **174**, 87–96.

Greig, D. G. & Travisano, M. T. (2004), 'The prisoners's dilemma and polymorphism in yeast suc genes', *Proc. R. Soc. Lond. B (Suppl.)* **271**, 25–26.

Grimm, V. (1999), 'Ten years of individual-based modelling in ecology: what have we learned and what could we learn in the future', *Ecological Modelling* **115**, 129–148.

Guckenheimer, J. & Holmes, P. (1983), *Nonlinear oscillations, dynamical systems, and bifurcations of vector fields*, number 42 *in* 'Applied Mathematical Sciences', Springer.

Hadeler, K. P. & Rothe, F. (1975), 'Travelling fronts in nonlinear diffusion equations', *Journal of Mathematical Biology* **2**, 251–263.

Haig, D. (1986), 'Conflict among megaspores', *Journal of Theoretical Biology* **123**, 471–480.

Haig, D. (1997), 'Parental antagonism, relatedness asymmetries, and genomic imprinting', *Proceedings of the Royal Society of London B* **264**, 1657–1662.

Haig, D. & Westoby, M. (1989), 'Parent-specific gene expression and the triploid endosperm', *The American Naturalist* **134**(1), 147–155.

Haig, D. & Westoby, M. (1991), 'Genomic imprinting in the endosperm: its effect on seed development in crosses between species, and between different ploidies of the same species, and its implications for the evolution of apomixis', *Phil. Trans. R. Soc. Lond. B* **333**, 1–13.

Hamilton, W. D. (1964), 'The evoltuion of social behaviour', *Journal of Theoretical Biology* **1**, 295–311.

Hamilton, W. D., Axelrod, R. & Tanese, R. (1990), 'Sexual reproduction as an adaptation to resist parasites (a review)', *Proc. Natl. Acad. Sci. USA* **87**, 3566–3573.

Harada, Y., Ezoe, H., Iwasa, Y., Matsuda, H. & Satō, K. (1995), 'Population persistence and spatially limited social interaction', *Theorectical population biology* **48**, 65–91.

Härdling, R. (2001), 'A model of triploid endosperm evolution driven by parent-offspring conflict', *Oikos* **92**, 417–423.

Harper, J. L. (1977), *Population Biology of Plants*, Academic Press.

Hassell, M. P., Comins, H. N. & May, R. M. (1991), 'Spatial structure and chaos in insect population dynamics', *Nature* **353**(6341), 255–258.

Hosono, Y. (1998), 'The minimal speed of travelling fronts for a diffusive lotka-volterra competition model', *Bulletin of Mathematical Biology* **60**, 435–448.

Hurst, L. D. & Peck, J. R. (1996), 'Recent advances in understanding of the evolution and maintenance of sex', *Trends in Ecology and Evolution* **11**(2), 46–52.

Iwasa, Y. (2000), Lattice models and pair approximations in ecology, *in* U. Dieckmann, R. Law & J. A. J. Metz, eds, 'The Geometry of Ecological Interactions', Cambridge Studies in Adaptive Dynamics, Cambridge University Press, chapter 13, pp. 227–251.

Iwasa, Y., Nakamaru, M. & Levin, S. A. (1998), 'Allelopathy of bacteria in a lattice population: Competition between colicin-sensitive and colicin-producing strains', *Evolutionary Ecology* **12**, 785–802.

Johri, B. M. & Ambegaokar, K. B. (1984), Embryology: then and now, *in* B. M. Johri, ed., 'Embryology of Angiosperms', Springer-Verlag, chapter 1, pp. 1–52.

Joshi, A. & Moody, M. (1995), 'Male gamete output of asexuals and the dynamics of populations polymorphic for reproductive mode', *Journal of Theoretical Biology* **174**, 189–197.

Joshi, A. & Moody, M. (1998), 'The cost of sex revisited: effects of male gamete output of hermaphrodites that are asexual in their female capacity', *Journal of Theoretical Biology* **195**, 533–542.

Judson, O. P. (1994), 'The rise of the individual-based model in ecology', *Trends Ecol Evol* **9**, 9–14.

Katori, M. & Konno, N. (1991), 'Upper bounds for survival probability of the contact process', *Journal of Statistical Physics* **63**, 115–130.

Kelley, S. E., Antonovics, J. & Schmitt, J. (1988), 'A test of the short-term advantage of sexual reproduction', *Nature* **331**, 714–716.

Kim, B. J., Kwon, Y. C., Kwack, Y. H., Lim, M. S. & Park, E. H. (1999), 'The mode of seed formation in *Allium senescens* and two Korean *Allium* species', *Plant Breeding* **118**, 435–438.

Klinkhamer, P. G. L. & de Jong, T. J. (1993), 'Attractiveness to pollinators: a plant's dilemma', *OIKOS* **66**(1), 180–184.

Koelewijn, H. P. & van Damme, J. M. M. (2005), 'Effects of seed size, inbreeding and maternal sex on offspring fitness in gynodioecious plantago coronopus', *Journal of Ecology* **93**(2), 373–383.

Kolmogoroff, A., Petrovsky, I. & Piscounoff, N. (1937), 'Etude de l'equation de la diffusion avec croissance de la quantité de matiere et son application á un problém biologique', *Moscow University Bulletin of Mathematics* **1**, 1–25.

Kondrashov, A. S. (1988), 'Deleterious mutations and the evolution of sexual reproduction', *Nature* **336**(1), 435–440.

Kondrashov, F. A. & Kondrashov, A. S. (2001), 'Multidimensional epistasis and the disadvantage of sex', *Proceedings of the National Academy of Science* **98**(21), 12089–12092.

Kopell, N. & Howard, L. N. (1973), 'Plane wave solutions to reaction-diffusion equations', *Studies in Applied Mathematics* **52**(4), 291–328.

Kot, M., Medlock, J., Reluga, T. & Walton, D. B. (2004), 'Stochasticity, invasions, and branching random walks', *Theoretical Population Biology* **66**(3), 175–184.

Krone, S. M. (2004), 'Spatial models: Stochastic and deterministic', *Mathematical and Computer Modelling* **40**, 393–409.

Laser, K. D. & Lersten, N. R. (1972), 'Anatomy and cytology of microsporogenesis in cytoplasmic male sterile angiosperms', *The Botanical Review* **38**(3), 425–454.

Law, R. & Cannings, C. (1984), 'Genetic analysis of conflicts arising during development of seeds in the Angiospermophyta', *Proceedings of the Royal Society of London B* **221**, 53–70.

Le Galliard, J. F., Ferriere, R. & Dieckmann, U. (2005), 'Adaptive evolution of social traits: Origin, trajectories, and correlations of altruism and mobility', *American Naturalist* **165**, 206–224.

Lewis, M. A. & Kareiva, P. (1993), 'Allee dynamics and the spread of invading organisms', *Theoretical Population Biology* **43**, 141–158.

Li, Q. J., Xu, Z. F., Kress, W. J., Xia, Y. M., Zhang, L., Deng, X. B., Gao, J. Y. & Bai, Z. L. (2001), 'Flexible style that encourages outcrossing', *Nature* **410**, 432.

Liggett, T. M. (1978), 'Attractive nearest neighbor spin systems on the integers', *Annals of Probability* **6**, 629–636.

Lotka, A. J. (1956), *Elements of Mathematical Biology*, 2nd edn, Dover Publications.

Lynch, M. (1984), 'Destabilizing hybridization, general-purpose genotypes and geographic parthenogenesis', *The Quarterly Review of Biology* **59**, 257–290.

Marsden, J. E. & McCracken, M. (1976), *The Hopf Bifurcation and Its Applications*, number 19 *in* 'Applied Mathematical Sciences', Springer-Verlag.

Matsuda, H., Ogita, N., Sasaki, A. & Satō, K. (1992), 'Statistical mechanics of population', *Progress of Theoretical Physics* **88**(6), 1035–1049.

Maynard-Smith, J. (1978), *The evolution of Sex*, Cambridge University Press.

Mayo, O. (1987), *The theory of plant breeding*, 2nd edn, Clarendon Press.

Michod, R. E. & Levin, B. R., eds (1988), *The evolution of sex: An examiniation of current ideas*, Sinauer Associates.

Mogie, M. (1992), *The evolution of asexual reproduction in plants*, Chapman and Hall.

Mogie, M., Britton, N. F. & Stewart-Cox, J. A. (submitted), Asexuality, polyploidy and the male function, *in* U. Grossniklaus, P. van Dijk, T. Sharbel & E. Hoerandl, eds, 'Apomixis: Evolution, Mechanisms and Perspectives', Regnum Vegetabile, IAPT.

Mogie, M. & Ford, H. (1988), 'Sexual and asexual *Taraxacum* species', *Biological Journal of the Linnean Society* **35**, 155–168.

Müller, H. J. (1932), 'Some genetic aspects of sex', *American Naturalist* **66**, 118–38.

Müller, H. J. (1964), 'The relation of recombination to mutational advance', *Mutational Research* **1**, 2–9.

Murray, J. D. (1989*a*), *Mathematical Biology, I: An Introduction*, Interdisciplinary Applied Mathematics, Springer.

Murray, J. D. (1989*b*), *Mathematical Biology, II: Spatial Models and Biomedical Applications*, Interdisciplinary Applied Mathematics, Springer.

Nakamaru, M., Matsuda, H. & Iwasa, Y. (1997), 'The evolution of cooperation in a lattice structured population', *Journal of Theoretical Biology* **184**, 65–81.

Nakamaru, M., Nogami, H. & Iwasa, Y. (1998), 'Score-dependent fertility model for the evolution of cooperation in a lattice', *Journal of Theoretical Biology* **194**, 101–124.

Nogler, G. (1984), Gametophytic apomixis, *in* B. Johri, ed., 'Embryology of Angiosperms', Springer Verlag, Berlin, chapter 10, pp. 475–518.

Noirot, M., Couvet, D. & Hamon, S. (1997), 'Main role of self-pollination rate on reproductive allocations in pseudogamous apomicts', *Theorectical and Applied Genetics* **95**, 479–483.

Nybom, H. (1985), 'Active self-pollination in blackberries (*Rubus* subgen. *Rubus*, rosaceae).', *Nordic Journal of Botany* **5**, 521–5.

O'Connell, L. M. & Eckert (2001), 'Differentiation in reproductive strategy between sexual and asexual populations of antennaria perlinii (asteraceae)', *Evolutionary Ecology Research* **3**(3), 311–330.

Okubo, A. (1980), *Diffussion and ecological problems: mathematical models*, Springer, New York.

Owen, M. R. & Lewis, M. A. (2001), 'How predation can slow, stop or reverse a prey invasion', *Bulletin of Mathematical Biology* **63**, 655–684.

Pailler, T., Humeau, L. & Figier, J. (1998), 'Reproductive trait variation in the functionally dioecious and morphologically heterostylous island endemic *Chassalia corallioides* (rubiaceae)', *Biological Journal of the Linnean Society* **64**(3), 297–313.

Pannell, J. (1997), 'The maintenance of gynodioecy and androdioecy in a metpopulation', *Evolution* **51**(1), 10–20.

Parker, G. A. & Macnair, M. R. (1978), 'Models of parent-offspring conflict. I. Monogamy', *Animal Behaviour* **26**, 97–110.

Peck, J. R. & Waxman, D. (2000), 'What's wrong with a little sex', *Journal of evolutionary biology* **13**, 63–69.

Perko, L. (1991), *Differential equations and dynamical systems*, number 7 *in* 'Texts in Applied Mathematics', Springer-Verlag.

Petrovskii, S., Morozov, A. & Li, B. (2005), 'Regimes of biological invasion in a predator-prey system with the allee effect', *Bulletin of Mathematical Biology* **67**, 637–661.

Queller, D. C. (1983), 'Kin selection and conflict in seed maturation', *Journal of Theoretical Biology* **100**, 153–172.

Queller, D. C. (1984), 'Models of kin selection on seed provisioning', *Heredity* **53**(1), 151–165.

Queller, D. C. (1989), 'Inclusive fitness in a nutshell', *Oxford Surveys in Evolutionary Biology* **6**, 73–109.

Raghib-Moreno, M. (2005), Point processes in spatial ecology, Phd, University of Glasgow, Department of Mathematics.

Rand, D. A. & Wilson, H. B. (1995), 'Using spatio-temporal chaos and intermediate-scale determinism to quantify spatially extended ecosystems', *Proc. R. Soc. Lond. B* **259**, 111–117.

Richards, A. J. (1986), *Plant Breeding Systems*, George Allen & Unwin (Publishers) Ltd.

Rutishauser, A. (1954), 'Die entwicklungserregung des endosperms bei peudogamen *Ranunculus*arten.', *Mitt. Naturforsch Ges Schaffhausen* **25**, 1–45.

Satō, K. (2000), Pair approximations, *in* U. Dieckmann, R. Law & J. A. J. Metz, eds, 'The Geometry of Ecological Interactions', Cambridge Studies in Adaptive Dynamics, Cambridge University Press, chapter 18, pp. 341–358.

Sato, K., Matsuda, H. & Sasaki, A. (1994), 'Pathogen invasion and host extinction in lattice structured populations', *Journal of Mathematical Biology* **32**(3), 251–268.

Schley, D., Doncaster, C. P. & Sluckin, T. (2004), 'Population models of sperm-dependent parthenogenesis', *Journal of Theoretical Biology* **229**, 559–572.

Schnable, P. S. & Wise, R. P. (1998), 'The molecular basis of cytoplasmic male sterility and fertility restoration', *trends in plant science* **3**(5), 175–180.

Scott, R. J., Speilman, M., Bailey, J. & GDickinson, H. (1998), 'Parent-of-origin effects on seed development in *Arabidopsis thaliana*', *Development* **125**, 3329–3341.

Sherratt, J. A. (1993), 'Transition waves that leave behind regular or irregular spatiotemporal oscillations in a system of three reaction-diffusion equations', *International Journal of Bifurcation and Chaos* **3**(5), 1269–1279.

Sherratt, J. A. (1994*a*), 'Irregular wakes in reaction-diffusion waves', *Physica D* **70**, 370–382.

Sherratt, J. A. (1994*b*), 'On the evolution of periodic plane waves in reaction-diffusion systems of a $\lambda - \omega$-type', *SIAM Journal of Applied Maths* **54**(5), 1374–1385.

Sherratt, J. A. (1998), 'Invading wave fronts and their oscillatory wakes are linked by a modulated travelling pulse resetting wave', *Physica D* **117**, 145–166.

Sherratt, J. A. (2001), 'Periodic travelling waves in cyclic predator-prey systems', *Ecology Letters* **4**, 30–37.

Sherratt, J. A., Lewis, M. A. & Fowler, A. C. (1995), 'Ecological chaos in the wake of invasion', *Proceedings of the National Academy of Science U.S.A.* **92**, 2524–2528.

Shigesada, N. & Kawasaki, K. (1997), *Biological Invasions: Theory and Practice*, Oxford Series in Ecology and Evolution, Oxford University Press.

Skellam, J. G. (1951), 'Random dispersal in theoretical populations', *Biometrika* **38**, 197–218.

Smith, C. C. & Fretwell, D. F. (1974), 'The optimal balance between size and number of offspring', *The American Naturalist* **108**(962), 499–506.

Smith, G. L. (1963), 'Studies in *Potentilla* l. i. embryological investigations into the mechanism of agomspery in British *P. tabernaemontani*', *New Phytologist* **62**, 264–282.

Smoller, J. (1983), *Shock-Waves and Reaction-Diffusion Equations*, Springer-Verlag.

Spencer, H. G. & Williams, M. J. M. (1997), 'The evolution of genomic imprinting: two modifier-locus models', *Theoretical Population Biology* **51**, 23–35.

Stearns, S. C., ed. (1987), *The evolution of sex and its consequences*, Vol. 55 of *Experimentia Supplementum*, Birkhauser Verlag.

Stebbins, G. L. (1950), *Variation and Evolution in Plants*, number 16 *in* 'Colunbia Biological Series', Columbia University Press.

Stebbins, G. L. (1976), Seeds, Seedlings, and the Origin of Angiosperms, *in* C. B. Beck, ed., '*Origin and Early Evolution of Angiosperms*', Columbia University Press, pp. 300–311.

Stewart-Cox, J. A., Britton, N. F. & Mogie, M. (2004*a*), 'Endosperm triploidy has a selective advantage during ongoing parental conflict via imprinting', *Proc. R. Soc. Lond. B* **271**(1549), 1737–1743.

Stewart-Cox, J., Britton, N. F. & Mogie, M. (2004*b*), Timescale separated pollination-colonisation models, *in* P. M. A. Sloot, B. Chopard & A. G. Hoekstra, eds, 'Cellular Automata, 6th International Conference on Cellular Automata for Research and Industry, ACRI 2004, Amsterdam, The Netherlands, October 2004 Proceedings', Vol. 3305 of *Lecture Notes in Computer Science*, Springer, pp. 765–774.

Stewart-Cox, J., Britton, N. F. & Mogie, M. (2005*a*), 'Pollen limitation or mate search need not induce an Allee effect', *Bulletin of Mathematical Biology* **67**(5), 1049–1079.

Stewart-Cox, J., Britton, N. F. & Mogie, M. (2005*b*), 'Space mediates coexistence of females and hermaphrodites', *Bulletin of Mathematical Biology* . (In press).

Sutherland, S. & Delph, L. (1984), 'On the iportance of male fitness in plants: patterns of fruit set', *Ecology* **65**, 1093–1104.

Trivers, R. L. (1974), 'Parent-offspring conflict', *American Zoologist* **14**, 249–264.

Turing, A. M. (1952), 'The chemical basis of morphogenesis', *Phil. Trans. Roy. Soc. Lond. B* **237**(641), 37–72.

van Baalen, M. (2000), Pair approximations for different spatial geometries, *in* U. Dieckmann, R. Law & J. A. J. Metz, eds, 'The Geometry of Ecological Interactions', Cambridge Studies in Adaptive Dynamics, Cambridge University Press, chapter 19, pp. 359–387.

van Valen, L. (1973), 'A new evolutionary law', *Evolutionary Theory* **1**, 1–30.

Verduijn, M. H., van Dijk, P. J. & van Damme, J. M. M. (2004), 'Distribution, phenology and demography of sympatric sexual and asexual dandelions (taraxacum officinale s.l.): geographic parthenogenesis on a small scale', *Biological Journal of the Linnean Society* **82**, 205–218.

Verhulst, P. F. (1838), 'Notice sur la loi que la population pursuit dans son accroissement', *Corresp. Math. Phys* **10**, 113–121.

Vijayaraghavan, M. R. & Prabhakar, K. (1984), The Endosperm, *in* B. M. Johri, ed., '*Embryology of Angiosperms*', Springer-Verlag, chapter 7, pp. 319–376.

Vinkenoog, R., Speilman, M., Adams, S., Dickinson, H. G. & Scott, R. J. (2002), Genomic Imprinting in Plants, *in* A. Ward, ed., 'Genomic Imprinting Methods and Protocols', Vol. 181 of *Methods in Molecular Biology*, Humana Press, chapter 25, pp. 327–370.

Volterra, V. (1931), *Animal Ecology*, McGraw-Hill, chapter Variations and fluctuations of the number of individuals in animal species living together.

von Neumann, J. (1966), *The Theory of Self-reproducing Automata, von Neumann*, The Theory of Self-reproducing Automata, von Neumann.

Walter, R. & Worsch, T. (2004), Efficient simulation of ca with few activities, *in* P. M. A. Sloot, B. Chopard & A. G. Hoekstra, eds, 'Cellular Automata, 6th International Conference on Cellular Automata for Research and Industry, ACRI 2004, Amsterdam, The Netherlands, October 2004 Proceedings', Vol. 3305 of *Lecture Notes in Computer Science*, Springer, pp. 101–110.

Westoby, M. & Rice, B. (1982), 'Evolution of the seed plants and inclusive fitness of plant tissues', *Evolution* **36**(4), 713–724.

Whitehouse, H. L. K. (1950), 'Multiple-allelomorph incompatibility of pollen and style in the evolution of the angiosperms', *Annals of Botany* **14**, 198–216.

Wilkins, J. F. & Haig, D. (2001), 'Genomic imprinting of two antagonistic loci', *Proceedings of the Royal Society, London B.* **286**, 1861–1867.

Williams, G. C. (1975), *Sex and Evolution*, Monographs in Population Biology, Princeton University Press.

Williams, J. H. & Friedman, W. E. (2002), 'Identification of diploid endosperm in an early angiosperm lineage', *Nature* **415**, 522–526.

Willson, M. F. & Burley, N. (1983), *Mate Choice in Plants*, number 19 *in* 'Monographs in population biology', Princeton University Press.

Wilson, W. (2000), *Simulating Ecological and Evolutionary Systems in C*, Cambridge University Press.

Wright, S. (1968), *Evolution and the gentics of populations*, University of Chicago Press.